Phthalocyanine langmuir-blodgett films and their associated devices

Baker, S.

PHTHALOCYANINE LANGMUIR-BLODGETT FILMS AND THEIR ASSOCIATED DEVICES

by

S. Baker, B.Sc.

A Thesis submitted for the Degree of Doctor of Philosophy in the University of Durham

March. 1985

DECLARATION

I hereby declare that the work reported in this thesis has not previously been submitted for any degree and is not being currently submitted in candidature for any other degree.

Signed S. Baker

The work reported in this thesis was carried out by the candidate.

Signed Gareth Roberts

McNeill

Directors of Studies

S. Baker

Candidate

ABSTRACT

Interest in the Langmuir-Blodgett (LB) technique has led to a number of investigations into different types of materials that can be deposited in the form of monolayers. For example, as well as the classic long chain fatty acids and alcohols, materials such as polymerisable molecules, aromatic hydrocarbons and dye substances can now all be produced in monomolecular form. Unfortunately, few of these materials yet fulfil the requirements of mechanical and thermal stability that will be necessary if LB films are to be used commercially. This work has dealt with the use of phthalocyanine, a substance well known for its thermal and chemical stability, in the production of LB films. Initially two compounds were investigated, dilithium phthalocyanine and tetra-tert-butyl phthalocyanine. Although it was found that both materials produced layers of reproducible quality which adhered tenaciously to various substrates and to each other, single monolayers were not obtained. More success has been achieved using an asymmetrically substituted phthalocyanine molecule.

Electron microscopy studies have shown that the majority of films are polycrystalline. However, a substitute CuPc proved to be a valuable exception. Multilayer films of this molecule were found to have domains of the order of 3 mm in size showing a preferred orientation. Even so, it has to be accepted that the phthalocyanine films produced to date are not as structurally perfect as for example, multilayers of ω-tricosenoic acid.

Our ability to produce monomolecular layers of phthalocyanine now extends the range of possible applications for this material. For instance it is known that the fine control of insulator thickness is crucial in the optimisation of photovoltaic and electroluminescent metal-insulator-semiconductor devices. Examples of both types of device have been demonstrated using our phthalocyanine films. For the bistable switch, a gallium arsenide substrate was used; both gallium phosphide and zinc selenide have been utilized in the electroluminescent structures. Moreover, in the case of phthalocyanine another possibility presents itself. It has long been known that the conductivities of this material and its derivatives are very sensitive to the presence of certain gases, particularly the oxides of nitrogen. The increased conductivity of such materials has been demonstrated to be confined to the surface of the crystal. Hence many phthalocyanine gas detector systems have been based on thin films. Unfortunately because phthalocyanine exhibits polymorphism, the exact structure of such films can be complicated, making interpretation of results and subsequent device optimisation difficult. Also the response and recovery times of these thin film devices can also be excessively long. It is possible that monomolecular LB films of phthalocyanine could well overcome some or all of these problems. Our experiments have concentrated on asymmetrically substituted copper phthalocyanine and its usefulness to detect nitrogen dioxide. Preliminary results show the response and recovery times for the simple gas structures to be faster than those previously reported for other thin film phthalocyanine devices. It is suggested that this is due to the more ordered structure of the LB film, which enables the gas to adsorb on, or desorb from the molecular sites more readily.

ACKNOWLEDGEMENTS

The production of a thesis requires the help and support of numerous people. I would like to acknowledge those who have been foremost in doing this. My supervisors Professor G.G.Roberts and Dr. M.C.Petty have been invaluable in both the work and realisation of this thesis; Mike for his clear perception of the way ahead and Gareth for his innovative drive and personal guidance extending beyond academic pursuit. I would like to thank Frank Spence for organizing the departmental workshop facilities and Brian Blackburn, with his associates, for their craftsmanship in constructing the equipment fundamental to my research to a truly excellent and professional standard. I am grateful to Dr. G.J.Russell for the electron microscope studies carried out in this thesis. Also many thanks are due to Norman Thompson for assistance with some of the diagrams. I gratefully acknowledge funding from the SERC and ICI and thank my industrial supervisors Dr. J.Cramp and Dr. R.Hann for the provision of materials and useful discussions. I would also like to thank many members of the Department for information and ideas accumulated during discussions, particularly John Batey, Jim Sharp and Mike Fowler. As always there are many personal friends who gave valued support but I would like to especially mention Dave Lazaro for his friendship and the valuable contribution he made proof reading this thesis. Above all I would like to thank my parents for the love and support which they have given throughout the years.

CONTENTS

CHAPTER 3

LANGMUIR BLODGETT FILMS

CHAPTER 4

EXPERIMENTAL TECHNIQUES

CHAPTER 5

PHTHALOCYANINE LANGMUIR-BLODGETT FILMS

CHAPTER 6

FILM CHARACTERIZATION

CHAPTER 7

DEVICE APPLICATIONS

CHAPTER 8

SUMMARY AND CONCLUSIONS

CHAPTER 1

INTRODUCTION

The Langmuir-Blodgett (LB) technique is a recently developed technology, where a compressed organic monolayer, supported on the surface of a subphase (usually water) is transferred to a substrate which is passed repeatedly through the monolayer. During the last decade the LB technique for depositing monomolecular layers has been the subject of increasing attention. Most interest has focused around the fact that the LB technique provides an excellent method for depositing thin, uniform, insulating films of accurately defined thickness. This permits their use in a variety of electronic device applications, such as field effect transistors, photovoltaic cells and light emitting diodes. However, there are deficiencies with conventional films made from fatty acid materials because of their lack of mechanical and thermal stability which renders commercial application impractical.

Phthalocyanine, commonly used as a dye and colourant in the chemical industry, has been shown to display excellent stability. It is resistant to attack from weak acids and alkalis, it has a high resistance to bleaching under high-intensity illumination and most phthalocyanine materials can be heated to 400°C before sublimation.

The aim of this work has been to develop techniques whereby

phthalocyanine can be deposited as an LB film. Although work with dye molecules has been carried out previously, it has invariably involved the use of long chain substitutions. This thesis covers the development of materials with little or no substitutions. The resulting phthalocyanine films therefore retain the intrinsic stability and high optical absorption coefficient associated with the basic phthalocyanine molecule.

LB films have been used previously in a "passive" way as insulators of precisely controlled thickness. This thesis reflects recent interest in using the films in an active role as part of the device. It is known that the electrical properties of phthalocyanine vary on exposure to certain gas ambients, especially halogens and the oxides of nitrogen and it is this property that has been exploited by using the film as an active part of gas sensing devices.

The thesis begins with a general review of phthalocyanine, its compounds, their preparation, characterisation and uses. Chapter 3 provides an introduction to LB films covering the basic concepts, the historical development of the technology and the materials used. The characterisation of the floating Langmuir films by means of pressure-area curves is also covered and this is followed by a review of the techniques used to investigate the deposited LB films. In chapter 4 a description of the LB trough used in this research is given, along with the constructional modifications which were made to facilitate work with phthalocyanine materials. It also contains a description of the equipment and procedures used to characterise the

phthalocyanine LB films and an account of the specially designed gas equipment for measuring the films' electrical response to gas ambients. In chapter 5 the newly developed techniques necessary for producing phthalocyanine LB films are explained. Firstly, the molecular synthesis and substitution methods are described, followed by the pressure/area curves and a discussion of their interpretation and finally the techniques and conditions necessary for optimum deposition. Chapter 6 deals with the characterisation of the phthalocyanine LB films. This is divided into three areas of assessment, namely structural, optical and electrical. Chapter 7 reports the incorporation of the phthalocyanine LB films in various electronic devices, where the films are shown to perform a valuable role in electroluminescent diodes and bistable switching devices. A detailed account is given of the use of the films in device structures which are sensitive to gaseous ambients. The thesis concludes with a summary of the results obtained from this research and some suggestions for future study. The overall view is that there is considerable promise for phthalocyanine LB films in the field of electronics. Although there is scope for improvement in their structure, their stability is of paramount importance and offers an advantage not possessed by other LB film molecules.

CHAPTER 2

PHTHALOCYANINE

2.0 INTRODUCTION TO PHTHALOCYANINE

The term phthalocyanine (Pc) was first used by Linstead (1) and is derived from the Greek terms for naphtha (rock oil) and for cyanine (dark blue). Interestingly, phthalocyanines were first discovered accidentally during an industrial operation at Grangemouth in Scotland. This occurred during the production of phthalimide. When ammonia was passed through molten phthalic anhydride in iron vessels, traces of a dark blue substance with great stability were noticed. This compound was isolated and identified as iron phthalocyanine.

The first patent describing phthalocyanine compounds was granted in 1929 to Dandridge, Drescher, and Thomas of Scottish Dyes, Ltd (2). Copper phthalocyanine was first manufactured by Imperial Chemical Industries in 1935. Commercial methods for the manufacture of phthalocyanine and copper phthalocyanine, as well as methods for eliminating crystallisation and flocculation of the pigment, were then developed. In addition, partially chlorinated and fully chlorinated copper phthalocyanines were produced for use in some applications.

Phthalocyanine dyes patented and developed in the thirty years following its discovery include Pc sulphonic dyes, Pc sulphonic chlorides, other water soluble Pc dyes, quaternary and

ternary ammonium salts of pyridyle derivatives of Pc, solvent-soluble dyes, azo dyes, vat dyes, leuco dyes, chrome dyes, triazine dyes and various dye precursors. Their main applications have been in writing inks (especially for ball point pens), colourants for paints, plastics, printing inks, and textiles, as well as for use in roofing granules, leather, petrol, oil, photographic colour prints and even food colouring. In recent years the photoconducting properties of certain morphological forms of phthalocyanine have been exploited in copying machines.

Phthalocyanine was first obtained in 1907 by Braun and Tcherniac (3) as a by-product of the preparation of o-cyanobenzamide from phthalamide and acetic anhydride. Diesbach and von der Wied (4) in 1927 obtained copper phthalocyanine by the reaction of o-dibromobenzene and copper cyanide in pyridene. The schematic representation of both these reactions is shown, fig. (2.1). A review of the commercial methods of manufacture for metal-free and copper phthalocyanine is given in the second volume of "The phthalocyanines" by CRC press (5).

This chapter seeks to provide: (a) a discussion of the structure and morphological forms of the metal-free, metal containing and substituted phthalocyanines, (b) a review of the preparation techniques used for phthalocyanine materials and the fabrication of devices, covering the preparation of single crystals, evaporated thin films and resin binder type layers and (c) a report of the physical properties of phthalocyanines

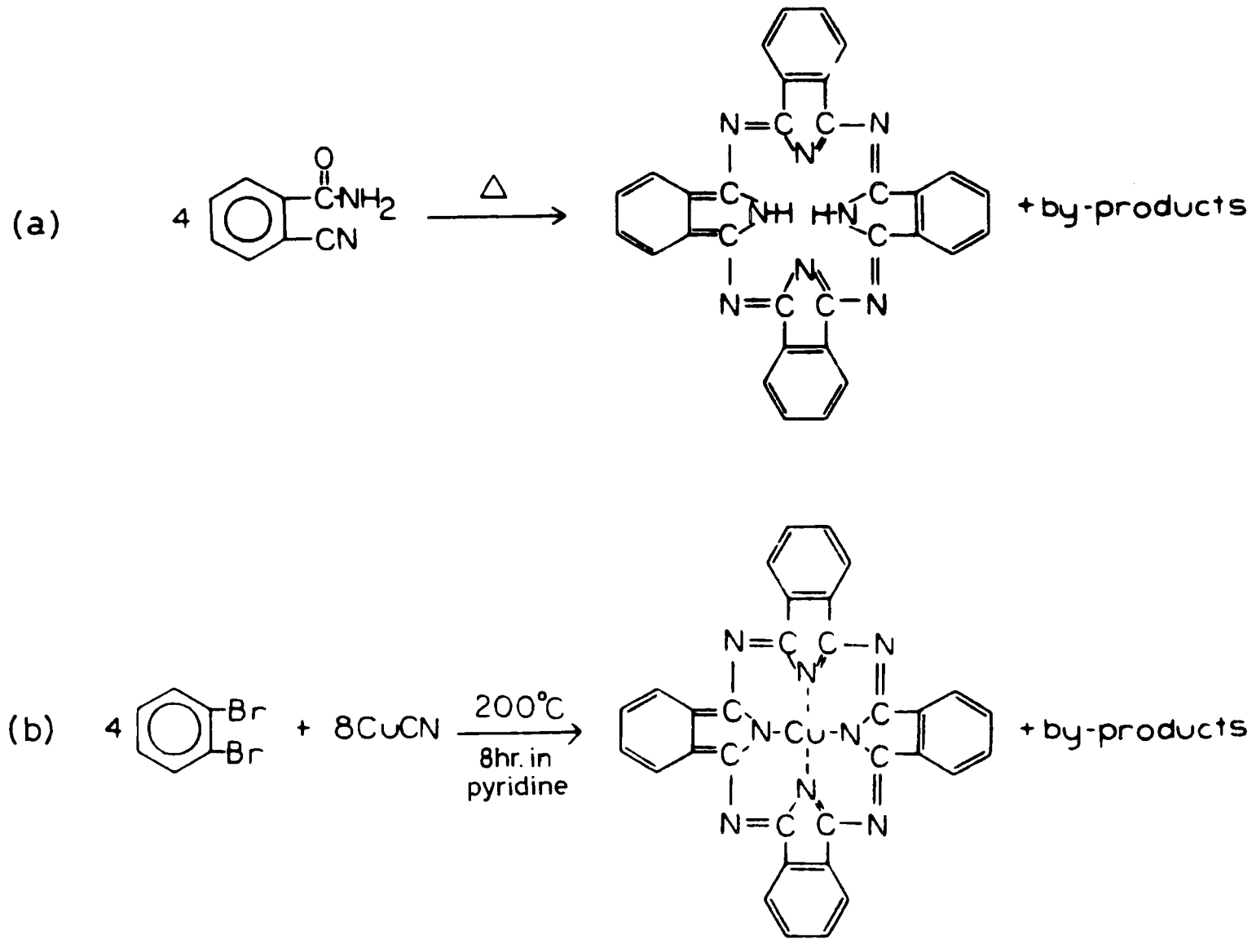

Figure 1. A schematic diagram showing the synthetic roots to phthalocyanine originally used by a) Braun and Tcherniac, b) de Diesbach and Von der Wied.

indicating their optical and electrical characteristics. This is then followed by a section covering the effect of various gas ambients on the above properties.

2.1 STRUCTURE OF PHTHALOCYANINE

One of the features of the material which accounted for the initial interest, is that the phthalocyanines and their metal derivatives form a beautifully crystalline series of compounds which, with the exception of the platinum derivative, are closely isomorphous. This made the series of compounds an ideal subject of study for the development of the isomorphous replacement and heavy atom methods of structure determination. Thus the phthalocyanines hold a place of great historical interest in the field of crystal and molecular structure determination. It was in fact the phthalocyanine molecule which was the first to yield an absolutely direct X-ray analysis which did not involve any assumptions, not even with regard to the existence of discrete atoms in the molecule. This work was reported by Robertson (6-10) in a series of classic papers.

2.1.1 Molecular structure

Metal-free phthalocyanine (or, as it is commonly termed, phthalocyanine) and its metal derivatives are quite closely linked to the naturally occurring porphyrins. The molecular structure of metal free phthalocyanine is shown in fig(2.2). As can be seen, the molecule contains a ring system of four

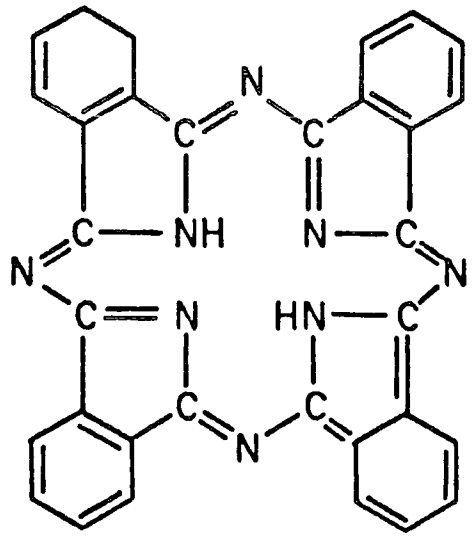

(A)

Figure 2. The molecular structure of phthalocyanine.

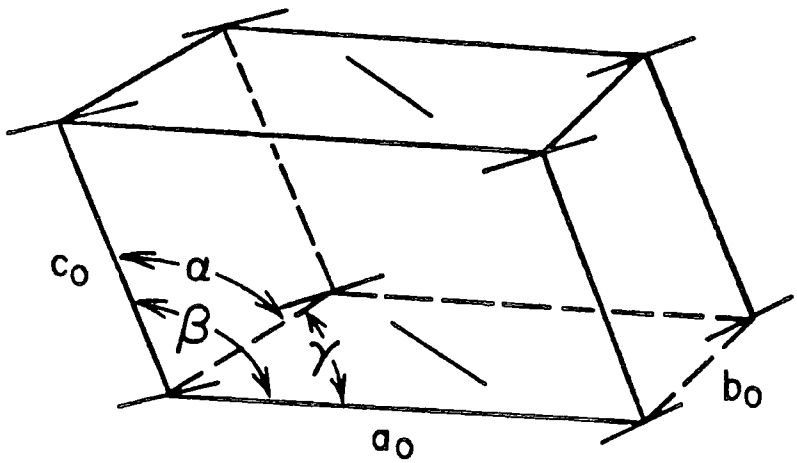

$\alpha = \gamma = 90°$

$\beta = 122°12'$

$a_0 = 19.85\,\text{Å}$

$b_0 = 4.72\,\text{Å}$

$c_0 = 14.8\,\text{Å}$

(B)

Figure 3. The unit cell of metal-free phthalocyanine, with cell parameters and positions of molecules indicated.

isoindole units linked by aza nitrogen atoms. Figure (2.3) shows a unit cell of the metal-free β-phthalocyanine, which indicates the cell parameters and the positions of the molecules. A structure determination of this compound and its metal derivatives was carried out by Linstead (11) in 1936.

2.1.2 Polymorphic forms

The phthalocyanines have been found to exist in at least two polymorphic forms, the α- and β-phases. Karasek and Decius (12) noted that the α-phase is obtained if the material is sublimed at pressures less than 50 Torr and the substrate temperature held at around room temperature. At higher sublimation pressures the β-phase is obtained. Fustoss-Wegner observed that this phase change occurred near 200° C and was irreversible (13). It is also possible to effect the change from the α- to the β-phase by grinding.

The β-form can be obtained as well-grown single crystals to which X-ray structure analysis can be applied, but the α-form exists in the form of very fine powder or vacuum-deposited film and the structure has not been fully analysed. (Platinum phthalocyanine is exceptional because it exists normally as the stable α-form in a single crystal.) The structure of the α-form of other phthalocyanine derivatives has been assumed to be isomorphic with the α-form of platinum phthalocyanine. However, this assumption is based only on the interplanar spacings of the fine crystals determined from a few diffuse lines in X-ray or

electron diffraction patterns. The remarkable development recently of high-resolution electron microscopy, both in the instrumental capability and in the observation technique, makes it possible to examine the structure of fine crystals through the direct observation of molecular images (14). This method is now widely recognized to be powerful, especially when the molecular structure is well known and only the packing or the arrangement of the molecules is in question. The method has been used to examine the polymorphs of ZnPc evaporated thin films (15) and shows that the film is not simply an α-form which is isomorphous with PtPc, but is composed of various polymorphs of the α-form.

In 1967 the observation of a novel crystalline form of metal-free phthalocyanine was described (16,17). This new crystal form was described as the X-phase and was prepared by extended milling of the α- or β-phases. This form, described as being "especially useful as a photoconductive material in electrophotography", can also be used to prepare polymers and is useful as a pigment in inks, paints and varnishes. It is reported by Sharp et al that a spectroscopic characterisation of the X-H_2Pc (18) and the X-CuPc (19) has been carried out and that the electronic spectra observed can be interpreted in terms of a dimer structure.

2.2 PREPARATION OF SINGLE CRYSTAL, EVAPORATED THIN FILMS AND RESIN BINDER TYPE LAYERS.

Interest in the use of phthalocyanine dyes and pigments as colourants and organic semiconductors has led to extensive work being carried out on methods for producing the material in different forms. The three common preparative techniques are now discussed in turn.

2.2.1 Preparation of single crystals of phthalocyanine.

Most investigations into the conduction properties of phthalocyanines have been carried out on single crystals. These crystals can be prepared from various organic solvents (20). However, growth of crystals in an inert gas from the vapour phase appears to be more successful than growth from solvents such as quinoline, α-chloronaphthalene, or sulphuric acid. It has been shown (21) that crystals grown from organic solvents are far from being perfect, evidently because it is difficult to control the nucleation. Investigations have shown that traces of the solvent are built in as part of the complexes, their presence contributing to large variations in electrical properties. Hence, the most common method of preparation is the entrainer sublimation method as described by Van Ewyk(22) and Fielding(23). In this method powdered phthalocyanine is placed in a ceramic boat which in turn is placed in a pyrex tube in a stream of oxygen-free nitrogen. Two temperature zones are

formed by the use of heating coils. The phthalocyanine powder sublimes from the boat which is positioned in the hot zone and is carried down the tube by the nitrogen stream where it condenses in the cooler zone. The crystals produced by this method are invariably long needle like crystals of a monoclinic structure. However, modification of the monoclinic structure has been observed due to the influence of a substrate. For example a transformation from the monoclinic to triclinic structure is observed when the film is deposited on muscovite surface (24).

2.2.2 Preparation of evaporated phthalocyanine films.

Although most fundamental characterisation work is carried out on single crystals of phthalocyanine, sublimation of the phthalocyanines seems to be the most common method used in the preparation of devices. In the vacuum deposition of the phthalocyanines it is common to use either a baffled source -such as the Mathis SO20- or a heated glass wool plugged column. This effectively prevents ejection of material from the source. A typical background pressure of 10^{-6} Torr would be used to carry out the deposition.

It has been demonstrated by Vincett et al (25) that control of the substrate temperature is important in optimizing the thin film properties. They describe a critical temperature T_c at which large differences are observed in crystallite orientation and size compared with those of films condensed at other

temperatures. The critical temperature is found to be closely related to the normal boiling point T_b of the material. (The relationship found being: $T_c / T_b = 1/3$) For phthalocyanine the critical temperature is approximately 12° C. This temperature is extremely reproducible for a given deposition rate, even in vacuum systems with different background pressures and for differing substrates, evaporation sources and film thicknesses.

2.2.3 Resin binder type layers incorporating phthalocyanine

Many methods of incorporating phthalocyanine dyes and pigments in resins and plastics have been investigated. One of the simplest methods of forming these layers is described by Loutfy and Hsiao (26). In their work the pigment (a substituted phthalocyanine, 52% of solid by weight) is suspended in a homogeneous solution of the dye (14%) and a polycarbonate, (34%). Organic films are then prepared by coating the substrate with the suspension. After the solvent has evaporated, a thin (0.8μm) uniform film of the pigment dispersed in the polymer is obtained. Other methods include the formation of polymer supported phthalocyanines. For example, various soluble metal-phthalocyanine derivatives can be incorporated into polymer chains, such as polyimides (27), polystyrene (28) and poly(2-vinylpyridine-co-styrene) (29). The method for depositing these films is quite simple, though many purification procedures must be carried out on the materials used. Hirabaru et al (30), in reporting on the deposition of these films, have

described the method simply as dipping the clean substrate into methanol containing 5% of the metal co-polymer and then drying it in air at 40° C for 40 minutes. The main interest in these poly-phthalocyanines is in their use as catalysts. For example, the iron(III) derivative is a remarkably effective catalyst for H_2O_2 decomposition (29).

A further interesting method is reported by Kovacs (31), whereby surface particulate monolayers are formed when appropriately deposited onto softenable organic polymer substrates. In this method the material is dispersed by vacuum evaporation onto a heated co-polymer. In addition to vacuum evaporation, and in particular for phthalocyanines, the material is finely dispersed in a liquid (eg methanol) which is a non-solvent for the polymer substrate. The dispersion is then coated as a thin liquid film by a gravure coating technique. After the liquid evaporates, a thin powder film is left which can easily be wiped off, and is clearly therefore above the substrate surface. If the substrate is now softened by heating, the dispersed particles become partially embedded. Complete embedding of the particles is achieved by exposure to a vapour which is a solvent for the polymer, enabling such embedded organic particulate structures to be applied in electrophotographic films.

2.3 GENERAL PROPERTIES OF PHTHALOCYANINE

2.3.1 Physical

The phthalocyanines are insoluble in water and virtually insoluble in most organic solvents. The best solvents for phthalocyanines are α-chloronaphthalene and tetrahydrofuran and even then they are only sparingly soluble. They are resistant to attack by weak mineral acids and alkalis and are also stable with respect to water vapour and many common gases in the absence of light. The phthalocyanines exhibit a very high involatility; films can be left for a year in air without displaying deterioration. They are also stable with regard to heat and light; the copper compound, for example, sublimes at 853K without decomposition (32). The colouristic properties of the phthalocyanines are known to vary with the particle size and shape. For example it has been shown that for copper phthalocyanine the intensity of visible light reflected from the pigment decreases when the size of the pigment particles is decreased by grinding (33). Also, measurements on oriented pigment crystals in films show that the transmission colour is reddish blue in the direction of the acicular axis of β-copper phthalocyanine and is greenish blue at right angles to the axis (34).

There is a tendency for phthalocyanines to form agglomerates during handling, storage and on mixing with plastics. Some studies (35) have been carried out on correlating the strength and other properties of agglomerates

formed with an instrumented tabletting machine. The ease of pigment agglomeration and the strength of the agglomerate are the major causes of difficulties encountered during dispersion in plastics.

The phthalocyanines lend themselves well to structure determinations carried out with X-rays, many comprehensive investigations having been carried out and presented for a variety of phthalocyanines. Because the structure of many phthalocyanines has been determined, this class of compounds is ideal for electron microscope studies. Direct electron microscopic observations of the copper phthalocyanine lattice show that the β-form consists of well ordered crystals, while the α-form shows many distorted spacings (36). As mentioned in section 2.1.1, molecular images of various phthalocyanines have been observed through the use of thin films and transmission electron microscopy. An interesting addition to these (37) comes out of the use of the field ion microscope, invented by Mueller, which makes visualisation of individual atoms in the surface of a metal tip possible, with a resolution approaching 2Å. A shadow outline of copper phthalocyanine is formed by surrounding the molecules with an ordered layer of evaporated platinum. The image observed is of the edge of the cavity formed in the platinum by the molecule. The success of this technique is due to the relatively high degree of atomic order in platinum layers deposited by vacuum evaporation on irridium tips at temperatures less than 130° C. Without some degree of order the resolution is greatly reduced.

2.3.2 Optical

The combination of the phthalocyanine molecule's stability, insolubility in most solvents and very high optical absorbance (phthalocyanines have an absorption coefficient of approximately 10^5) has led to its substantial use in the dye industry. Consequently there exists a wealth of information on its optical properties. A comprehensive review of the literature is given in "The Phthalocyanines" by CRC press (38). Phthalocyanines belong to the general category of materials described under the heading of the organic state. The bonding in these systems is weak and is ascribed to Van der Waals forces between molecules of the lattice. As a result, the absorption of light by an organic solid is molecular in nature and can be simply represented by the discrete transition between the ground and excited electronic states of the free molecule. Since electron exchange is weak, electron-phonon interactions dominate and vibrational structure is observed to accompany the electronic transition.

This is in marked contrast to classical inorganic semiconductors which are normally characterised by strong covalent or ionic bonding between atoms of the lattice. Strong bonding of this kind results in the formation of bands, rather than discrete atomic energy levels, which are associated with the entire crystal. Hence the absorption of light normally involves the transition of an electron from the valence band to the conduction band. The electron and the resulting hole in the

valence band are then free to move through the crystal. Since electron exchange is much stronger than electron-phonon interactions, no vibrational structure is observed and the latter can be treated as a perturbation which results in occasional scattering of the carrier as it moves through the crystal lattice. A comparison of the idealized electronic transitions occurring in the organic and inorganic solid state is shown in fig. (2.4)

The general absorption properties of the organic solid state as described above are exhibited by phthalocyanine. Optical absorption spectra are reported which cover vacuum deposited films, single crystals, solutions and the vapour state (for example references 39 and 40). Figure (2.5) shows the absorption spectra for single crystals, evaporated films and a solution of metal-free phthalocyanine. Only qualitative similarity is indicated since the ordinate scales for the three curves are different. The solution spectrum is characteristic of the free molecule, and the observed peaks are due to electronic transitions from the ground singlet, or highest filled state, to excited singlet states. The singlet states, characteristic of the free molecule, are undoubtedly broadened and shifted to lower energies by interaction with the crystal field in the solid. This is observed in both the film and single crystal, and accounts for the similarity which exists in the regions of absorption observed. It is therefore assumed that optical absorption observed in the crystals in the region below 800nm is due to electronic transitions from the ground

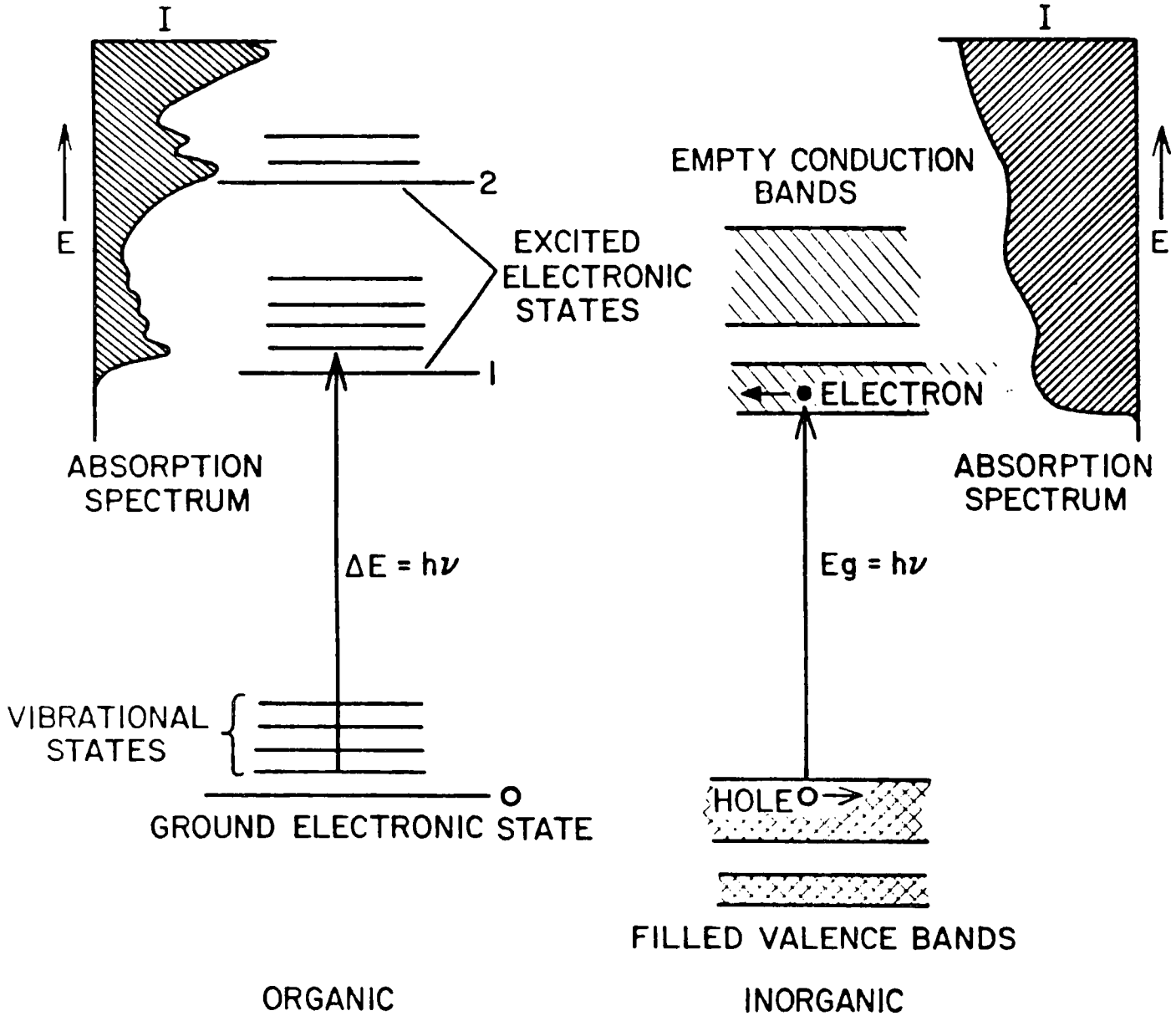

Figure 4. The idealized electronic transitions occurring in an organic material and an inorganic semiconductor, with the resultant absorption spectrum.

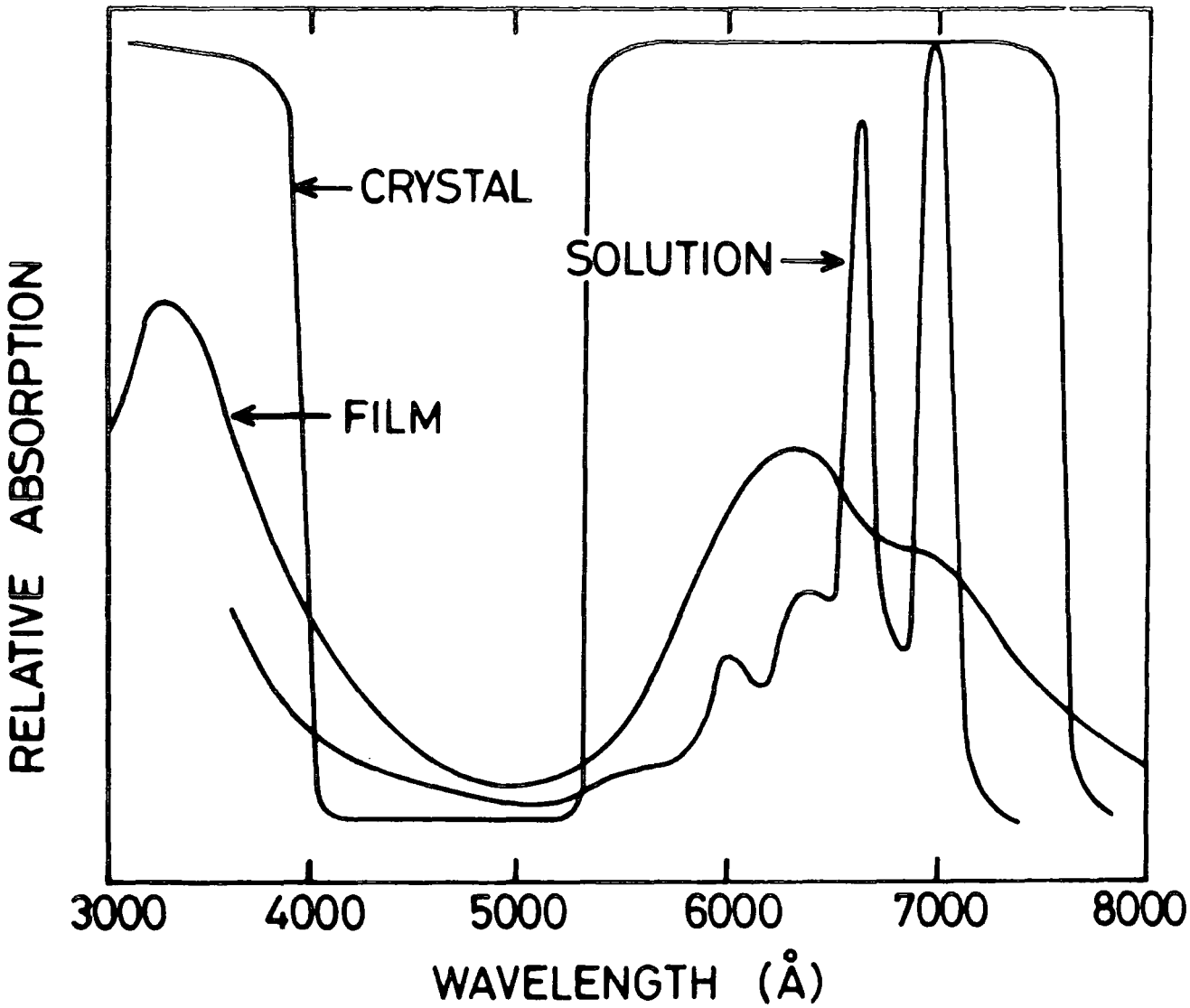

Figure 5. The absorption spectra of metal-free phthalocyanine single crystal, evaporated film, and solution in 1-chloronapthalene (film and solution spectra by Assour, crystal spectra by Heilmeir).

state to the broadened, shifted, and slightly overlapping, excited singlets of the metal-free phthalocyanine molecule. However, it is important to note that the optical absorption spectrum of the crystal retains much of the character of the free molecule. This indicates relatively weak interaction between molecules in the crystal lattice as one might expect from the relatively weak intermolecular bonding (40) due to Van der Waals forces. Much work has been carried out to investigate the effect on the spectra of various ligands (for example reference 41). Here the absorption spectrum of phthalocyanine in sulphuric acid was found to be characterized by a band which was displaced differently by various π-metal ligands.

Many phthalocyanines have been found to exhibit either fluorescence, phosphorescence or both. Fluorescence can be defined as the process of passing between states of the same multiplicity with the emission of light. In almost all cases fluorescence occurs from the lowest excited level of a given multiplicity. Phosphorescence can be generally defined as the process of passing between states of different multiplicity with the emission of light. More specifically, however, phosphorescence is defined as the radiative transition between the lowest triplet state and the ground state of the molecule. The corresponding absorption process is strongly forbidden and hence the natural lifetime of phosphorescence emission is much greater than that for fluorescence emission and usually varies from 10^{-3} s to several seconds. Zinc phthalocyanine is a well documented example of a phthalocyanine which exhibits both (42).

The fluorescence spectra of the three polymorphs of metal-free phthalocyanine are shown in Fig. (2.6). As can be seen the spectrum is not highly structured -this is due in part to the fact that the specimen consists of polycrystals with different orientations. An interesting feature in all the fluorescence spectra shown is the peak at about 900 nm. Menzel and Jordan (43) have interpreted the fluorescence in terms of a two level scheme. Two distinct fluorescing sites are proposed, where the 900nm band is attributed to an excimer state, and the 800nm band is assigned to molecular fluorescence.

2.3.3 Electrical

There have been a number of reports of the electrical properties of phthalocyanines. Most research has been carried out on metal-free phthalocyanine and its copper derivative. Defects are of paramount importance in determining the conduction properties of molecular materials, as is the level of purity. Stress has been laid on the purification procedures for trace metals, and for organic impurities which may form charge complexes with the phthalocyanines and result in enhanced conductivity above that for the pure compounds (44).

In general the metal phthalocyanines have a higher electrical conductivity than the metal-free phthalocyanines. In the case of copper phthalocyanine this can be attributed to increased π-orbital delocalisation owing to the inclusion of the central metal atom. The increase in delocalisation leads to

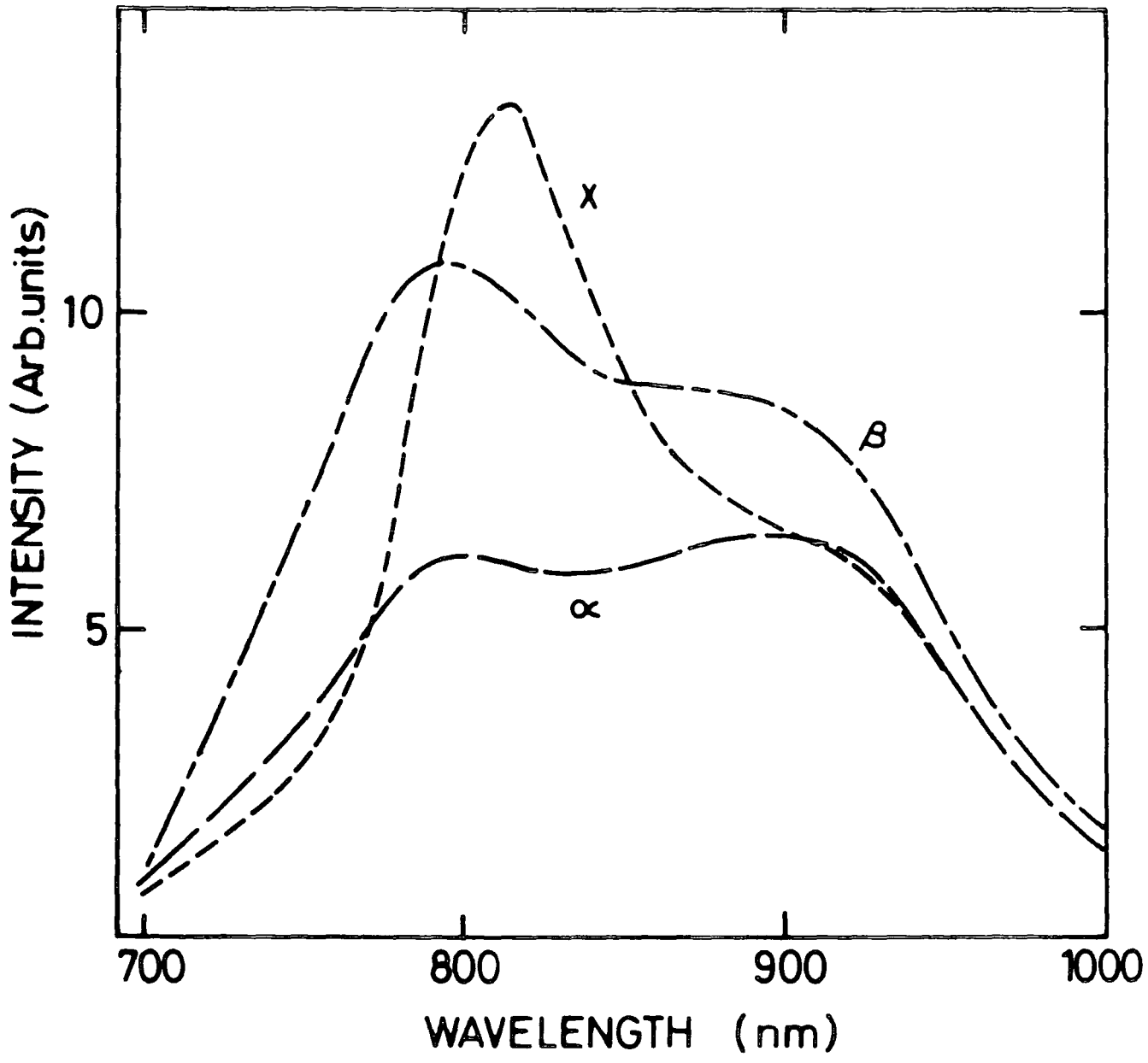

Figure 6. The fluorescence spectra of compressed pellets of α-, β-, and X-metal-free phthalocyanine; (after Menzel and Jordon 1978).

larger intermolecular wavefunction overlap and thus a greater mobility for charge carriers (45).

The dependence of the conduction on the crystal phase of phthalocyanines has also been investigated (46), the α-phase being found to have the lower resistivity. However there is some conflict in the literature, some authors believing that the crystal phase transformation from α to β (and vice versa) has no influence on conductivity (47). The source of the apparently higher conductivity of the α-phase is attributed to the stronger propensity for oxygen absorption in this phase.

Studies of the dc bulk conductivity in a single crystal can yield much information about the electronic traps in a solid. However, with molecular crystals there are many difficulties, in the main associated with the problem of making good ohmic contact to the material. In the absence of ohmic contacts, dc measurements are plagued by polarisation effects.

Kleitman et al have described (48) the current voltage characteristic for crystals of metal free phthalocyanine. They found an ohmic region for electric fields up to 10^3 V/cm. Heilmeir and Warfield extended these measurements and reported (49) similar ohmic behavior up to 10^4 V/cm, and a square-law dependence thereafter. Interpreting the high field results in terms of space-charge-limited-currents (SCLC), they calculated trap densities of 10^{12} -10^{14} /cm^3, by means of an activation energy analysis. These investigations were taken further by Sussman (50,51) who performed measurements of SCLC on evaporated films of copper phthalocyanine. In this work, which comprised a

complete study of current as a function of voltage, temperature, thickness and illumination, he obtained results consistent with the assumption of a trap distribution that decreases exponentially with energy as the distance from the valence band edge increases. Some systematic correlation was also found between annealing and parameters governing the trap distribution.

In a further study of the ohmic and space-charge-limited regions, Barbe and Westgate (52,53) carried out careful conductivity measurements on β-metal-free phthalocyanine. Using a vacuum ambient of 5×10^{-9} Torr they established the thickness and voltage dependences for both the ohmic and non-ohmic current regions, and thus provided direct proof that the square law region relates to a space charge limited current. Figure (2.7) shows the dependences of the ohmic current density and the SCL current density on crystal thickness. Figure (2.8) shows that the SCLC has an activation energy of 0.38 eV over the complete range of thermal measurements, while the activation energy for ohmic conduction takes the values 0.38eV below 90° C and 1.05 eV above 90° C. The temperature dependence of both the ohmic and SCLC can be explained fairly precisely by a model based on a level 0.38 eV below the conduction band edge having $10^{19} - 10^{20}$ /cm^3 trapping centres and $10^{12} - 10^{13}$ /cm^3 donors.

In a comprehensive report on charge transport in nickel phthalocyanine crystals carried out by Cox and Abdel-Malik (54) the conduction is again found to fall into ohmic and space-charge-limited regions. From measurements of the

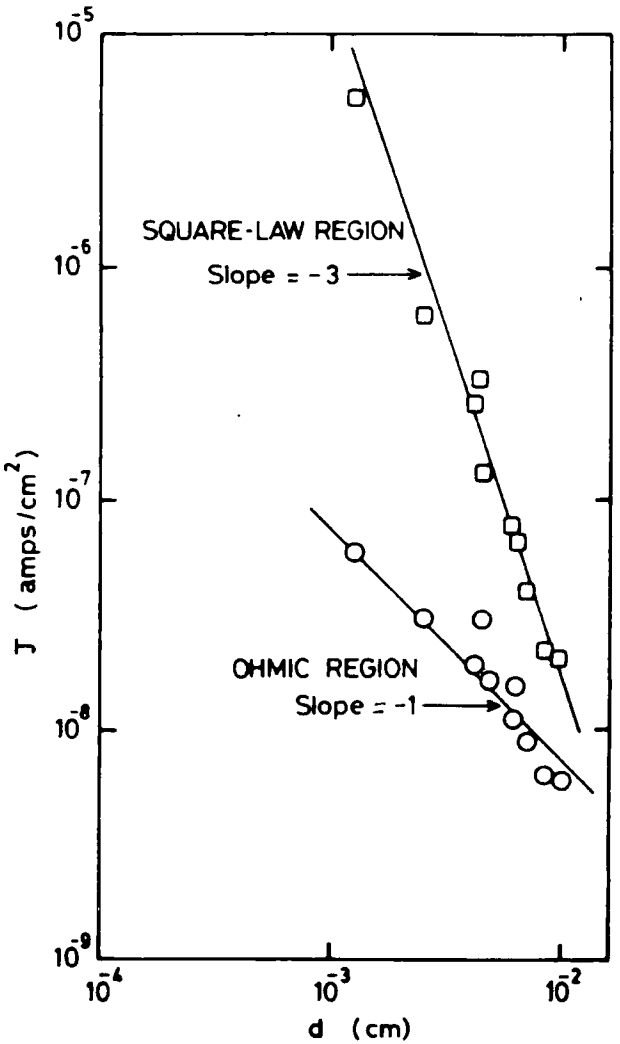

Figure 7.

Current density versus crystal thickness for the Ohmic region at 100V (o) and for the square-law region at 400V (□) (after Barbe and Westgate).

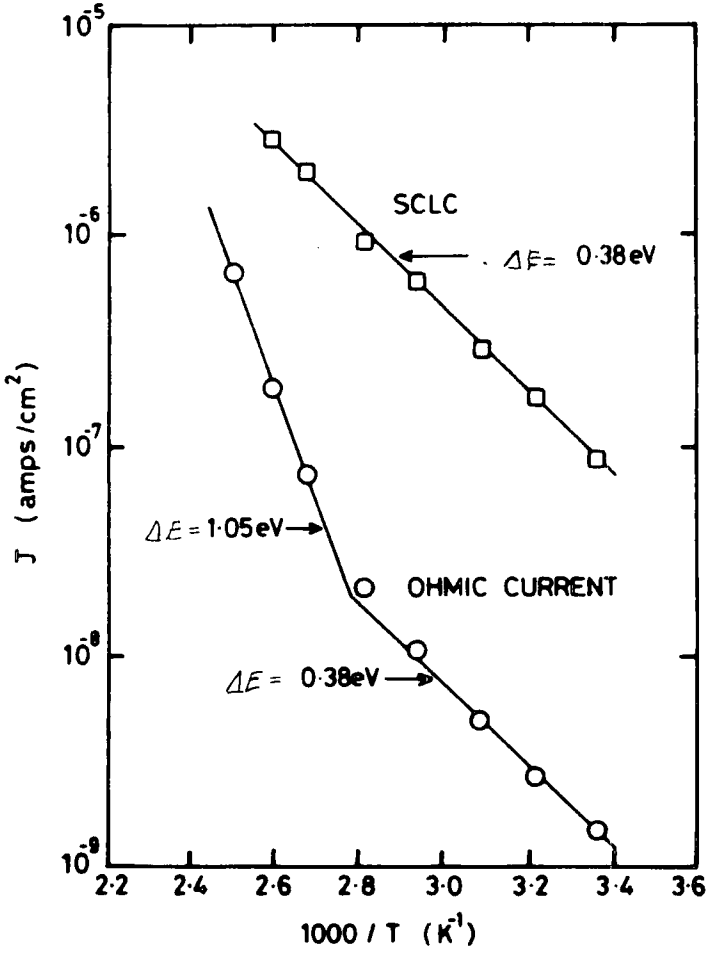

Figure 8.

Current density versus reciprocal temperature for the Ohmic region at 10V (o) and the space-charge-limited region at 4000V (□) (after Barbe and Westgate).

temperature dependence of the ohmic and space-charge-limited (SCL) bulk currents flowing in the c′ direction, these authors located the statistically important energy levels and their state densities in this molecular solid. The activation energies obtained for the ohmic and SCL regions indicated the presence of a discrete electron level 0.43 eV below the conduction band, with a state density of 5×10^{19} cm^{-3}, and a hole level 0.64 eV above the valence band having a state density of 3×10^{12} cm^{-3}. The thermal band gap is 1.63 eV. Further to this work an investigation of the Seebeck effect in NiPc revealed that the conduction was n-type over the temperature range 325-425 K, the excess donor concentration being 8×10^{11} cm^{-3}.

Interest has also been shown in lead phthalocyanine as it is considered to be a one-dimensional conductor (55). This is because in crystalline lead phthalocyanine, the molecules are stacked linearly in the direction of the c-axis and the interatomic distance between lead atoms within a molecular column is only slightly larger than that in lead metal.

Investigations concerning the fundamental process of conduction, including an evaluation of the drift mobility of the charge carriers, have also been carried out. Cox (56,57) measured the electron and hole drift mobilities at temperatures between 290 to 600K along the c-direction of metal-free phthalocyanine by means of a pulsed-laser technique to excite carriers. Carrier mobilities at 373K were found to be 1.4 $cm^2/V.s$ for electrons and 1.1 $cm^2/V.s$ for holes, the mobility at a given temperature being obtained from a plot of reciprocal

transit time versus field strength . He found that the mobilities for both carrier types decreased with increasing temperature, fitting a mobility-temperature relation of the form $\mu=AT^{n}$. Typical values for the parameter n for electrons and holes were found to be 1.5 and 1.3, respectively. These are consistent with an interpretation in terms of energy band theory, where the mobilities of both carrier types is controlled essentially by lattice phonon scattering.

Similarly, Aoyagi reports (58) that in copper phthalocyanine the drift mobility for holes is about 0.35 $cm^2/V.s$ and the drift mobility for electrons is somewhat below this. He reports that extrapolated values of mobility at the graphical position corresponding to 1/T=0 are about 17-43 $cm^2/V.s$. i.e. much larger than the corresponding drift mobility measurement for metal-free phthalocyanine. This result suggests that the metal ion in phthalocyanine enhances the probability of charge transfer from molecule to molecule.

Mizuguchi has reported (59) on the fast photoconduction decays in evaporated thick films of β-copper phthalocyanine. The decay curves consist of two regions, as shown by the log-linear plot of photocurrent versus time in fig (2.9). One of these components is quite fast, being 1-2μs over the near ultra-violet to near infra-red region. The other component is slightly slower and has an approximate value of 3-4μs. For the samples studied, he also observed the photoconductivity to increase as the decay times became longer. These results were speculatively interpreted as being due to traps linked with

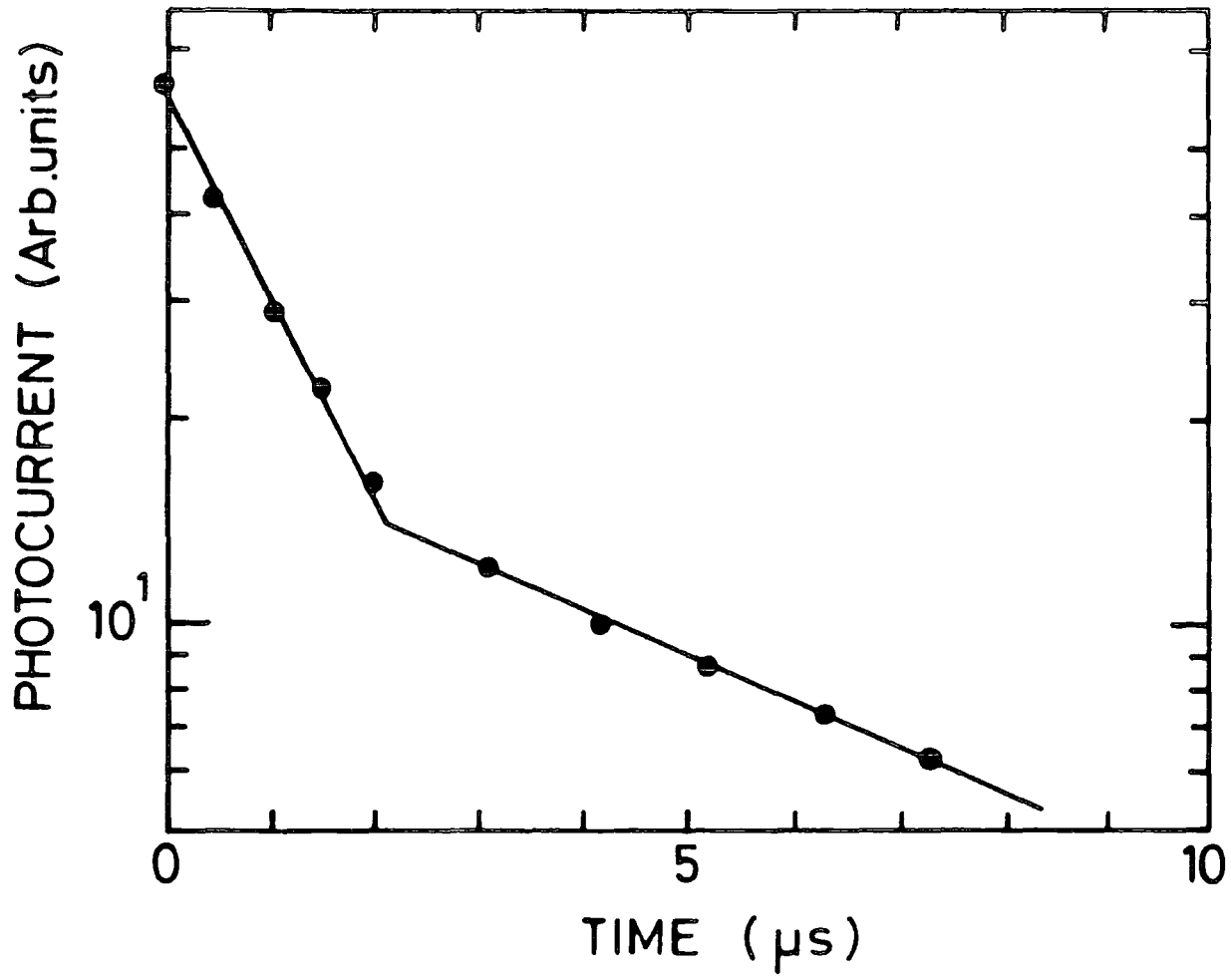

Figure 9. A log-linear plot of the transient behaviour of photocurrent versus time (after Mizuguchi).

either imperfections in the crystal, inclusion of absorbed oxygen in the bulk during the evaporation of the phthalocyanine, or diffusion of oxygen from the surface to the bulk. Further work by Mizuguchi showing how ambient atmospheres influence the photosensitivity and response time are referred to in the next section of this chapter.

Interest is developing in the use of thin organic films in the areas of photoconduction and photovoltaics. Photovoltaic conversion can be achieved by a number of materials with different efficiencies, but no particular material or combination of materials provides, as yet, a cheap enough system to compete with the cost of large scale, fossil-fuel-generated electricity. While intensive research is being carried out to reduce the cost of conventional inorganic devices, there is considerable interest in organic thin-film devices, because of the intrinsically low energy cost involved. There are three major advantages to be gained by the use of organic materials: First, the compounds are highly coloured; absorption coefficients greater than 10^5 cm^{-1} in the visible are observed, sometimes over large wavelength ranges. Second, the semiconductor properties of porphyrin-type molecules are well documented, and third, the conductivity can be altered by suitable doping.

Chamberlain (60) has reviewed the state of the art for organic solar cells and has reported on the use of porphyrin type molecules as the photoactive layer in MIM structures. Although a major problem with organic devices is their

instability at high light intensities, Chamberlain has found that cells incorporating merocyanine and phthalocyanine -as first described by Fan and Faulkener (61)- show long term stability. The main factors contributing to decay of organic cells appear to be a) build up of oxide layers on the barrier metal surface and b) photo and thermal degradation of the dye. Chamberlain has also reported an enhancement of the photocurrent on doping the cell with O_2, H_2O, and especially I_2. The photocurrent was found to increase by several orders of magnitude on exposure to iodine vapour. Further aspects of this work will be discussed along with other reports on the effects of external ambients on the conduction of phthalocyanine in the following section.

The papers considered to mark the main developments in the electrical characterisation are summarised in table 2.1 at the end of this section. As can be seen from table 2.1 there is quite a spread in the values reported for both the conductivities and trap densities. This can be explained by the fact that in organic materials the conduction tends to be dominated by lattice defects which vary according to the method and conditions of preparation.

2.3.4. Gas reactions

The electrical conductivity of the phthalocyanines has been shown to alter in the presence of certain ambients. The bulk of references found in the literature deal mainly with the

Table 2.1 Review of the main papers reporting the electrical properties of phthalocyanine

Author and Reference	Material	Summary of Results	
Heilmeier and Warfield (49)	Single crystal metal-free pc	Conductivity trap density	- 1.9×10^{-13} $\Omega^{-1} cm^{-1}$ - $10^{12} - 10^{14}$ cm^{-3}
Sussman (50)	Evaporated CuPc	Conductivity Fermi Level Trap density Mobility	- 7×10^{-10} Ω^{-1} cm^{-1} - 0.56eV above the valence band - $1 \times 10^{16}/cm^3$ - 0.02 $cm^2/Vsec$
Barbe and Westgate (52, 53)	Single crystal Metal-free pc	Trap density - Trap level Donor concentration	- 5×10^{19} cm^{-3} - 0.38eV below conduction band - 2×10^{12} cm^{-3}
Cox (56, 57)	Single crystal Metal-free pc	Conductivity Trap density Trap level Donor concentration Electron mobility Hole mobility	- 10^{-10}-10^{-14} Ω^{-1} cm^{-1} - 7×10^{16} cm^{-3} - 0.32eV below conduction band - 2×10^{7} cm^{-3} - 1.2 cm^2 V^{-1} s^{-1} - 1.1 cm^2 V^{-1} s^{-1}
Cox (54)	Single crystal β-nickel phthalocyanine	Conductivity Electron trap level Trap density Hole trap level Trap density	- 1×10^{-13} Ω^{-1} m^{-1} - 0.43eV below conduction band - cm^{-1} 5×10^{19} cm^{-3} - 0.64eV above valence band - 3×10^{12} cm^{-3}

following three areas; absorption of oxygen, of halogens, and of the oxides of nitrogen. For example, the electrical conductivity of metal-free and copper phthalocyanine single crystals has been measured in vacuum, nitrogen, and oxygen by Assour (62). His results indicate increased surface conduction due to reversibly adsorbed oxygen. In an extension of their work on characterising the bulk and surface properties of metal-free phthalocyanine crystals, Barbe and Westgate (63) identified two types of electronic states. They reported that there are at least 10^{11} cm^{-2} slow surface states on metal free phthalocyanine crystals and that the time constants of these states depend on the gas ambient. There are also three sets of fast surface states having densities of the order of 10^{10} -10^{11} cm^{-2} within 0.17 eV of mid band gap. The parameters of these states are not affected appreciably by oxygen or hydrogen ambients. Fast surface states are usually attributed to the effect of the termination of the crystal lattice at the surface, and slow states are usually due to foreign atoms adsorbed on the surface.

A study of the surface photovoltage (64) indicates that when oxygen adsorbs onto a nickel phthalocyanine polycrystalline film, one form adsorbs reversibly while the other adsorbs irreversibly and can only be removed by heating the sample to 433K. The latter causes an order of magnitude increase in photovoltage. Mizuguchi has produced a comprehensive series of papers (65-68) covering the effect of oxygen and hydrogen on transient photocurrents and on the thermal quenching and

thermally assisted optical quenching of photocurrents in evaporated thin films of β-copper phthalocyanine. He observed that oxygen and hydrogen respectively produce an increase and a decrease of the dark conductivity. However, he also reports an anomaly in the photoconductivity results in that the efficiency decreased in oxygen and increased in hydrogen, opposite to the effect normally observed. The decrease in photocurrent in oxygen is caused by thermally assisted photodesorption, annihilating holes. The increase in hydrogen is interpreted in terms of an adsorption scheme whereby hydrogen removes electron traps, causing both types of photocarrier to contribute to the photocurrents.

Yamamoto et al (69) have described the use of a palladium/copper phthalocyanine junction for use as a hydrogen sensing element. The effect arises out of the change in Schottky barrier height due to the change in metal work function which occurs due to the ability of palladium to disolve hydrogen. In the case of inorganic semiconductors, metal contacts with covalent semiconductors give barriers almost independent of the electronegativity of the metal. The independence of the barrier height is considered to be due to either the effect of surface states on the semiconductor, or the structural change of the boundaries caused by diffusion of the chemical components across the interface. On the other hand "ionic" semiconductors make Schottky barriers with metals. Thus, metal junctions with copper phthalocyanine can be used as good gas sensor elements.

Curry (70) reported changes in the resistivity of copper phthalocyanine of eleven orders of magnitude on exposure to various halogens. He also established that the resistivity change occurred with no discernable change in the structure as determined by X-ray crystallography. Yamamoto et al reported that the absorption spectra of thin-films are greatly influenced by the halogens (72). Figure (2.10) shows the absorption spectra for undoped and doped copper phthalocyanine and metal-free phthalocyanine films. The long wavelength edges of the first absorption bands around 700-800 nm of both phthalocyanines show a blue shift and are significantly deformed after exposure to iodine. In addition it can be seen that new absorption bands appear at 540nm and 470nm in copper phthalocyanine and metal-free phthalocyanine respectively. These results are due to the formation of a charge transfer complex. The electron transfer in this process produces unoccupied electronic states in the valence band of the phthalocyanine. These unoccupied electronic states, or holes, may possibly play a fundamental role in the observed increase in conductivity.

Chamberlain, in his work on organic solar cells (60), investigated the mechanism of the increased photoresponse of indium /phthalocyanine photocells on exposure to iodine vapour. He postulated a number of mechanisms and by process of elimination found that the iodine forms charge transfer complexes with the phthalocyanine molecules. Under illumination these excited complexes dissociate in the built in field. The

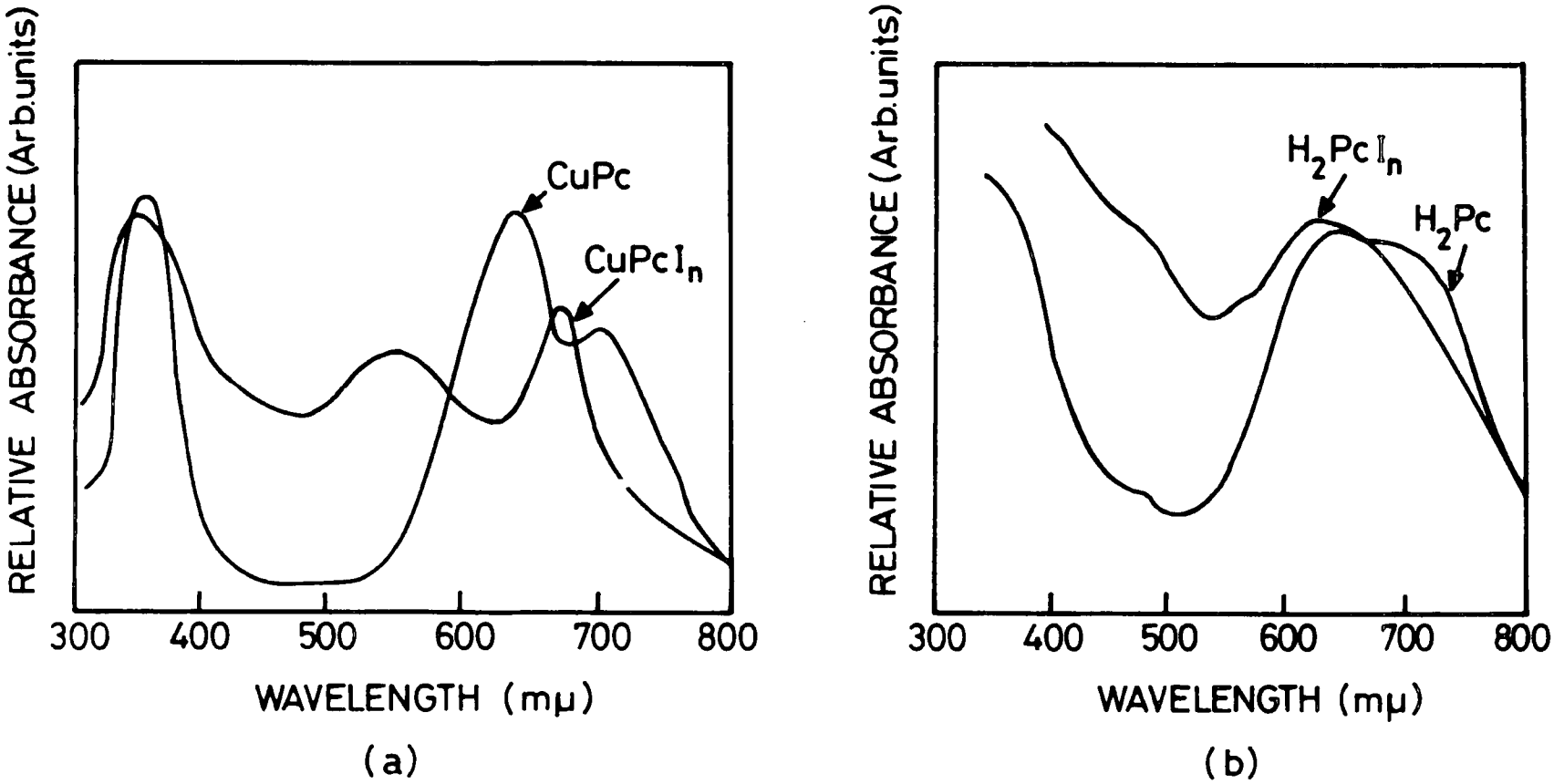

Figure 10. The absorption spectra of a) copper phthalocyanine and b) metal-free phthalocyanine films both undoped and doped with iodine.

electrons and holes so formed constitute a negative and positive space-charge respectively. The photocurrent is then limited by the drift of the space-charge by electron hopping to the electrodes under the influence of the built-in field.

The enhancement of dark d.c. conductivity in a range of thin film organic semiconductors including phthalocyanines, by the oxides of nitrogen is reported by Honeybourne (72,73). The phthalocyanines were found to have a uniquely high conductivity response to electron acceptors, and a unique capacity for the physisorption of NOX. Figure (2.11) shows the effects of NOX on the electronic spectrum of α-phthalocyanine, before and after exposure to the gas, and finally after the film has been heated at 150° C. The spectra indicate the generation of the radical cation, because they are similar to the solution spectrum of the cation of the tetrasulphonate of copper phthalocyanine. The neutral organic species is regenerated on heating. He also reports an increase of six orders of magnitude on exposure to 10 ppm of NOX. However, equilibrium is not reached until 20 minutes have elapsed.

Further work has been carried out in this field by Wright and co-workers. They report (74) on quantitative studies of the magnitude, rate and reversibility of changes in the surface semiconductivity of single crystals of phthalocyanines as a function of ambient gas. NO_2 and N_2O_4 were found to increase the surface conductivity by factors of up to 10^8. At low pressures the magnitude of the increase followed the Freundlich adsorption isotherm, while the rate obeys the Elovich equation.

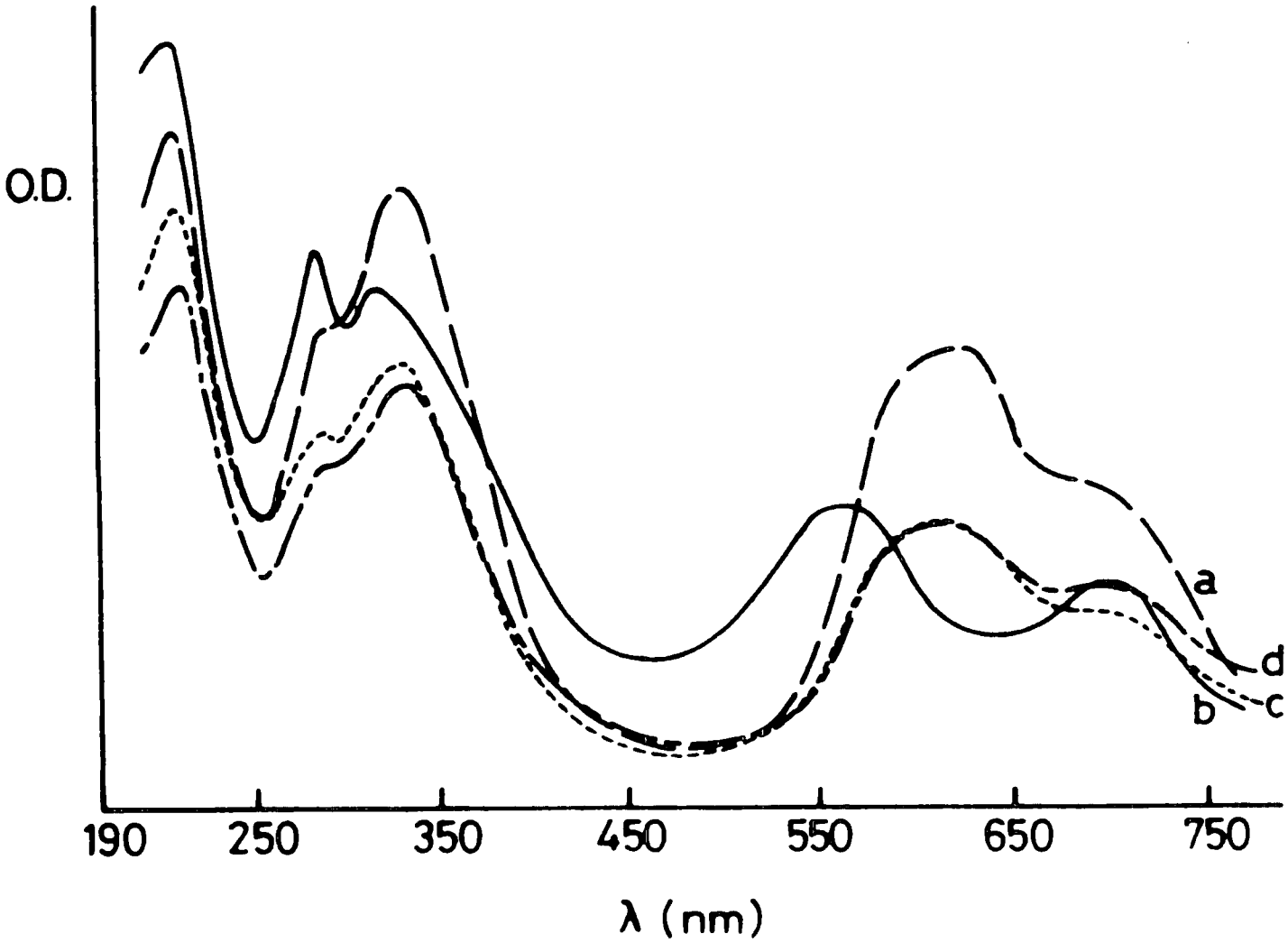

Figure 11. The effects of NOX on the electronic spectrum of a-phthalocyanine: a) before NOX, b) after NOX, c) the film heated to 150° C, d) the film further heated to 200° C (after Honeybourne and Ewen).

The saturation conductivity was found to be similar for all phthalocyanines and corresponds to complete surface coverage, each adsorbed molecule producing one ionised state. However, reversibility of the effect on evacuation, was found to be dependent on the metal substitution. The resistivity of metal-free, nickel, copper and zinc phthalocyanines increased by factors of between 50 and 1000, whereas little change was observed in the resistivities of cobalt, manganese and lead phthalocyanines. The conductivity changes are interpreted in terms of the production of ionised states following weak chemisorption involving donor-acceptor interactions. In a continuation of the above study (75) they have reported on the effects of oxygen, nitrogen dioxide and trifluroborane on the photoconductivity of phthalocyanine single crystals. The photoconduction is found to be enhanced by a factor of 100 and the photoconduction action spectra change to resemble the absorption spectrum, rather than its reverse in vacuo. However, though the photoconductivity is found to be more sensitive to low gas concentrations than dark semiconductivity, it has less potential for gas detection due to the poor reversibility of the effects.

A thesis by J.J.Miasik (76) reports the effect of NO_2 on evaporated films of both zinc and lead phthalocyanine. Figure (2.12) shows a typical result for zinc phthalocyanine. As can be seen, a delay is found before the sample responds to the gas (4ppm NO_2), and the sample takes 15 hours to reach the equilibrium state. After removal of the NO_2 from the gas stream

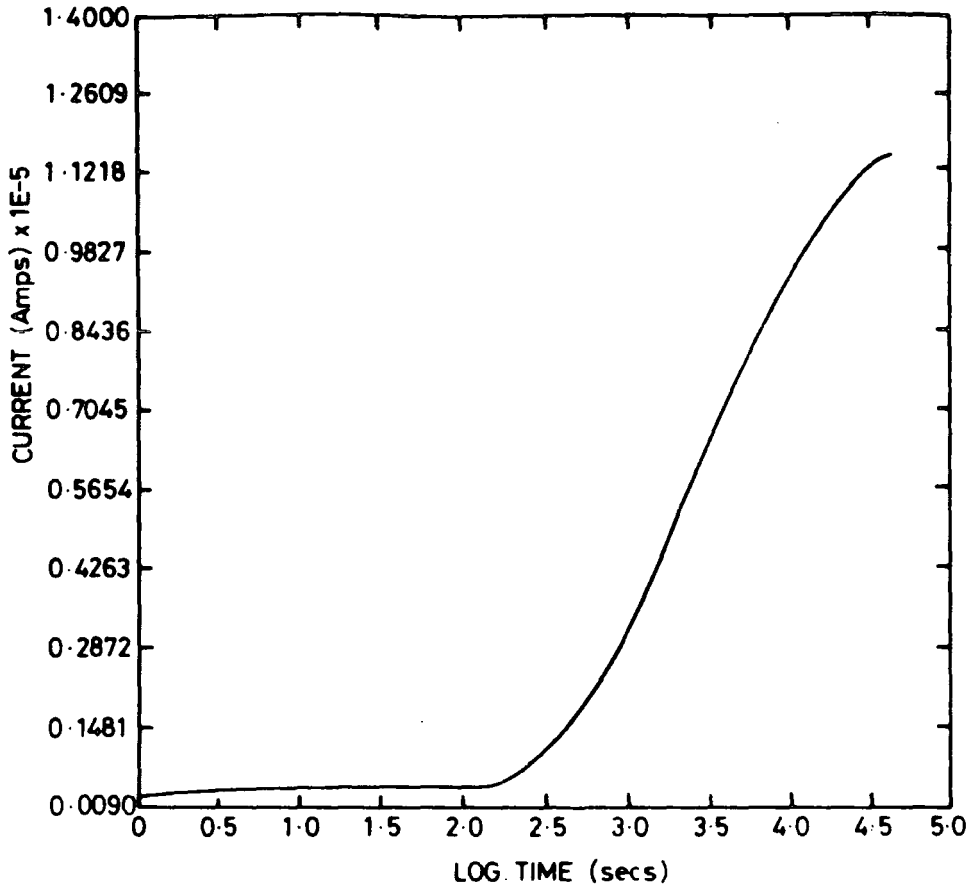

(a)

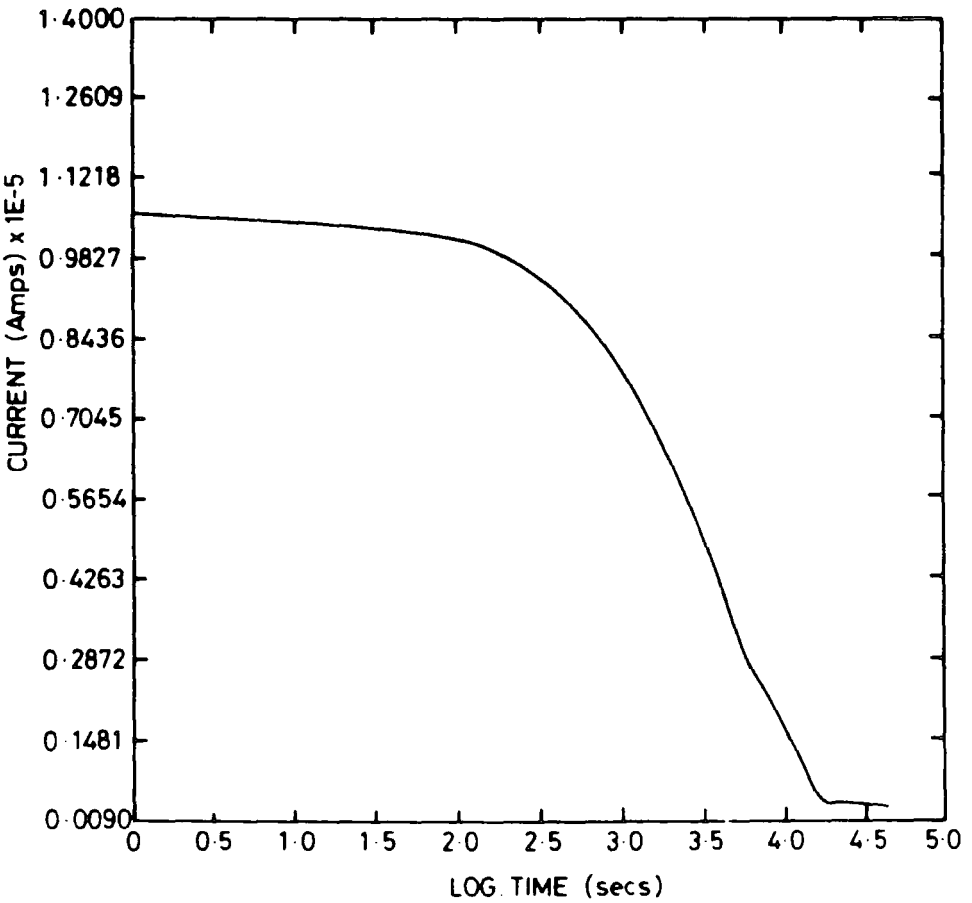

(b)

Figure 12. The response of a zinc phthalocyanine film to a) a 4ppm NO_2 ambient, b) removal of the NO_2 from the gas stream (after Miasik).

the sample takes 5 hours to recover.

This high degree of phthalocyanine sensitivity to NOX has formed the basis of a detector for air-borne NOX contaminants.

A report by Bott describes a device based on lead phthalocyanine (77). The devices were operated at temperatures in the range 100-170° C and results show that the response time of the device fell from 10 minutes at 130° C to 1 minute at 170° C. Figure (2.13) shows the variation of the conductance of the lead phthalocyanine with time, following a step change into 50 ppb NO_2 and return to air. With this device the time taken to reach saturation is six minutes.

A patent by Heiland (78) describes a gas sensor for the detection of the anaesthetic gas halothane. He found the device to have a sensitivity of approx 1ppm to halothane but reports that the device can only detect levels of NO_2 above 10,000ppm. The detector is operated at room temperature and effectively acts as a memory device because after exposure to the gas the conductivity decays from the elevated value very slowly. The authors suggest that the device could be used to monitor the total exposure of a patient to the anaesthetic by an integration of the current versus time plot. Figure (2.14) shows a schematic of the device, a response to exposure to the gas, and the decay of the current level after exposure.

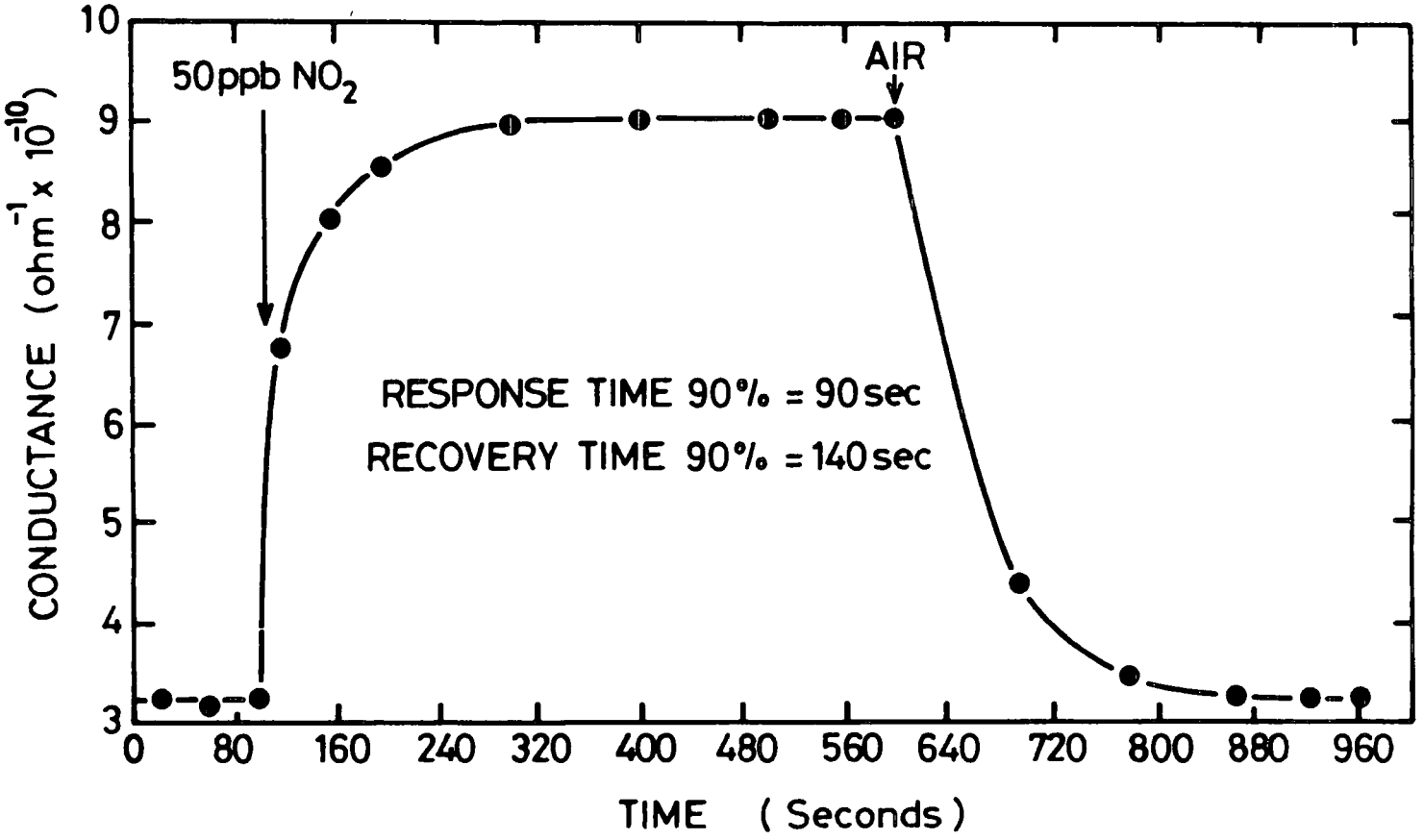

Figure 13. Variation of conductance of lead phthalocyanine film with time following a step change of 50ppb NO_2 and return to air (after Bott).

(a)

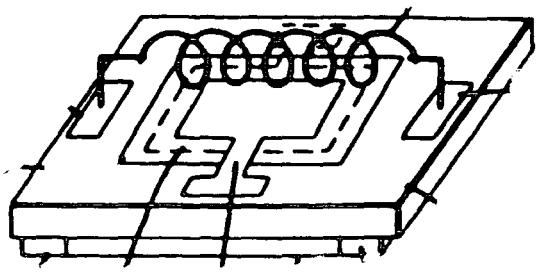

(b)

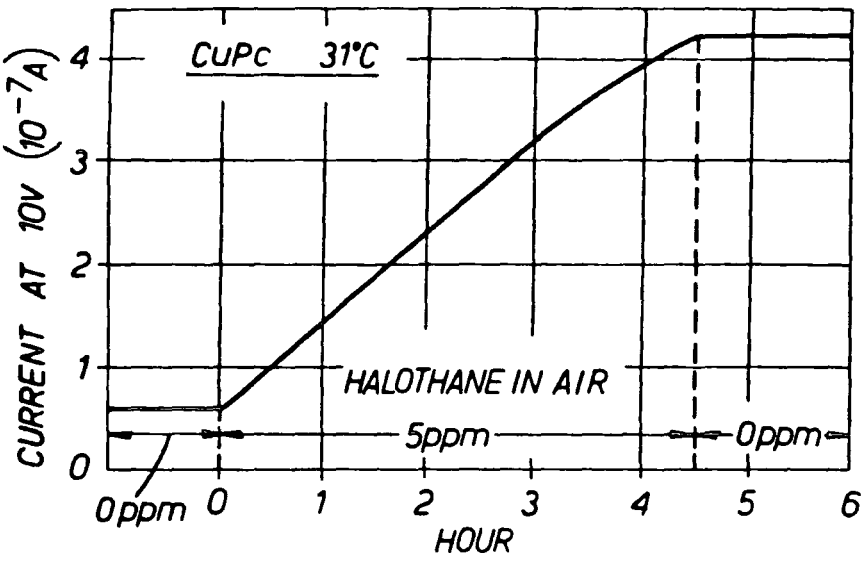

(c)

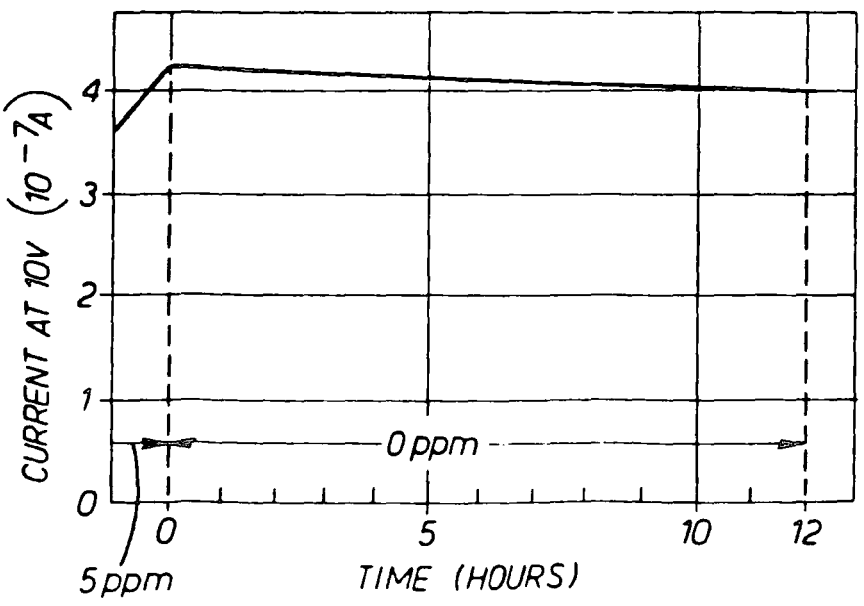

Figure 14. A) schematic diagram of the gas sensor b) the decay of current level after exposure to the gas, c) the decay of current level after removal of the gas ambient (after Luars and Heiland).

CHAPTER 3

LANGMUIR BLODGETT FILMS

3.0 HISTORICAL REVIEW.

Before discussing in detail the equipment for the deposition of Langmuir Blodgett films, it is perhaps useful to look at the historical development of the subject. The earliest reports are attributed to Benjamin Franklin, the versatile American statesman who in 1774, during his frequent visits to Europe, carried out his original experiments on the behaviour of oil on water. His communication (1) to the Royal Society vividly describes his experiments on the spreading of oil on stretches of English waters; he reported as follows:

> "At length being at Clapham where there is, on the common, a large pond, which I observed to be one day very rough with the wind, I fetched out a cruet of oil, and dropped a little of it on the water. I saw it spread itself with surprising swiftness upon the surface...the oil, though not more than a teaspoonful, produced an instant calm over a space several yards square, which spread amazingly and extended itself gradually until it reached the leeside, making all that quarter of the pond, perhaps half an acre, as smooth as a looking glass."

In 1891 Pockels(2) described the first methods for manipulating these films and in 1899 Raleigh(3) proposed that they were only one molecule thick. In 1917 Irvine Langmuir began to develop the theoretical concepts (4) that attempted to explain previous observations. Later, with Katharine Blodgett (5), he devised a process to control and transfer these monolayers onto substrates.

The original trough used by Langmuir and Blodgett in their early work was made of tin, the inside of which was coated with paraffin wax to make the surface hydrophobic. The trough was then filled to the brim with water and a metal control barrier which had also been rendered hydrophobic was used to clean the surface of the water simply by passing it across the surface and forcing all the surfactant material into the unused region behind the control barrier.

The material to be used, dissolved in an appropriate solvent, could then be applied to the surface of the subphase. The spread layer was then compressed using piston oil which was separated from the film by a waxed silk thread, which was fastened to each side of the trough. The piston oil maintained a constant pressure as the substrates were raised and lowered through the film by means of a hand driven winder. This was used because it was "difficult to lift a slide slowly with forceps held in the hand without an occasional backward hitching motion."

A detailed account of these and other fascinating early

studies in surface chemistry, may be found in the excellent series of articles by Giles and Forrester(6). A discussion of some of the developments which have taken place since these early pioneering experiments can be found in the book by Gaines(7). The most comprehensive source relating to present day work in the field can be found in the proceedings of the first international conference on LB films(8). Recent activities are described in the review article by Roberts(9). The modern troughs used today are still based on the principles described above, but are much more sophisticated, both in their mechanical construction and in the instrumentation used to control the procedure. Details of the troughs used in this work are given in the following chapter.

3.1 BASIC CONCEPTS

The basic requirement for the production and study of Langmuir Blodgett films (henceforth called LB films) is an enclosed clean water surface, the area of which is capable of being varied and compressed. Langmuir films (floating monolayers) are produced by applying a solution of an appropriate organic material on the surface where, if the correct choice of solvent has been made, the solution will spread over the surface; the solvent then evaporates leaving behind an evenly spread layer of the solute. The materials most commonly used are of the fatty acid type. These materials have a hydrophobic part and a hydrophilic part. Thus the molecule

tends to align itself with the hydrophilic part in the water and the hydrophobic tail sticking out (see fig. (3.1a)). If the area containing the layer is now decreased, so compressing the layer, the molecules will move together and align themselves in an ordered way. This ordered layer can now be transferred to a substrate which is drawn through the layer. Successive movements though the layer are used to build up multilayers of known thickness (see fig. 3.1b,c and d). Full details of the processes of layer formation and deposition are given later in section 3.4.

The subphase is required to be extremely pure to avoid affecting the properties of the monolayer. To attain this the subphase is subjected to purification procedures before use. Water is normally used as the subphase as it is a readily available polar liquid which has an established technology in methods of purification. The materials used are commonly those of the stearic acid type which are amphipathic, this property being responsible for the alignment of the molecules on the water surface. (However it is possible to use materials which do not fall into this category. The materials reported in this thesis and others such as the merocyanines investigated at the University of Durham, depart from this requirement.) To ensure a consistent film quality it is important to hold the surface pressure constant during deposition. This has been achieved by a variety of means; Langmuir added a tiny drop of oleic acid to the water at one end of the trough. This was separated from the Langmuir film by a floating silk thread. The hydrophobic oil

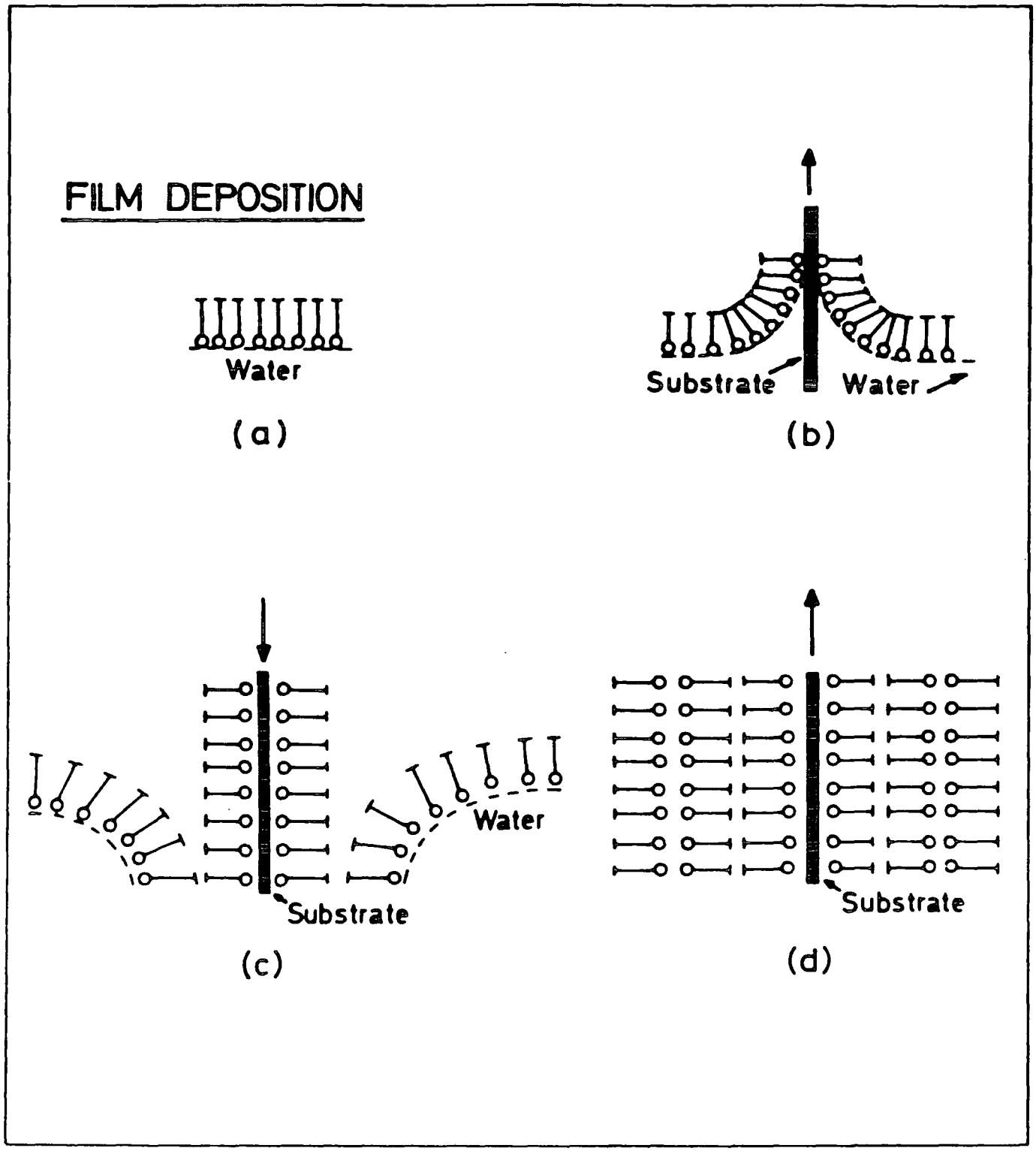

Figure 1. Diagram showing a) the alignment of amphipathic materials with the subphase and b), c) and d) the successive steps in the formation of a multilayer.

was found to have molecules that spread out to consume all the available area thus exerting a defined pressure on the perimeter. The excess material gathered on the surface in small lens-like globules. The oil spread immediately from these lenses to occupy the new area as the silk thread barrier moved in response to the removal of the Langmuir film. Thus the oleic acid spread at one end of the trough acted as a piston to compress the LB films at the other side of the barrier to a constant surface pressure.

Modern trough systems achieve this control of the surface pressure by the use of a Wilhelmy plate connected to a microbalance. The plate makes a zero contact angle with the subphase surface, thus converting a horizontal pressure to a vertical force. The compression of a surface monolayer can be thought of as being analogous to the compression of a gas. In both cases the material passes through a gaseous, liquid and solid phase. Once compressed into a two dimensional solid, the layer can be transferred to a substrate by passing it through the layer-subphase interface. The layer can be transferred to the substrate by one of three methods of deposition, namely the X,Y, and Z types. These respective labels correspond to deposition on the way down only, in both directions and on the way up only. Figures relating to these modes of deposition can be found accompanying section 3.4.

3.2 ORGANIC CHEMISTRY OF LANGMUIR BLODGETT MATERIALS

3.2.1 Introduction.

The main constraint upon scientists wishing to investigate LB films is the availability of suitable film forming materials. Although some of the simpler materials can be obtained from chemical suppliers, others requiring special substituents have to be synthesized from basic materials. Langmuir Blodgett materials must possess several characteristics, e.g. (i) they must be soluble in a suitable solvent, (ii) the material must be stable with respect to the subphase, i.e. it must be resistant to dissolution. This is normally accomplished by having a large non polar moiety. Typically there is also a highly polar group at one end, to prevent aggregation and to ensure correct alignment. These amphiphilic compounds must also be stable against collapse once formed into a film.

3.2.2 Langmuir-Blodgett materials

Fatty acids and their derivatives.

The alkanoic acids and their salts are amongst the organic materials which have been most widely investigated. These compounds combine the necessary hydrophobic part (an alkyl chain) with a hydrophilic part (carboxylic acid group). The alignment of these materials is with the hydrophilic part

sitting on the water surface with the hydrophobic part orientated at an angle (often 90 degrees) to the surface. Typical examples are provided by stearic and arachidic acid, about which a large body of data, concerning surface chemical behaviour and the LB films that they form, has now been accumulated. The structure of stearic acid ($C_{17}H_{35}COOH$) is shown, fig. (3.2a). The thickness of a monolayer of stearic acid is about 2.5nm while that of arachidic acid is about 10% greater.

To improve the shear resistance and cohesion of the fatty acid monolayers it is common practice to introduce a divalent metal ion (usually in the form of a chloride) into the subphase. This replaces the H^+ ions in the polar group of two acid molecules thus forming the metal salt. This linking results in greater lateral stability (10). The structure of the cadmium salt is shown in, fig. (3.2b).

Compounds which are very similar to the simple fatty acids can be created by replacing the alkyl group with chains containing one or more double bonds . It can be seen by the use of simple molecular models that introducing a double bond into the chain interferes with its ordering. However if the double bond is placed at the terminal position this disruption is considerably reduced. A well known material falling into this category is w-tricosenoic acid (the structure of which is shown in, fig. 3.2c). This molecule has been studied extensively by Barraud because of its potential use in electron beam lithography (11). It is possible also to replace the alkyl

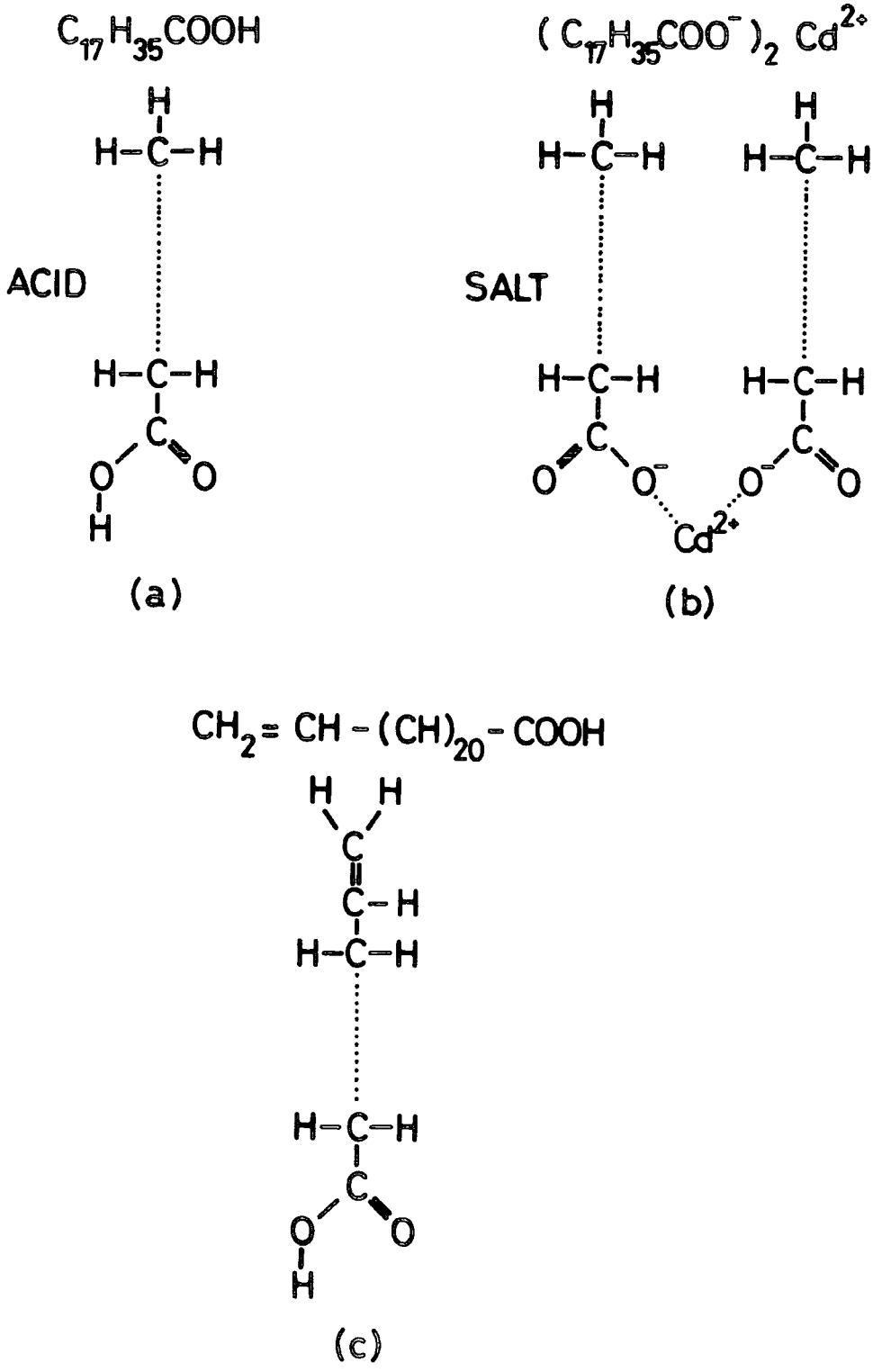

Figure 2. The molecular structure of a) stearic acid, b) cadmium stearate and c) w-tricosenoic acid.

chain with one containing triple bonds. In this respect the diacetelenic acids have been widely investigated because of their polymerizability. Films of the diacetelenic acids have been deposited and investigated in the monomer and preformed polymer form.

The use of polymerizable materials to form LB layers was an important step in the approach to forming stable layers, for with conventional fatty acids there is the problem of lack of physical and thermal stability. The introduction of cross linking between molecules by the use of polymerization was the method by which it was hoped that this problem would be overcome. It is in part the need to create films of even higher stability that has prompted the work carried out in this thesis.

Aromatic molecules.

In the case of aromatics, many of the molecules of interest do not readily form a monolayer on the surface of the subphase and they must be modified in some way in order to render them suitable for use with the LB technique. The simplest method of achieving this is to mix the material with a conventional fatty acid in order to form a mixed Langmuir film (12) or alternatively cause the material to be adsorbed onto a fatty acid film (13).

Alternatively the molecule can be substituted with long hydrocarbon chains. Early work carried out in this field with photoactive molecules by Kuhn (14,15) and Sugi (16) used both

these techniques. In this case though, the specific property of interest is necessarily diluted and the resulting films have limited mechanical and thermal stability. However, through the technique of molecular engineering, whereby innovative chemistry can provide the tool to substitute various ring compounds with short aliphatic side chains, materials such as 3-(10-butyl-10anthryl) propanoic acid have indeed proved to be effective. Multilayers of excellent quality with interesting electrical and optical properties have been reported by Vincett et al. (17). This research has demonstrated that through the use of molecular engineering, and by careful addition of suitable side groups to selected molecules, complex structures with properties totally different from those of the parent compound can be achieved. The main interest in such materials is that many derivatives of polycyclics are highly fluorescent in daylight. Thus LB films formed from such materials might find application in electronic displays.

Porphyrins, Merocyanines and Phthalocyanines.

There have been many studies of porphyrin derivatives involving a wide number of groups attached to the periphery of the ring system. Substitution of the central hydrogen atoms by a metal ion has also been carried out. It has been found that the orientation of the flat ring system depends on the length of the alkyl chain. Extensive work carried out by Tredgold's group at Lancaster University on simple esterified porphyrins (18) has

shown that some porphyrin esters orientate vertically and deposit Z type. However, work carried out by Barrauds group (19) on tetra-phenyl-porphyrins substituted with long alkyl chains show these molecules deposit as Y-type layers with the molecules lying flat on the water surface.

Merocyanine compounds have been studied by Sugi (20,21) in the form of mixed LB films. The reported anisotropic photoconduction observed in mixed LB films of merocyanine dyes (22) is shown to depend on the molar ratio af the dye and the arachidic acid.

The interest in phthalocyanine arose out of the early awareness that the device potential of Langmuir-Blodgett thin films would be greatly widened if at least part of the aliphatic structure of the more traditional materials were replaced by a structure with the electrically more interesting pi-electron system. Early work carried out by Kuhn (23) involved phthalocyanines substituted with long alkyl chains, and the use of mixed monolayers. This approach however leads to a dilution of the properties of the phthalocyanine. The work in Durham has concentrated on the use of lightly substituted phthalocyanines involving both symmetrical and asymmetrical substitution of the periphery of the molecule and their associated metal complexes. The monolayer assemblies formed from these lightly substituted phthalocyanines are very robust, an important factor in practical LB film devices. The formation and deposition of these layers are reported in detail in chapter 5 of this thesis.

3.2.3 Future developments.

Although the examples given represent only a few of the materials which have been examined, it will be evident that many interesting physical characteristics have been identified in the films formed, yet little work has been carried out to access the potential of related organic systems. Much could be gained by extending the range of groups used in making up the molecules. For example, the nature of the hydrophilic polar group could be extended from COOH to a range of other hydrophilic functions; for instance amide, alkylamino, sulphoxide, nitroxide and hydroxymethyl groups might be employed. Also the location and number of unsaturated linkages in the elongated molecular structure could be varied significantly. One method of exploring this potential range of materials would be to encourage organic chemists to synthesise attractive new materials for exploratory studies of both the chemical behaviour of the compounds on the water surface and their LB film forming capacity. The area in which the largest gain is to be made can be seen in recognising that the general approach to the synthesis of LB materials has been an ad hoc one, in that it has relied mainly on the modification of known LB film materials. Here a combination of synthetic organic and physical chemistry is required to obtain quantitive information on the relationship between the chemical structure and the properties of the molecule in forming a layer, and the physical properties of the layer itself. Only by a substantial study on

the correlation of structure and function in LB film-forming materials, will the myriad of future experiments implied in the ad hoc approach be reduced.

3.3 DEPOSITION EQUIPMENT AND INSTRUMENTATION.

3.3.1 Trough and barrier.

Although there is more than one type of trough system in use, they have a number of common features. The trough itself is usually formed of an inert material (commonly glass), which holds the subphase (normally highly purified water). The barrier mechanism sits at the subphase/air interface. The three basic types of trough system currently in use are summarized below.

Single movable barrier.

With troughs of this type the container is an integral part of the boundary of the compression system. A seal must be incorporated between the edge of the trough and the movable barrier. The principle of operation is similar to that first described by Langmuir(24).

Rotating barrier.

It is also possible to produce LB films in a circular trough using the type of radial compression barrier first devised by Sucher(25). In a modern version described by Fromherz(26) there are two independent drive barriers enclosing the monomolecular film thus enabling the monolayer to be

compressed as well as transported on the liquid surface.

Constant perimeter barrier.

The type of barrier system used at Durham is the constant perimeter type. It is similar to that described by Blight, Cumber and Kyte(27). The barrier is composed of a fabric belt which has been rendered hydrophobic by treating it with teflon. This belt is then configured by a system of six teflon rollers which is in turn secured by two mobile overarms which move symmetrically inwards or outwards thus maintaining the barrier taut at all times. The use of this type of barrier eliminates problems with leakage of material and water level adjustment, problems associated with the other two systems.

3.3.2 Deposition system.

There are several methods for transferring monolayers from a subphase to a solid substrate. The most common is to move the substrate vertically through the the compact monolayer, this normally being achieved with a motor-driven micrometer drive. However, other geometries such as movable belts or a rotating substrate (28) are possible.

During deposition of the monolayer it is particularly important to maintain the monolayer at the desired surface pressure. Most modern troughs have a control box which is used to monitor the surface pressure and compare it with a preset value. As molecules are removed from the subphase the barriers

then move so as to maintain the constant preset surface pressure during dipping. In most cases the speed of response to pressure changes during dipping is determined by the viscosity of the monomolecular layers and not by the limitations of the servomechanism.

3.4 TYPICAL PROCEDURE FOR THE DEPOSITION OF STEARIC ACID AND ITS SALTS.

The following section describes the preparation and procedures that are carried out for the deposition of stearic acid and its salts. The values quoted are typical of those used. It is mentioned here in order to provide the reader with a standard against which to compare the more complicated methods involved with producing phthalocyanine LB films.

3.4.1 Subphase cleanliness.

It is essential that the subphase used be clean both from bulk contaminants and surface contaminants. The purity of the subphase is obtained by firstly filtering the water supply with a coarse filter for removing large particulate matter from the supply (e.g. peat), then passing the water through a micron filter to remove smaller particles. The water is then passed through an ion exchange resin (Elga system). This water is then used as a source for a Millipore water system which incorporates three filters (two carbon and one ion exchange). Finally the

water passes through a filter of submicron size. Thus the water does not contain any bulk contaminants which can affect the film. For the deposition of stearic acid the subphase is now treated in two ways; firstly, the pH is adjusted by the addition of dilute hydrochloric acid to a value of 5.8 and secondly an amount of cadmium chloride is added to make the subphase in to a solution of concentration 2×10^{-4} M/l. The addition of the cadmium salt is important in forming layers of a stable nature. (The effect on the isotherms obtained for stearic acid due to the addition of cadmium chloride is shown, fig. 3.3). The water surface must also be cleaned of any surface active contaminant (e.g. dust or an old film). This is normally achieved by using a suction pipe with a glass tube pulled to a small diameter. The cleaning procedure normally involves collapsing the area to its minimum value and cleaning the surface inside the barriers by moving the nozzle to and fro over the water surface. This action sucks up small quantities of water and any other material residing on the surface.

3.4.2 Monolayer spreading.

The monolayer is spread from a solution of the LB material dissolved in a suitable solvent. Typically the solvent will have the properties of (i) being a good solvent for the LB material being used, (ii) being immiscible with the subphase and (iii) possessing a moderate evaporation rate. Solvents that are too volatile can lead to inadequate spreading of the LB material

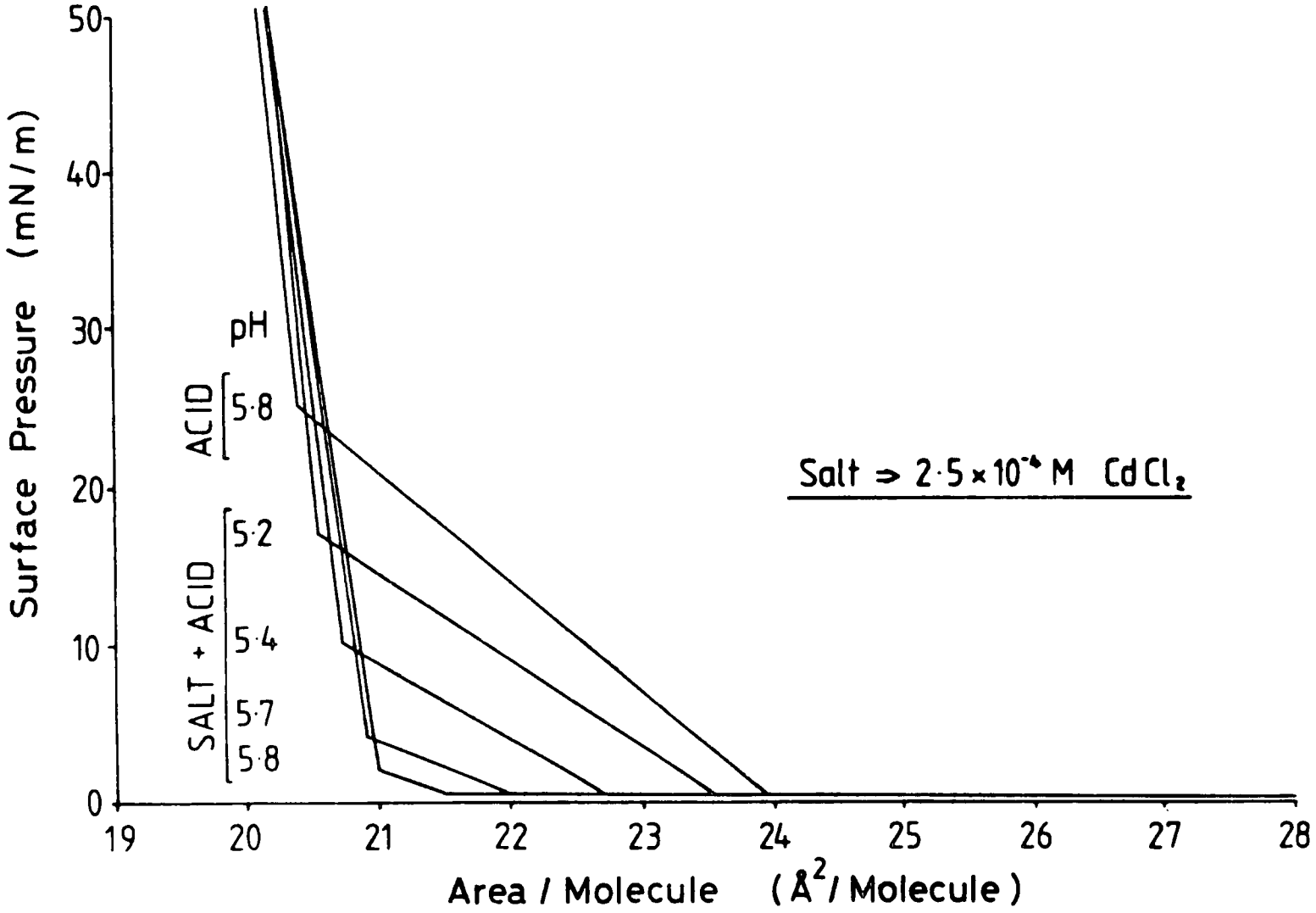

Figure 3. Isotherms for stearic acid showing the effect of both pH variation and the use of cadmium chloride in the subphase.

on the subphase and solvents that are slow to evaporate may remain to some degree and be incorporated in the compressed layer. In the case of stearic acid, a solution of concentration 1mg/cc in chloroform fulfills the above requirements. The solution is usually applied to the surface of the subphase using a micrometer syringe which allows material to be applied in a controlled and quantitative manner. After each drop, a short period is usually allowed for spreading and some evaporation to take place before the next drop is applied. This prevents excessive build up of solvent which could lead to poor spreading. After the monolayer has been spread, a reasonable period is left for evaporation of the solvent to take place (five minutes in the case of stearic acid) before manipulating the film.

3.4.3 Monolayer compression.

The characteristics of the monolayer can be monitored as it is compressed. The compression is carried out by slowly reducing the area available to the film. A typical speed of compression is $6.5cm^2/s$ for stearic acid.

An isotherm for stearic acid obtained for the optimum subphase conditions is shown in fig. (3.4). When the surface area is large, a decrease in area leads to no apparent rise in surface pressure. This is likened to a gaseous phase where the molecules can be thought of as being spread evenly over the enclosed water surface having little or no interaction with each

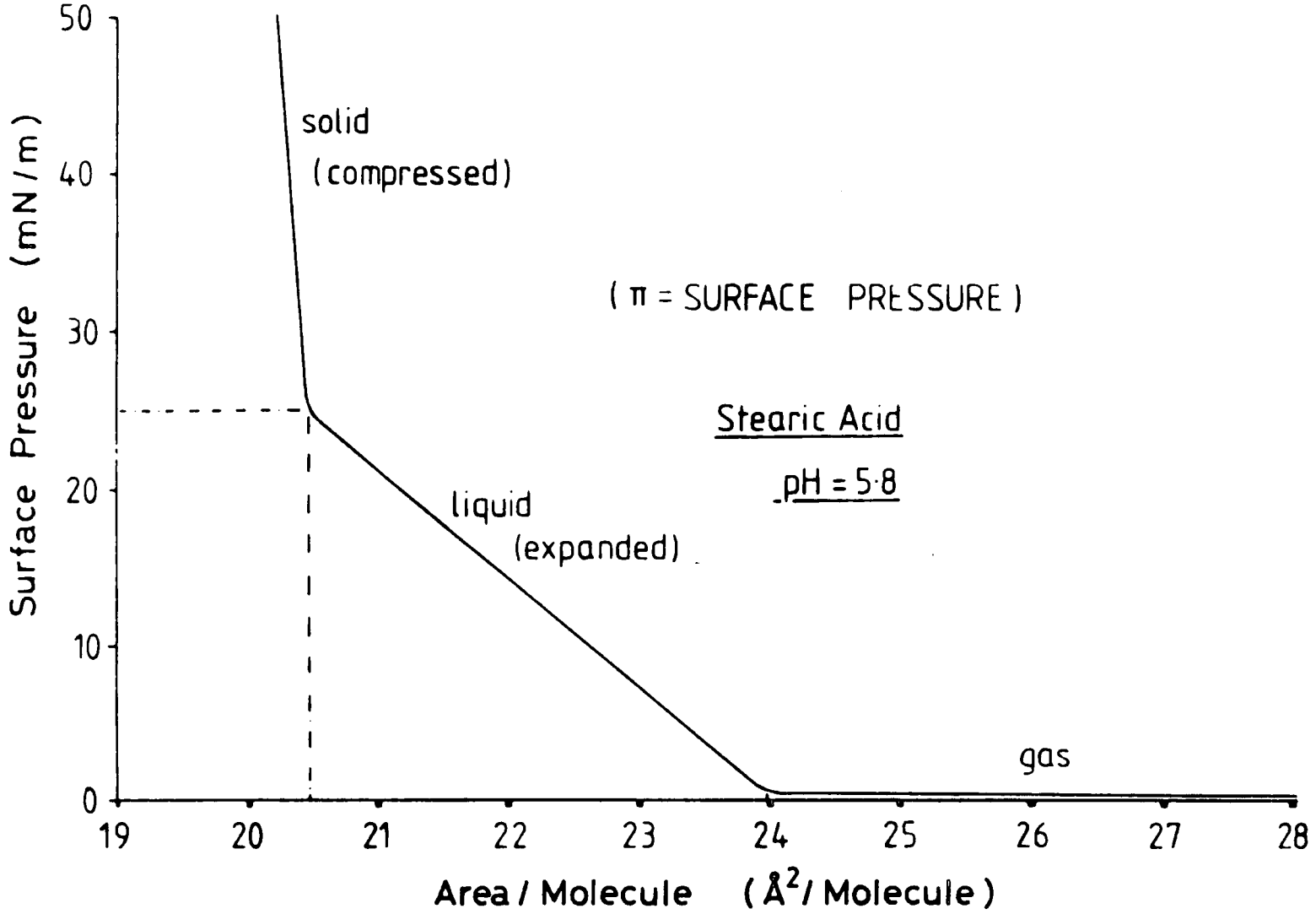

Figure 4. A typical isotherm for stearic acid obtained for the optimum subphase conditions.

other. As the enclosed water surface is further decreased the surface pressure begins to rise. This part of the isotherm can be equated to a liquid state. Here the molecules can be thought of as being in close proximity to one another. At this stage the molecules rather than being orientated randomly upon the water surface begin to align themselves vertically. As the area is decreased still further there is a sharp change in the slope of the isotherm. This can be regarded as the solid phase where the molecules have formed a condensed layer upon the surface and are capable of little further realignment. The solid line rises steeply until at a certain pressure the layer collapses. It is common to extrapolate back the solid line to zero surface pressure, this value of area being taken as the area per molecule in the condensed layer. It can be seen from fig. (3.4) that this gives a value of 20.7Å^2 for the area per molecule for stearic acid, which corresponds to the typical value accepted for the molecular packing of stearic acid.

The effect of varying the pH of the subphase on the isotherm characteristics is seen in fig. (3.3). The variation in pH affects the chemical equilibrium between the acid and salt. At a pH such as 6 the monolayer consists mainly of cadmium stearate but as the acidity of the subphase is increased the proportion of stearic acid also increases until, at a pH of approximately 5, the film consists mainly of stearic acid.

3.4.4 Film deposition.

Once a material has been spread and compressed to form a condensed layer, the monomolecular film can be deposited onto a variety of substrates. This is achieved by moving the substrate by means of a dipping mechanism. After a vertical traverse downwards through the film, the direction of travel is then reversed and the substrate brought back up through the film. The speed of deposition has been found to be very important and care is taken to ensure that the speed is kept constant throughout the deposition. It has been observed that a prime factor in the formation of high quality multilayer films is the quality of the first layer. The method described by Peterson et al(29) of depositing an aged layer very slowly first with subsequent layers being deposited at a faster rate, is often followed.

It is essential that throughout the deposition the monolayer is maintained at a constant pressure, this being achieved by the use of a feedback mechanism which adjusts the position of the barrier to compensate for changes in surface pressure. The mode of deposition for stearic acid has been found to be Y type. However, in certain circumstances, for example when a hydrophilic substrate is dipped, pick-up rarely occurs on the initial passage of the substrate down through the film. In these cases the method of beginning the dipping sequence with the substrate immersed is employed. Fig. (3.5) shows schematically the pick-up of the monolayer and the

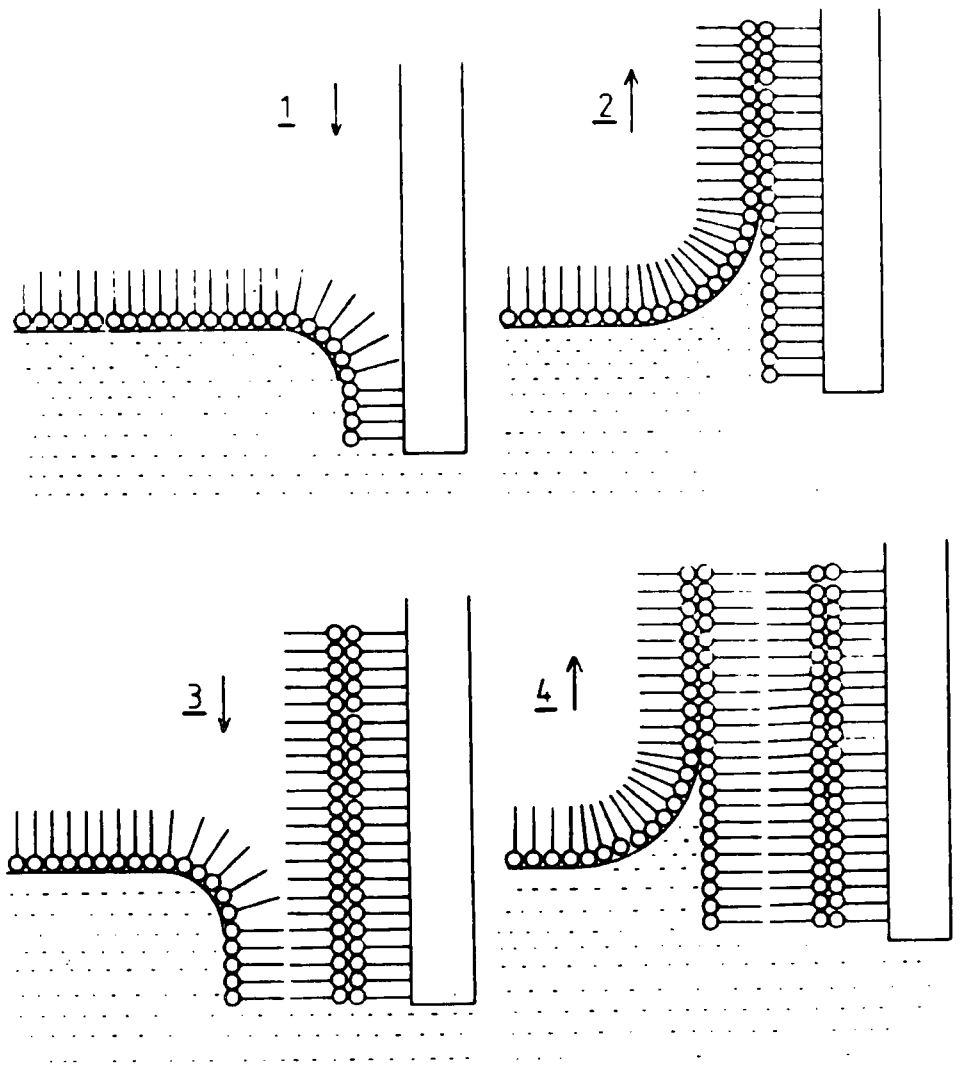

Figure 5.

A schematic representation of the pick-up of a monolayer and the subsequent build-up of a multilayer for a Y-type material.

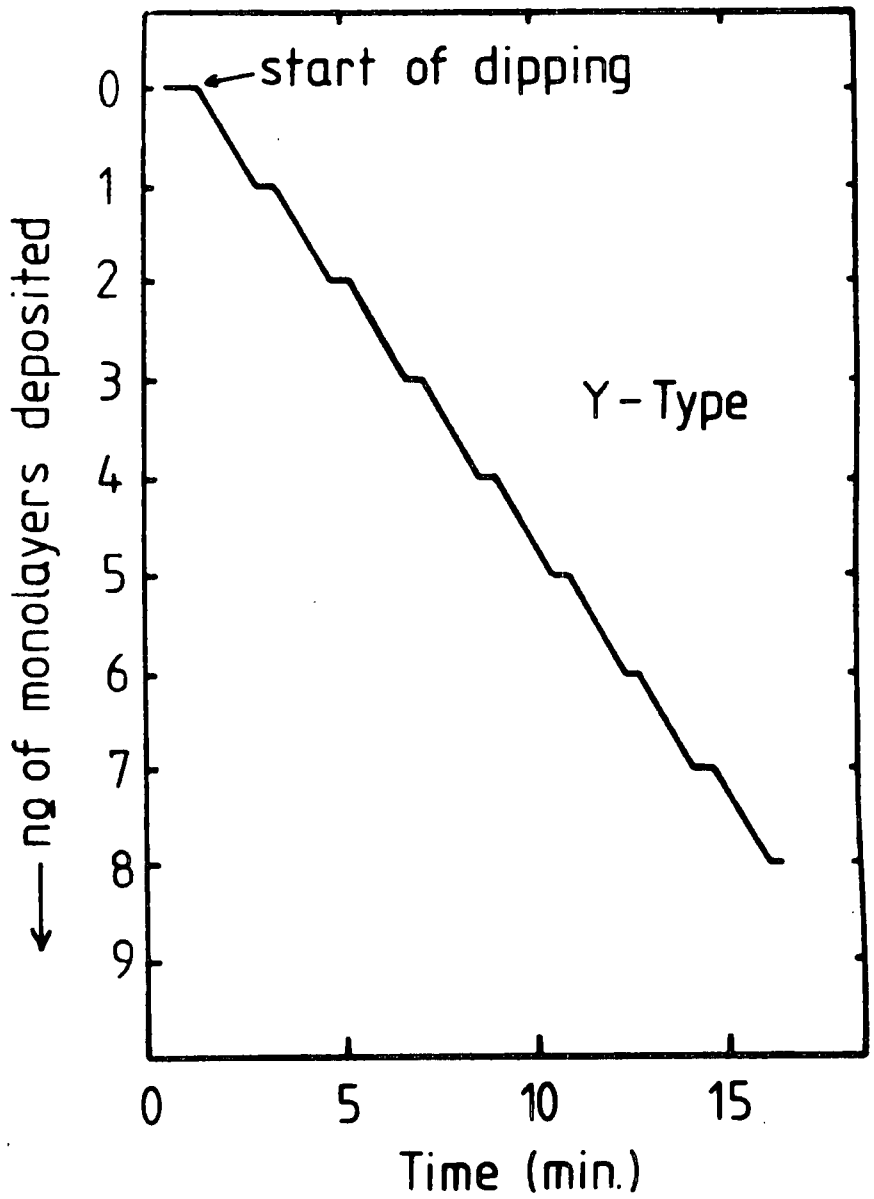

Figure 6.

A plot of film area versus time for the deposition of a Y-type material.

subsequent build up of a multilayer on it. The structure obtained is the typical head to head, tail to tail type associated with Y-type deposition. Fig. (3.6) shows the record of area versus time for the transfer. The figure also includes a trace recording of the surface pressure versus time showing that the pressure was maintained at a constant level by the feedback system. Fig. (3.7) shows for comparison the type of multilayer arrangement achieved with X and Z type deposition. The structure shows a head to tail to head type pattern.

Although the procedure given here is for stearic acid and its salts many materials have been developed for LB films and can be deposited on a variety of substrates. Such standard materials which exist at the moment include saturated and unsaturated long chain fatty acids, substituted diacetelenes and anthracenes with many other materials being developed. They can be dipped onto a variety of substrates including glass, metals, metallised surfaces and semiconductors.

3.5 BASIC CHARACTERIZATION.

It is essential when thinking of device applications that basic characterization experiments are first carried out on the deposited films. There are many methods that have been used to assess film quality. The methods most commonly used are summarized in: Table 3.1

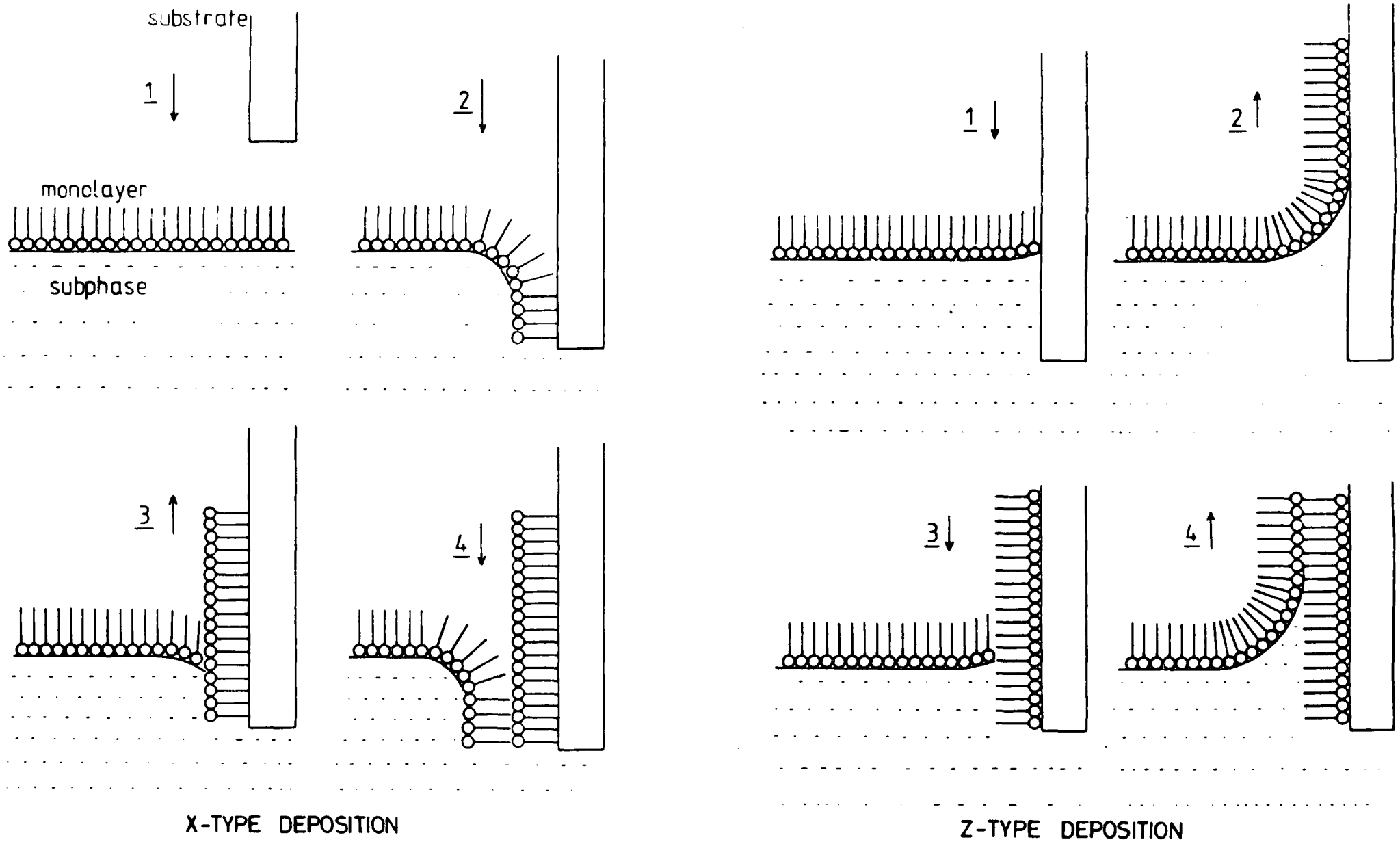

Figure 7. A schematic diagram of the multilayer arrangement achieved with X and Z-type deposition.

TABLE 3.1 TECHNIQUES USED IN THE CHARACTERIZATION OF LB FILMS

X-ray diffraction (30)	The technique has proved useful in the elucidation of the structural details of deposited films. Results have been obtained and quantitatively explained by Nicklow et. al. down even to a monolayer. Fig. (3.8) shows X-ray diffraction data from a film of 43 layers of perdeuterated manganese stearate on a substrate of monocrystalline silicon.
Neutron diffraction (31)	Nicklow et. al. have observed neutron diffraction from as few as three monolayers of manganese stearate. The unusually high sensitivity that allows observable diffraction from less than 1μg/cm of material is a consequence of the low angle Bragg peaks.
RHEED (32)	Reflection High Energy Electron Diffraction is a useful, substantially non destructive technique facilitating rapid identification of LB film structures.
TED (28)	For a more detailed investigation of the LB film structure, Transmission Electron Diffraction has been used with samples prepared by the Walkenhorst-Zingsheim method. A diffraction pattern from 21 layers of w-tricosenoic acid is shown in fig. (3.9)
XPS (33)	The X-ray photoelectron spectroscopy technique can be used to gain an appreciation of the quality, control of thickness and reproducibility of the multilayer assemblies, by studying electron mean free paths.
AC measurements (34)	Electrical measurements are extremely sensitive to pinholes and other defects in the deposited film and hence provide a straight-forward test of the structural integrity of the monomolecular assemblies. Fig. (3.10) shows capacitance data for cadmium stearate LB films on a highly doped InP substrate as a function of the number of deposited layers. The linear dependence demonstrates clearly the reproducibility of the monolayer capacitance and hence thickness from one layer to the next.

TABLE 3.1 TECHNIQUES USED IN THE CHARACTERIZATION OF LB FILMS

Electron spin resonance (18)	The application of this technique can provide information about the electronic and structural properties of systems containing paramagnetic species. Electron spin resonance measurements performed on merocyanine dyes by Kuroda, Sugi and Iizima, have shown that the generation of stable spin species in high concentration is closely related to chromophore aggregation in mixed layer systems.
Polarized resonance Raman spectroscopy (35), (36)	A sensitive technique which has been shown by Vandevyver and Ruaudel-Teixier to give information on the angular molecular distributions inside LB films. The technique is best suited to the study of conjugated molecules in the form of LB films and with these materials could be used with as little as one layer.
I R Dichroism (37)	This technique has been used for the determination of the in-plane anisotropy and the multilayer structure of behenic acid and w-tricosenoic acid. Investigation of the aliphatic tilt angle is also possible using IR dichroism performed at a variable angle of incidence using transverse magnetic polarization. In the study by Chollet and Messier, preferential tilting was observed along the withdrawal direction.
IETS (38)	In investigations of monolayers using inelastic tunnelling spectroscopy the vibrational modes excited are the same as those in conventional Raman and IR spectroscopy. The composition of the film predicted on the basis of IETS data has been found to be in excellent agreement with that expected. But perhaps the most remarkable point is that inelastic tunnelling is seen at all, as this bears a high testimony to the structural perfection and uniformity of these films.
Neutron Reflection (39)	This technique has been used by Highfield and Thomas to observe interference fringes from LB multilayers of cadmium arachidate-d on glass. Their results show that a model which proposes a reduction in the thickness of the first few layers gives a good fit to the interference and Bragg diffraction data.

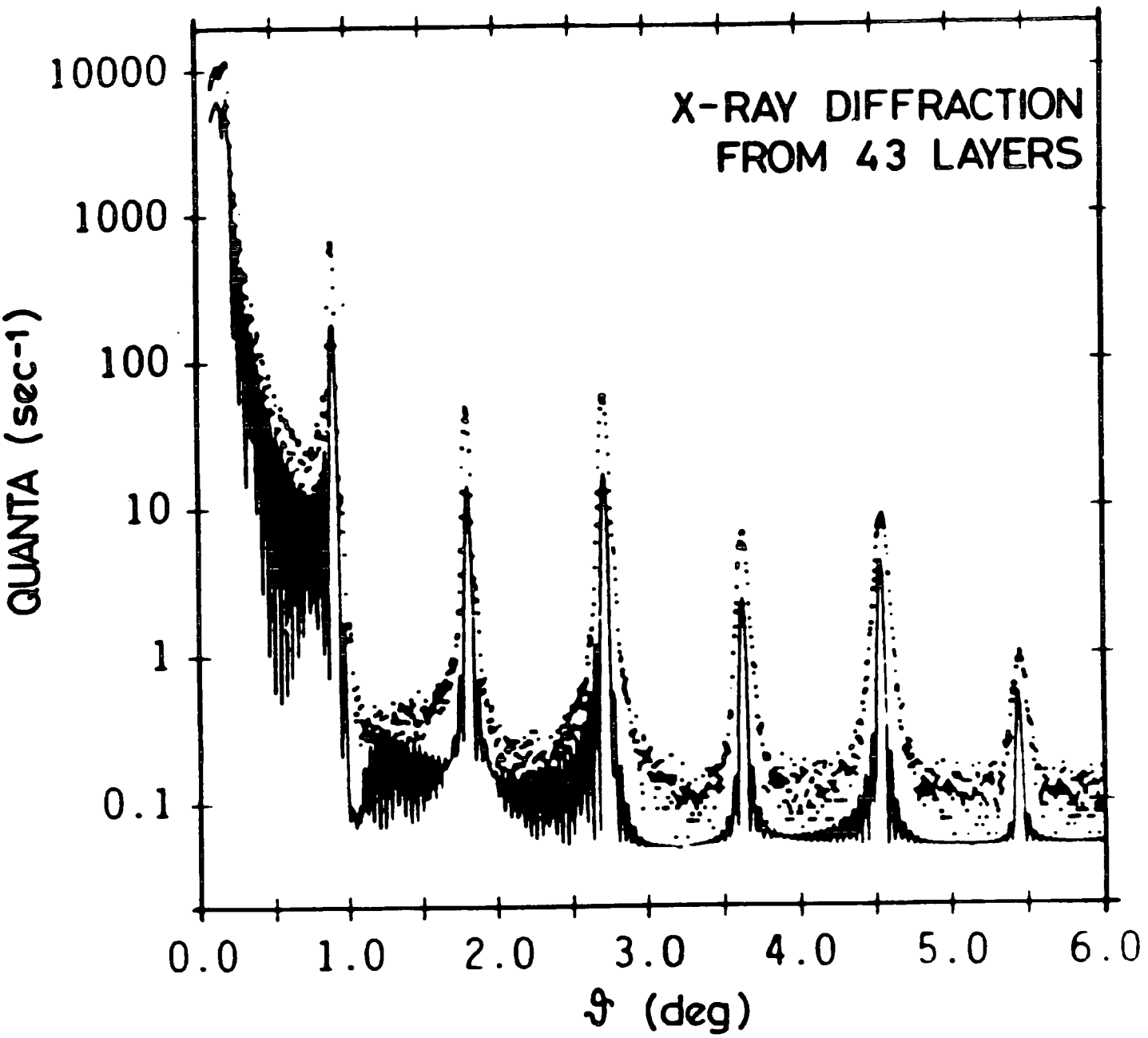

Figure 8. Results showing X-ray diffraction data from a film of 43 layers of perdeuterated manganese stearate on a substrate of monocrystalline silicon. (After Nicklow et al)

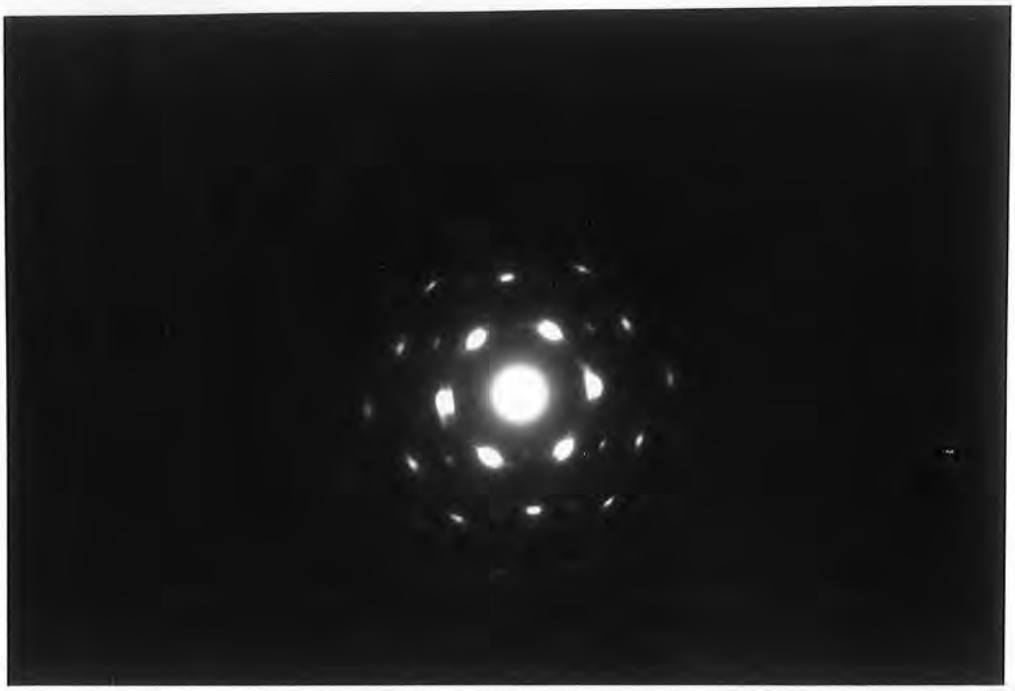

Figure 9. A photograph showing the diffraction pattern from 21 layers of w-tricosenoic acid. (After Peterson et al)

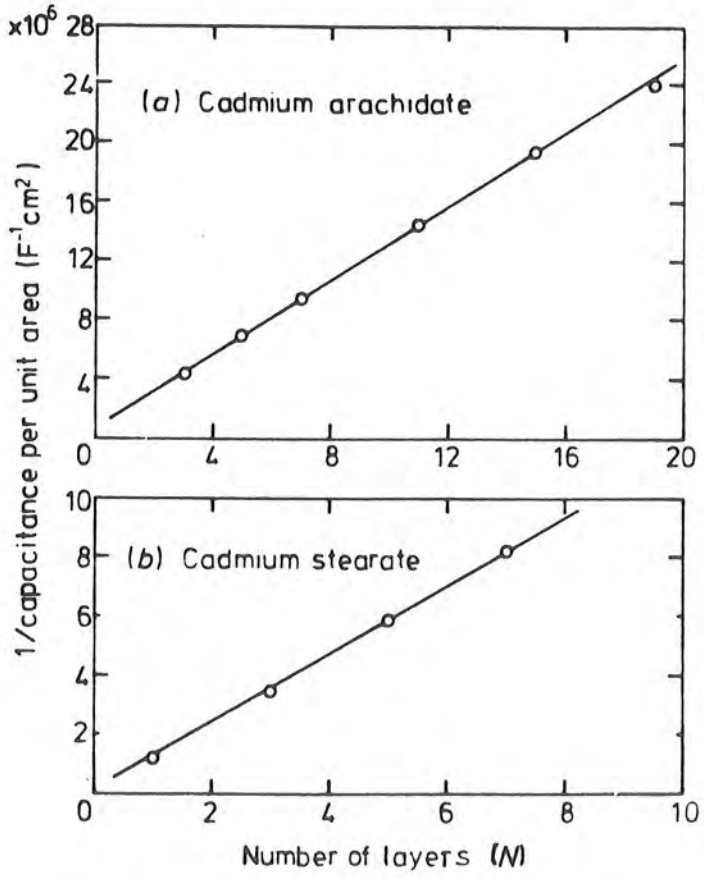

Figure 10. Capacitance data for cadmium stearate LB films on a highly doped InP substrate as a function of the number of deposited layers. (After Roberts et al)

3.6 APPLICATIONS AND FUTURE DEVELOPMENTS.

One of the major advantages of the LB technique is the precise control of thickness that it offers. It provides a tool whereby it is possible to fabricate structures which possess a layer whose thickness can be varied in multiples of the individual molecule's length. Another advantage is that the Langmuir trough technique is a low temperature deposition process. This circumvents the difficulties which arise out of using energetic processes such as evaporation, sputtering or growth from a plasma. Experience has shown that such methods often produce a surface damaged layer that invariably dominates the electrical characteristics of the junction formed. The technique also lends itself to the possibility of building up complex structures by the use of specially chemically engineered interlocking molecules, which basically allow assemblies to be built up on a molecular lego basis as shown and exploited in the elegant work by Hans Kuhn(40). It is also possible, depending on the material used, to give these layers various inherent properties, for example in producing insulating or semiconducting layers. Some of the suggested applications for LB films are outlined below.

Dilute and standard radioactive sources

The potential of obtaining thin organic films suitable for measuring the range of electrons with energy <1keV is realised by depositing a dilute radioactive source using the LB technique. The range is assessed by subsequently depositing standard monolayers which act as absorbers of precisely controlled dimensions (41). This technique provides positive advantages over the usual method whereby absorption characteristics are measured using radioisotope Auger electrons from the L-shell. In the latter method owing to the relatively low energy of the sources used, difficulties arise because of self-absorption.

Biological membranes.

The close resemblance of LB films to naturally occurring biological membranes and the use of the Langmuir trough technique to assemble materials of interest in the biological field such as chlorophyll-a, has long been noted by bioscientists. This has stimulated interest in areas of biotechnology involving the ionic permeability characteristics of membranes, basic research having been carried out in this field by Franks and Snook (42). Other areas include the formation of biocompatible hydrophilic surfaces from monomolecular films to, for example, prevent blood coagulation (43). Some of the groups investigating the use of LB films as

biosensors believe that incorporation of biological molecules such as enzymes into the films may form the basis of novel integrated solid state devices able, for example, to monitor immunological response.

LB films on semiconductors

When considering materials for integrated circuits silicon has an inherent attractiveness which derives in part from the fact that the material possesses a naturally insulating surface layer. In the fabrication of practical devices a relatively thick additional layer of silicon oxide is grown and then microlithography is used in order to define precisely the regions where subsequent films are to be deposited. Improvements in the microlithographic process have been achieved by a move away from conventional photolithography to techniques involving X-rays and electron or ion beams. This allows sub-micron resolution to be achieved, resulting in improved packing density and performance. However, the main disadvantage with electron beam systems lies with their electron scattering characteristics. It is found that a reasonable resolution is obtained only when using very thin layers of resist. Problems arise though because conventional spin coated polymer films, below a thickness of 1μ, exhibit unacceptably large pin hole densities and variations of thickness. The LB technique thus provides the better method of depositing suitable materials onto a substrate to aid microstructure fabrication.

At the University of Durham a wide variety of work has been carried out concerning the deposition of insulating LB films onto semiconductors other than silicon, thus creating new opportunities in microelectronics. Two main types of device have been studied and are outlined in the following sections.

Metal-insulator semiconductor tunnelling devices.

The technique of using LB films to aid the injection efficiency of minority carriers into semiconductors has been used at Durham to optimise the performance of both MIS solar cells (44) and electroluminescent cells (45,46). The main advantages are gained by having the critical control of the insulator thickness required to obtain optimum performance. The control available with monomolecular films is down to dimensions as low as fractions of 1nm.

Field effect devices.

The charge distribution at the surfaces of semiconductors can be modified by the use of an insulating layer. The use of LB films in providing this layer for several important semiconductors including cadmium mercury telluride (47), for which no natural insulating layer exists, show the ease with which a variety of single crystal surfaces can be accumulated, depleted or inverted with an applied voltage. The first field effect transistor incorporating monomolecular layers were

reported by Roberts et. al. in 1978 (48). The use of an organic layer in a transistor structure opens up many possibilities for sensor and transducer applications, as advantages are gained in (i), the degree of control afforded by the LB technique and (ii), the fact that organic compounds normally respond more positively than inorganic materials to external stimuli such as pressure and temperature.

Summary

Although only a few of the fascinating possibilities are outlined in the above examples it is hoped that they provide a feel for the range of exciting prospects in future developments and applications. Supermolecular designs leading to novel superconductors, three dimensional memories and conducting polymers now appear to be worthwhile goals. However, to achieve them, much solid research requiring the close cooperation of physicists, chemists, biologists and electronic engineers must be carried out.

CHAPTER 4

THE LANGMUIR BLODGETT TROUGH AND OTHER EXPERIMENTAL TECHNIQUES

4.0 INTRODUCTION

This chapter describes in detail the Langmuir-Blodgett trough and the other experimental equipment used in this work. An account is also given of the experimental procedures and techniques used in the preparation and characterization of the phthalocyanine films.

4.1 THE LB TROUGH

The LB trough system used in this work is shown in fig. (4.1). The photograph shows the trough housed in its protective cabinet alongside its associated instrumentation. As in any device-processing technology, cleanliness is of paramount importance, and for this reason the troughs in Durham are housed in a microelectronics class 10000 clean room. The system can be broken down into seven sections, namely; the trough which contains the subphase, the barrier and associated drive and monitoring system, the dipping mechanism, the instrumentation, the control system, the auto-cycle used for automatic dipping, and the housing and support for the trough. Each of these is discussed separately in the following section:

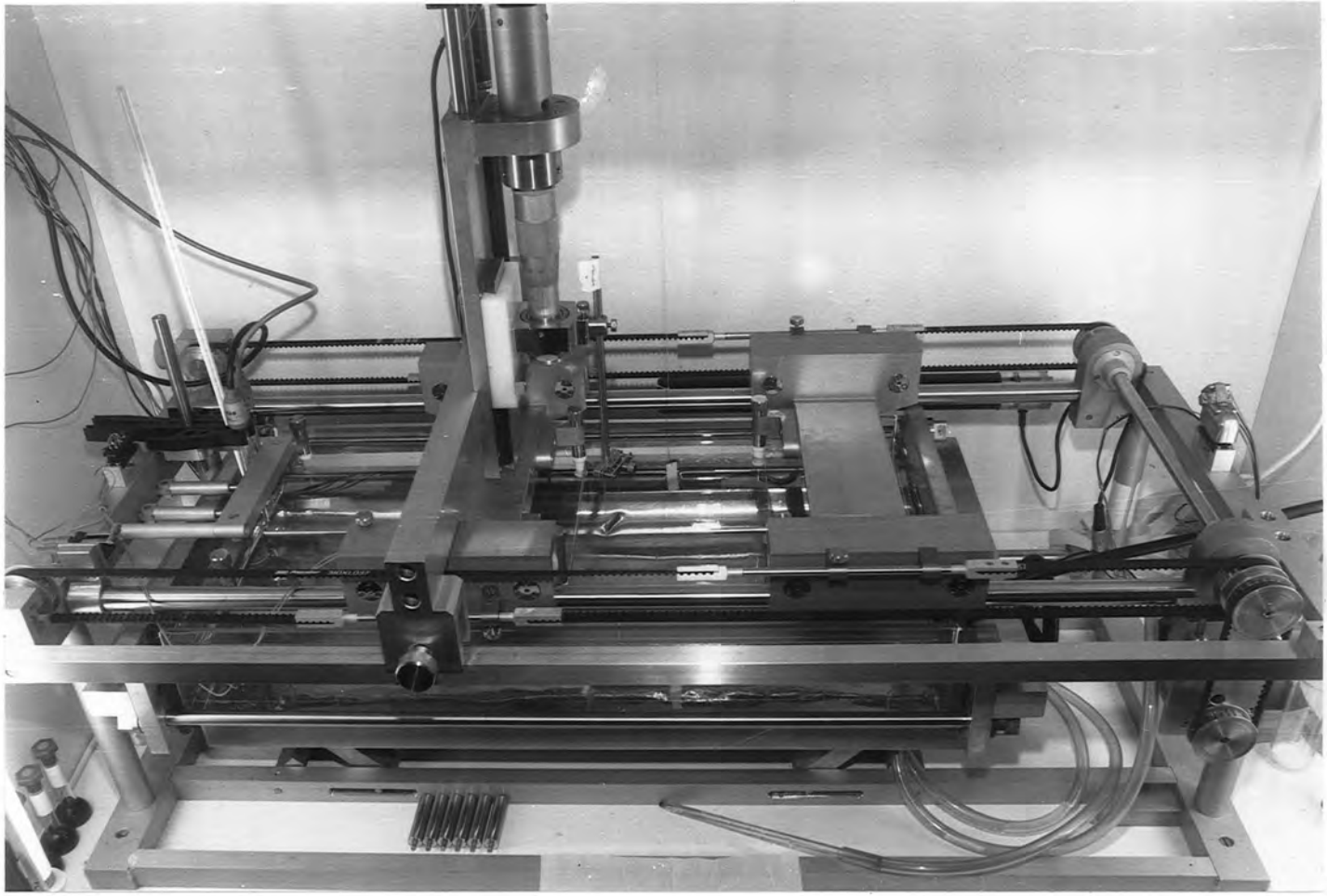

Figure 1. A photograph of the LB trough system used in this work.

The trough

The trough is composed of glass sections fitted together and is used to contain the subphase. As even a low level of contamination present in the subphase can significantly affect film quality, the materials used in the trough construction are all of an inert type. The trough manufacture involved the use of a sheet of plate soda-glass which was shaped into a "U" by forming around a stainless steel mould in an oven. This "U" section is sealed at both ends with glass plates held in place by two external metal endplates which are compressed by four metal rods. The rods can be tightened using adjustment nuts which have sprung washers to help maintain a constant tension, irrespective of temperature variation. The actual seal is made by a gasket of PTFE; this material was chosen because of its inert nature. A simpler method of putting endplates on the "U" section would be to use an adhesive that should be relatively inert once it had set. This alternative was tried using plate glass and a silicon based adhesive. However, in subsequent tests there was found to be a significant amount of contamination reaching the water surface.

Before the trough was used it was "leached" by steeping in a solution of dilute sulphuric acid for twenty four hours. This effectively prevented contamination of the subphase by ions diffusing out of the glass.

One of the major considerations in trough design was that it should be of a size and construction which allowed the

dipping of large substrates but still facilitated removal and cleaning. To further aid in this respect, the trough was supported on a platform which could be raised and lowered, thus increasing the ease with which the trough could be removed, inserted and positioned.

The barrier system

The barrier used was of the constant perimeter type reported by Blight, Cumper and Kyte (1) and is shown in the photograph in fig. (4.1). The barrier is supported and configured by six PTFE rollers, four of which are attached to the two moveable overarms, enabling the area to be altered. (the principle of operation is shown schematically in the inset of fig. 4.6). The two rear rollers are fixed and attached to the trough frame, they are both sprung and responsible for maintaining the tension in the barrier ribbon. The barriers themselves are composed of fabric to prevent stretching and are coated with teflon to make them hydrophobic; this is necessary as the contact angle formed with the barriers has been found to be important in the production of reproducible isotherms. This type of barrier is thought to cause less distortion to the film as the area is decreased. It also solves the problem of leakages from the corners of a box and piston type construction. A further advantage is that the water depth is not critical and can be set at any level within the width of the barrier ribbon.

The barriers were driven by a geared down electric motor

through the drive belt system shown in fig. (4.1). The power for the motor was supplied by the automated control box. A potentiometer fitted to the drive shaft of the barriers gave an analogue signal which was used to relate the position of the barriers to the area of the trough.

The basic design of the trough was as outlined above but various improvements were made during the course of the work. Moreover, some of the functions were specially tailored for the type of molecules that were used. One of the improvements incorporated was the facility to dip large area substrates without having to replenish the material on the subphase too often (this being an involved procedure requiring an operator). This facility is required for the fabrication of large area solar cells, flat panel displays and large area sensors. Consequently the width of the trough was increased, bringing the total surface area to approximately 1000 square centimeters. However this introduced another problem for the dipping of very small area samples: very little movement of the barriers was required, in order to maintain a constant surface pressure during deposition. The potentiometers fitted to the shaft which drove the barriers were originally ten turn, wire-wound potentiometers and, as such, gave a stepped output. Unfortunately it was found that the resolution of these potentiometers was inadequate for monitoring small movements of the barriers. To solve this problem a Penny and Giles hybrid linear potentiometer was fitted. These potentiometers are essentially wire wound with a coating of conducting plastic;

this gives virtually infinite resolution. With this potentiometer, it was possible to detect and record barrier movements of 1/2000 inch, (equivalent to 1.25 micrometers,). This is equivalent to an area loss of approx 5.10^{-3} cm^2.

Deposition mechanism

The dipping mechanism consisted of a micrometer-driven dipping platform which was positioned above the enclosed area of the trough. Various sample holders can be attached to this platform allowing substrates to be positioned immediately above the water surface. The platform is moved vertically into and out of the water surface by the micrometer drive. The stage itself runs in a dove tail. A photograph of the deposition mechanism is shown in fig. (4.2).

A requirement of the stage movement was that it be confined to a variable set of limits which could be set to take into account substrate size. This was initially achieved by using a pair of micro-switches. However, this meant that, for deposition processes involving variance of the area of sample covered, (e.g. stepped structures) the cabinet had to be opened and the trough disturbed to reset the limits. This problem was resolved by fitting another Penny and Giles hybrid linear potentiometer, allowing the position of the dipping head to be monitored by the control box. The limits could then be set externally from the box, removing any need to disturb the trough.

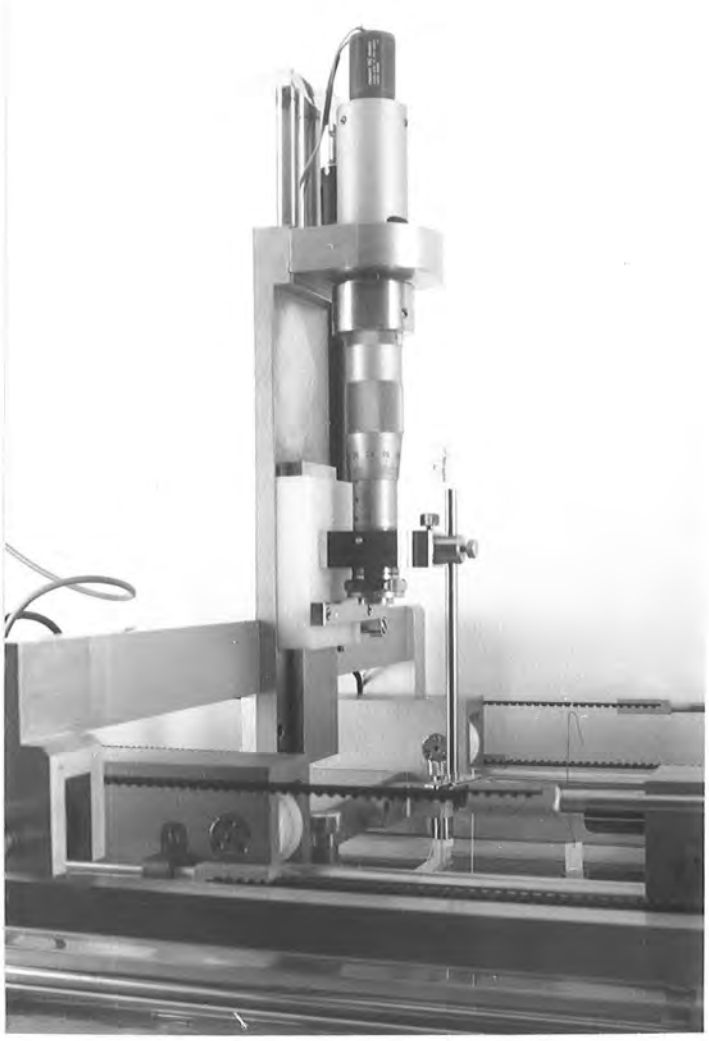

Figure 2. A photograph of the deposition mechanism used with the LB trough.

The fitting of this potentiometer again highlighted various problems in the movement of the head, both in the vertical movement of the platform and in the circular movement of the micrometer drive. The problem of viscosity on the vertical runner of the platform was thought to be due to the fact that the two running faces were made of brass, which is renowned for the formation of a sticky layer on its surface. The moving part of the dipping platform was therefore changed for one made of Delrin (polyacetal). This served two useful functions; first, as Delrin is a self lubricating material, the problem of the formation of a viscous layer was removed; second, the load lifted by the dipping motor was reduced. Since one of the original considerations in the construction of the dipping head was to keep it massive in order to dampen any vibration from the motor or the mechanical movement, the brass supporting structure was retained.

The tight spots discovered in the rotation of the micrometer drive were found to be due to small misalignments of the micrometer with the vertical axis of the dipping head movement. Despite being able to adjust the alignment so that the movement was free, frequent use invariably upset the fine setting required. This was overcome by fitting a gimbal to the platform side of the micrometer, allowing the necessary degree of freedom required to cope with any small misalignment which might occur.

Instrumentation

The instrumentation surrounding the trough is shown in fig. (4.3). The surface pressure is measured by a Beckman LM 600 microbalance via a Wilhelmy plate arrangement. The balance is situated on the top of the cabinet housing the trough. The output of the balance is fed to a Bryans 1900 X-Y recorder to record the pressure-area curves. The analogue output representing the area was derived from the linear potentiometer associated with the barrier arms. The output of the Beckman was also fed to a Bryans 312, 2 channel Y-t recorder for the recording of surface pressure during deposition. Finally an output was also supplied to the control box.

The pH was monitored by a Pye Unicam PW9409 pH meter. A secondary electrode was used to provide temperature compensation.

The control box

The trough was driven and controlled from a control box shown in the photograph in fig. (4.4). The right hand side of the box deals with the control of the dipping head. The linear potentiometer, fitted between the dipping head support and the dipping platform, permitted the position of the head to be monitored, which allowed the controls of the box to be used to set the upper and lower limits of travel. In the "set limits" mode, the movement of the head was performed quickly. The

Figure 3. A photograph showing the instrumentation associated with the LB trough system.

Figure 4. A photograph of the control box used to drive and automate the trough processes

dipping section also had an automatic cycle mode which when activated caused the head to cycle between the preset upper and lower limits. The number of cycles to be performed was entered into the front panel and a counter displayed the number remaining. The speed of the dipping head in the cycle mode was set on the front panel, the range of speeds being from 0.7 mm/min to 0.4 mm/sec.

The controls situated in the middle of the panel deal with the barrier movement. The barriers could be moved together and separated at a range of speeds, each action being set separately on the potentiometers mounted on the front panel.

It was essential that both the dipping head and the barriers were driven at a constant speed. This was achieved by using the accurate speed control circuit shown in fig. (4.5). Here, the motor drive op-amp forms the heart of the output stage. To compensate for resistance in the motor winding and wiring, a signal proportional to the motor current is generated across a resistor connected in series with the motor and fed back to the non-inverting input of the op-amp. The effect of the motor resistance is exactly cancelled if the sensing resistor is made equal to the motor and the wiring resistance. Thus, changes in torque (and hence armature resistance) are automatically compensated for by an increase in the drive current resulting in the speed of the motor being held constant.

The barriers can also be operated in a control mode. In this mode the surface pressure is measured by the Beckman electrobalance and the signal fed to the control box where it is

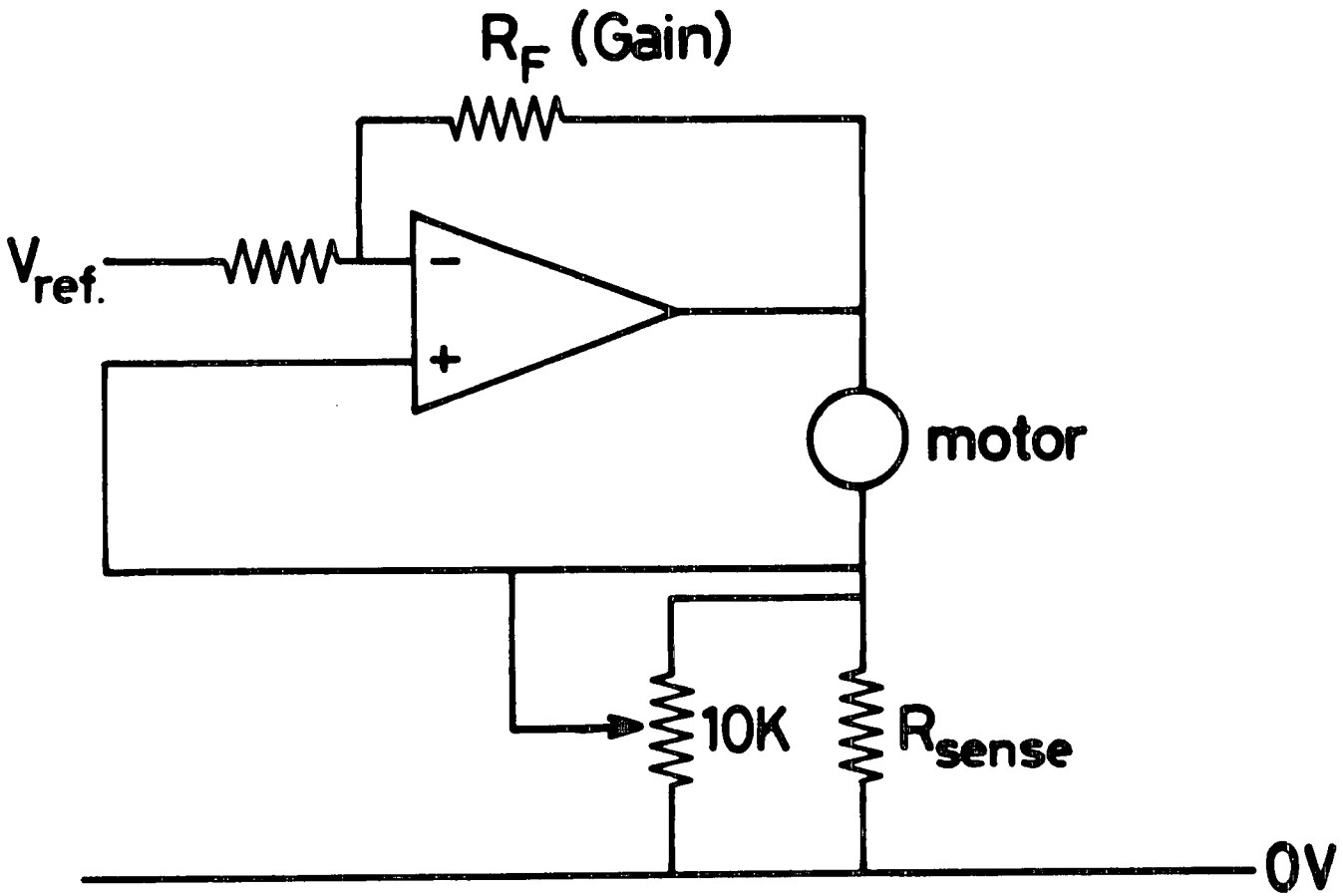

Figure 5. A schematic diagram of the automatic speed control circuit used to control both the barrier and dipping head drive.

compared to the value of the preset pressure dialled. The barriers are driven until the two are equal. The control mode was used to maintain a constant surface pressure as material was removed during deposition. A schematic diagram of the feed-back loop between the electrobalance and the barrier motor is shown in fig. (4.6).

The final position of the barrier control switch is the auto cycle position used for materials which deposit Z-type.

The auto cycle for Z-type deposition

The materials used in this work, namely various phthalocyanine derivatives; were found to deposit in a Z-type fashion i.e. material was deposited only as the substrate was removed from the subphase. A novel method of monitoring this Z-type deposition was therefore developed. This can be seen by reference to fig. (4.7a) which shows the method usually adopted to monitor the deposition of an LB film. The film area is simply recorded as a function of time. While this method is relatively straightforward it does suffer from the disadvantage that variations in the deposition ratio can be obscured by changes in the speed of dipping. Fig. (4.7b) shows a technique which overcomes this difficulty; in this case the film area is plotted as a function of dipping head (i.e. substrate) position, rather than time. Transfer of the film to the substrate on the upward motion of the dipping head starts at point A. This deposition terminates at B as the substrate

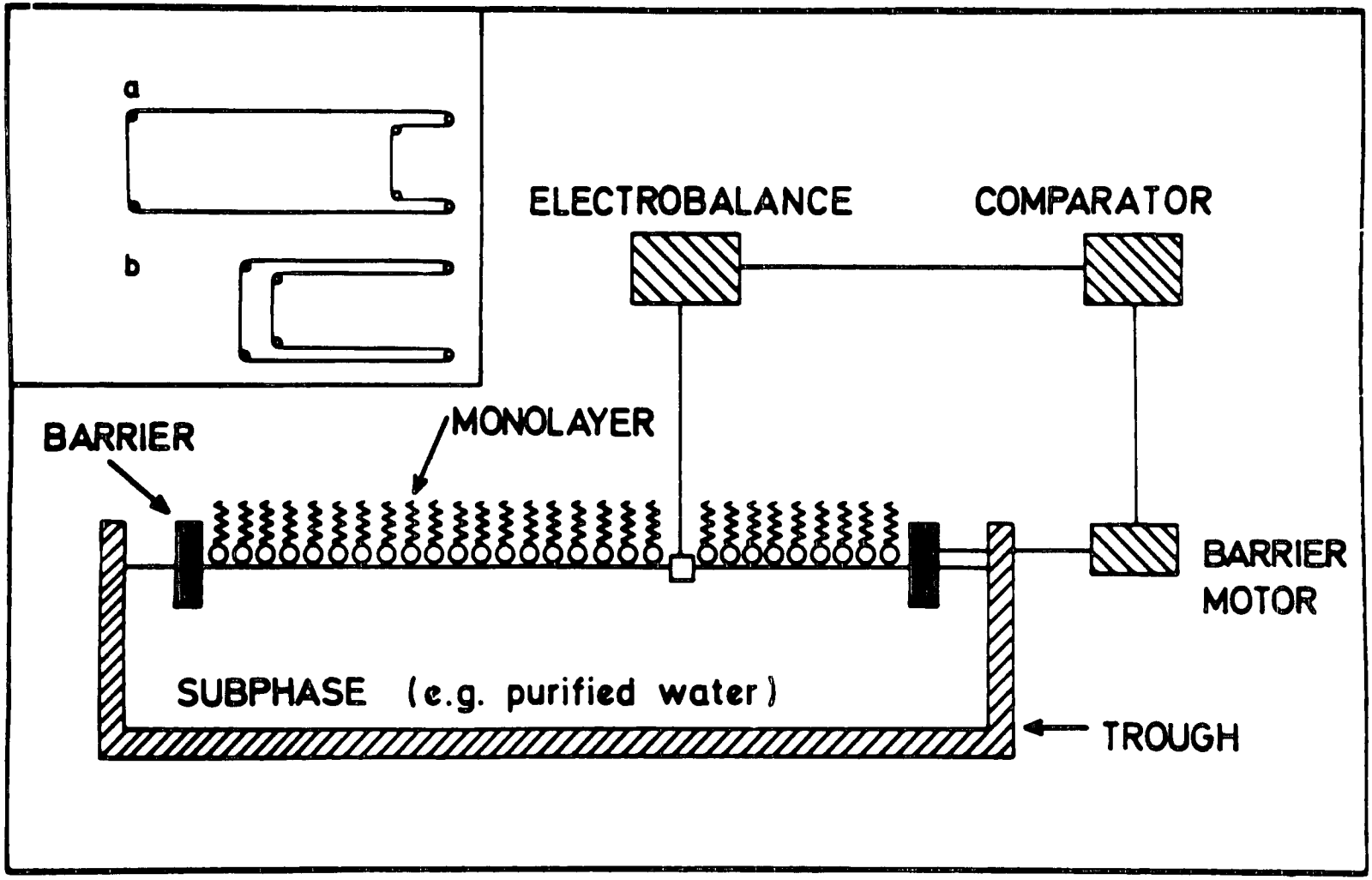

Figure 6. A schematic diagram of the feed-back loop between the electrobalance and the barrier motor. The inset shows the opperation of the barriers.

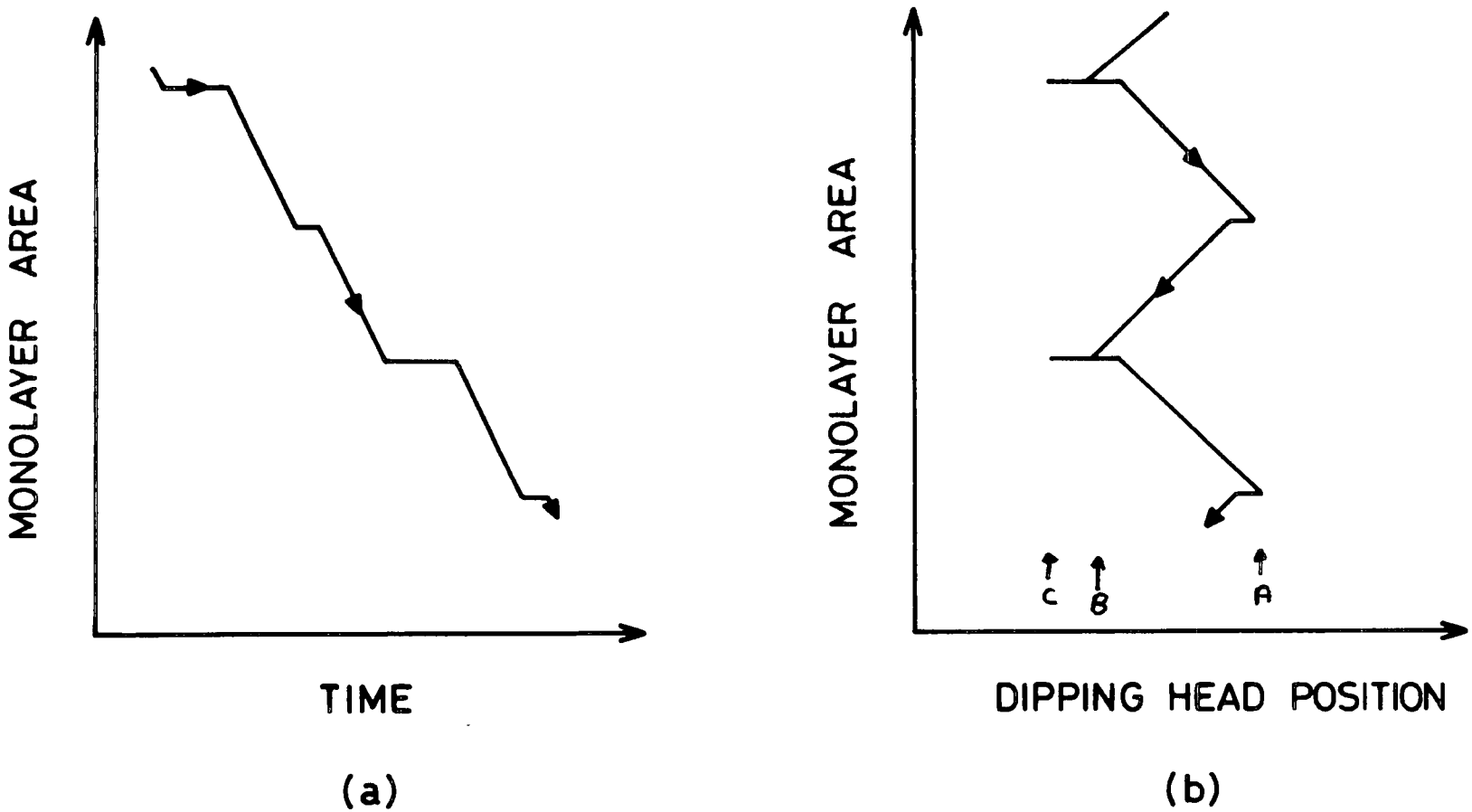

Figure 7. Schematic representations of a) the standard deposition of an LB film, where the film area is simply recorded as a function of time and b) an alternative method of monitoring the deposition, where the area is plotted as a function of the dipping head position.

leaves the surface of the subphase. At C the direction of substrate motion changes. With Z-type deposition no film is removed from the surface of the subphase as the substrate is lowered through the film/air interface, resulting in the horizontal lines in fig. (4.8a).

The initial procedure required that, after a single layer had been transferred on the substrate upstroke, the floating film was removed before the substrate was again lowered. A fresh layer was subsequently spread onto the subphase surface. This was necessary to ensure that absolutely no film was transferred to the substrate on its downstroke. For the deposition of a large number of layers, the procedure was obviously very time consuming. However, it was discovered that films of similar quality could be obtained simply by expanding, rather than removing, the floating film before lowering the substrate into the subphase. Consequently the control system of the L.B. trough was modified to perform this task automatically. The film area/dipping head position diagram for the complete autocycle used for the Z-type deposition of phthalocyanine is shown in, fig. (4.8b). The cycle starts at the top right of the diagram with the barriers open and the dipping head at the upper limit of its travel. In step 1 the dipping head is lowered with the barriers expanded. On reaching the lower limit of its travel the barriers compress the layer (step 2) until the preset surface pressure is reached. A time delay of 1 to 6 minutes is allowed for the layer to stabilise and then the dipping head is raised to the upper limit of its

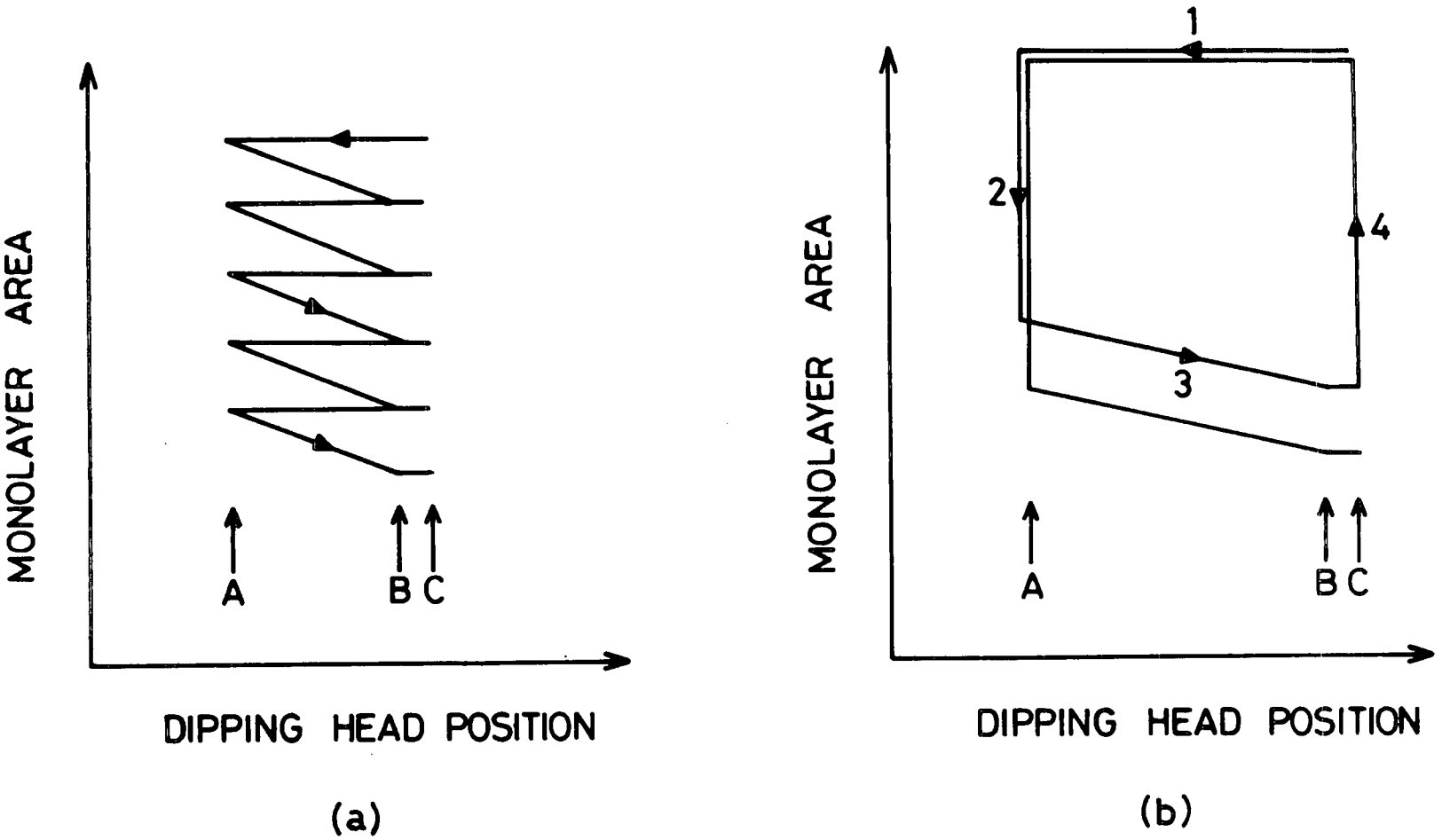

Figure 8. Schematic representations of a) a deposition plot of area versus dipping head position for a z-type material and b) the film/ dipping head position diagram for the complete autocycle used for z-type deposition.

travel at the preset dipping speed (step 3). Finally the barriers are expanded (step 4). There is a time delay of 5 to 30 minutes before the commencement of the next cycle. Such an automated procedure considerably simplifies the deposition of a large number of layers of the phthalocyanine material and is probably useful for the Z-type deposition of many other molecules.

Trough housing and support

The trough was housed in a cabinet which was designed to act as further protection against airborne contaminants. The cabinet has as one of its features, an extractor fan which was used to remove fumes from the evaporating solvents. It was supported on a Newport anti-vibration table. This was used particularly during the day, when vibration levels were at their highest.

4.2 GENERAL PREPARATION TECHNIQUES

4.2.1 Cleaning and etching procedures

Glass slides.

The research work sometimes required the use of high quality, smooth, transparent substrates. Slides made from Corning 7509 glass satisfy these criteria. The slides were prepared using the following procedure:

(i) one half hour sonification in 10% decon 90 solution.
(ii) one half hour sonification in de-ionised water.
(iii) three hours reflux in iso propyl alcohol.

Semiconductor substrates

In this work many semiconductors were used, namely InP, Si, SiO_2 ZnSe, CdTe and GaP. All of these were prepared by using standard cleaning procedures as outlined below.

Indium phosphide

(i) reflux in iso-propyl alcohol for three hours.
(ii) polish with 1% bromine/methanol etch.

Silicon

(i) etch in 5% HF.
(ii) rinse in millipore water.

Silicon dioxide

reflux in iso-propyl alcohol for three hours.

Zinc selenide

reflux in iso-propyl alcohol for three hours.

Gallium phosphide

polished using an etch composed of potassium ferricyanide and potassium hydroxide in water. The etch was used at 80° C.

4.2.2 The vacuum deposition of metals for metallization and the formation of back contacts

The preparation of metallized glass slides

Once again Corning 7509 glass was used after following the cleaning procedure outlined previously. The metallization was carried out in an Edwards E306 vacuum system at a pressure of less than 10^{-5} torr. The metals most commonly deposited were aluminium, gold and lead. For the evaporation of aluminium a tungsten spiral was used as a source, whilst for gold and lead a molybdenum boat was used. Both types of source were fired before use by operating them, in a vacuum, at a temperature higher than that used for the evaporation. After the deposition of the metal a period of half an hour was left to allow the slides to cool.

These metallized slides were then used for three purposes: (i) as back contacts for MIM structures, (ii) for interdigitated

structures for use in lateral conduction and gas measurements, and (iii) for the preparation of specially developed substrates for analysis with the transmission electron microscope.

ELECTRICAL CONTACTS WITH SEMICONDUCTORS

Forming back contacts

In the case of electrical devices incorporating semiconductors, electrical connection was made by evaporating the appropriate metal in the Edwards evaporator, utilising the metallization procedure. The procedures already outlined for the surface preparation of each type of semiconductor were followed. In the case of Si or SiO_2 the back of the slice was commonly treated with 40% HF, immediately prior to metal evaporation, ensuring the removal of any native oxide. Normally, two contacts were deposited so that ohmicity could be evaluated on a curve tracer. Contact was made to the metal electrode via a wire and silver paste.

Top contact evaporation

The biggest problem in evaporating top contacts on to LB films is the burning or diffusing of the evaporant metal through the layer. Stearic acid, for example, has a bulk melting point of only 70° C, although that for $CdSt_2$ is slightly higher, and in monomolecular form may be higher still. There are two main

approaches to solving this problem; firstly the evaporation can be carried out with the substrate cooled (e.g. on a cold finger using liquid nitrogen as the coolant). This method is not always satisfactory due to problems caused by mismatches in the thermal expansion coefficents of the substrate, LB films and metal.

Secondly the evaporation may be carried out in stages with a very low deposition rate. A typical staged evaporation is outlined below.

5 angstroms at 1 angstrom per second
5 angstroms at 1 angstrom per second
10 angstroms at 1 angstrom per second
15 angstroms at 1 angstrom per second
15 angstroms at 1 angstrom per second
20 angstroms at 1 angstrom per second
20 angstroms at 1 angstrom per second
20 angstroms at 1 angstrom per second

The above evaporation would be carried out at a pressure of less than 10^{-5} torr, with a time period of approx 20 minutes between each stage.

The metal most commonly used to make the top contact is gold but often aluminium would be used as it evaporates at a much lower temperature, and therefore is much less likely to cause thermal damage to the LB layer. In the case of the aluminium evaporation procedure, gold is used for the last 20 angstroms as this avoids contacting problems with the surface oxide of the

aluminium. Electrical connection is made to the device by a gold ball pressure contact.

4.2.3 Device fabrication

The fabrication of lateral conduction structures.

The cleaning and metallization procedures already outlined were followed. The samples were then coated with a photoresist and exposed through a mask giving an interdigitated electrode pattern. The unexposed resist was then removed using a commercial developer, followed by the removal of the exposed aluminium using the following etch:

30 parts orthophosphoric acid
2 parts acetic acid
0-7 parts water
(parts by volume)

The remaining photoresist was then removed by rinsing in acetone. The slide was finally prepared for deposition by refluxing in iso-propyl alcohol for three hours. Electrical contact was made to these devices via a wire placed in mechanical contact with the stem of the electrode and then coated with conducting silver paste. With aluminium there exists a native oxide which could lower the efficiency of the device by placing a high resistance in the circuit. Attempts to solve this problem were made by using gold as the metal for the electrode deposition. Unfortunately it was found that the gold

tended to diffuse into the glass and form a conducting surface. This problem could alternatively be approached by using a metal with a conducting oxide.

The fabrication of transmission electron microscopy samples

To examine a sample by transmission electron diffraction (TED) entails certain requirements; firstly the sample must be thin enough to allow transmission of the electron beam. In this respect LB films present no problems as thicknesses can be produced with the dimension of one molecule. One difficulty arises however, when considering how to support this layer, as the substrate must also be thin enough to allow transmission of the electron beam. The method used to overcome these problems was the Walkenhorst-Zingsheim technique (2,3). This involves the deposition of the LB films onto an anodized aluminium slide, and the subsequent transfer of the film plus the anodic oxide support, to an electron microscope copper grid. The procedure used was as follows: first the cleaning and metallization procedure for aluminium already outlined was performed; the anodisation was then carried out at 4.5V in a 3% solution of diammonium hydrogen citrate; the substrate was then rinsed and refluxed with isopropyl alcohol before being coated with the LB films; the slide was then placed in a Petri dish and filled with a solution of mercuric chloride and acetic acid. The dish was filled to a level slightly higher than the slide surface, but not so high as to flood the slide. As a result of the etching

of the aluminium layer, the LB film with its alumina substrate would float on the water surface and it could then be lifted from below onto an electron microscope copper grid and drained on filter paper.

4.3 STRUCTURAL ASSESSMENT

The TEM examination was performed in a JEM 120 transmission electron microscope, operated at 80 kV and using a goniometer diffraction stage positioned below the projector lens. The region of sample in this position which contributed to the diffraction was about 200 μm in diameter. The microscope was capable of operating at two beam voltages, 80kV and 100 kV; the lower value was used so as to reduce the risk of burning the film, a common problem when investigating organic materials.

Other electron microscopy investigations which were carried out included RHEED and scanning electronmicroscopy. The RHEED studies were again carried out on the JEM 120 at 80 kV, the substrate used being highly polished InP. This material has been successfully used with the fatty acids to obtain satisfactory diffraction patterns (4). The scanning electron microscopy was carried out on a Cambridge stereo scan 600, operated in secondary emission mode. Again, the layers under investigation were invariably dipped on to highly polished InP. This normally resulted in good contrast between the substrate and the film as the secondary emission of electrons from the heavy indium atoms is much higher than that from the lighter

elements present in the phthalocyanine.

4.4 ELECTRICAL MEASUREMENTS

The electrical investigations that were carried out on the various device structures fell into two basic areas; capacitance measurements and conduction measurements. In both cases they were performed in the sample chamber which is shown in the photograph in fig. (4.9). The chamber was made from brass as this was found from experience to give the best insulation from electrical noise. It was then nickel chrome plated to avoid problems with tarnishing. The chamber could also be used for measurements in various gas ambients, including some oxidising gases. Thus, the plating protected the chamber from attack from these reactive gases. The connecting pipes and taps were all made from stainless steel because of the corrosive properties of the gases used. The inside of the chamber contained a platform made of Delrin upon which a sample could be mounted. A moveable probe -also made of Delrin - was positioned above the platform; this held a gold ball for making contact with the top of the sample. The sample chamber also contained a holder which could be filled with a desiccant, normally silica gell or anhydrone. Electrical contact was made to the inside of the chamber by four BNC connectors.

The capacitance measurements were carried out using a Brookdeal 9502 Ortholoc instrument operating as a two channel phase sensitive detector. The Ortholoc allowed the monitoring

Figure 9. A photograph of the sample chamber used to make capacitance and conductance measurements.

of the capacitance and the quadrature component, i.e. the conductance. In general, the capacitance was measured both as a function of frequency and as a function of thickness for stepped structures. The Ortholoc was also used to carry out capacitance and conductance versus voltage measurements for MIS structures. The general procedure involved placing the sample in the measurement chamber and leaving it for two hours in a nitrogen environment, to allow stabilisation of temperature and humidity.

For capacitance versus thickness measurements, the Ortholoc would be set at the required frequency. Both channels would be first zeroed, using the offsets on the device, and then calibrated using a standard capacitor. Calibration was accomplished by placing the standard capacitor across the measurement terminal and then adjusting the phase angle until the output of one of the channels was zero. This channel was then designated for conductance and the other for capacitance.

For capacitance and conductance versus voltage plots, a mixing box was used to provide the ac signal with a dc offset. The outputs of the capacitance and conductance channels were fed to the Y inputs of a two pen X-Y recorder, and the X-channel was connected to the voltage ramp, used to provide the sample voltage scan.

For capacitance and conductance versus frequency plots, the Ortholoc required re-calibrating each time the frequency was altered. The dc conduction measurements were carried out using a Time Electronics voltage source and a Keithley picoammeter. The measurements were carried out on both sandwich and lateral

conduction structures.

4.5 OPTICAL MEASUREMENTS

Optical measurements were carried out using a Cary 2300 spectrophotometer. The measurements taken included transmission and reflectance readings for layers deposited on glass slides or semiconductors. Reflectance readings were taken using the Cary reflectance accessory (N° 87-175-872). The transmission sample holders were purpose built in Durham. The spectrophotometer was also used to assess the concentrations and purity of solutions prepared for LB film deposition. In this case the measurements were made using a pair of matched quartz, 1 cm path length, cells. In all cases, standard procedures were followed for obtaining a zero baseline reading before any data were taken.

The samples were also examined under a Vickers M17 industrial microscope, this particular model being equipped with dual illumination. This meant that it was possible to view the samples with both incident and transmitted light. The lenses were also of a type which allowed the sample to be viewed under bright or dark field illumination. This was useful in that it often allowed various, normally invisible structural features to be seen. For example, in films of polymerised diacetylenes the material exists in two forms; red and blue. Under bright field illumination this can not normally be observed, but the two types are quite readily distinguished under dark field illumination. The illumination source was also fitted with a

Figure 10. A photograph of the equipment used to measure the conductivity of the phthalocyanine films in the presence of various ambients.

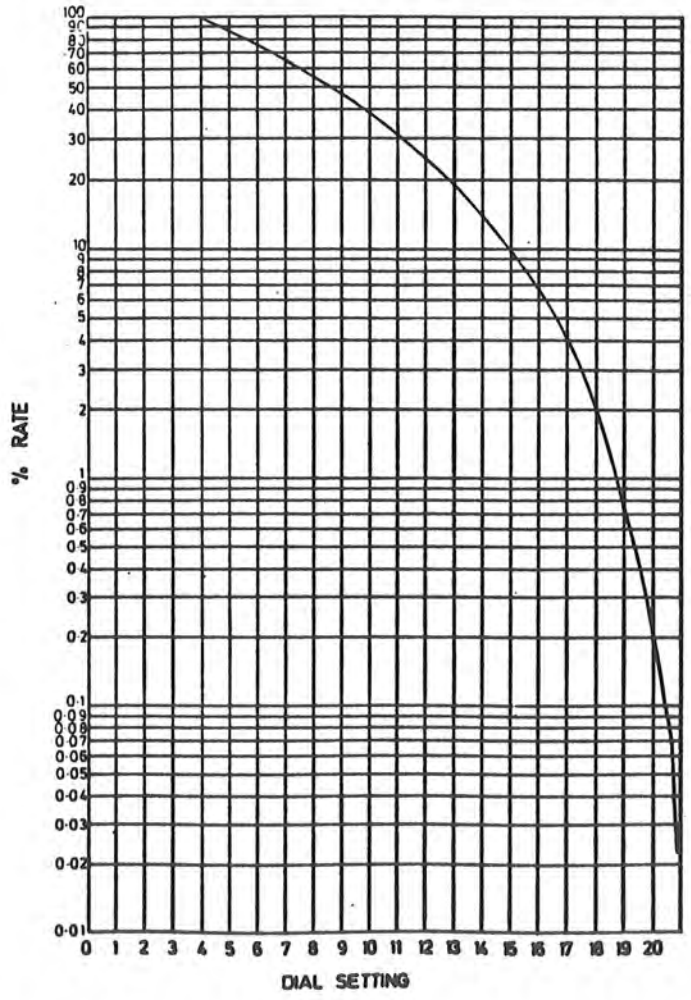

Figure 11. A plot showing the calibration curve supplied for the gas blender.

polarizer which allowed observations to be made with polarized light.

4.6 GAS MEASUREMENTS

Measurements of the conductivity of phthalocyanine in the presence of various ambients were also made. The special equipment used in these experiments is shown in the photograph, fig. (4.10). It comprises a Signal series 850 gas blender which can provide a complete range of gas concentrations of two source gases. The calibration curve supplied for the gas blender is shown in fig. (4.11). As can be seen, the curve of gas concentration versus dial reading levels off, so that only a very small change in the dial setting (at the higher values) produces a large shift in the gas concentration. To overcome this an already diluted gas was used, and further diluted in the blender. This technique also circumvented the problem of having to handle the concentrated gas with its highly corrosive properties. The gas blender outlet was connected, through stainless steel piping, to a purpose-built stainless steel sample chamber, made in the Departmental workshops. All inlets and outlets to the chamber were controlled by valves. These valves were used to operate the system in one of four modes. Mode one allowed the system to be evacuated using the rotary pump shown. In mode two the valves were set so that the chamber was flushed with gas directly from the gas blender, the gases exhausting into an adjacent fume cupboard. In mode three the

valves were set so that the system could be flushed directly from the diluent gas cylinder. In mode four the valves were set so that the blender would exhaust directly to the fume cupboard. This was useful in that it could be used to allow the gas mixture from the blender to reach equilibrium before the gases were directed to the sample chamber.

The sample chamber contained a platform upon which samples could be supported. Connection to the sample was made from the outside of the chamber via eight BNC connectors and a lead-through. Four of these connectors could be used for making connection to the sample and two made connection to a thermocouple positioned on the sample platform. The remaining two made connection to a resistive heater positioned underneath the sample platform. In general, only two of the four connectors used for making contact with the sample were needed. These were used to connect a voltage source across the sample (the voltage applied being 30 V) and to connect in series a Keithley picoammeter, the output of which was fed to an X-t recorder. The sample platform could be heated, by the resistive heater, to temperatures up to 200° C; the temperature of the platform was monitored by a nickel-chrome thermocouple. The general procedure used with the system was to mount the samples on the platform using a simple screw clamp. In order to measure the response time of the device, following the sudden influx of the test gas, the system would first be operated in mode two and the sample flushed with the diluent gas from the blender. The output from the picoammeter would be monitored with time and the

base current level assessed. The system would then be operated in mode four and the required gas concentration dialled in. After five minutes, the system operation would be changed back to mode two, the timing of the change being noted and marked on the chart recorder.

If the measurement to be made was one of variation of response versus gas concentration, the system would be operated in mode two and flushed with diluent gas. Half an hour after a base level had been established the first concentration would be dialled in. The response was then monitored with time and when it had become steady, the level was noted and the next gas concentration dialled in.

CHAPTER 5

PHTHALOCYANINE LANGMUIR-BLODGETT FILMS

5.0 INTRODUCTION

In any practical device incorporating organic films it is essential that the layers have greater stability (thermal and structural) than those of simple molecules customarily used in monolayer investigations. This chapter describes the results of a study carried out into the preparation of LB films of phthalocyanine, a material which is well recognised in the chemical industry as possessing excellent stability. Its importance as a photovoltaic pigment is well established (7,8), although experimental results using evaporated films or dispersions in a resin binder are complicated because phthalocyanine exhibits polymorphism. Phthalocyanine compounds have received little attention in the LB field on account of their almost total insolubility in organic solvents. Other less stable dyes have been used successfully but normally only after substitution with long hydrocarbon chains (9) or dilution with a fatty acid to form a mixed layer (10). Ordered layers of dyes on the surface of semiconductors have also been used to study the transfer of charge carriers from the photoexcited dye to the semiconductor (dye sensitization) (11). It is hoped that the novel phthalocyanine films described in this thesis may be used for a similar purpose and, because of their stability, be

applied in electronic device structures.

5.1 SYNTHESIS OF PHTHALOCYANINE COMPOUNDS

The following section describes the synthesis of the phthalocyanine compounds used in this work. Some of the materials were received from ICI Ltd, but for completeness a brief description of their synthesis is also included.

Dilithium phthalocyanine

Dilithium phthalocyanine was synthesised following the published method (12) by the reaction of phthalonitrile with lithium metal in amyl alcohol and extraction of the product with acetone to give crystalline material with a purple lustre.

Tetra-4-tert-butyl phthalocyanines

The tetra-4-tert-butyl phthalocyanines were prepared by the method of Mickhalenko et al (13). This involved the synthesis of 4-ter-butyl phthalonitrile. The procedure adopted was the synthesis of 4-ter-butyl-o-xylene from o-xylene and ter-butylchloride using ferric chloride as a catalyst. The 4-ter-butyl-o-xylene was oxidised to 4-ter-butyl-phthalic acid with alkaline potassium permanganate. This was converted to 4-ter-butyl phthalic anhydride by heating with urea at 170° C to give 4-ter-butyl phthalimide. This, when stirred with ammonia

at room temperature for 24 hours gives 4-ter-butyl phthalamide, which reacts with phosphoryl chloride in the presence of anhydrous pyridine to give 4-ter-butyl phthalonitrile.

4-ter-butyl phthalocyanine condenses in sodium/iso-amyl alcohol solution in the presence of a catalytic amount of ammonium molybdate at 180°-190° C to give metal-free 4-ter-butyl phthalocyanine. This material was purified by column chromatography on alumina using chloroform as a solvent.

Metal substituted Tetra-4-ter-butyl phthalocyanines

Metal substituted Tetra-4-ter-butyl phthalocyanines were prepared in a similar way by the addition of appropriate transition metal ions in the reaction mixture and then purified by column chromatography on alumina using chloroform as a solvent.

5.2 PREPARATION OF LANGMUIR FILMS

In the formation of a floating monolayer there are a number of steps which must be carried out. First, the preparation of a suitable solution from which the material can be spread. Second, the establishment of the required conditions for good layer formation. This section covers the development of these stages.

5.2.1 CHEMISTRY OF DILITHIUM PHTHALOCYANINE FILMS

The first material that we wished to deposit as an LB film was metal-free phthalocyanine. However metal-free phthalocyanine is insoluble in all the common solvents and is only sparingly soluble in others. The approach used was the novel one of using dilithium phthalocyanine which is unusual in that it is soluble in a number of common organic solvents, e.g. ethanol and acetone. Relatively little is published about this most interesting compound which we abbreviate to Li_2Pc. However, it is known that it can be rapidly hydrolysed to metal-free phthalocyanine and can undergo metal exchange reactions in alcoholic solutions.

$$Li_2Pc + H_2O = 2LiOH + PcH_2\downarrow$$

$$Li_2Pc + M(NO_3)_2 = MPc\downarrow + 2LiNO_3$$

Where M is typically a first row transition metal.

Thus, a solution of Li_2Pc in acetone, when carefully transferred onto an aqueous surface will form in situ insoluble metal-free phthalocyanine in the form of a surface layer; and under appropriate conditions (pH, metal ion concentration, subphase) it is possible to form films of various metal phthalocyanines.

5.2.2 SOLVENTS

The solvent most commonly used for the spreading of Langmuir films is chloroform. Not only is it a good organic solvent but also it is almost immiscible with the subphase and has a moderate evaporation rate. Few phthalocyanines, however, are soluble in chloroform apart from some of the substituted phthalocyanines. Also, it must be remembered that it is not enough to find a solvent which dissolves phthalocyanine; the solvent must also satisfy other essential criteria, such as insolubility in the subphase.

Another difficulty which manifested itself in the process of developing methods of preparing phthalocyanine LB films was that the Langmuir films were found to have a high surface viscosity. This resulted in the problem that when material was removed from the surface during the deposition of the film it did not flow so as to replenish the supply.

This section covers the different spreading solvents which were prepared to solve these problems. An optical characterisation of these solutions is included in chapter 6.

Dilithium phthalocyanine

As mentioned in section 5.2.1, this material could be easily dissolved in acetone. However the solution had to be prepared freshly each day, as problems were encountered with the hydrolysis of the material to the metal-free on extended

storage. Li_2Pc solutions were prepared by dissolving the material in acetone (previously dried with a molecular sieve) to make a solution of 1mg/cc concentration. This starting solution was then diluted with various other solvents to form the required spreading solvents. A common additive was chloroform which was used to try and improve the spreading characteristics. The solution normally required filtration before use to ensure the removal of any hydrolysed material. This immediately presents a problem if area calculations are required as the concentration of the solution must be known. This was established by the following procedure: First, a sample of known volume was taken from the filtered solution and evaporated to dryness in a container of known weight. On reweighing the container the weights are subtracted to give the mass of material in the known volume, hence a value for the concentration of the solution can be calculated. Second, the optical absorbance of another sample was measured at the same time, and from these measurements a value for the optical absorption coefficient was calculated. This was then used on subsequent occasions to determine the concentration of other solutions. From these measurements a value of 1.54×10^5 was obtained for the extinction coefficient.

However when film preparation alone was to be carried out and no area calculation was required, it was a laborious procedure to have to filter the whole solution each time. Also the practice was wasteful of material. A practical solution to this problem was devised whereby a small filter holder was

designed to act as an "inline filter" which could be fitted over the end of the micrometer syringe. A schematic diagram of the device is shown in fig. (5.1).

Mixed layers

An approach which has been used with some dyes in order to achieve good deposition is to incorporate the dye into a fatty acid matrix. This alternative approach to depositing the dye in a monomolecular layer was also attempted with the phthalocyanines. The spreading solution was prepared by mixing aliquot parts of dilithium phthalocyanine dissolved in acetone and stearic acid dissolved in chloroform. In the work presented here, various molecular mixtures of stearic acid and dilithium phthalocyanine were investigated.

Manganese phthalocyanine

The solubility problem experienced with the metal-free phthalocyanine is also present with manganese phthalocyanine. However it is known that the material can be dissolved in tetra-hydro-furan (THF) and therefore solutions were prepared using this solvent. The material did not dissolve instantly in the solvent, but appeared to dissolve slowly over a period of an hour or so.

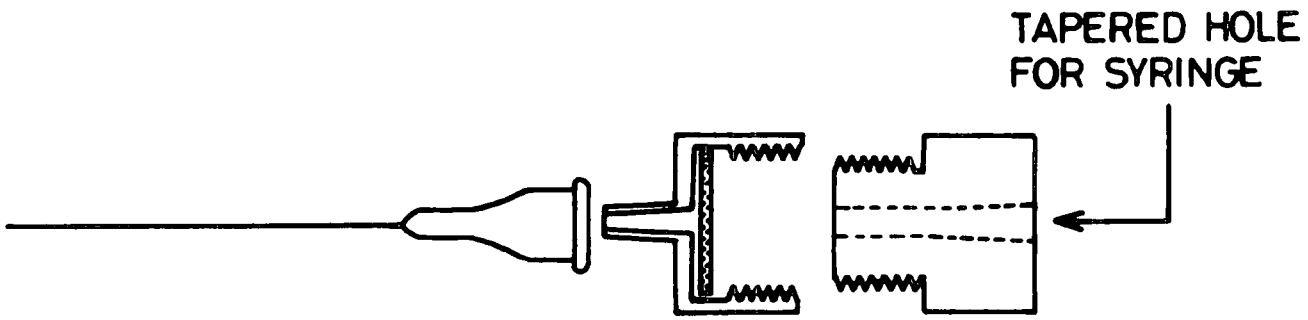

IN-LINE FILTER FOR METAL-FREE PHTHALOCYNINE SOLUTIONS

Figure 1. A shematic diagram of the "in line" filter used when spreading metal-free phthalocyanine

Tetra-tert-butylphthalocyanines

The great advantage of these compounds is that the tetra-tert-butyl substitution gives the material solubility in solvents such as toluene, xylene and chloroform. Moreover, for most of the metal-free and metal substituted compounds, the solution is stable and can be kept indefinitely.

Asymmetric copper phthalocyanine

This material is similar to the tetra-tert-butyl compounds in that it is also soluble in a range of solvents such as toluene, xylene and chloroform. The solution is again quite stable with no deterioration being observed over storage periods of many months. The solution concentration used was approximately 0.5 mg/cc.

5.2.3 Subphase preparation

As mentioned earlier the subphase is critical in the production of high quality Langmuir films. Apart from the asymmetrically substituted copper phthalocyanine, the stability of which was found to be pH dependent, the phthalocyanines were found to be unaffected by the pH of the subphase. The pH was allowed to settle at 5.54 (the value at which the pH naturally levelled out due to absorption of atmospheric carbon dioxide) for the preparation of films of the metal-free and the

tetra-tert-butyl compounds. However for the asymmetrically substituted copper phthalocyanine the pH was found to be best above 7.0 and was normally set initially at 9.0. At low pH values the area covered by the film was observed to decrease owing to the dissolution of the material into the subphase. Fig(5.2) shows the rate of collapse at low and high pH. The dissolution of material at low pH can be explained in terms of protonation of the amine group which gives the material water solubility. The lower the pH the greater the protonation of the amine groups in the phthalocyanine molecule until all three groups are protonated, this species having quite a high solubility in water. For the preparation of the mixed layers the usual dipping conditions for stearic acid were followed i.e. a pH value of 5.8 and $CdCl_2$ added to a concentration of 2.10^{-4} M/l. The addition of simple metal salts to the subphase was not found to affect the stability of the Langmuir films.

One of the problems encountered in the preparation of multi-layer LB films of some of the phthalocyanines, was poor adhesion of layers following the initial layer. It was observed that although material was removed from the slide when the barriers were expanded, no material was removed if the film was maintained under compression. However this could not be used as the normal deposition method because some material was deposited in the form of striations on the substrate. This was interpreted as the surface pressure of the film counteracting the surface tension of the water which would tend to pull the layer from the slide. Thus if a subphase was used which had a

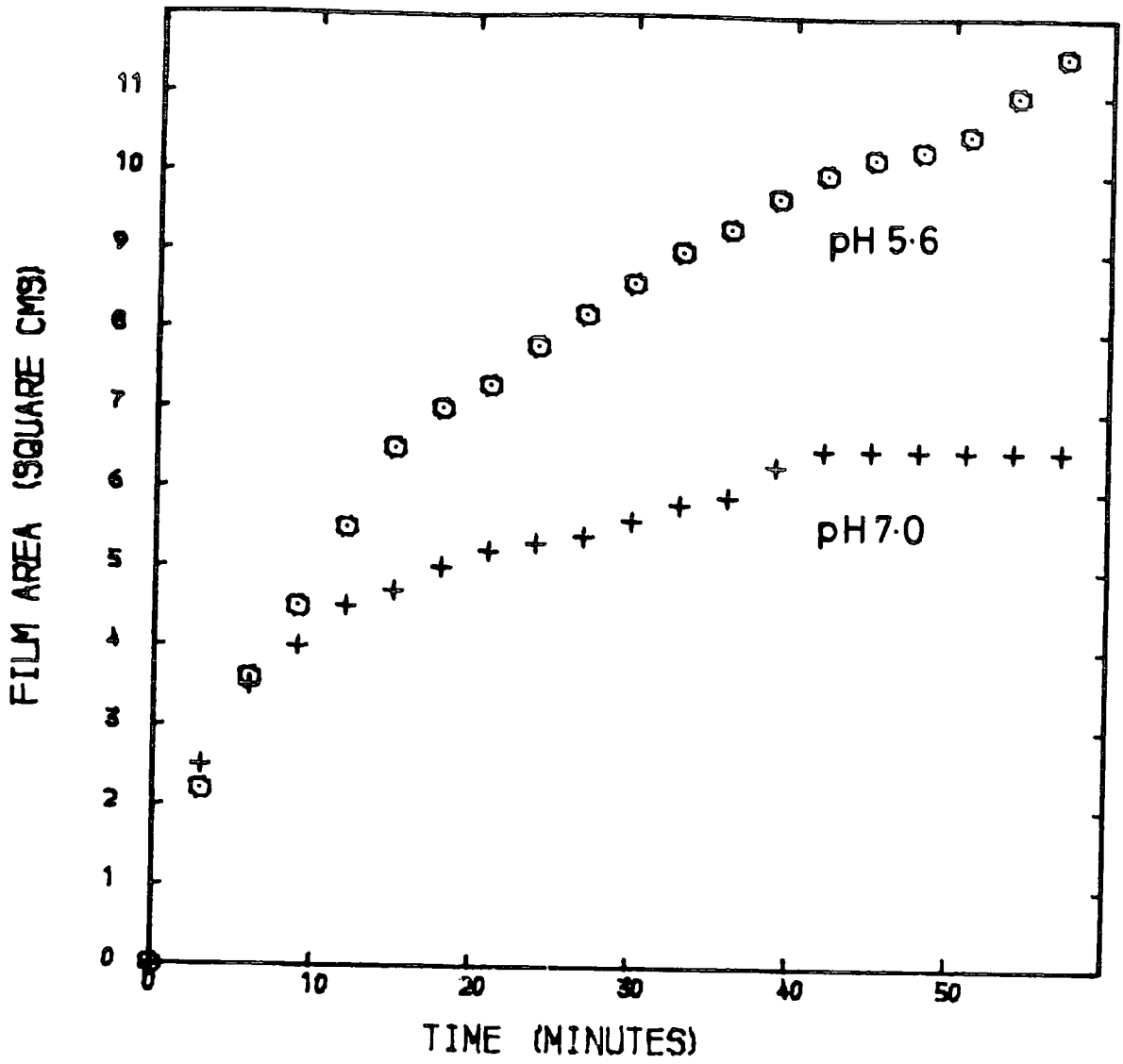

Figure 2. Variation of the area decay of a Langmuir film of ASY-CuPc with the pH of the subphase.

lower surface tension, it could improve the quality of the multi-layer films. Various organic liquids were investigated, but it was found that a certain surface pressure was required to enable droplets of solution to spread on the surface. The drops either formed lenses on the surface, or in the case of liquids with a very low surface tension, were not supported on the surface at all, and thus sank to the bottom of the container.

An alternative approach was tried using a mixed subphase. A graph showing the surface tension for various mixtures of water and ethanol is given in fig (5.3). From this it can be seen that a pressure reduction of 15 dynes/cm can be achieved with the incorporation of only 5% ethanol. Various mixtures were evaluated and a mixture containing 2% ethanol was found to be the optimum; mixtures with a higher percentage suffered from poor spreading of the dispersing solvent. Results showing the type of isotherm obtained with this subphase and the effect on deposition are described in sections 5.3 and 5.4 respectively.

5.3 ISOTHERMS

The isotherms of phthalocyanine were obtained as outlined in chapter 4. The information which can be extracted from these, can be broken down into two main areas; First, the area per molecule as calculated from the isotherm can be used together with the known cross-sectional areas of the molecule to give an indication of its orientation. Second, the form of the isotherm can be used to provide information on phase transitions

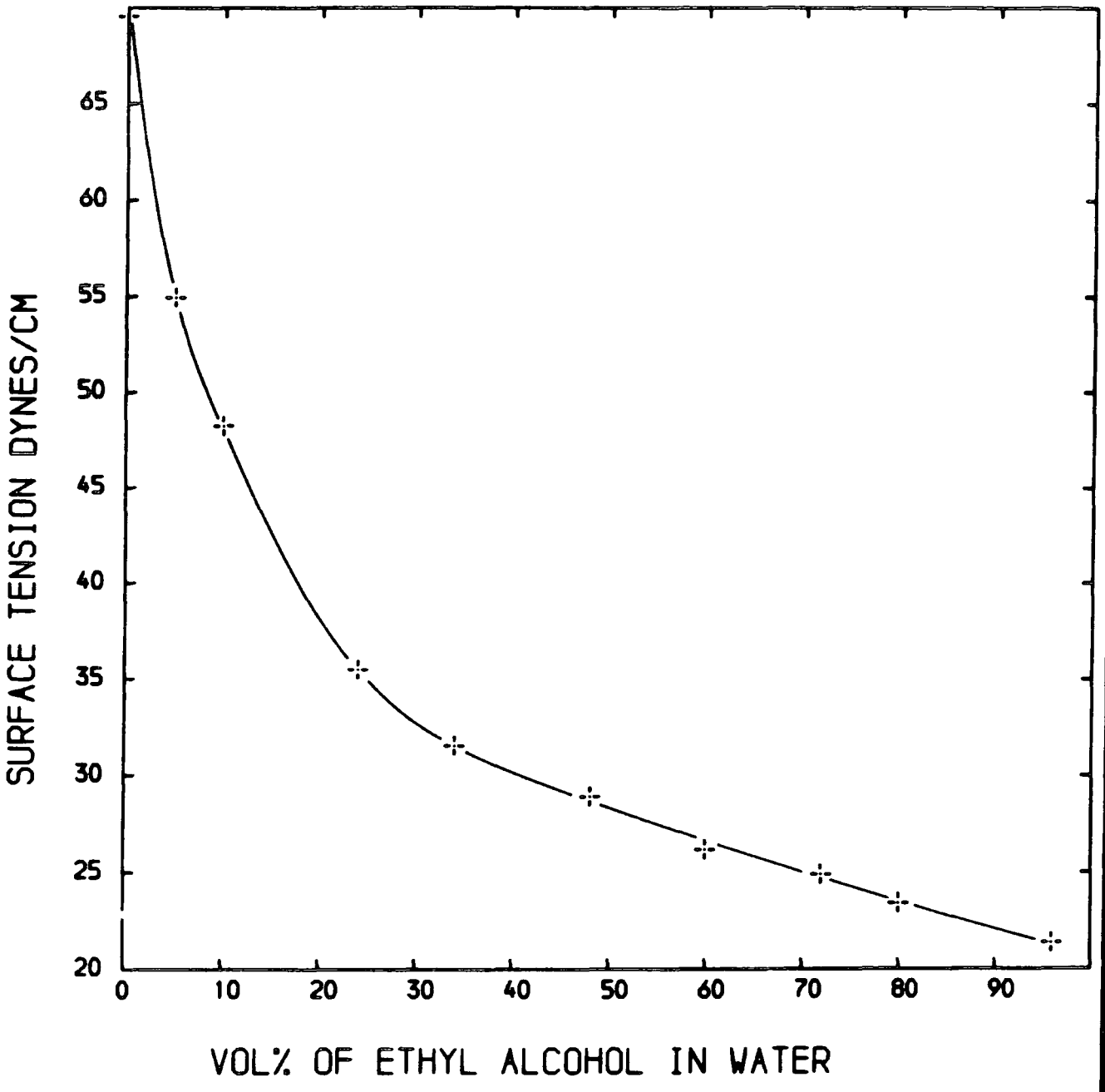

Figure 3. The variation of surface tension with various mixtures of water and ethanol.

occurring within the layer. On this latter point it should be mentioned that, in general for phthalocyanines, no distinct structure is observed in the isotherm, unlike those obtained for the fatty acids. The absence of sharp transitions between the different phases is due to molecular realignment occurring throughout the gaseous and liquid stages of the isotherm. This is also the accepted explanation for the short chain aromatic compound, C4 anthracene (14) and other molecules showing similar types of isotherm such as merocyanines (15) and porphyrins (16). The form of the isotherm depends critically on the metal ion at the centre of the molecule, the form of substitution and the spreading solvent, pH etc. We now outline our efforts to obtain optimum conditions for the floating Langmuir film in order that good quality phthalocyanine layers can be deposited on suitable substrates.

5.3.1 Isotherms for metal-free unsubstituted phthalocyanine

This sub-section includes isotherms for metal-free phthalocyanine spread from the dilithium phthalocyanine solutions described previously. Two distinct types are discussed: (a) Isotherms prepared directly from the solvent used to affect dissolution of the material, and (b) those obtained using various solvent mixtures to enhance the spreading and deposition properties of the Langmuir film.

Simple solvent

Fig. (5.4) is a typical isotherm obtained for metal-free phthalocyanine spread directly from acetone. The figure shows both the compression and expansion isotherms. The first observation to be made from the isotherm is that the area per molecule as calculated from the isotherm, is 8.8 $\mathring{A}^2$. This is considerably smaller than that expected for a configuration corresponding to the molecule packing edge on (40 $\mathring{A}^2$) or packing face down on the subphase (160 $\mathring{A}^2$). This implies that in this type of deposition the molecules are stacked, or have formed aggregates on the surface of the subphase. The second observation relates to the form of the two isotherms. The compression isotherm is curved with no distinctive features, whilst the expansion isotherm appears to consist of a gaseous and condensed phase only. Subsequent compression isotherms were found to take the form of the expansion isotherm. Further discussion, and an explanation of the shape of the isotherm will be covered when describing the next set of isotherms.

The films were also found to have a high surface viscosity. This was evidenced by a simple "suction test" which was carried out on all materials: this was accomplished by holding the film under constant pressure in the control mode; material was then removed from the dipping area by the use of the suction pipe used for cleaning the surface of the trough, and the barriers observed for signs of movement. In general three typical responses could be identified. With a material such as stearic

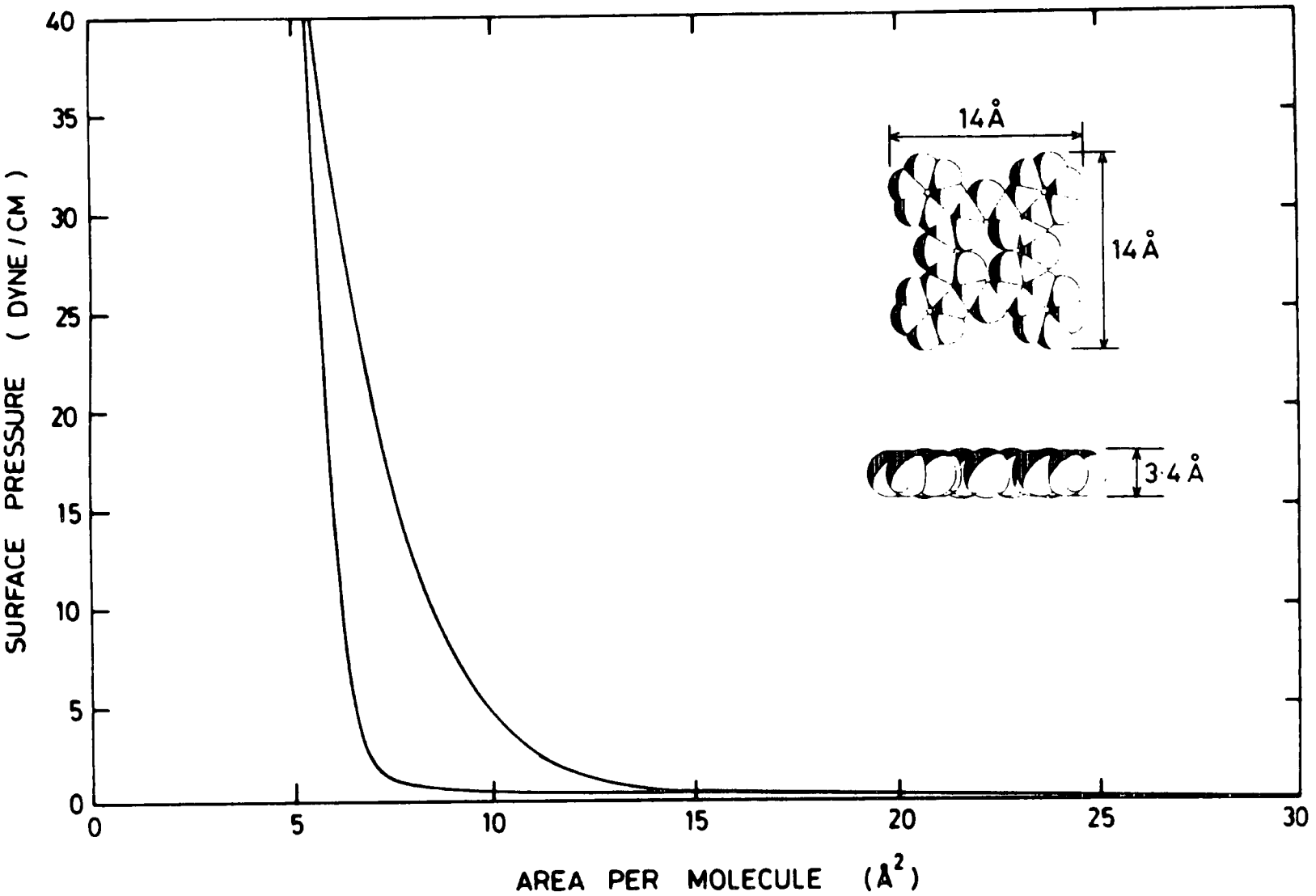

Figure 4. A typical isotherm for metal-free phthalocyanine spread from acetone.

acid, the barriers were observed to respond instantly to removal of the film. Any material which behaved likewise was classed as giving a type A response. Materials where a delayed or sluggish response was observed were classed as type B and materials which gave little or intermittent response were classed as type C. In the case of the metal-free phthalocyanine spread from acetone, the Langmuir films were found to fall in to class C.

Mixed solvent

The isotherm discussed previously showed that the Langmuir film obtained for metal-free phthalocyanine spread from acetone, has a smaller area per molecule than expected and suffers from rigidity due to the high surface viscosity of the layer. The isotherms shown in fig. (5.5) were taken for metal-free phthalocyanine spread from various modified solvents. Fig. (5.5a) shows the type of pressure-area isotherms obtained using a simple mixture of solvents, namely acetone and chloroform. The chloroform was added to aid the spreading of the solution, as observations on the spreading of the acetone solution showed that some material appeared to be entering the subphase. This could be expected to some extent, as acetone is miscible with water. As can be seen from the isotherm, the incorporation of chloroform increases the calculated area per molecule to 14.7$\AA^2$, an increase of 67%. This increase can be attributed to two factors; first, an improvement in the spreading of the material leading to less aggregation occurring, and second, a reduction

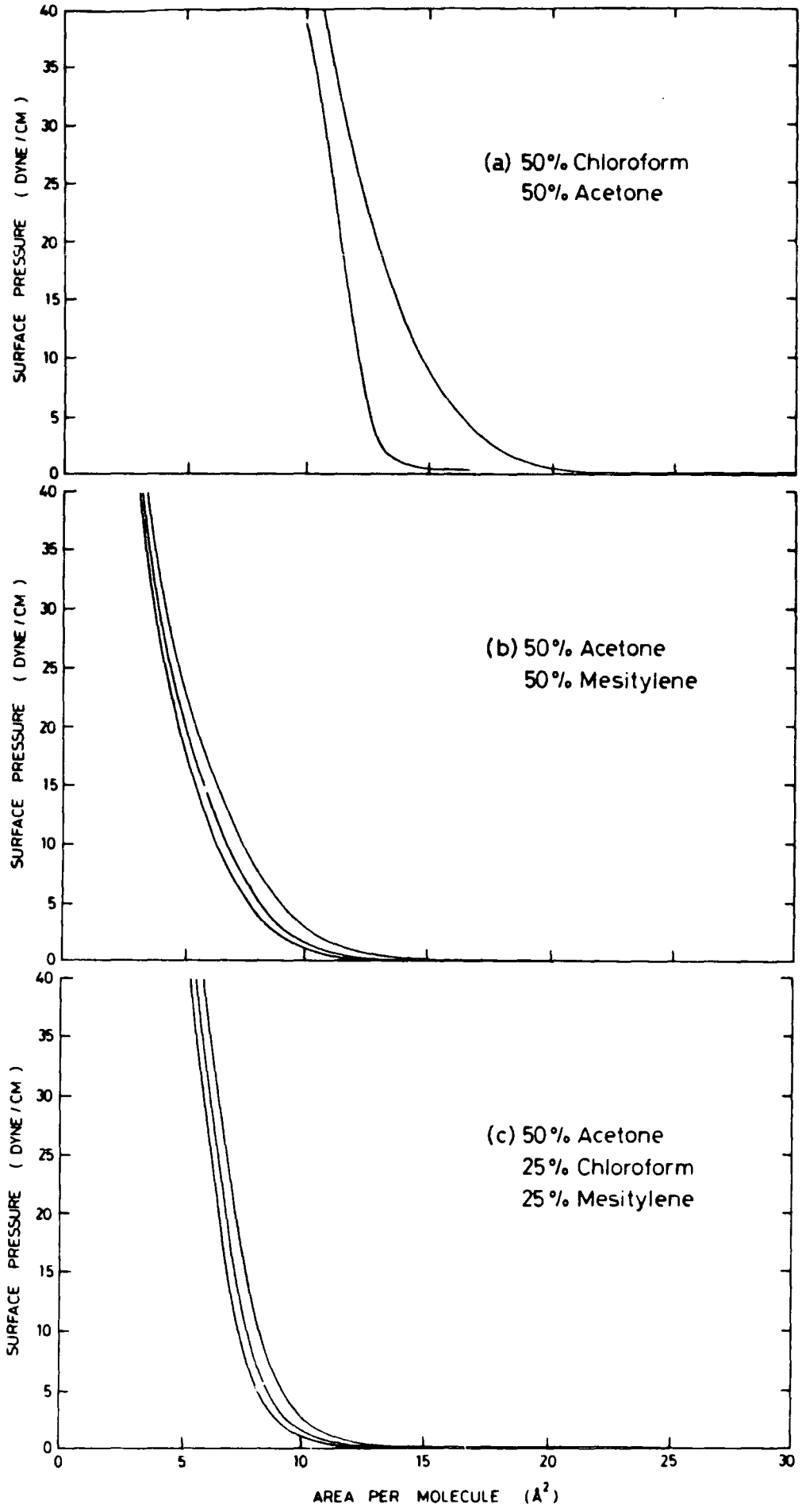

Figure 5. A range of isotherms for metal-free phthalocyanine showing the variation with spreading solvent.

in the interaction of the acetone with the water, thereby reducing the amount of material lost to the subphase.

As with the isotherms obtained for metal-free phthalocyanine spread from acetone, the chloroform/acetone mixture produces a curved isotherm with no distinctive features. The recompression produces an isotherm which again appears to consist of gaseous and condensed phases only. Subsequent compressions enhance this distinction, whilst the area per molecule remains the same after the second compression. The change in the character of this isotherm and that for material spread from acetone, can be interpreted as follows; during the first compression the molecules are free to move and align themselves relative to each other as they are compressed, producing an intermediate state between the gaseous phase and the condensed phase. However, once brought in to close contact in the condensed state the molecules tend to lock together and, on expanding the area, remain locked together in small plates. On recompression these plates come back together resulting in the isotherm showing less intermediate behavior due to there being little realignment between molecules during the compression.

When tested with the suction test these films were again found to be rigid, and gave a type C response. It should also be noted that when compressed, the above films form an extremely stable layer with no appreciable collapse being evident over a period of many hours.

Lubricating solvent

The problem of rigidity in a Langmuir film is a very important one as it is a major factor in characterising the ease with which it may be deposited as a Langmuir Blodgett film. The films so far described were found to be very rigid as evidenced by the type of response they exhibited with the suction test. In fact it could be observed during the test that as material was removed, it left a hole in the film which was not filled by material replacing it from the surrounding area. For this reason we decided to further modify the spreading solvent by the incorporation of slowly evaporating solvents whose purpose was to provide "lubrication" for the molecules, thus enabling them to move more freely in the layer. Figure (5.5b) shows the pressure-area isotherm using a spreading solution containing equal proportions of acetone and mesitylene (1,3,5 trimethyl benzene). The first compression again produces a curved isotherm with no distinctive features. On recompression however, in contrast to the simple solvent case, little change is observed in the form of the isotherm, indicating that the locking together of molecules has been and continues to be, inhibited over several compressions.

Three component solvent

Using the above principle it was possible to improve the rigidity, fresh and aged films exhibiting type A and B responses, respectively, to the suction test. However, the area per molecule obtained using this combination of two spreading solvents is smaller than the area obtained using acetone by itself, indicating an extremely poor quality layer. The next step was to try and incorporate the superior spreading qualities of the chloroform mixture with the more fluid properties obtained by the incorporation of mesitylene. Figure (5.5c) shows a typical isotherm obtained using a spreading solution comprised of 50% acetone, 25% chloroform and 25% mesitylene. The isotherm is very similar to that described for the previous mixture but with slightly less curvature. The film was found to exhibit a type B response to the suction test for both fresh and aged layers. The calculated area per molecule is 8.8 A which is comparable to that observed for layers obtained using acetone solution.

Summary

The above results indicate that using simple mixtures of solvents, the films produced on the subphase are very rigid and therefore difficult to transfer to a substrate. The addition of mesitylene, which evaporates relatively slowly, provides the required "lubrication" and enables transfer of the film to a

substrate. However, the area occupied by the molecule in the film is less than the surface area of the edge (40 $\AA^2$) or the face of the phthalocyanine molecule (160 $\AA^2$), indicating that the molecules in the film are stacked. The stacking appears to be reproducible, since similar values for the area per molecule are obtained under a wide range of film preparation conditions. Most importantly however, the films produced are not rigid and therefore can be transferred to a substrate.

Experiments were carried out with many other solvent combinations during the course of this work. The examples covered illustrate the main features and the optimum combinations that were found. A selection of results is summarised in table (5.1).

A further experimental observation which emphasizes the problem of rigidity with these materials is outlined below. Before the commissioning of the trough described in this thesis, a small experimental trough was used to obtain some preliminary results. Two interesting observations were found when the area per molecule was calculated for various amounts of material spread from the chloroform/acetone mixture, a) a variance in the value obtained and b) the smaller the area enclosed by the barriers the larger the calculated area per molecule. This was attributed to fact that the rigidity of the film prevented it moving into the legs of the barriers as the film was compressed (in the case of the small trough the area of the legs is quite significant -at minimum area they occupied 50% of the total area). Table (5.2) shows the values obtained for the films as

AREA ENCLOSED BY BARRIERS (CM^2)	AREA PER MOLECULE ($\mathring{A}^2$)	CORRECTED AREA PER MOLECULE ($\mathring{A}^2$)
122	15.3	10.1
164	12.4	9.5
198	10.7	8.8

Table 5.2 Showing the change in calculated area per molecule with barrier position.

calculated from the isotherms and adjusted so as to neglect the area occupied by the legs. It can be seen that the molecular areas obtained with the barrier leg area neglected correspond more closely with one another, having a variance of 0.7 compared to 2.7 for the raw data. Perfect agreement is unlikely to be achieved as the assumption that absolutely no material enters the leg is unlikely to be strictly valid. A further possible explanation is that the material in the legs is unlikely to be in a state of equilibrium with the material in the main section enclosed by the barriers. This effect was not observed on the trough used in this thesis, but of course the relative area occupied by the legs was much smaller.

5.3.2 Isotherms for mixed layers of Li_2Pc and fatty acids

When it has proved difficult to deposit a material using standard techniques, one solution has been to incorporate it into a layer formed by one of the fatty acids. This has been successfully carried out for materials such as the merocyanines and various other dye-type materials. In our case the dilithium phthalocyanine was spread along with stearic acid. The form of the isotherms differed from a standard unstructured phthalocyanine type of isotherm in that the degree of structure observed in the mixed film depended on the amount of stearic acid present. A range of isotherms showing this variation is presented in fig. (5.6). At the lowest percentage used (10.6%), the form of the isotherm (e) is curved and similar to

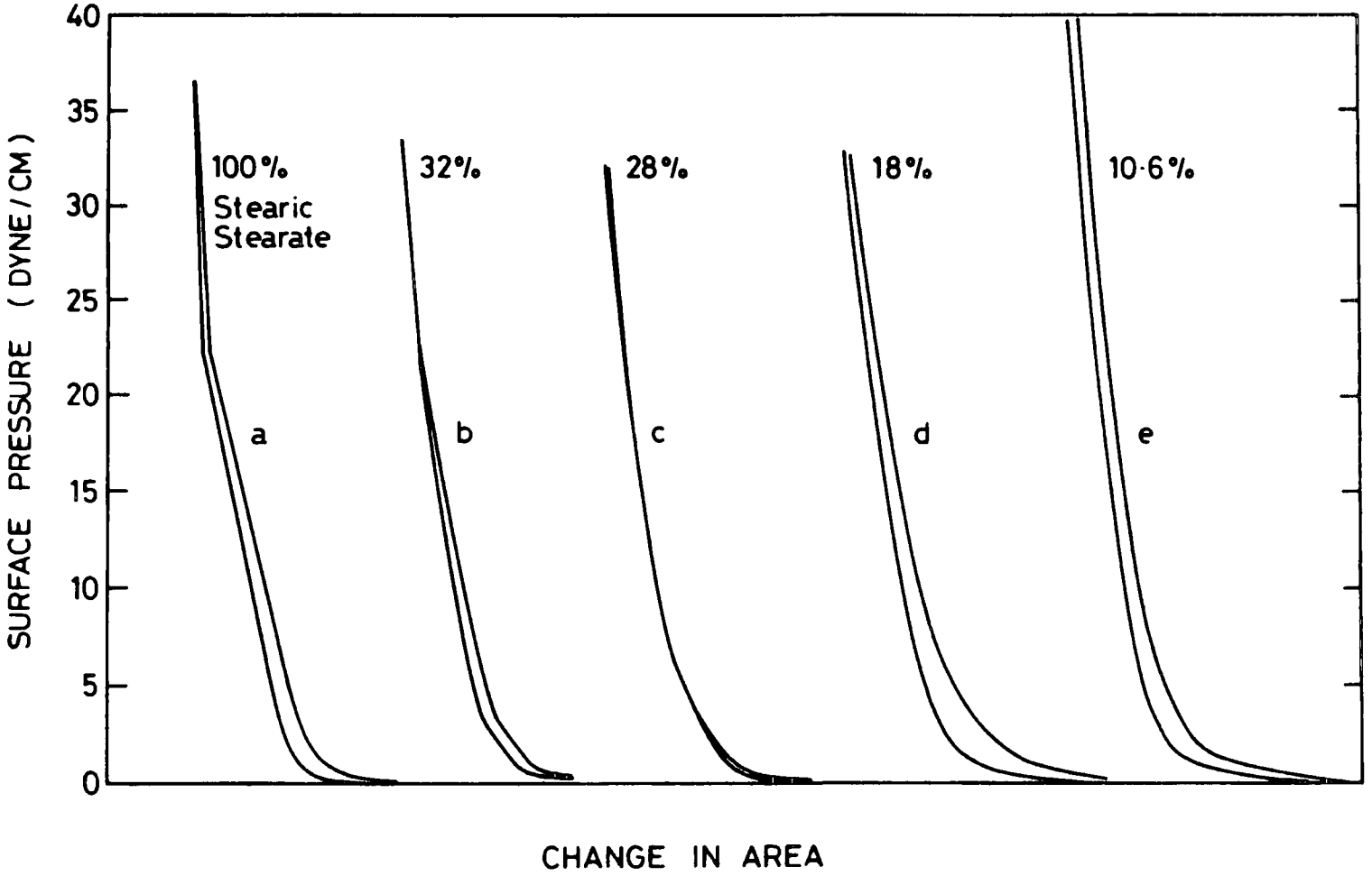

Figure 6. A range of isotherms showing the variation with percentage of incorporated stearic acid.

those obtained for an acetone or chloroform/acetone mixture; however, the second compression follows the first reasonably well. With the film containing 18% stearic acid, the isotherm (d) shows a more gradual slope to the curve. With 28% stearic acid in the film a slight structuring can be observed in the isotherm (c) and with 32% (b) a definite structure becomes apparent.

The area that would normally be occupied by the stearic acid in the film can be calculated from the solution concentration. This value may then be subtracted from the total area occupied by the mixed film and the area per molecule for the phthalocyanine calculated. The calculated area per molecule obtained is invariably smaller than that expected for the true molecular cross section, and in some cases is found to be less than zero. This result indicates that the phthalocyanine is being squeezed out of the film.

5.3.3 Isotherms for unsubstituted manganese phthalocyanine

This material was obtained from the Eastman Kodak company and screeening tests were carried out to see if the inclusion of a metal ion in the central part of the molecule would alter its film-forming properties. The material was found to dissolve in tetra-hydro-furan (THF) and was spread upon the trough using this as a spreading solution. As can be seen from the isotherms in fig. (5.7) there is no structure and very little curvature. However, the area per molecule obtained is 76$\AA^2$ which is a

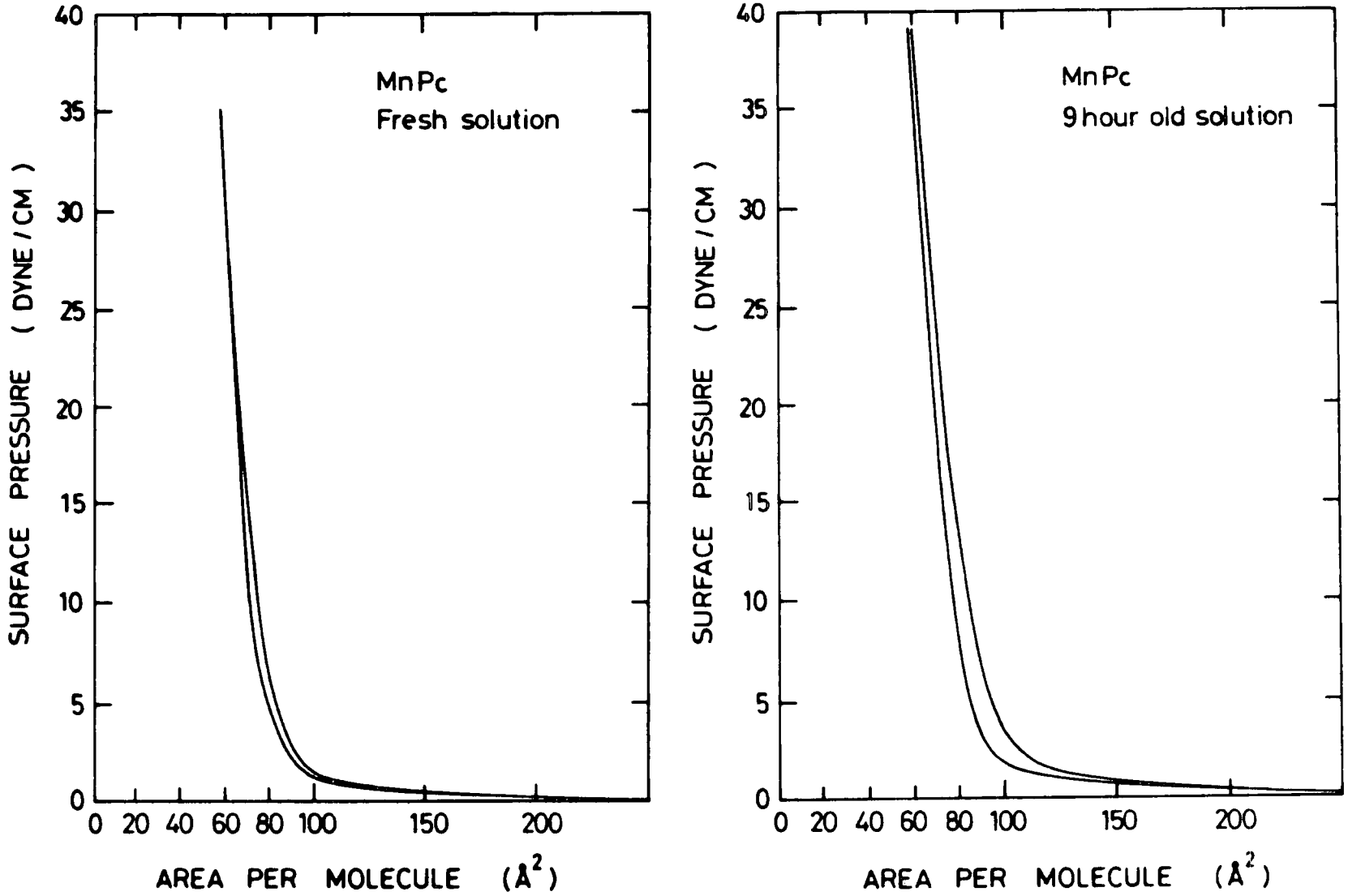

Figure 7. Isotherms for manganese phthalocyanine taken for both a fresh and a 9 hour old solution.

considerable improvement on that obtained for metal-free films. This value is consistent with the cross-sectional area of the edge of the molecule, indicating that the molecules are stacked vertically edge on in the film. The inclusion of a metal in the central co-ordinating region of the molecule therefore makes a large difference to the packing of the molecules. The metal atom is known to alter the intermolecular distance, which possibly interrupts the stacking and hence reduces the level of aggregation.

When the solution was prepared it was coloured blue, but after a number of hours the colour was observed to have changed to green. This can be interpreted as an alteration in the oxidation state of the manganese. Fig.(5.7) shows the isotherms obtained from both a freshly prepared solution and the same solution left for 9 hours. Little difference is observed in either the form or indicated area per molecule, implying that this change in oxidation state plays no real part in the alignment of the molecule. Further isotherms were measured on the dilithium phthalocyanine using THF as the solvent, to eliminate the possibility that the improvement observed with the manganese phthalocyanine could be due to the use of the THF as the spreading solvent; these however did not produce any significant difference from the isotherms already mentioned.

5.3.4 Isotherms for 4-ter-butyl phthalocyanines

Two types of 4-ter-butyl phthalocyanine were investigated; metal-free and metal substituted molecules. The metal containing compounds investigated were copper phthalocyanine, zinc phthalocyanine, and manganese phthalocyanine. All materials mentioned could be used to produce Langmuir films, but of varying quality depending on the solvents used. The following section covers firstly, the type of isotherm obtained with the metal-free form and secondly, those found with the metal substituted materials. Finally, the effect of using different solvents with these materials is discussed.

Metal-free 4-ter-butyl phthalocyanine

The metal-free 4-ter-butyl phthalocyanine was found to be an easy material to handle. The solvent used to effect dissolution of the material was toluene and this was diluted with chloroform to aid spreading. The material formed a much higher quality film, with a higher area per molecule than the metal-free phthalocyanine. A typical isotherm is shown, fig. (5.8). As can be seen, the calculated area per molecule is 34.3Å^2. The minimum expected molecular cross-sectional area would be 60Å^2, if interlocking of the ter-butyl groups is assumed. The value obtained is thus less than that expected and is indicative of either the formation of a bilayer or of a certain degree of aggregation occurring within the film. The

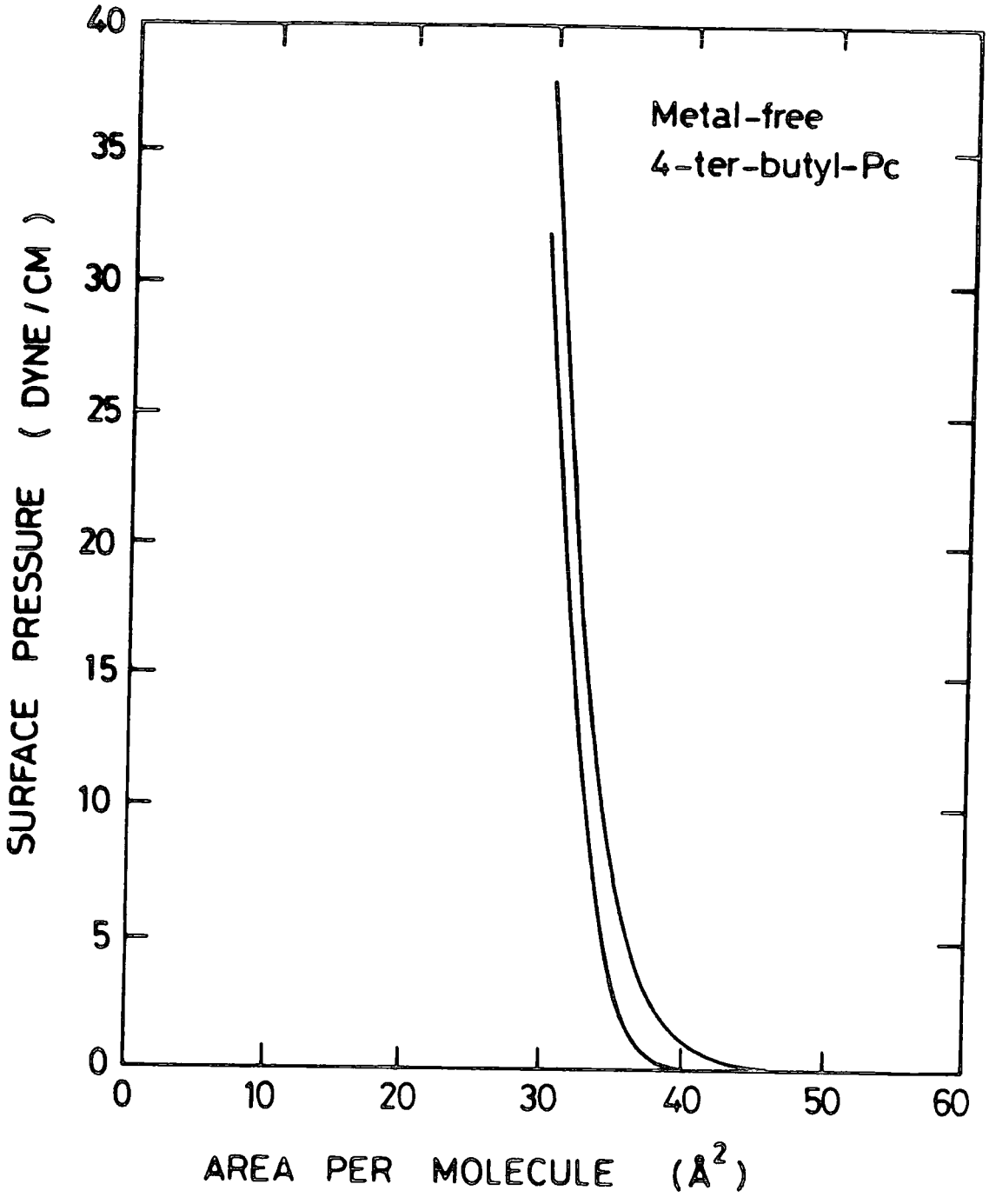

Figure 8. Isotherm for metal-free 4-ter-butyl phthalocyanine.

form of the isotherm again shows a smooth transition from the gaseous to the solid stage, but the curve is more gently sloped than the isotherm obtained for metal-free phthalocyanine.

Metal substituted 4-ter-butyl phthalocyanines

The metal substituted phthalocyanines were the next materials studied. They were found to exhibit better film forming properties than the metal-free form, although a variation of the film properties was found with different spreading solvents. For illustrative purposes isotherms will be shown for films spread from both chloroform and xylene. The main feature of these isotherms is that the area per molecule obtained is much higher than for those materials covered so far. A comparison can also be drawn between the metal-free phthalocyanine and manganese phthalocyanine. For in this case also, the incorporation of the metal atom into the molecule seems to improve the film formed, in that the calculated area per molecule is higher and the film is not as rigid as the metal-free form.

Copper 4-ter-butyl phthalocyanine

Figure (5.9) shows the isotherm for copper 4-ter-butyl phthalocyanine spread from xylene; the molecular structure is shown in the inset. The area per molecule obtained is 87.4$\AA^2$ which can be related to the molecule standing on its edge on the

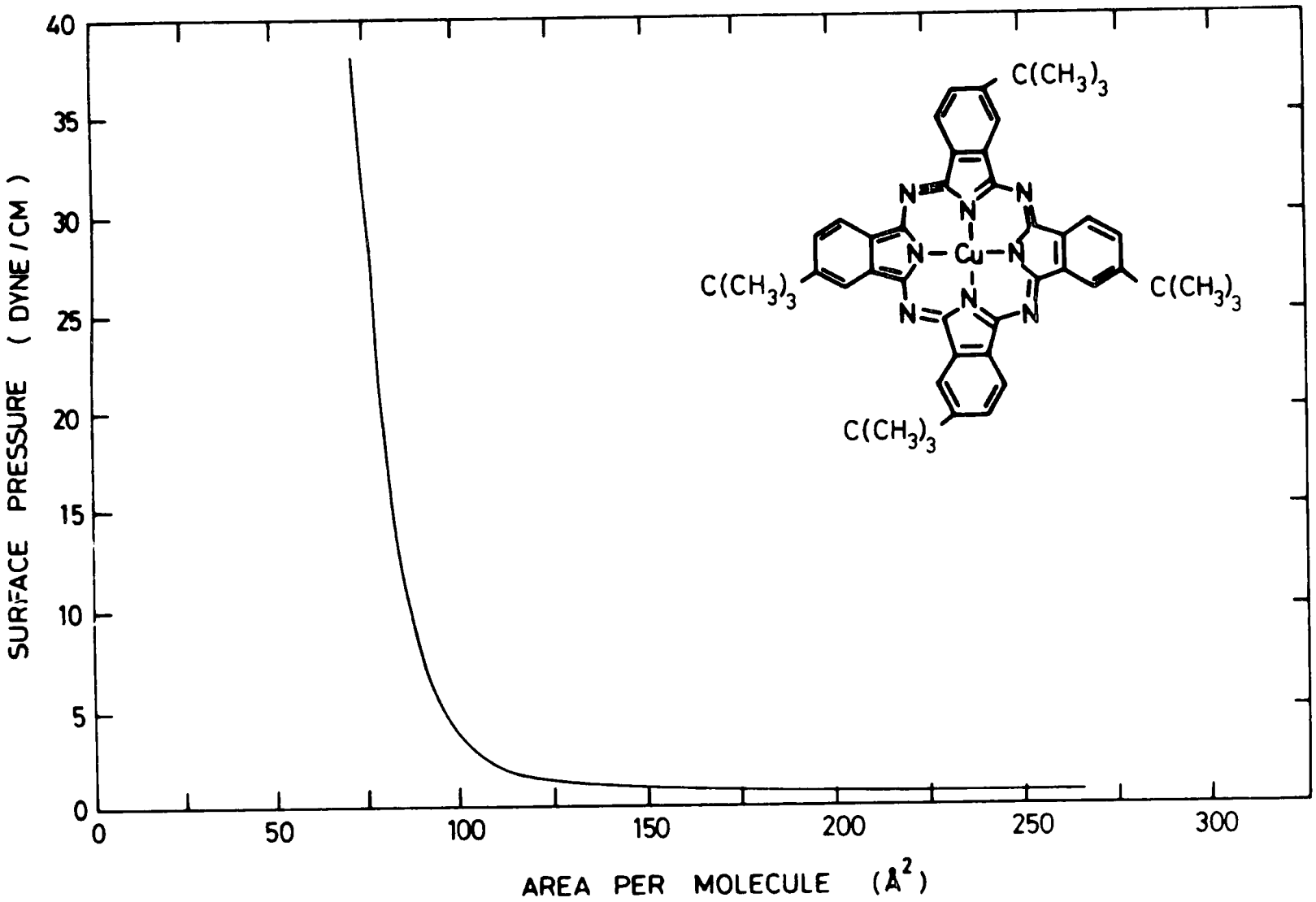

Figure 9. A typical isotherm for copper 4-ter-butyl phthalocyanine spread from xylene.

subphase. It should be borne in mind that the calculated area per molecule alone, does not provide conclusive evidence of the molecule's orientation. For example in the present case an alternative explanation would be that the molecules are lying flat and stacked five high on the water surface. Confirmation of the orientation must come from other independent measurements. Various methods of achieving this are discussed in the following chapters covering the characterisation of the films. No isotherm is shown for the material spread from chloroform, as considerable aggregation was observed upon spreading and throughout the compression.

Zinc 4-ter-butyl phthalocyanine

Fig. (5.10) shows isotherms obtained for zinc 4-ter-butyl phthalocyanine spread from both chloroform and xylene. The calculated areas per molecule obtained from both graphs (92Å^2 and 91Å^2 respectively for the chloroform and xylene spreading solutions) are fairly similar to that obtained for the first compression. However the expansion isotherm for the film spread from chloroform gives quite a different value, indicative of rigid layer formation. The responses of the film to the suction test, were type C with chloroform as the speading solvent and type B with xylene. Again the calculated areas per molecule are best explained by the molecule being stacked edge on.

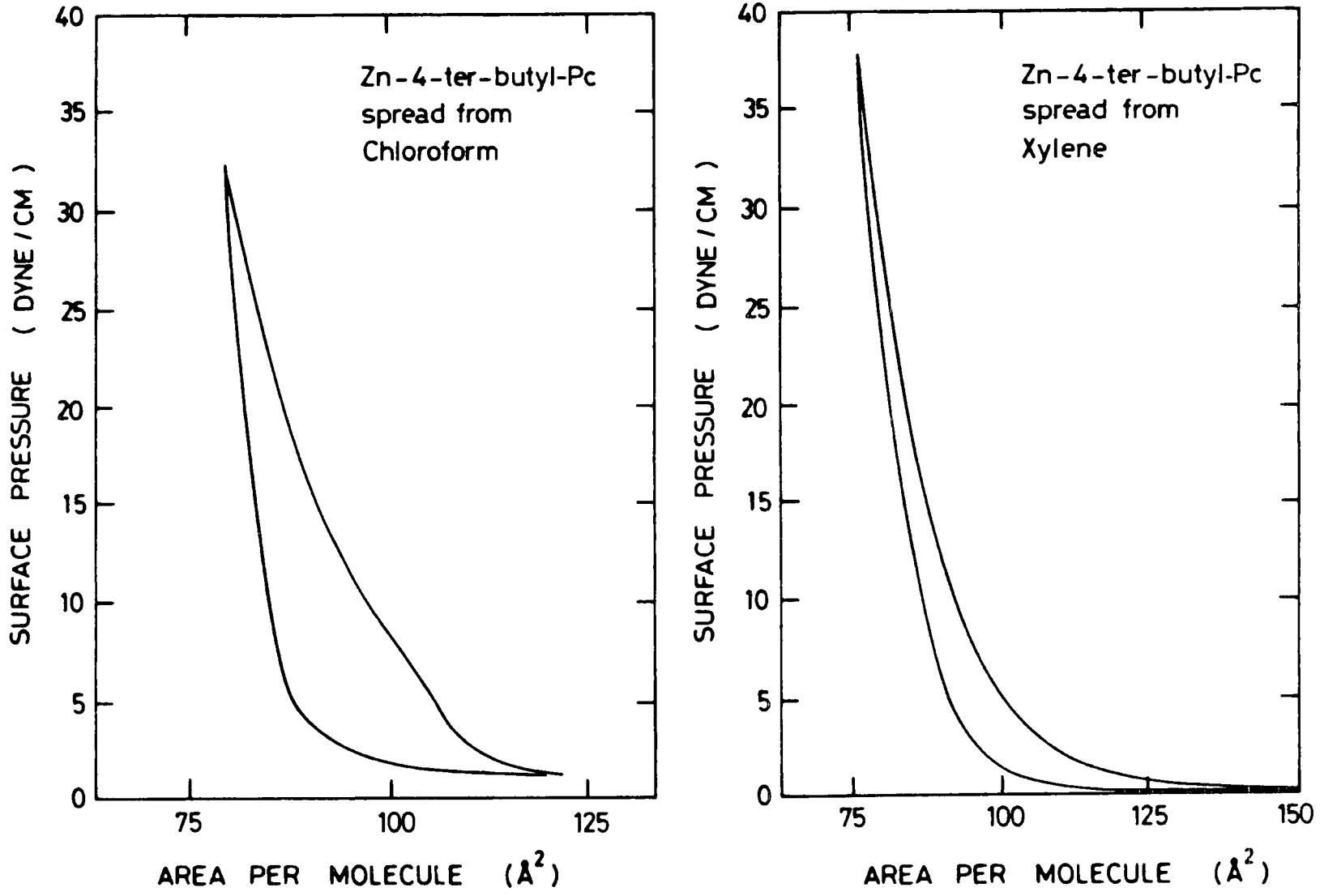

Figure 10. A typical set of isotherms for zinc 4-ter-butyl phthalocyanine spread from chloroform and xylene.

Manganese 4-ter-butyl phthalocyanine

The set of isotherms for manganese 4-ter-butyl phthalocyanine spread from both chloroform and xylene are shown fig. (5.11). The distinguishing feature between the two isotherms is that the film spread from chloroform shows evidence of structure. This is, in fact, the only phthalocyanine compound examined which showed such a distinctive amount of structuring. Attempts were made to enhance the structure by reducing the compression and expansion speeds right down to the minimum values. However, this actually reduced the amount of structure observed although it did not remove it. Both films were found to give a type B response to the suction test.

The calculated area per molecule is about 30% smaller than that for the copper or the zinc form, but still falls within the minimum value which might be expected for edge on packing. Apart from this problem, the floating monolayer, although fairly fluid, was still slightly too rigid to transfer multilayers. From the previous results it can be seen that a major factor in determining the properties of the monolayer is the spreading solvent. One line of thought pursued was that solvents like chloroform are protic solvents. That is, they tend to donate protons and, for example, when mixed with water tend to render it slightly acidic. This type of solvent tends to leave the material it has dissolved rather quickly, which in turn tends to make the material brittle. Solvents such as xylene are a neutral type of solvent and materials spread from it do tend to

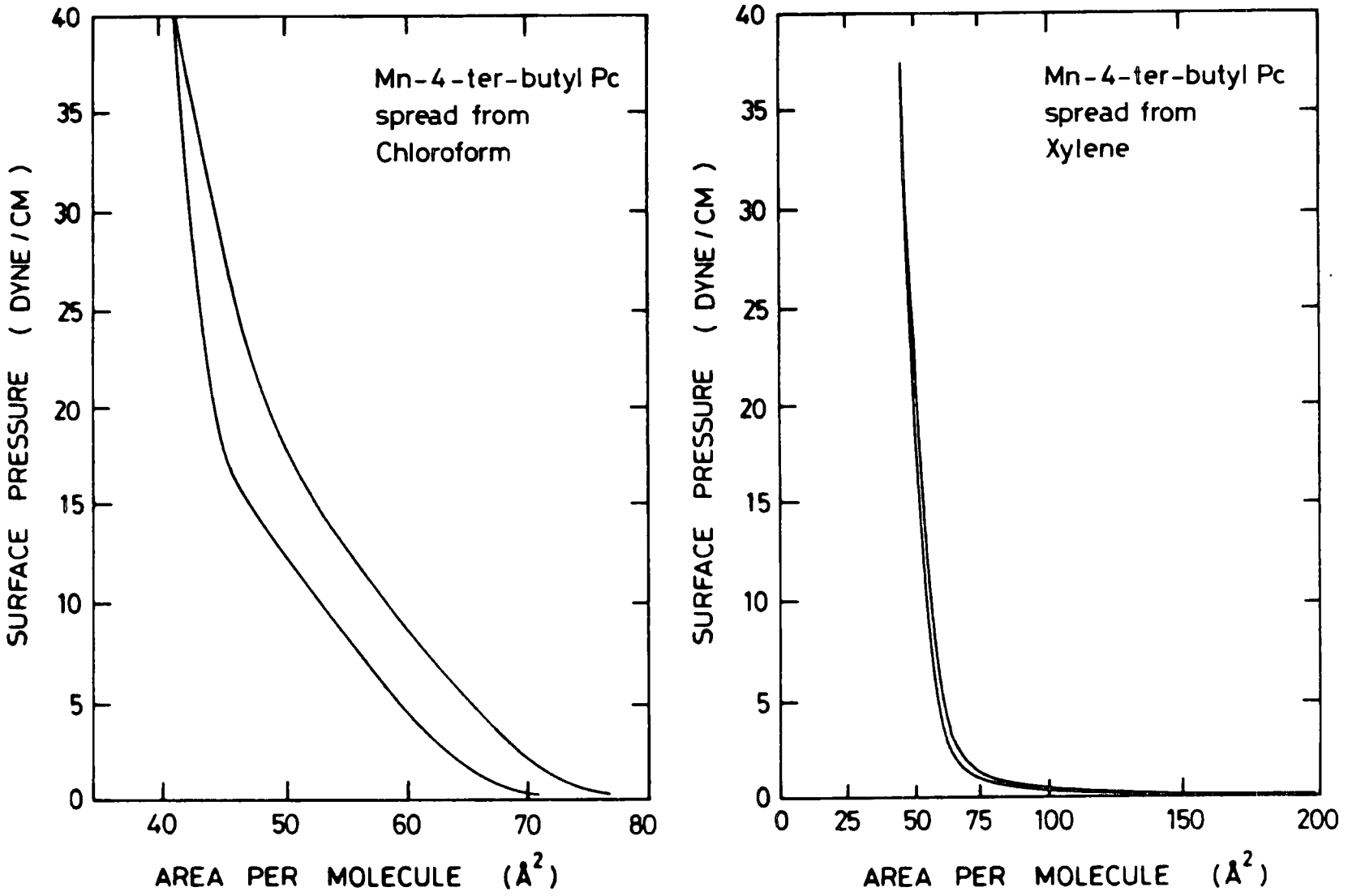

Figure 11. A typical set of isotherms for manganese 4-ter-butyl phthalocyanine spread from chloroform and xylene.

be less rigid. Hence, it appeared a logical choice to use an aprotic solvent. Di-methyl formide was thought to be appropriate in that it dissolves manganese 4-ter-butyl phthalocyanine. However films spread from this solvent, although exhibiting an improved reaction to the suction test, gave a lower value for the calculated area per molecule. This could be attributed to loss of material to the subphase, as di-methyl formide is miscible with water. Various mixtures of the di-methyl formide solution with xylene were tested to try and improve the situation without actively destroying the advantage gained by using an aprotic solvent. This produced an interesting result in that when the area per molecule obtained was plotted against the percentage of xylene in the mixture, the curve showed a maximum. The result described above is shown in fig. (5.12). The optimum can be explained in the following way: Firstly, solutions containing low percentages of xylene tend to lose material to the subphase by the interaction of the di-methyl formide with the subphase and secondly, solutions containing a high percentage of xylene produce films with a higher degree of aggregation. The optimum represents a compromise between these extremes.

The optimisation results reported here are for materials received before our purification procedures were perfected. A further improvement was achieved with material of a higher purity, the final value of calculated area per molecule obtained being $86\mathring{A}^{2}$ which is comparable with that for the other 4-ter-butyl phthalocyanines.

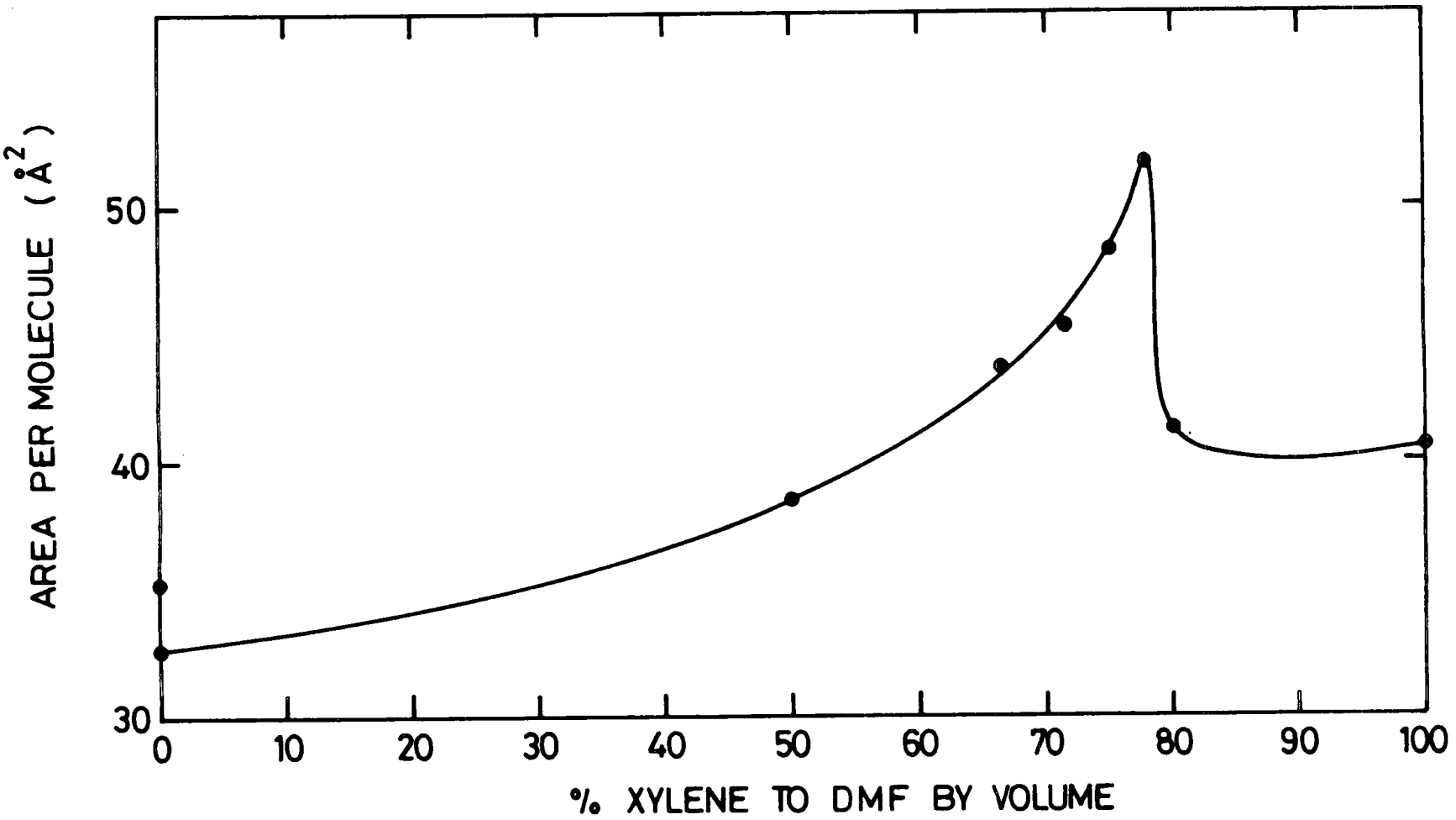

Figure 12. The variation of calculated molecular area with spreading solvent mixture.

5.3.5 Isotherms for an asymmetrically substituted copper phthalocyanine

The particular form of copper phthalocyanine described in this sub-section is asymmetrically substituted and is thus completely different from the other materials described in this thesis. The asymmetrical phthalocyanine [CuPc tris($CH_2NHC_3H_7$-iso)] was found to produce a curved isotherm with no structure. The amount of curvature with this compound (abbreviated to ASY-CuPc) suggests little rigidity in the film. This was further confirmed by the film exhibiting a suction test which was almost stearic-like, the response being type A for a freshly spread monolayer and B for an aged layer. Fig. (5.13) shows an isotherm for this material spread from chloroform. As can be seen, the isotherm is curved, and also subsequent compression isotherms follow the first, another indication of there being little rigidity in the layer. No advantage was obtained in spreading this material from other solvents. The area per molecule obtained is almost consistent with the molecule sitting edge-on in the water, the short chains pointing towards, and overlapping with the neighbouring molecules. As shown by the inset, the average space taken up per molecule in this configuration would be approximately 4.0 Å x 18.0 Å x 18.0 Å.

A point of interest with this particular material is that the amine groups can be protonated. Results presented in section 5.2.2 show that at low values of pH, the material slowly

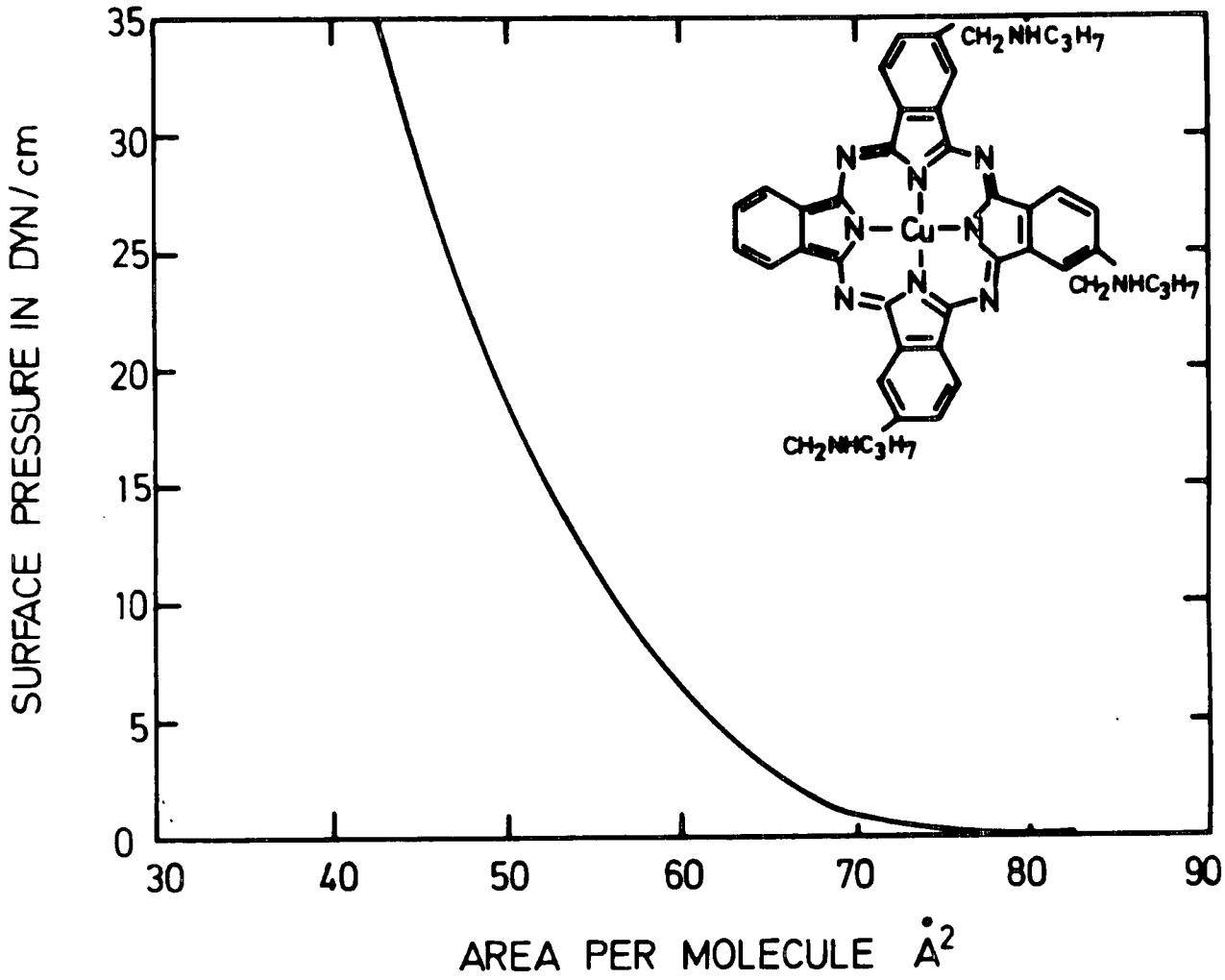

Figure 13. A typical isotherm for the asymmetrical copper phthalocyanine spread from chloroform.

dissolves. However variations in pH do not seem to affect the form of isotherm obtained. It should also be remembered that the constant pressure facility in our modern trough can cope with materials which dissolve gently in the subphase.

5.3.6 Isotherms for mixed layers of asymmetric copper phthalocyanine and fatty acids

As outlined in section 5.3.2 another approach in achieving good deposition is to incorporate the phthalocyanine molecule into a stearic acid matrix. This section reports the results obtained with mixed layers covering the full molecular composition range from 100% stearic to 100% asymmetrically substituted copper phthalocyanine. A selection of isotherms is shown in fig. (5.14). As may be seen, with a film containing a 90% molecular mixture of stearic acid, the isotherm still shows some structure but is less defined than that for a pure stearic acid film. With 80% stearic acid incorporated, the isotherm now appears as a smooth curve with no apparent structure. The subsequent curves leading up to 100% ASY-CuPc show no distinguishing features, except a general trend towards decreasing curvature.

Subsequently, calculations were made of the area per molecule occupied by the stearic acid and phthalocyanine molecules. It was found that if the area per molecule for the stearic was assumed to be constant, the value calculated for the asymmetrically substituted copper phthalocyanine was less than

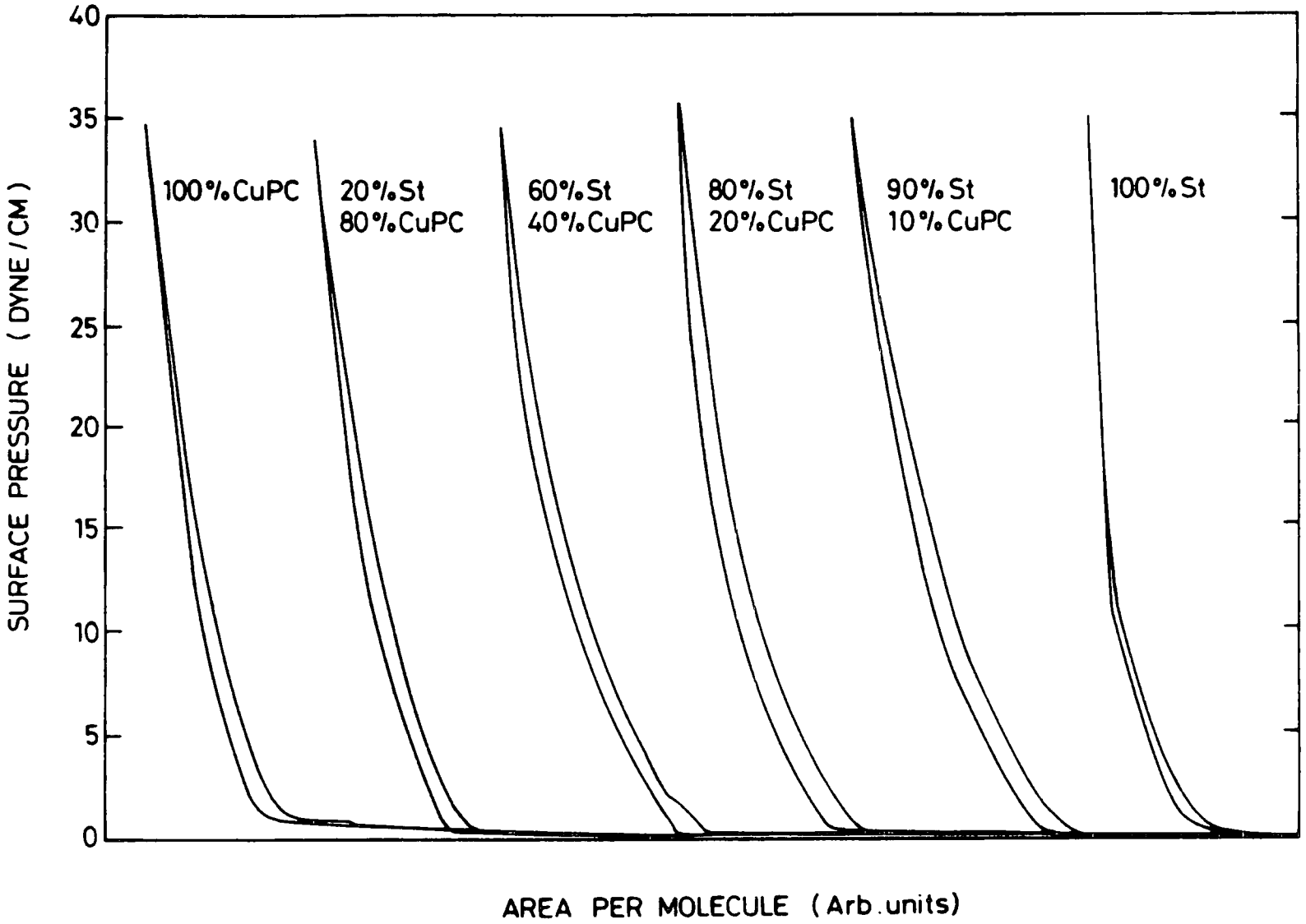

Figure 14. A series of isotherms showing the variation in form of the isotherm with various percentage mixtures of stearic acid and ASY-CuPc.

expected. A similar explanation to that given for the metal free mixed layers can be used. That is, the phthalocyanine molecules appear to be squeezed out of the film. Results obtained on LB films deposited using the solutions described here are contained in section 5.4.5 of this chapter.

5.3.7 Isotherms using a subphase containing alcohol

The reasons for introducing alcohol into the subphase are outlined in section 5.2.3. The spreading behaviour and isotherms for various phthalocyanine compounds were investigated, but the results presented here will focus on the asymmetric copper phthalocyanine. A series of isotherms were taken using both chloroform and methylene chloride as solvents. For these materials, the maximum percentage of alcohol to water that could be used was 10% and 6%, respectively. Above these values lenses formed on the surface and very poor spreading was observed.

Fig. (5.15) shows a series of isotherms obtained with a range of alcoholic subphases. The first isotherm shows that the inclusion of 2% alcohol results in increased curvature; the suction response observed was type A ie. the Langmuir film behaved classically on removal. As the percentage of alcohol is increased some structure is apparent in the isotherm. The area over which the new state occurs is seen to increase with the alcoholic content of the subphase. The area per molecule obtained from the most steeply-rising part of the isotherm

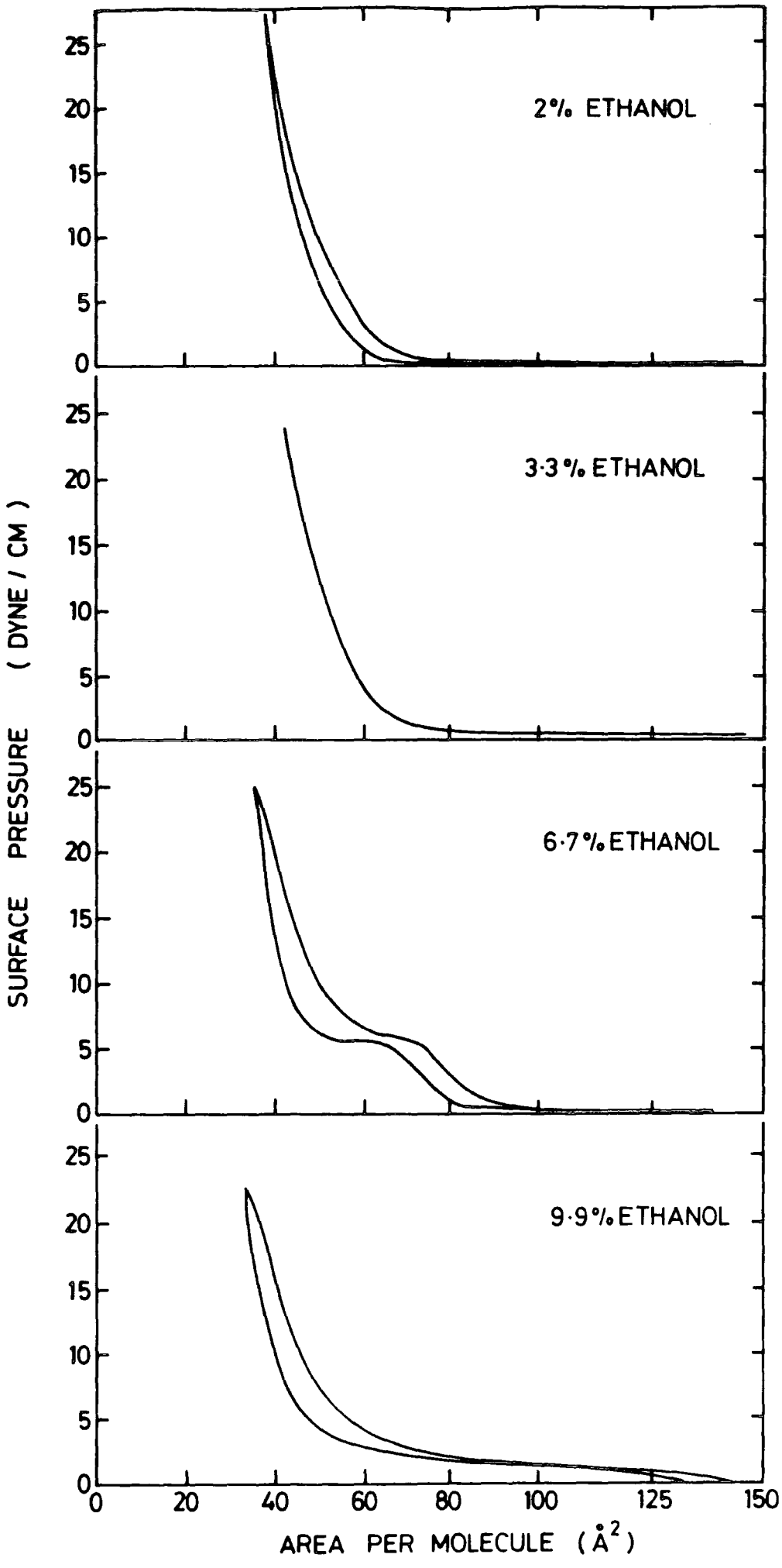

Figure 15. A series of isotherms obtained with a range of alcoholic subphases.

Material	Solvent	Suction Test Response	Calculated Area/molecule $Å^2$	
Metal-free pc	Acetone	C	8.8	Problems encountered with the acetone entering the subphase and aggregation occurring
Metal-free pc	Acetone/chloroform	C	14.7	Some aggregation observed
Metal-free pc	Acetone/mesitylene	A/B	6.3	Aggregation could be clearly seen
Metal-free pc	Acetone/chloroform/ mesitylene	B	8.8	Slight aggregation could sometimes be observed
Manganese pc	Tetra-hydro-Furan	C	76	No aggregation observed but layer appeared quite rigid
Metal-free 4 ter-butyl pc	Toluene/Chloroform	B	34.3	No aggregation observed and layer appeared reasonably fluid at low
Cu 4-ter-butyl pc	Xylene	B	87.4	No aggregation observed and layer appeared reasonably fluid.
Cu 4-terbutyl pc	Chloroform	-	-	Intense aggregation observed with this solvent
Zn 4-ter-butyl pc	Chloroform	A	92	The Langmuir film formed possessed excellent qualities but unfortunately underwent rapid photo-oxidation
Zn 4-ter-butyl pc	Xylene	B	91	
Mn 4-ter-butyl pc	Chloroform	B	54	This material clearly exhibited an optimum area/molecule with a spreading solvent comprising 78% xylene 22% dimethyl formide
Mn 4-ter-butyl pc	Xylene	B	58	
Mn 4-ter-butyl pc	Xylene/di-methyl formide	A	86	
Asy-Cu pc	Chloroform	A	57	A good response to the suction test which was maintained even after many hours

remains consistent throughout, corresponding to edge-on stacking as observed in the absence of alcohol in the subphase. This leads us to the conclusion that a) the part of the isotherm which is being altered is that relating to the liquid part of the compression and b) what is being observed is an extension of the transition between the liquid and solid state. The effect on deposited multilayers of using alcohol in the subphase is included in the following section.

5.4 Film deposition

In the preceding sections of this chapter we have covered the stages required to form phthalocyanine Langmuir films. These floating layers were assessed by evaluating pressure-area curves obtained on the compression and expansion of the film. From these isotherm measurements it was possible to calculate the occupied area/molecule. The role of the spreading solvent was found to be crucial in optimising the properties of the Langmuir film. Slowly evaporating solvents were found to reduce the surface viscosity of the layers and in some cases to improve the structure, as evidenced by the area/molecule values. In the case of the ASY-CuPc and metal-substituted 4-ter-butyl Pc's these values were found to be consistent with the formation of a monolayer with edge-on stacking of the molecules. However, further verification of this is required from other independent measurements, some of which are presented in chapter 6. Thus having covered the methods of preparation of these layers we now

go on, in the following section, to cover the deposition techniques which were developed in order to transfer the floating Langmuir films onto a substrate.

5.4.1 Metal-free unsubstituted phthalocyanine

These films were very difficult to transfer, especially when large samples or multilayer structures were required. The problem was mainly due to the rigidity of the films; it was found that material moved insufficiently to replenish film removed from the subphase during deposition. The only reasonable degree of success was achieved with a spreading solvent containing mesitylene. Layers spread from this solvent could be successfully transferred, but the dipping conditions required a very slow dipping speed. Fig. (5.16) shows the pick up profile for such a film. Normally the trace on either side of the actual pick-up is level, showing no change of area: in this case there is a sloping tail due to the slow evaporation of mesitylene still incorporated in the layer. The mesitylene can be eliminated by allowing full evaporation to take place. However, if this is allowed, the film becomes too rigid to transfer. From the table shown in fig. (5.16) it can be seen that if the amount of film removed is compared with the area of sample covered, a transfer ratio can then be calculated. In this case it is found that the transfer ratio is greater than one, i.e. the area of film removed is greater than the physical area of sample covered. This is explained simply by the fact

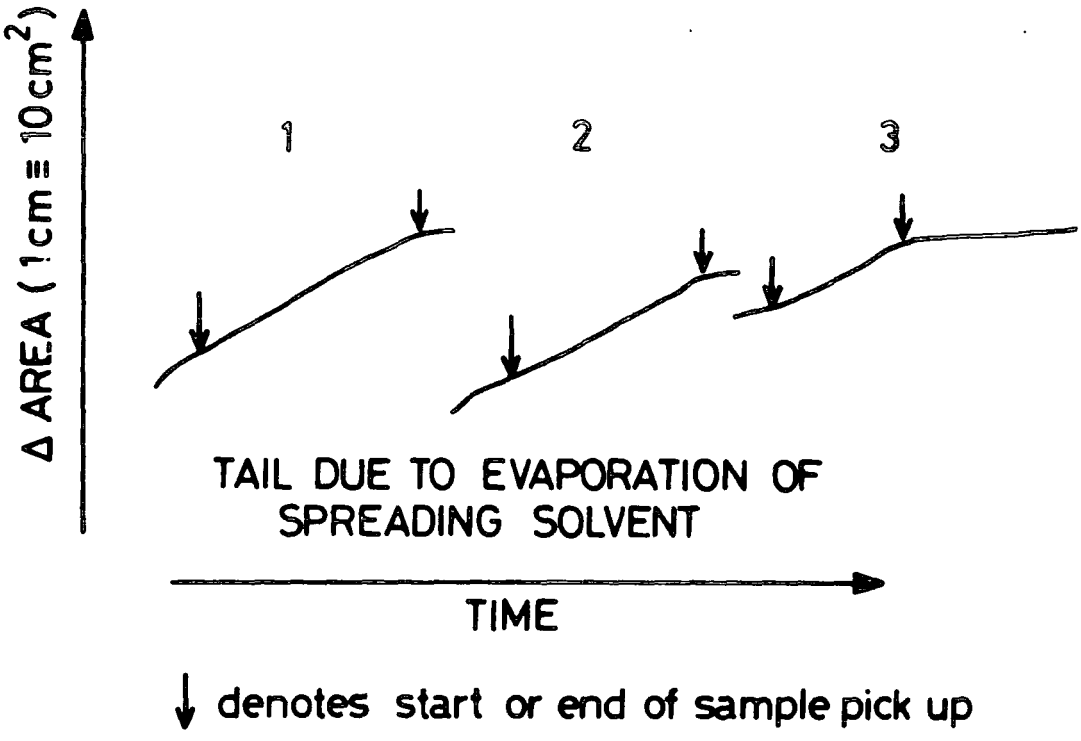

	INDICATED AREA OF FILM REMOVED	AREA OF SAMPLE COVERED	TRANSFER RATIO
1	20	17·5	1·14
2	16	15	1·07
3	12	10·5	1·14

Figure 16. A record of the deposition of metal-free phthalocyanine, with a table showing the calculated transfer ratios.

that part of the indicated area-decrease represents area loss due to the evaporation of the remaining solvent in the layer.

5.4.2 Mixed layers of phthalocyanine and stearic acid

In view of the improved Langmuir film quality observed with the mixed layers, good deposition would be expected. The mixtures used for deposition contained approximately 30% stearic acid, this being the molecular mixture which showed a stearic acid like isotherm structure. It was found, however, that poor pick-up was obtained, material being transferred adequately on the removal of the substrate from the subphase, but being partially stripped off on reinsertion. Fig. (5.17) shows the trace observed for the transfer of such a film. As may be seen, upon reinsertion of the substrate, a rise in the surface pressure of the compressed layer is observed which is indicative of material being removed from the substrate.

In section 5.2.2 we mentioned that the area per molecule measurement indicated that the phthalocyanine molecules were actually being squeezed out of the layer. This would probably lead to the situation sketched in fig. (5.18a), where the film exists in the form of a packed stearate layer with a covering of phthalocyanine molecules. During reinsertion of this structure, these molecules exhibiting little bonding with the substrate, would be stripped off resulting in a rise in surface pressure.

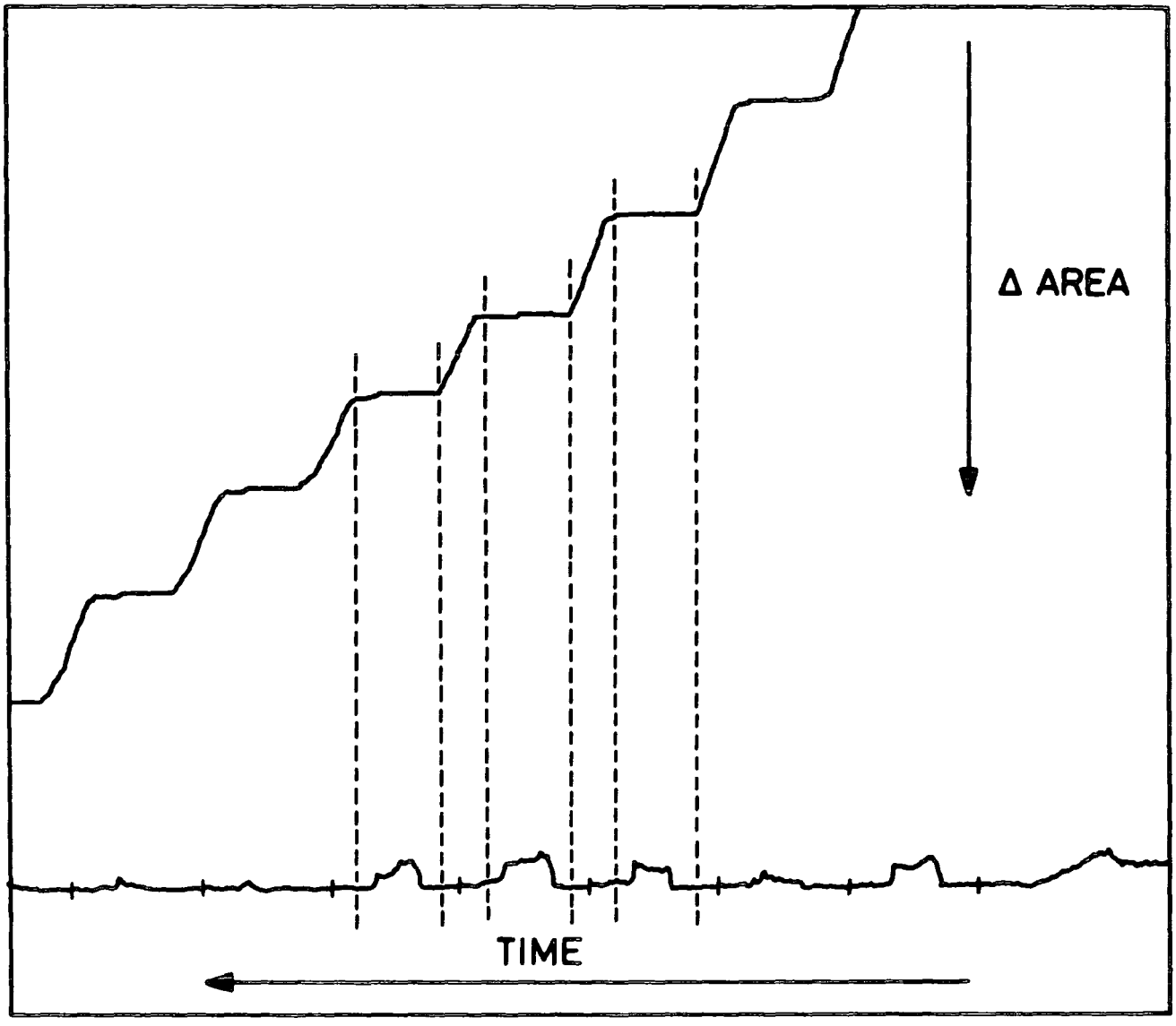

Figure 17. A record of the deposition of metal-free phthalocyanine in a mixed layer with stearic acid.

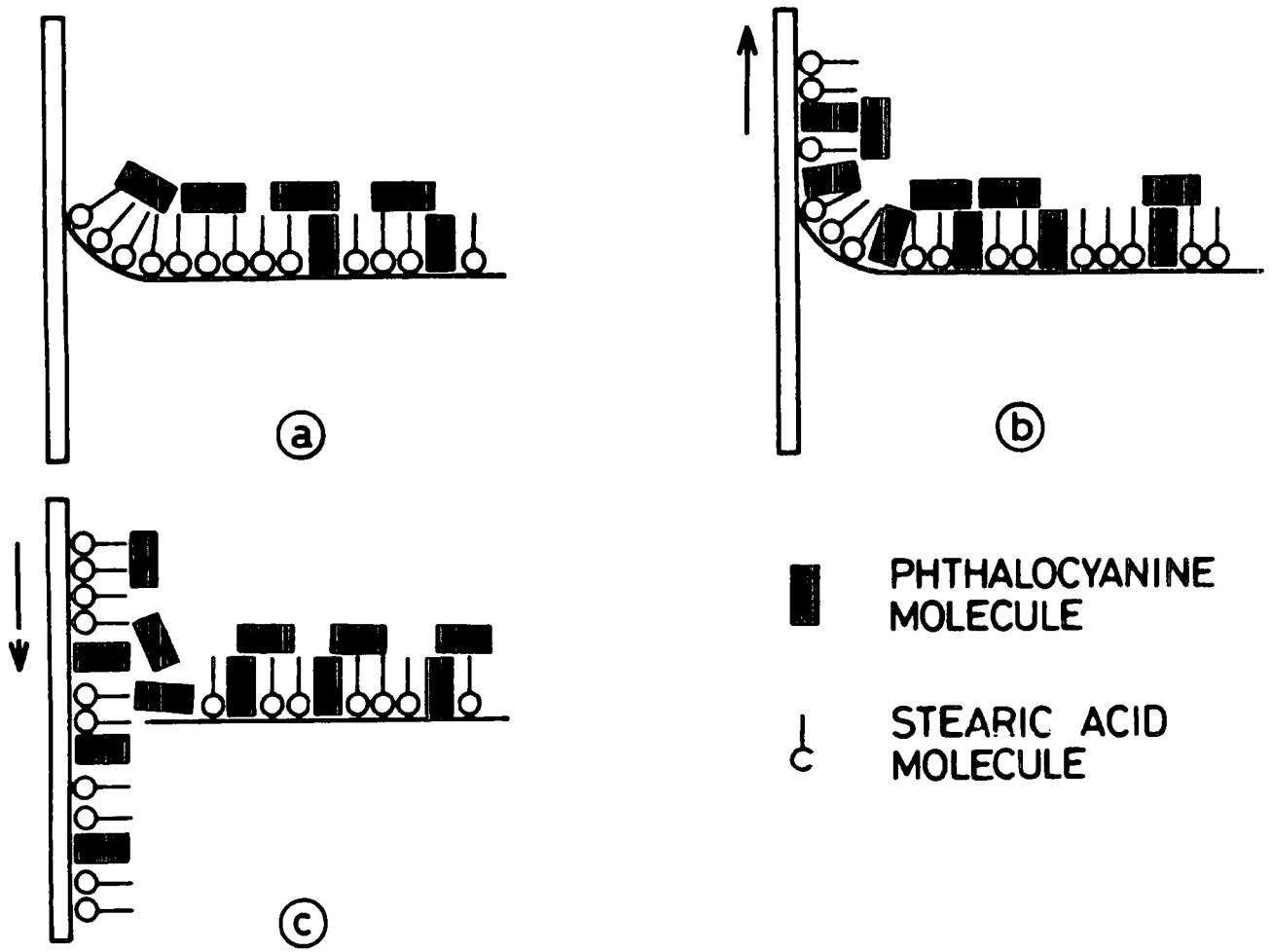

Figure 18. A schematic diagram showing the possible packing arrangement of the ASY-CuPc and stearic acid molecules, b) the transfer of this layer and c) the effect of this packing on deposition when the substrate is reinserted into the subphase.

5.4.3 Unsubstituted manganese phthalocyanine

The rigidity of the monolayers caused problems with this material; although effective transfer could be achieved for films held at low compression for the first layer, poor pick up was observed for subsequent layers.

5.4.4 4-ter-butyl phthalocyanines

With the metal-free ter-butyl phthalocyanine it was found that deposition could be achieved at pressures of around 20 dynes/cm. Values above this tended to make the layer rigid. The value of pH was found to have no effect upon the quality of film transfer.

Of the metal containing, symmetrically substituted phthalocyanines, only the manganese form was investigated in any depth as far as dipping characteristics were concerned. This was because only a very small quantity of the copper compound was available and even this was relatively impure. In the case of the zinc form it was known that the solution underwent rapid photo-oxidisation and that it was not possible to transfer the material except, possibly, if it was deposited under an atmosphere of nitrogen. This left manganese the clear contender for a full screening of the deposition conditions. Also the manganese form was in plentiful supply and it was possible additionally to explore the effect of various purification procedures. A dipping profile for the manganese 4-ter-butyl

phthalocyanine is shown in fig. (5.19). The material was spread from the optimised solvent described in section 5.3.4 and held at a control pressure of 25 dynes. Pressures higher than this tended to lead to rigid layer formation as for the metal-free 4-ter-butyl compound mentioned earlier. The material shows good pick-up, with a transfer ratio of 0.95. The adhesion of the films is seen to be fair and to improve, to a certain extent, with the number of layers deposited.

5.4.5 Asymmetric copper phthalocyanine

There are clearly many problems to be overcome in first forming a suitable Langmuir film of phthalocyanine and then transferring it to a substrate. Of all the materials studied the asymmetric copper phthalocyanine was found to exhibit the best transfer characteristics and fortunately they were maintained even after many hours. It was, however, necessary to address an adhesion problem with this material when fabricating multilayer structures. It was found that after the deposition of the third to fifth layer, material started to be removed on reinsertion of the substrate. This was improved in two ways; Firstly, it was recognised that the amine groups were capable of being protonated and in this state imparted a degree of solubility to the molecules. Figure (5.20) shows the improvement achieved by raising the pH of the subphase above 7. The first trace indicates a loss of 25% of material on the second dip, and 80% on the third. By comparison, the second

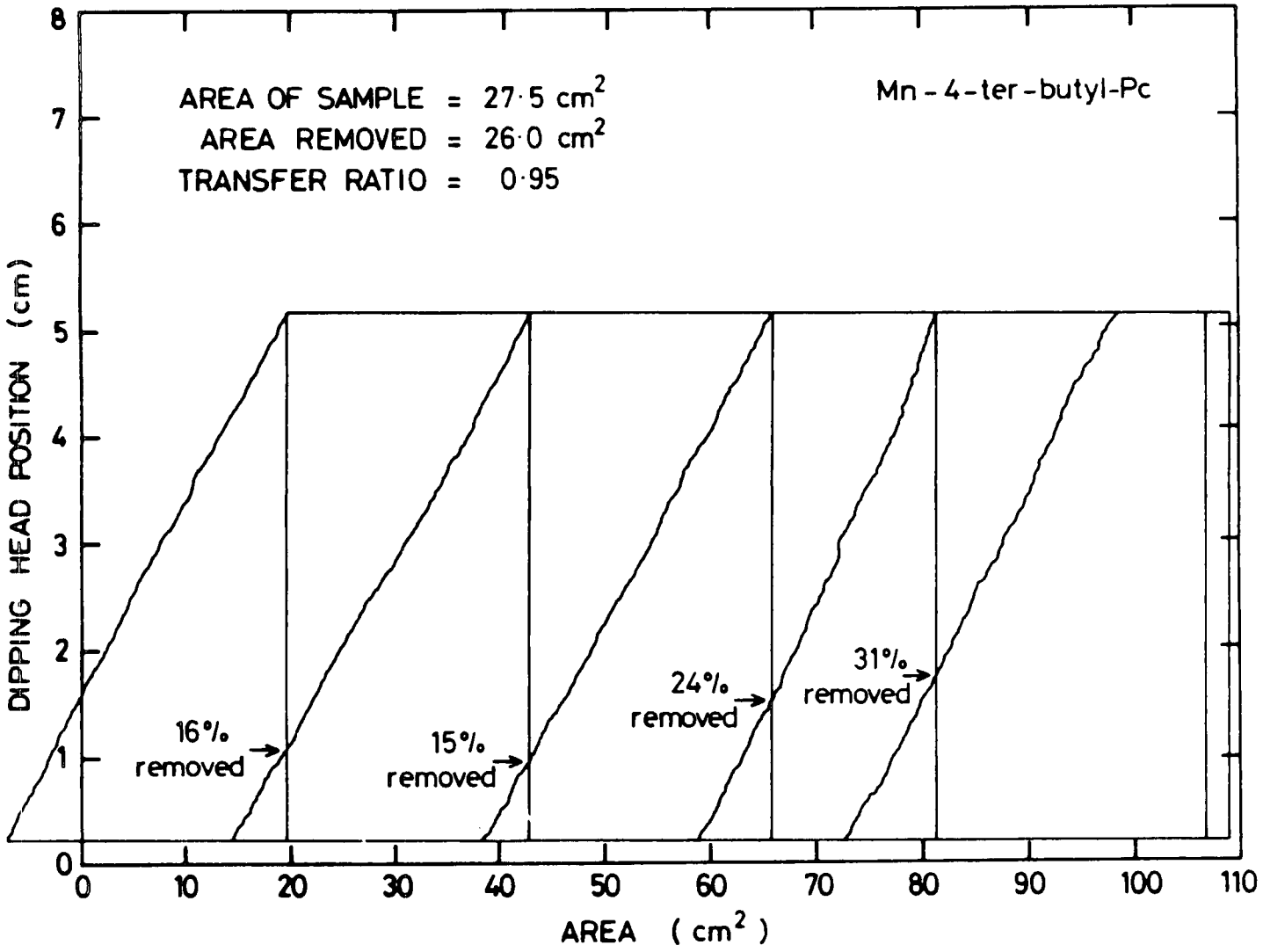

Figure 19. A record of the deposition of manganese 4-ter-butyl

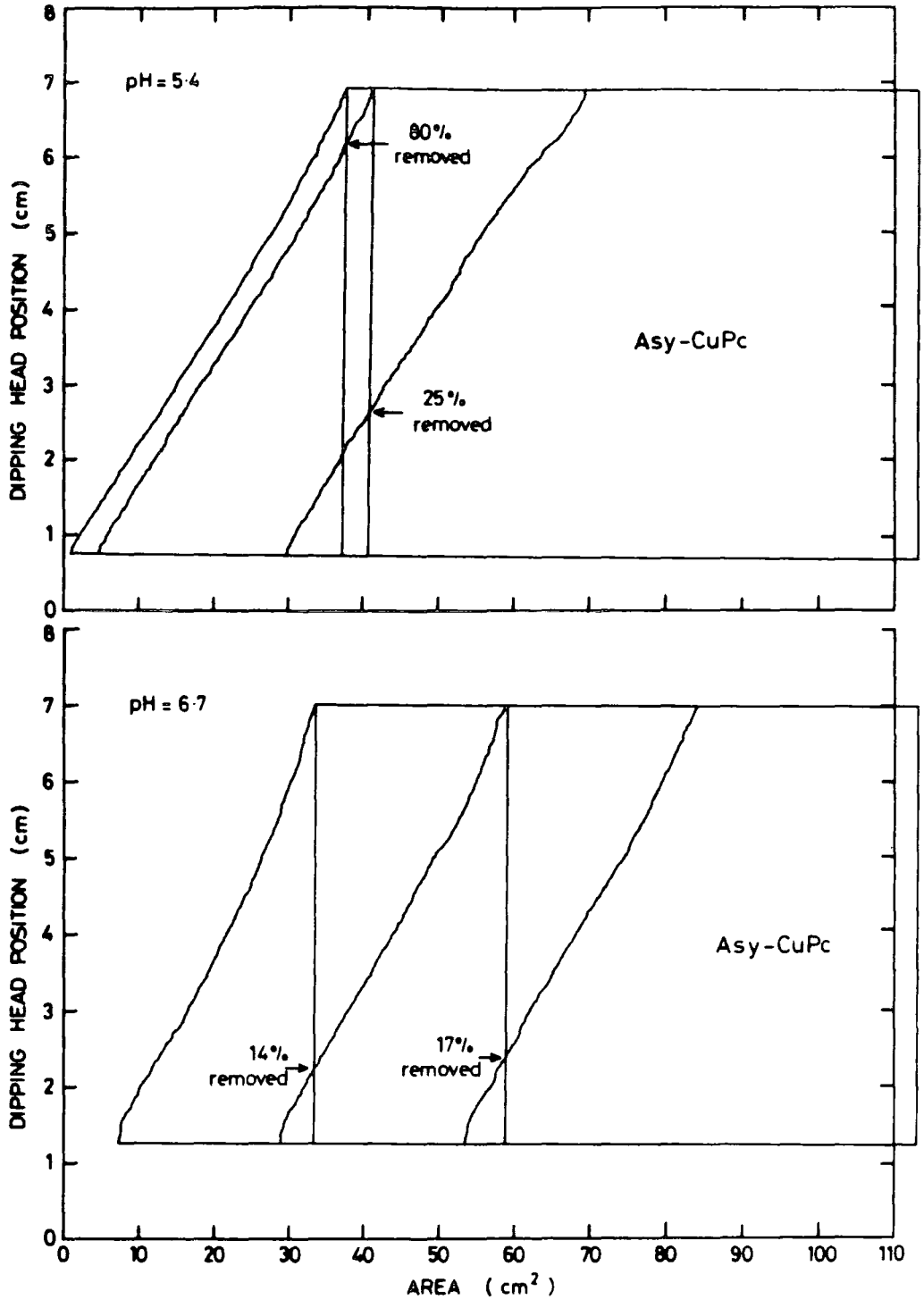

Figure 20. Deposition profile showing the improvement in deposition achieved by raising the pH of the subphase.

profile indicates a loss of 17% of material on the second dip and 14% on the third. The increased absorbance of these films reflects this improvement (fig. 5.21). The second method was the use of a subphase containing a certain percentage of alcohol, in an attempt to reduce the surface tension which is responsible for stripping the film. The result of using a subphase containing 2% alcohol is seen in fig. (5.22). In the first profile, with the subphase consisting of only millipore water, 22% of the total amount of material is lost, whereas a total loss of 11% is found in the second profile. No further improvement was observed in the deposition of the films as the volume % of alcohol was increased above 2%. Above 6% an actual deterioration was observed this coinciding with the deterioration in the spreading characteristics at these concentrations, as discussed in section 5.3.5. Thus, effective transfer of these monolayers was achieved at a pH of above 7, using a subphase containing 2% alcohol. The dipping pressure used was 25 dynes/cm and the dipping speed 5 mm/min.

5.4.6 Mixed layers of asymmetric copper phthalocyanine

With a predominantly stearic acid film, good deposition could be expected. Indeed this is observed for films containing 80% or more stearic acid molecules. However, as the percentage of stearic acid is decreased a systematic decline in the standard of deposition is observed. Figure (5.23) shows the deposition profile for a range of mixed layer films. For a film

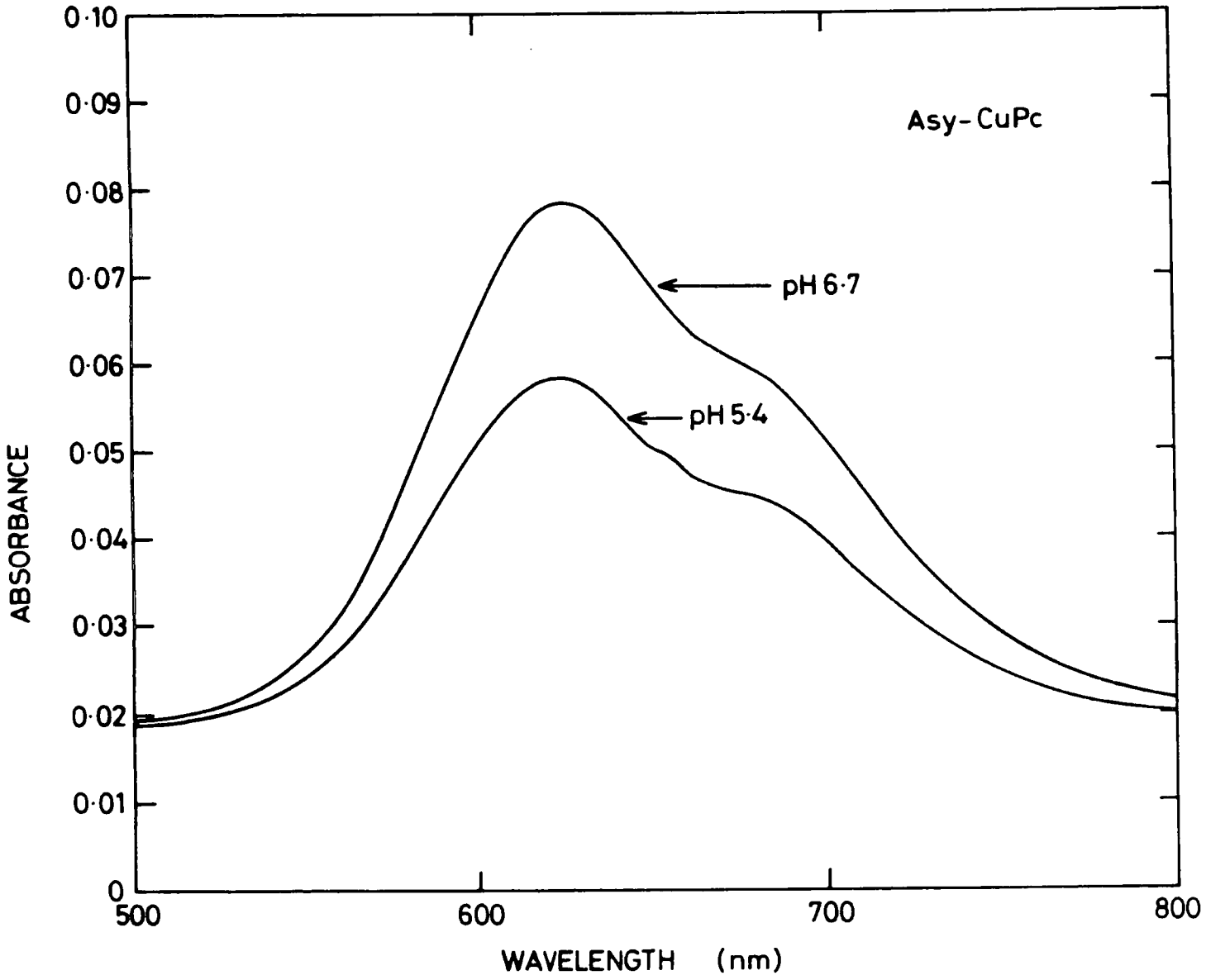

Figure 21. An optical absorbance plot of deposited films ASY-CuPc reflecting the improvement obtained at elevated pH.

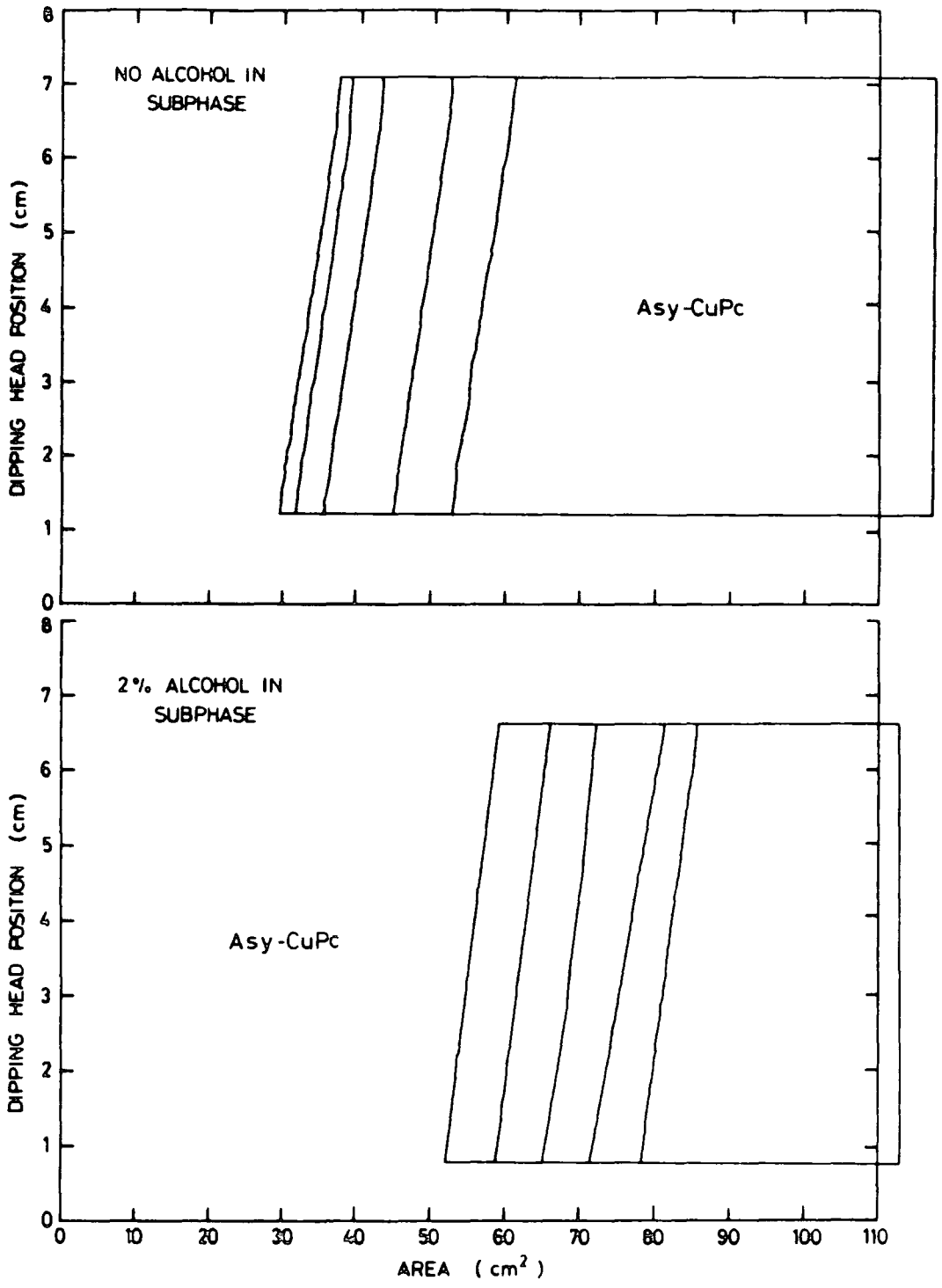

Figure 22. Deposition profile illustrating the improvement in deposition achieved by incorporating alcohol in the subphase.

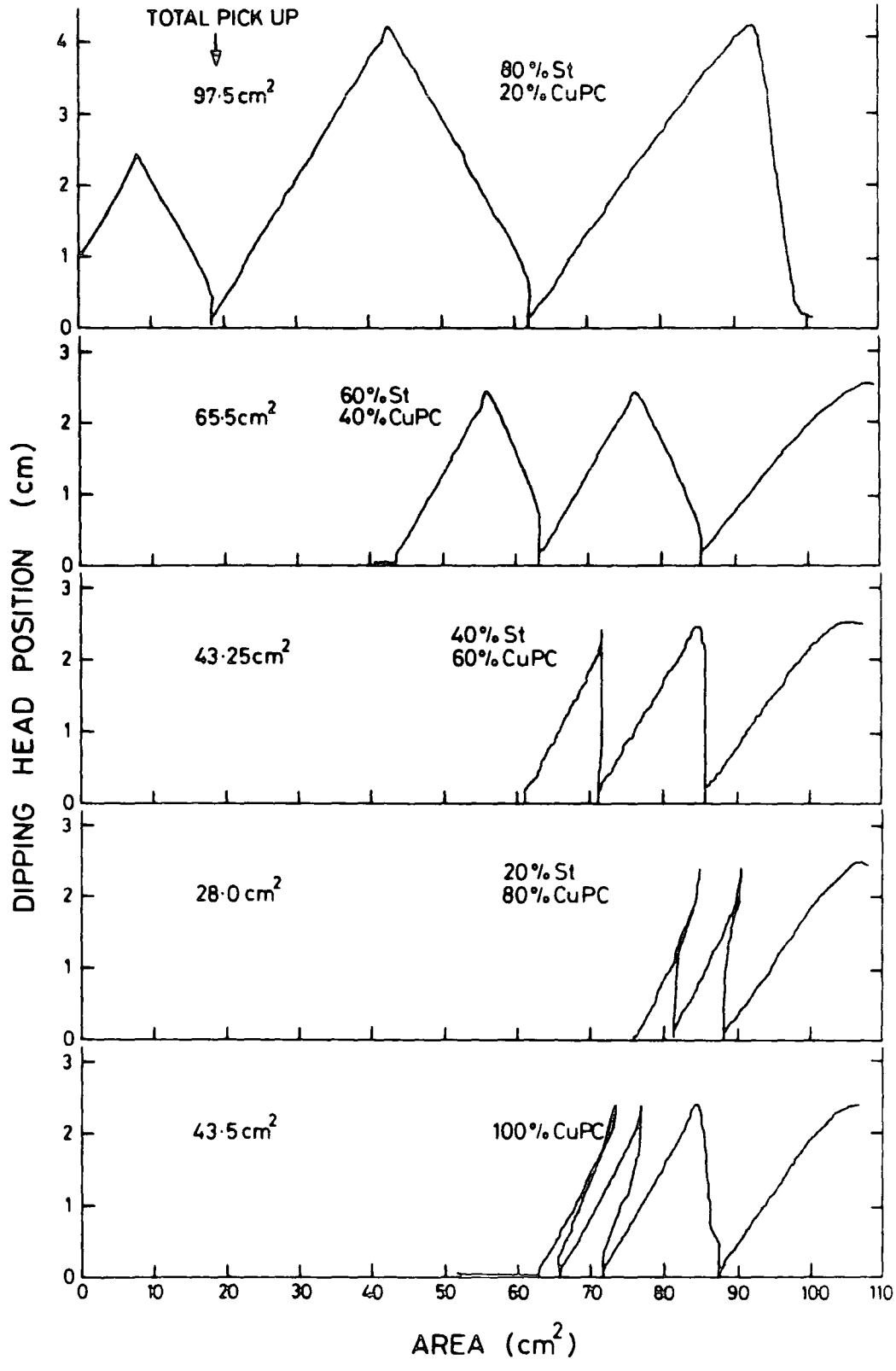

Figure 23. A series of deposition records showing the variation in film transfer with various percentage mixtures of stearic acid and ASY-CuPc.

containing 80% stearic acid an even deposition is achieved on insertion and removal of the substrate from the subphase. However, with a film including 60% stearic acid it can be seen that less material is transferred on insertion of the substrate and with a 40% mixture the deposition surprisingly appears Z-type, indicating that no material is being transferred on insertion. For this particular ratio, observation of the meniscus formed during deposition shows it to be flat, indicating that the surface of the substrate is no longer hydrophobic. This would be consistent with the explanation that the surface is now dominated by the characteristics of the phthalocyanine. This is to be expected for, although the molecular ratio is 60% stearate to 40% phthalocyanine, the size of the phthalocyanine molecule (if edge on stacking is assumed) is four times that of the stearate.

With lower percentages of stearic acid a decided deterioration in the deposition occurs, where material is observed to be removed during insertion of the substrate. This again can be explained by reference to fig. (5.18) where it can be seen that molecules of phthalocyanine which have been squeezed out of the film are particularly vulnerable to removal on reinsertion as they are not held tightly in a compact layer.

SUMMARY

This chapter has described in detail the preparation procedures for the deposition of a variety of phthalocyanine materials. The major problems encountered with these materials lie in a) their tendancy to form aggregates which results in a low value for the calculated area/molecule and b) the formation of floating Langmuir films of a high surface viscosity which leads to difficulties in deposition. The use of modified spreading solvents proved to be an important step in overcoming these problems. In particular the use of solvents which left the spread layer relatively slowly were found to produce a marked improvement in both the the value of area/ molecule obtained and in the deposition characteristics. The choice of metal ion and peripheral substitution also played an important role in the film forming ability of the materials. In general the metal substituted compounds gave the best area/molecule values with the asymmetrically substituted phthalocyanine exhibiting the best transfer characteristics.

We have shown that with the correct choice of subphase and spreading solvent that it is possible to deposit LB films of phthalocyanine. The next stage involved the characterisation of the deposited layers and this was performed in three main areas namely; structural, optical and electrical. The result of these investigations is reported in chapter 6. Following the characterisation of the films their potential use is assessed in a number of device structures including electroluminescent

diodes, MISS bistable switching devices and a gas detecting MIS and lateral conduction structures. The use of phthalocyanine LB films in these devices is reported in chapter 7.

CHAPTER 6

CHARACTERISATION OF PHTHALOCYANINE LB FILMS

6.0 INTRODUCTION

This chapter covers the characterisation of the phthalocyanine LB films described in the previous chapter. The account is divided into the three areas of structural assessment, optical properties, and electrical properties. The structural section describes observations of the films using RHEED and TEM; also included is a description of the physical stability of the films i.e. their resistance to abrasion. The section covering optical properties deals mainly with the absorbance spectra of the films. The final section describes measurements carried out on both metal and semiconducting substrates in order to obtain values of both bulk and surface electrical conductivity for the LB films.

6.1 STRUCTURAL ASSESSMENT

6.1.1 Adhesion

Good film adhesion to the substrate is obviously extremely important in a device structure. The phthalocyanine films of all the molecules studied were found to excel in this regard and to stick tenaciously to a wide range of solids. This was

especially true in the case of the metal-free films which were found to form extremely stable layers. The strongest adhesion was found when the materials were deposited onto metal or metallized substrates. This can be explained by the phthalocyanine interacting with the metallized substrate and forming a chemical bond. A simple test was carried out on a deposited film of the asymmetrically substituted copper phthalocyanine in which the absorbance of a film deposited on a glass slide was first measured; then a strip of cellotape was placed over the sample and torn off; the absorbance of the sample was finally remeasured and the percentage of material removed calculated. The absorbance values in this case, were obtained by transmission measurements. On the samples tested, the absorbance was found to fall by 6.5% indicating that only this percentage of material had been removed along with the cellotape.

6.1.2 Electron Microscopy studies

The films were investigated by transmission electron diffraction (TED), reflection high energy diffraction (RHEED), and also by scanning electron microscopy (SEM).

RHEED investigations

The photograph in fig. (6.1) shows the RHEED diffraction pattern observed for three layers of the metal-free phthalocyanine deposited on aluminised glass. It shows the diffraction pattern taken from the unaluminised side and reflects the properties of the phthalocyanine. (The diffraction pattern obtained for the aluminised side showed the characteristics of evaporated aluminium.) This pattern was used as a calibration to determine the interplanar spacings corresponding to the diffraction rings in fig. (6.1). The presence of a set of rings indicates that the film is polycrystalline in form, and the absence of any arcs of intensity confirms that the grains of which it is comprised do not have any specific preferred orientation. The d-spacing obtained from the pattern and corresponding to the only sharp and intense diffraction ring is 0.359nm which is in good agreement with the interatomic spacing of the crystal form. The d-spacings of the other rings are listed in table (6.1) which is located at the end of the section on SEM investigations. Also included in table 6.1 are the ASTM index values for the d-spacings for the main diffraction lines for metal-free phthalocyanine. As can be seen these match quite closely with the experimentally determined values for the LB film of the same material.

The photograph in fig. (6.2) shows the RHEED pattern obtained from a film of metal-free 4-ter-butyl phthalocyanine

Figure 1. The RHEED diffraction pattern observed for three layers of metal-free phthalocyanine deposited on glass.

Figure 2. The RHEED diffraction pattern obtained for metal-free 4-ter-butyl phthalocyanine deposited on InP

deposited on InP. This particular semiconductor was often used in experiments of this kind for three reasons. First, the surface of this material can be highly polished giving a very smooth surface onto which LB films may be deposited. Secondly, the diffraction pattern obtained from the InP can be used as a calibration for the print. Thirdly, such substrates have been found to increase the degree of order found in LB films of the fatty acids. The pattern again indicates that the films are polycrystalline with small grain size without any preferred orientation of the grains. The d-spacing corresponding to the main diffraction ring is 0.338nm which is approximately the same as the interatomic distance.

The RHEED patterns for all the materials were very similar to the patterns described for both the metal-free phthalocyanine and the 4-ter-butyl phthalocyanine in that they all featured one predominant ring which gave a d-spacing of the order of the intermolecular separation. No preferred orientation of the grains was indicated in any of the RHEED patterns observed.

TED investigations

Some of the deposited LB films were observed in the TED mode of the TEM, the samples having been prepared as described in chapter 4. These samples showed only polycrystalline order as revealed by the RHEED observations. This was an unexpected observation considering the much smaller area of sample from

which the pattern is derived using this method and it thus confirms the particularly small grain size of these films (<1μm). However, in the case of the asymmetrically substituted phthalocyanine, a preferred orientation of the grains was observed. This can be seen in the TED pattern in fig. (6.3) in which the preferred orientation is indicated by the arcs of intensity. This preferred orientation was not observed to change significantly as the sample was moved across the beam, and persisted in some cases for specimen movements of approximately 3mm. The d-spacings given by the diffraction arcs in fig. (6.3) are 0.329nm and 0.121nm where the larger value again corresponds to the intermolecular separation. Other rings which might be expected (for example, spacings corresponding to the distance between layers, - 1.8nm) would fall very close to or under the beam stop which obscures the main beam and would therefore not be observed. The d-spacings for all the films reported here are summarised in table 6.1.

SEM investigations

Further characterisation of the films was carried out using the scanning electron microscope. The photograph in fig. (6.4) shows a scanning electron micrograph of a layered structure of metal-free phthalocyanine on InP. The layered structure of the sample can be seen quite clearly, with a sharp change in contrast being observed between the InP and the edge of the

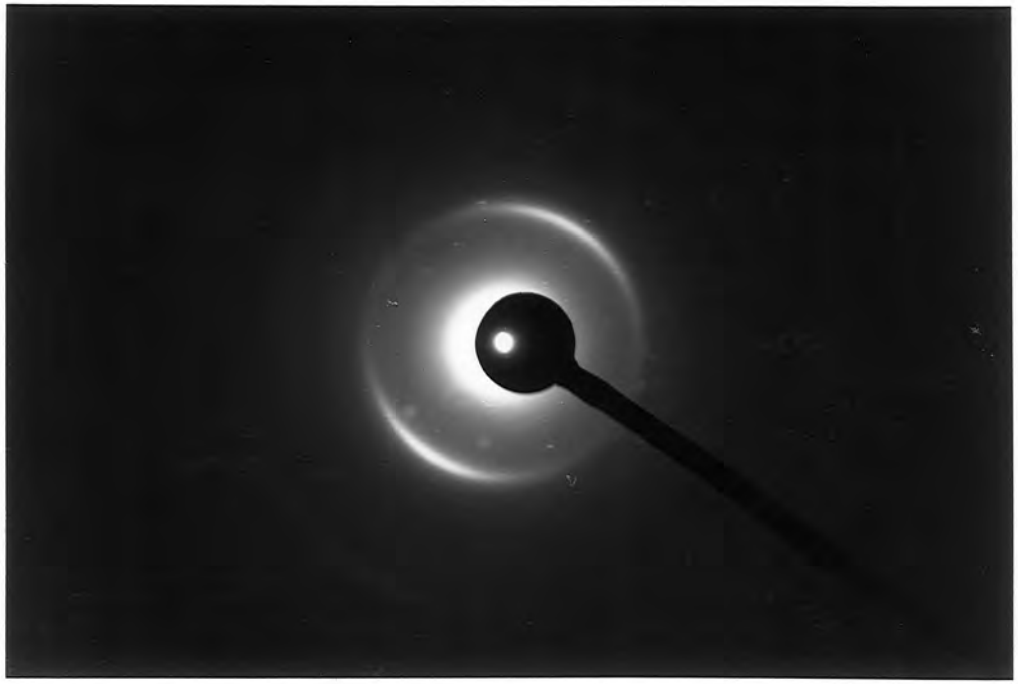

Figure 3. A TEM micrograph of asymmetrically substituted copper phthalocyanine showing a preferred orientation, indicated by the arcs of intensity which are present.

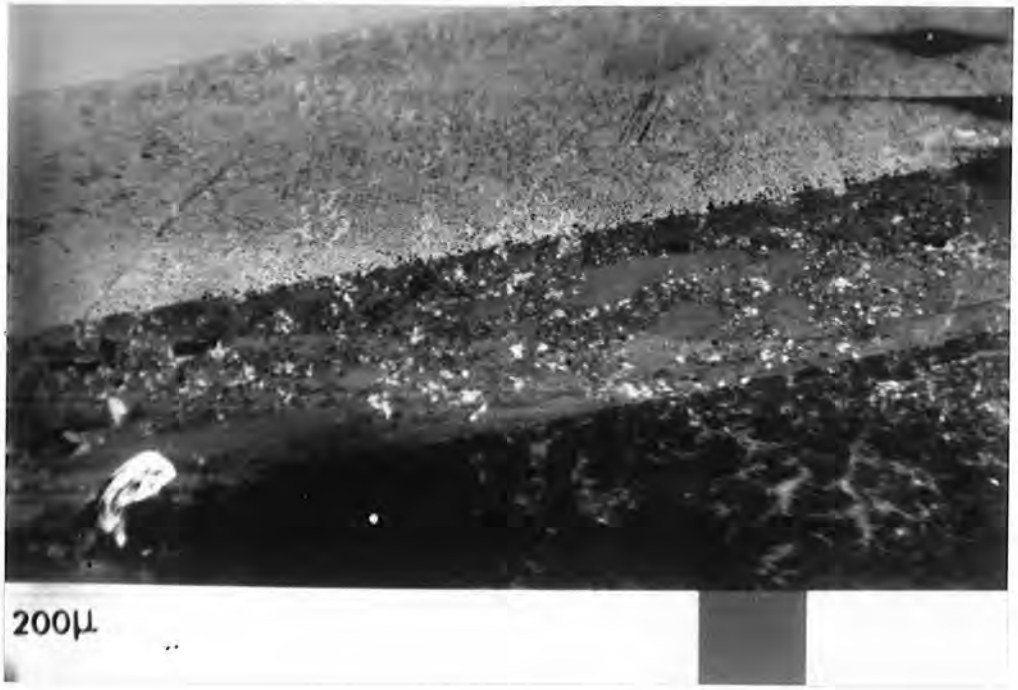

Figure 4. A scanning electron migrograph of a layered structure of metal-free phthalocyanine on InP.

Figure 5. An enhanced view of the layered structure shown in fig.4 showing the degree of aggregation present in the film.

Material	d-spacings (in nanometers) corresponding to main diffraction lines			
Metal-free phthalocyanine values from ASTM index *	0.345	0.325	0.179	0.164
Metal-free phthalocyanine LB films	0.359	0.328	0.174	0.164
Metal-free 4-ter-butyl phthalocyanine LB film	0.338	0.221	0.164	
Asymmetric copper phthalocyanine LB film	0.329	0.121		

Table 6.1 Showing the d-spacings observed for various phthalocyanine LB films

* included for reference with the values obtained for the various phthalocyanine LB films

film. The main aspect under consideration here was the uniformity of the film. It can be seen that the film appears to be very patchy with many small aggregates present in the layers. This is more evident in the photograph shown in fig. (6.5), which was taken at twice the magnification. Indeed it was not unusual with this material to actually observe small aggregates both in the floating layer on the subphase, and in the deposited films. However, in spite of the presence of these aggregates it does appear as if overall coverage has been achieved. In contrast, the scanning electron micrograph shown in fig. (6.6) for the asymmetrically substituted copper phthalocyanine (taken at the same magnification) has a much more uniform appearance. This correlates with the improved isotherms and dipping profiles obtained with this material. Similar results were observed with the manganese 4-ter-butyl phthalocyanine, again demonstrating a basic connection between the quality of deposition and the structural order of the film. It is interesting to note at this point that the shape of the meniscus which can be seen in the micrograph (see fig. (6.6)) alters from the first layer to the subsequent layers. This is because the surface of the clean InP is very hydrophilic, and therefore, on initial insertion of the substrate, the meniscus rises up the sample to form a low contact angle. On subsequent insertions the surface comprises a phthalocyanine layer. The phthalocyanine, although by no means hydrophobic, is not as hydrophilic as the InP, the actual observed contact angle with the water being perpendicular to the substrate after insertion.

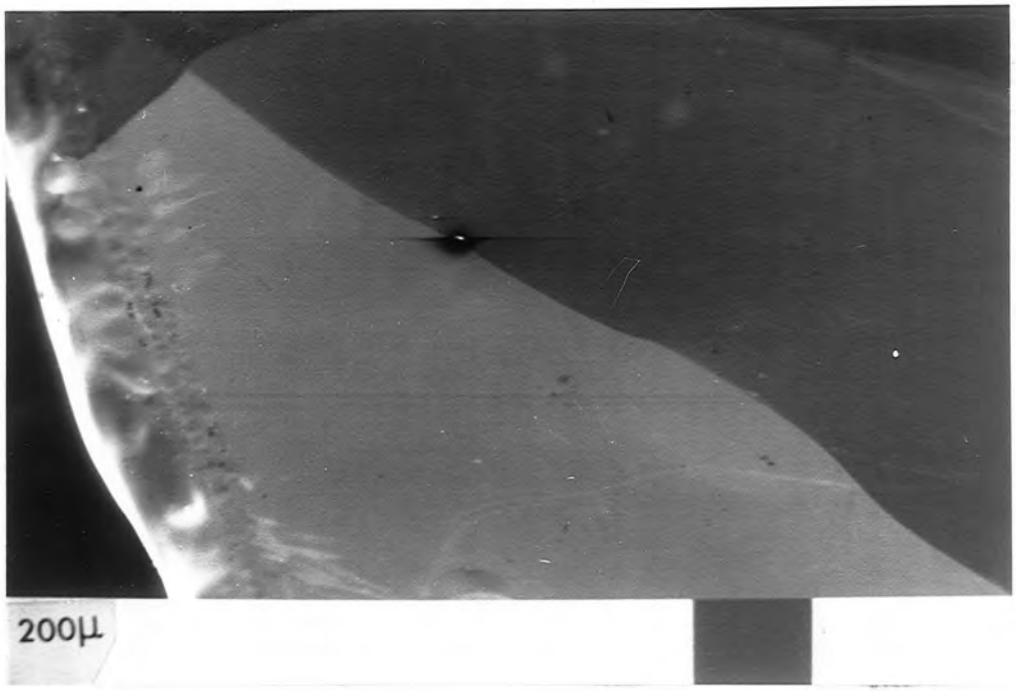

Figure 6. A scanning electron micrograph for the asymmetrically substituted copper phthalocyanine.

SEM contrast mechanisms

Some discussion is merited here on the reasons why contrast is observed between the film and the InP. There are basically four mechanisms which might give rise to the contrast observed:
a) Topographical contrast which is caused by variation in the orientation of different parts of the surface.
b) Atomic number contrast in which elements of higher atomic number give rise to an enhanced probability of secondary electron emission, due to their inherent higher electron density.
c) Charging effects which can arise when examining insulating films when charge build up occurs and leads to enhanced secondary emission.
d) The formation of a potential barrier by the presence of the film leading to the surface becoming depleted of carriers. This would cause a decrease in the secondary emission.

From inspection of fig (6.6), it can be seen that the area covered by film is darker than the bare exposed InP surface. This enables the third mechanism (c) to be rejected on the grounds that it would lead to the film appearing in lighter contrast than the InP. The topographical contrast argument (a) can also be rejected as both the indium phosphide and the phthalocyanine film are smooth. This then leaves mechanisms (b) and (d) to be considered. Further information relating to this matter is provided by the series of experiments on a layered

structure (0,1,3,10) of manganese 4-ter-butyl phthalocyanine. Figures (6.7a&b) show the observed scanning electron micrograph for this structure on InP, with beam energies of 1.5keV and 7.5 keV, respectively. With the 1.5keV beam (fig. (6.7a)), the layers can be clearly distinguished and a dark band of contrast at the start of the 10 layer region can also be observed. This band is an artifact due to a build up of material caused by variations in the level of the meniscus during dipping. For a 1.5keV beam the information emanates predominantly from the immediate surface of the sample and mechanism (b) adequately explains the observed intensities of the different layers. This is because the In has a relatively high atomic number of 49, compared with the phthalocyanine which is made up predominantly of low atomic number elements; consequently the uncoated InP appears in light contrast. However, the electron micrograph for the 7.5keV beam (fig. (6.7b)), while showing contrast between the InP region and the first two steps in thickness of the phthalocyanine layers, does not show any appreciable contrast between the last two steps (3 and 10). This cannot be explained simply by invoking the explanation used for the 1.5keV beam as the depth of penetration of the at 7.5keV is of the order of a micron and the thickest section of the phthalocyanine film is only 200Å. Thus, the observed contrast can only be explained by invoking both mechanisms and suggesting that both processes compete against one another in the thicker layers, which results in almost the same intensity being observed for both. Indeed the barrier mechanism will also be operative with the 1.5keV

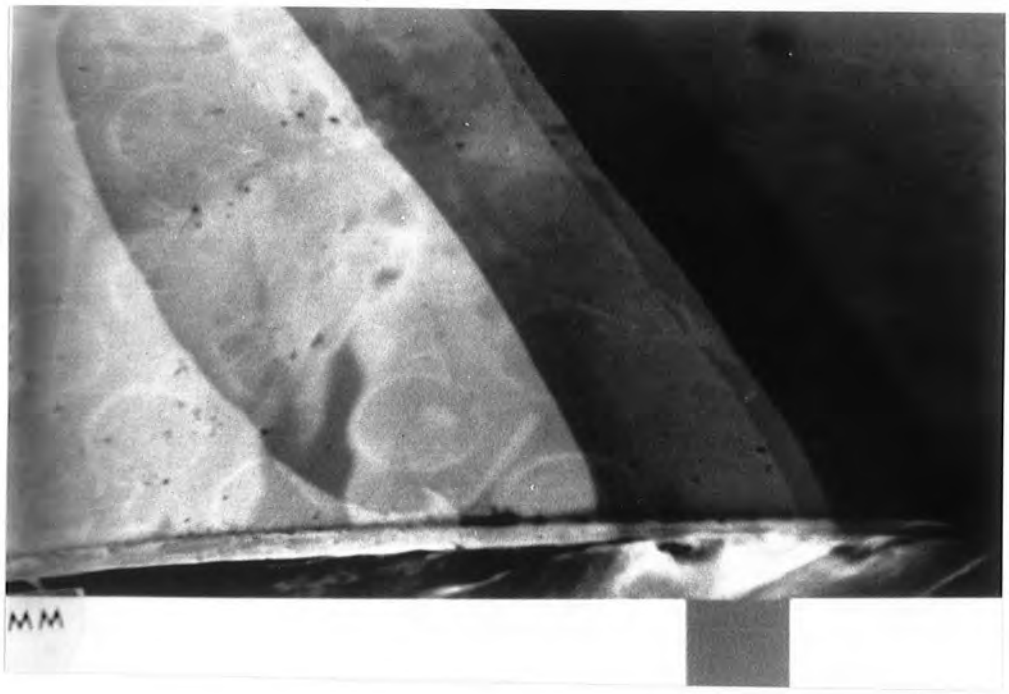

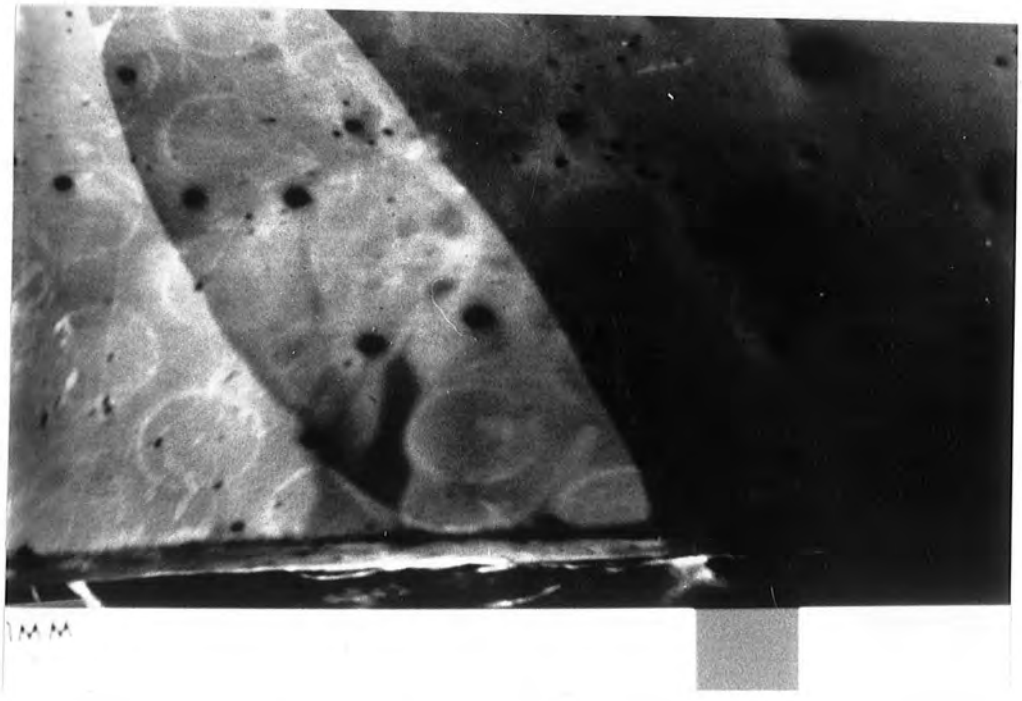

Figure 7. A scanning electron micrograph of manganese 4-ter-butyl phthalocyanine, taken with a beam strength of, a)1.5kV and b) 7.5kV.

beam, but because most of the emitted secondary electrons come from the very top surface the atomic number mechanism is more dominant.

The sample was also observed with the SEM operating in an absorbed current mode. The micrographs were observed to be the complement of those obtained in the secondary emission mode. showing that the reduction in intensity is due to the electrons being absorbed by the sample.

6.2 OPTICAL PROPERTIES

In this section the absorbance spectra of the various phthalocyanine LB films are compared with the solution spectra. The Beer-Lambert law is checked for both the solutions and the LB films. In the case of the phthalocyanine LB films, the peak absorbance is plotted versus the number of deposited layers to check for uniformity of deposition.

Solution characterisation

The optical characterisation of the phthalocyanine films began with an assessment of the solutions from which they were prepared. The absorbance spectra of a series of solutions of diminishing concentration, prepared by successive dilutions of the original solution, were measured. Data were thus obtained to ascertain whether the absorption peaks shifted as the

concentration was varied and to test the validity of the Beer-Lambert law: (A=ecd) where A is the absorbance, e the molar extinction coefficient, c the concentration in moles/litre and d the path length. For the Beer-Lambert law to be obeyed, a plot of absorbance versus concentration will follow a linear relationship.

Absorbance versus concentration plots are presented for dilithium, manganese 4-ter-butyl, and asymmetrically substituted phthalocyanine, in fig. (6.8). As can be seen plots a and b for dilithium and manganese 4-ter-butyl phthalocyanine both yield linear plots, showing that the Beer-Lambert law is obeyed in this region. The plots give molar extinction coefficients of $0.87x10^{5}$ and $0.63x10^{5}$ for the dilithium and manganese form respectively. These values being of the order expected for phthalocyanine materials.

The plot for the asymmetrically substituted copper phthalocyanine, however, shows a departure from linearity at higher concentrations. The deviation from the Beer-Lambert law appears to be due to the formation of a dimer complex in the solutions of higher concentration. This can be quantified further by reference to fig. (6.9) where the spectra obtained for two solutions, one of concentration $8.6x10^{-6}$ moles/litre the other $71.1x10^{-6}$ moles/litre. As can be seen there are two main peaks, the main absorption peak occuring at 674nm and a smaller broader peak at 614nm. In previous studies, the long narrow longer wavelength absorption has been attributed to a monomeric phthalocyanine complex, and the broad partially resolved

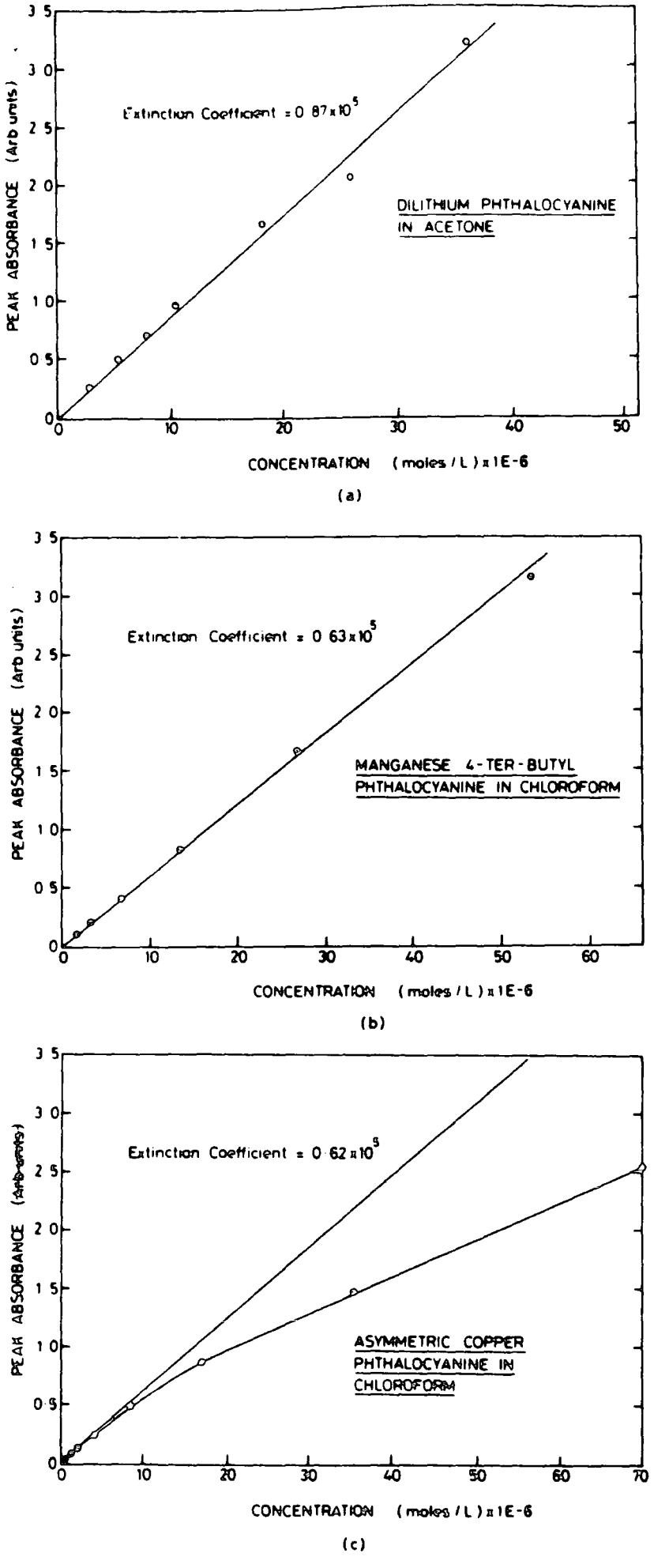

Figure 8. A plot of absorbance versus concentration for; a) dilithium phthalocyanine, b) manganese 4-ter-butyl phthalocyanine, c) asymmetrically substituted copper phthalocyanine.

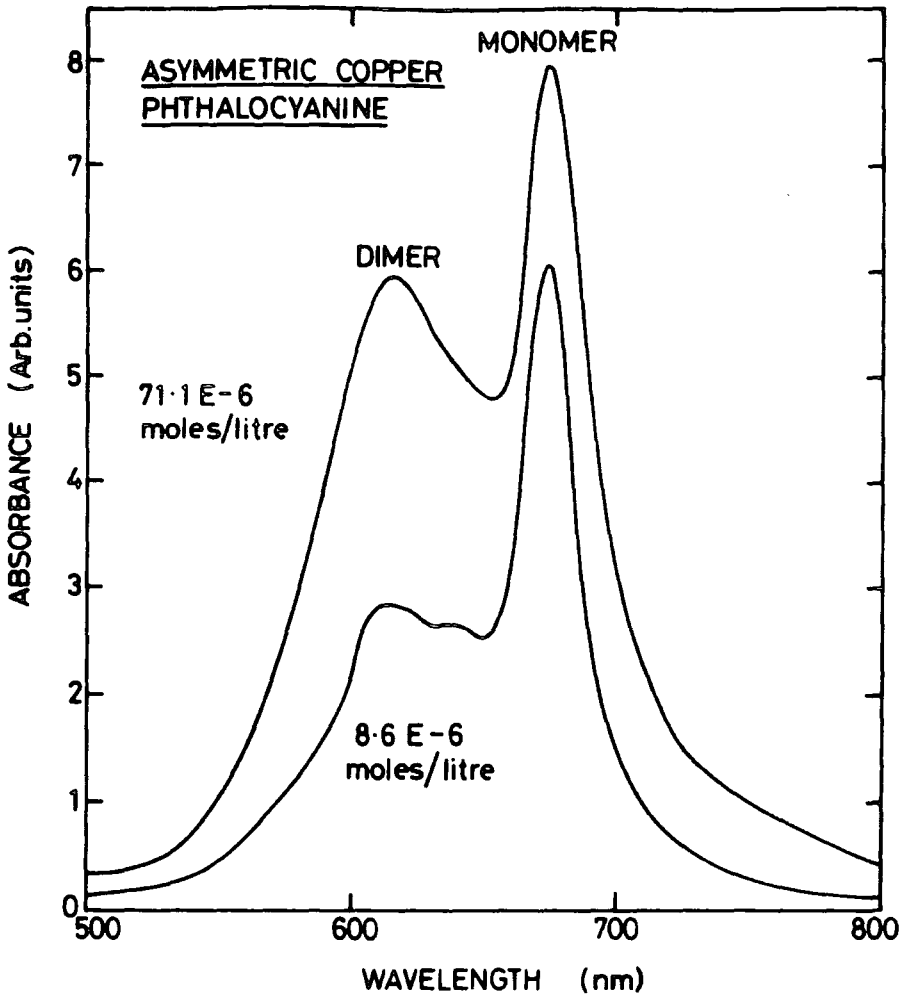

Figure 9. The absorbance spectra for two solutions of concentration 8.6×10^{-6} and 71.1×10^{-6} moles/litre showing the growth of the dimer peak with increasing concentration.

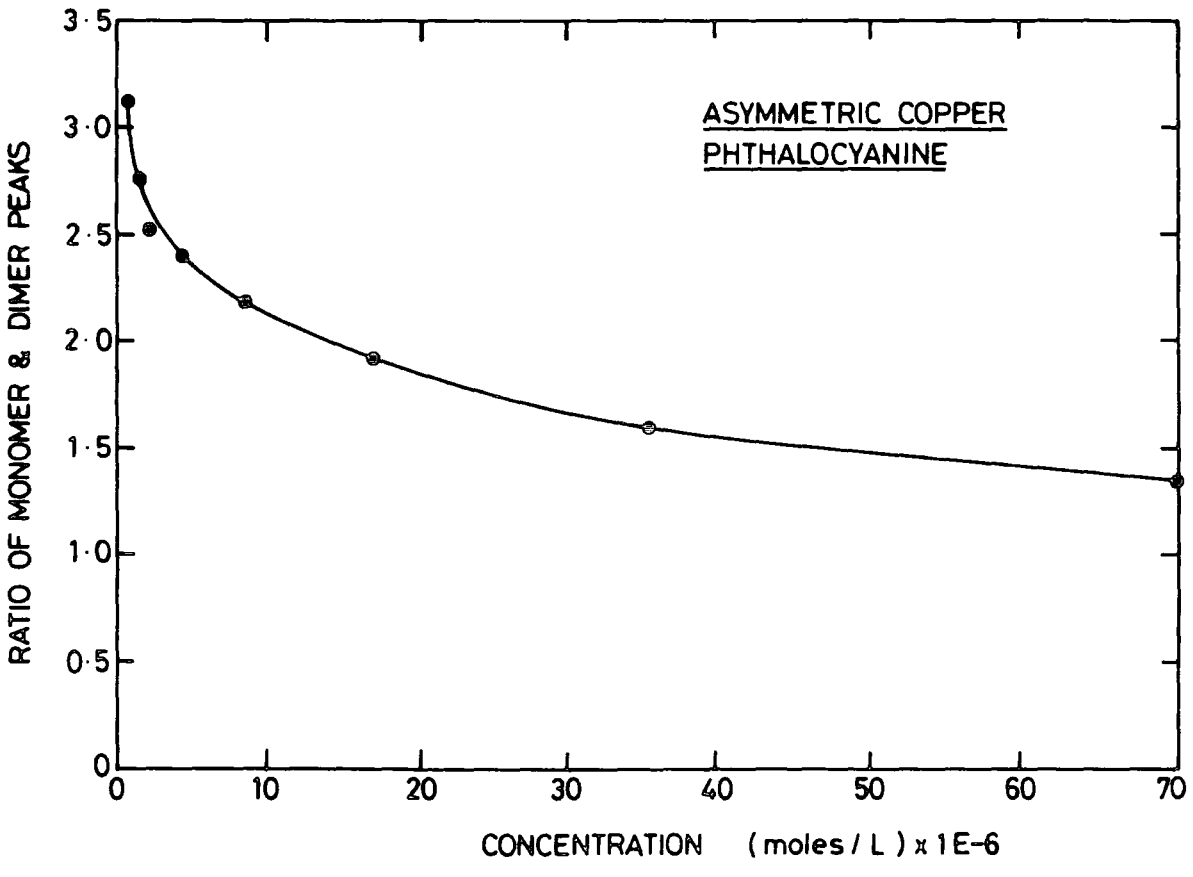

Figure 10. A plot of the ratio of the heights of the monomer and dimer peaks versus concentration, showing the increase of dimer formation with increasing

absorption has been attributed to a dimer complex (1,2 and 3) It can be seen on comparing the relative heights of the monomer and dimer peak for the two solutions, that the dimer peak has increased in height for the solution of higher concentration. Thus the departure from linearity of the absorbance versus concentration plot can be explained in terms of the increasing degree of formation of the the dimer complex. The degree of dimer formation can be seen in fig. (6.10) where the ratio of the monomer and dimer peak is plotted as a function of concentration. It can be seen that the rate of dimer formation in concentrations above $15x10^{-6}$ moles/L is found to level off; this explains the second linear section in the absorbance versus concentration plot. Finally an extinction coefficient of $0.625x10^{5}$ can be calculated for the solution concentrations below 10^{-6} moles/litre, where the Beer-Lambert law appears to be obeyed. This value is in good agreement with the values obtained for the dilithium and manganese forms.

Phthalocyanine LB films characterisation

Fig. (6.11) shows the absorption spectra for both a solution of dilithium phthalocyanine, and a deposited LB film of metal-free phthalocyanine. As can be seen the absorption spectra for the solution consists of the lowest allowed transition at 662nm with two additional vibrational maxima, located at 632 and 598nm. In comparison, the metal-free film is

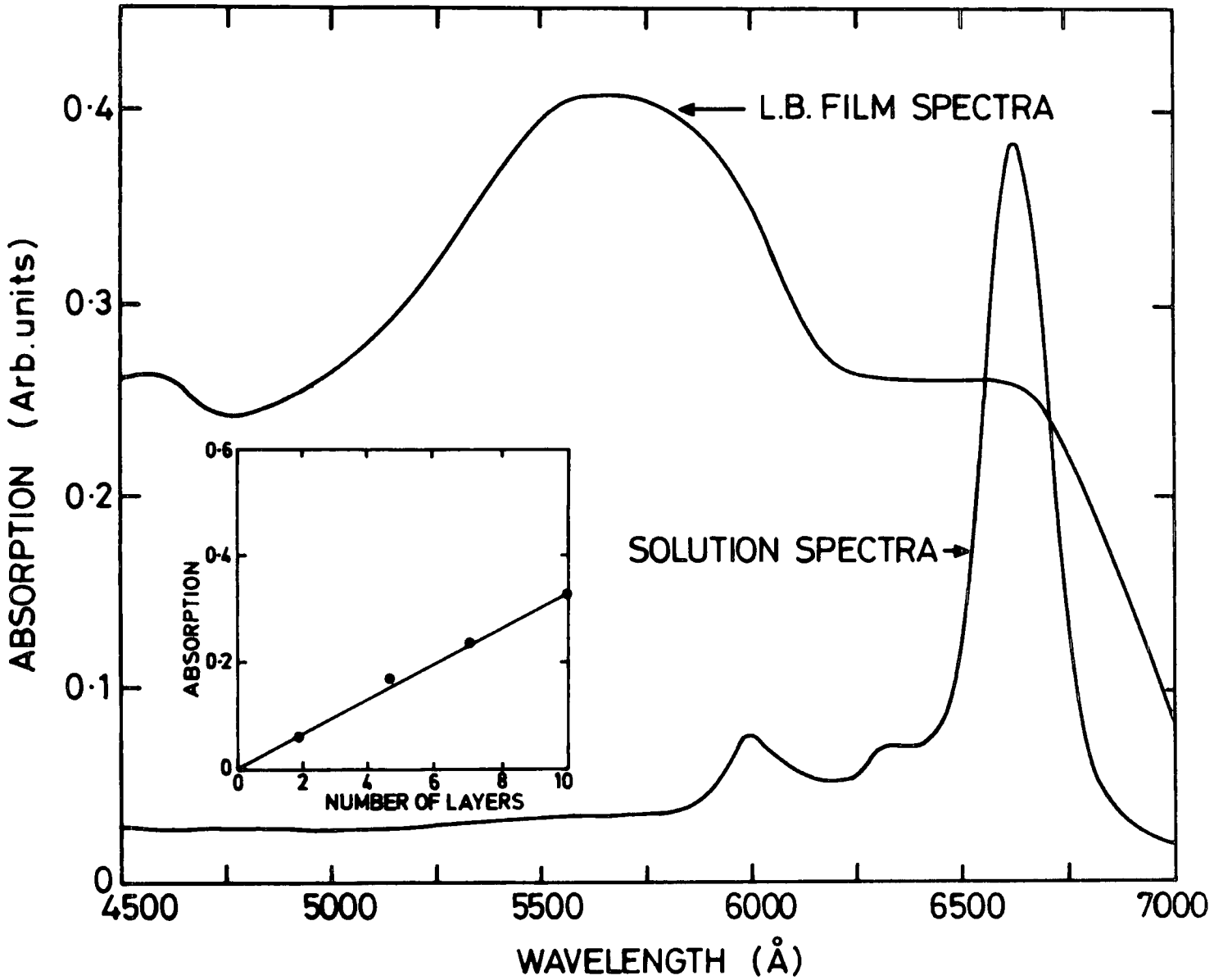

Figure 11. Absorbance spectra for both a solution of dilithium phthalocyanine, and a deposited LB film of metal-free phthalocyanine.

much broadened and shows no vibrational structure. There is a crystal field shift of 2785 cm^{-1} from the 0-0 solution transition at 662 nm, and the two observed electronic transitions at 568 and 662 nm result from a dipole-dipole interaction between adjacent molecules in the film. This indicates that the dipoles are not aligned parallel but are inclined at an angle to one another. This results in the two peaks, one which is blue shifted and the other which is red shifted, from the absent 0-0 transition. The inset in fig. (6.11) shows the linear response of absorbance with the thickness of the deposited layers.

A schematic representation of the changes in the electronic levels due to the crystal field and dipole-dipole interactions is shown on fig. (6.12). Figure (6.13) shows the expected peak shifts for the three possible dipole-dipole alignments; a) shows the blue shift, from the (0,0) electronic transition for the free molecule, expected for parallel alignment of the dipoles. b) shows the red shift expected for parallel but opposite alignment of the dipoles, and c) shows the splitting observed for dipoles orientated at an angle to each other. It should be noted that these bands can all be further shifted by the crystal field.

Figure (6.14) shows the absorption spectra for both a solution and an LB film of metal-free 4-ter-butyl phthalocyanine. The solution spectra shows two electronic transitions owing to the symmetry of the molecule. These transitions are located at 700 and 664 nm; vibrational maxima are also present at 642 and 600 nm. The film spectrum is again

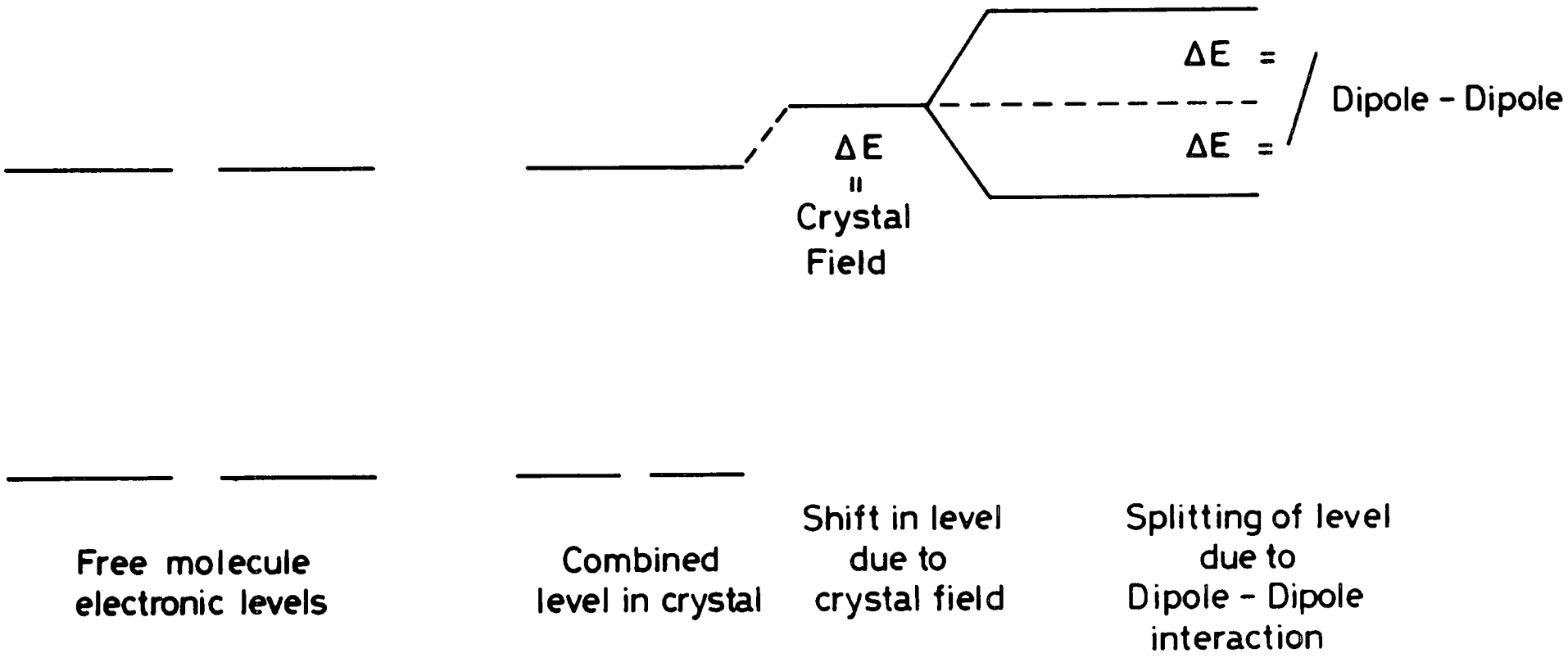

Figure 12. A schematic representation of the changes in the electronic levels due to the crystal field and dipole-dipole interactions.

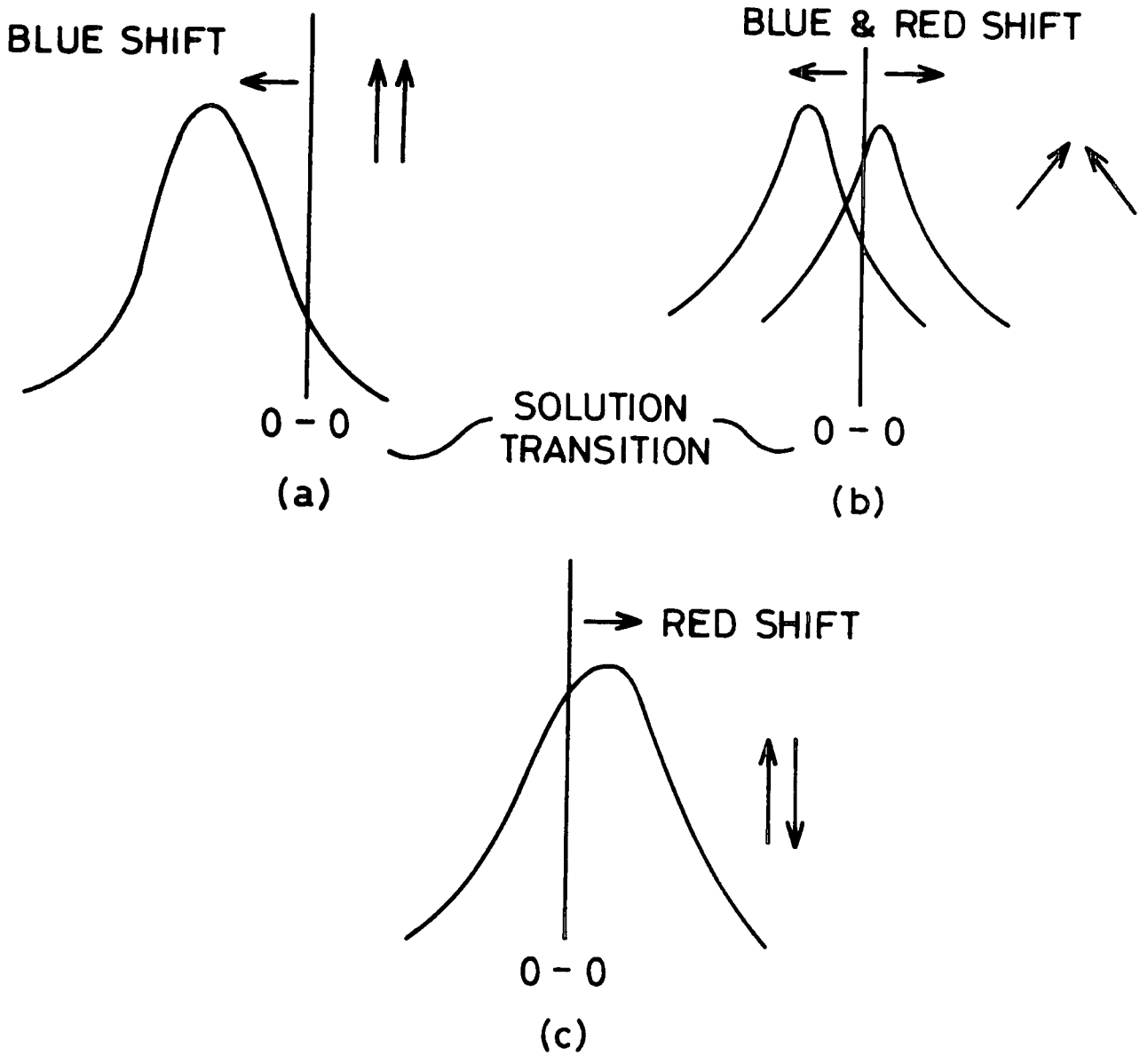

Figure 13. A schematic diagram showing the expected peak shifts for the three possible dipole alignments; a)parallel alignment, b) parallel but opposite alignment, and c) angular alignment.

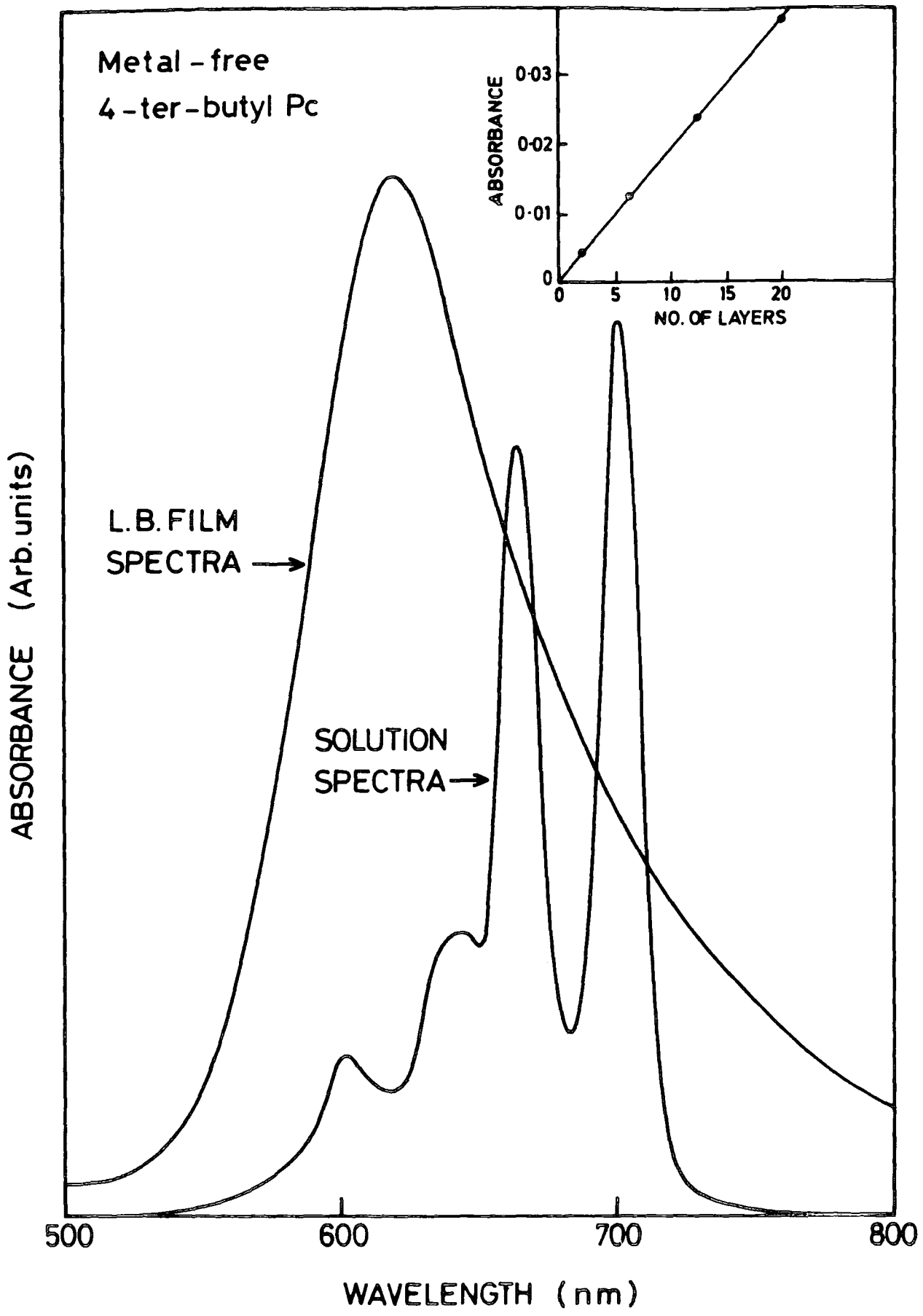

Figure 14. Absorbance spectra for both a solution and a deposited LB film of metal-free 4-ter-butyl phthalocyanine.

broadened and blue shifted, but there is no evidence of a red shifted band. This indicates that the dipoles are aligned parallel and complementary to one another (see fig (6.13)). The inset again shows that the relationship between the number of layers dipped and their absorbance is a linear one.

The absorption spectra for the solution and LB film for both the asymmetrically substituted Cuℓ and the manganese 4-ter-butyl phthalocyanine are shown in figs. (6.15&16) respectively. Both follow a similar scheme, in that the spectra of the solutions show a clear 0-0 electronic transition and additional vibrational maxima. Also the film spectra show broadening due to the crystal field and exhibit no vibrational structure. In both cases the peak is split, showing a blue and red shift, indicating that the dipoles of the molecules are inclined at an angle to one another in their respective films.

Mixed layer characterisation

The results reported here are for asymmetrically substituted phthalocyanine contained in a stearic acid matrix. It was found that the spectra observed for the mixed layers were all very similar to the spectra obtained for . LB films formed from the pure asymmetrically substituted phthalocyanine. The substrates used to check the deposition of layers containing various percentages of stearic acid (reported in section 5.4.5) were also used to check if the expected proportion of phthalocyanine had actually been incorporated in the deposited

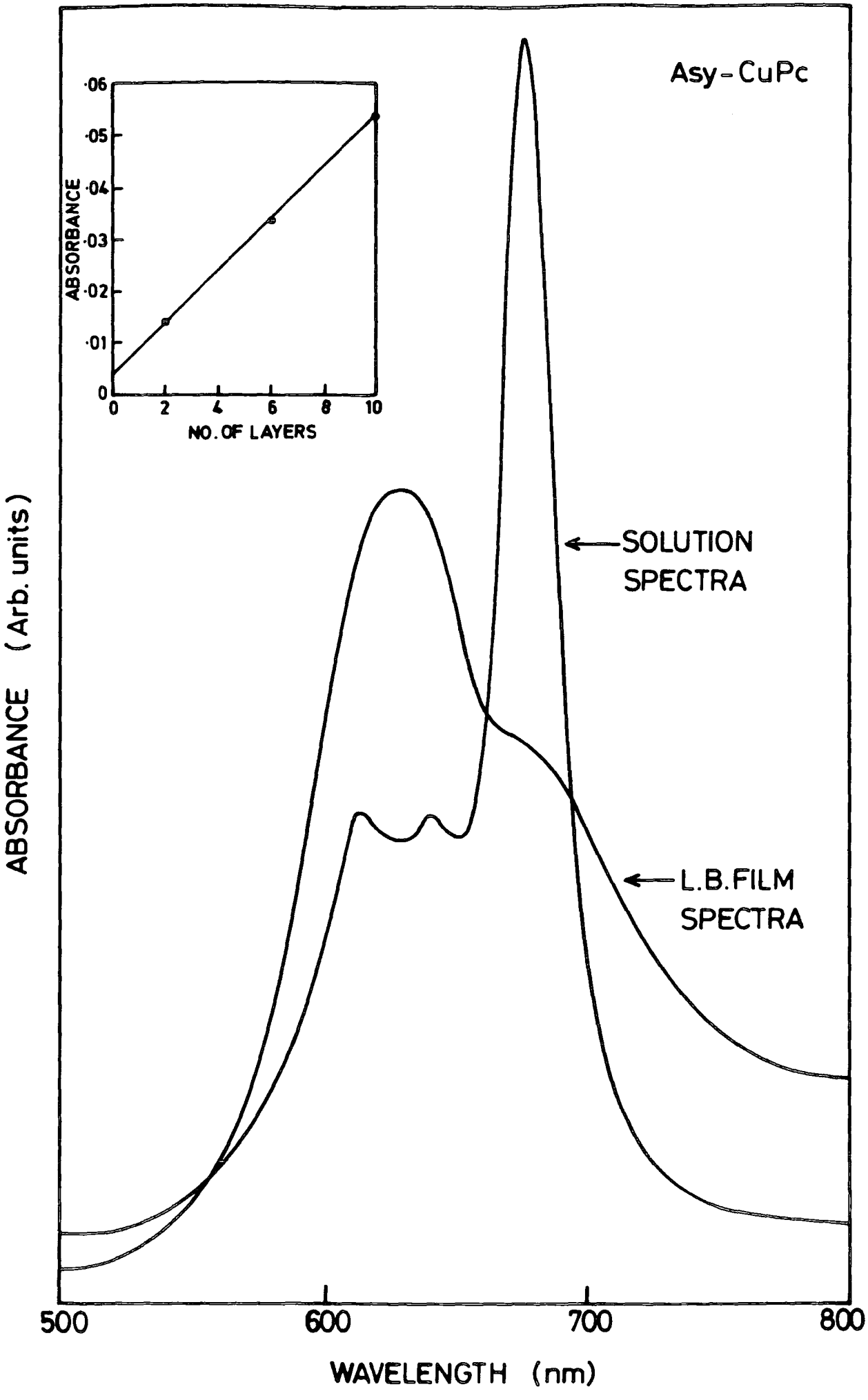

Figure 15. Absorbance spectra for both a solution and a deposited LB film of asymmetrically substituted copper phthalocyanine.

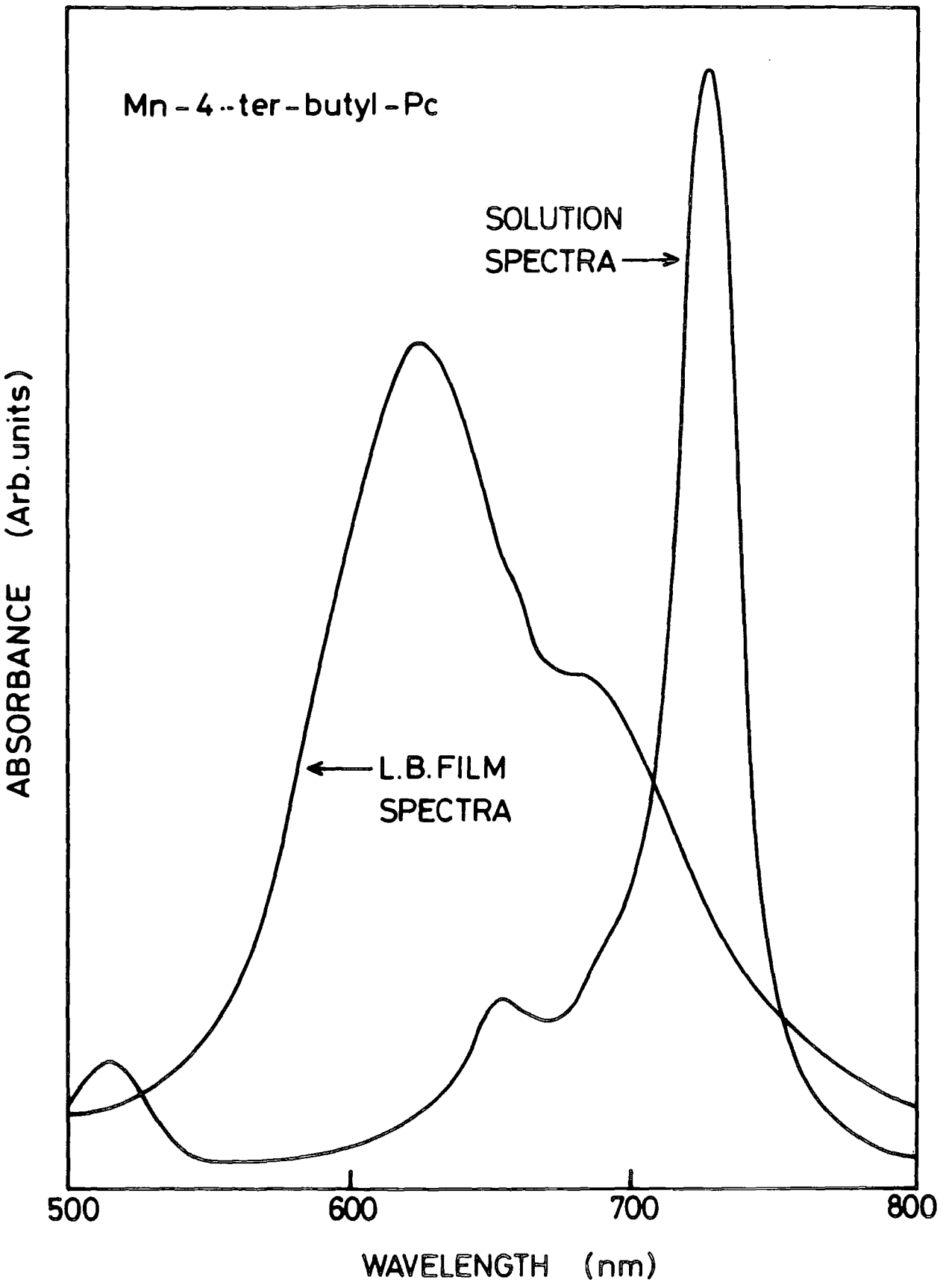

Figure 16. Absorbance spectra for both a solution and a deposited LB film of manganese 4-ter-butyl phthalocyanine.

layers. This was achieved by plotting the measured absorbance of each sample against the percentage of phthalocyanine contained. As can be seen with reference to fig. (6.17a) the expected linear relationship is not observed indicating that full deposition is not being achieved on each dip. Indeed as reported in section 5.4.5 this is the case and the deposition was seen to deteriorate for stearate mixtures containing more than 80% stearic acid. The results shown in fig. (6.17a) were corrected by calculating the total area transferred and normalising the results to absorbance per unit area dipped. Replotting this value against the percentage of phthalocyanine in each film gave the expected linear relationship as shown in fig. (6.17b).

As mentioned previously the spectra of these films were very similar to the spectra obtained for a LB film of the asymmetrically substituted phthalocyanine, a dominant broad peak being observed at 624 nm with a shoulder at 670 nm. However, one feature that was observed was that as the concentration of phthalocyanine in the film fell the structure of the shoulder at 670 nm became more distinct. It was concluded that this was due to the reduction in the crystal field experienced by the phthalocyanine molecules. It would follow then that if the dilution was carried out further the spectra should become even more distinct and ultimately if a high enough dilution was used it should be possible to eliminate the dipole-dipole interactions and return back to the free molecule spectra. With the time and equipment available it was possible to prepare a

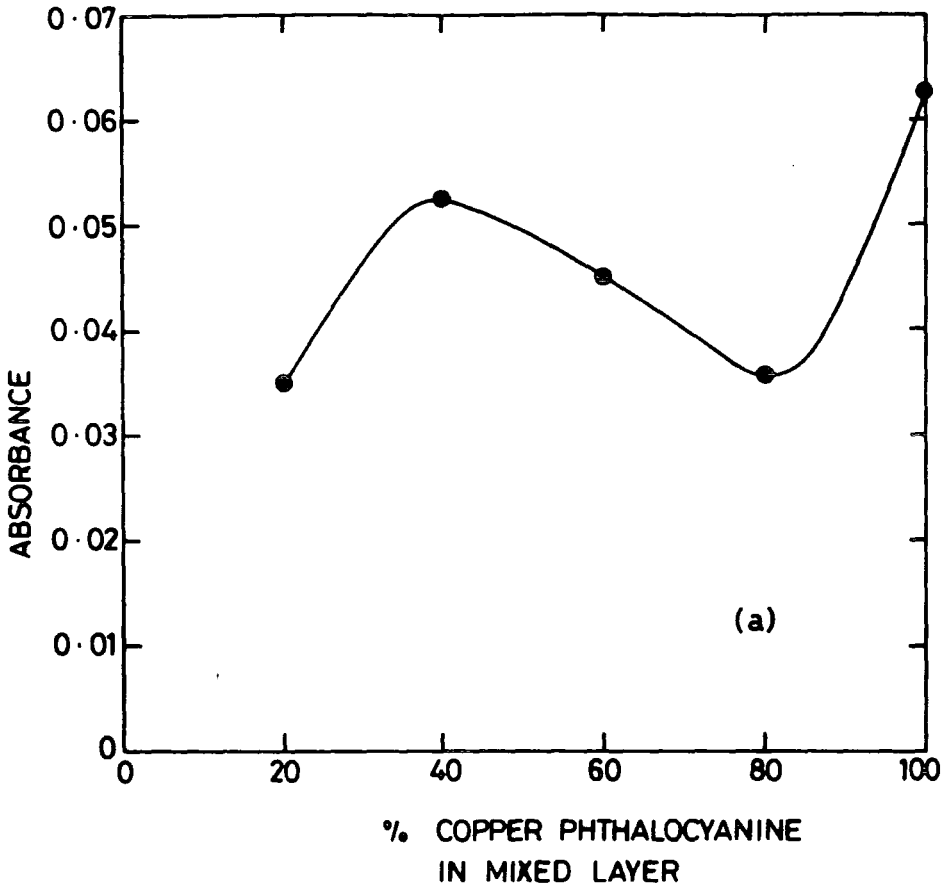

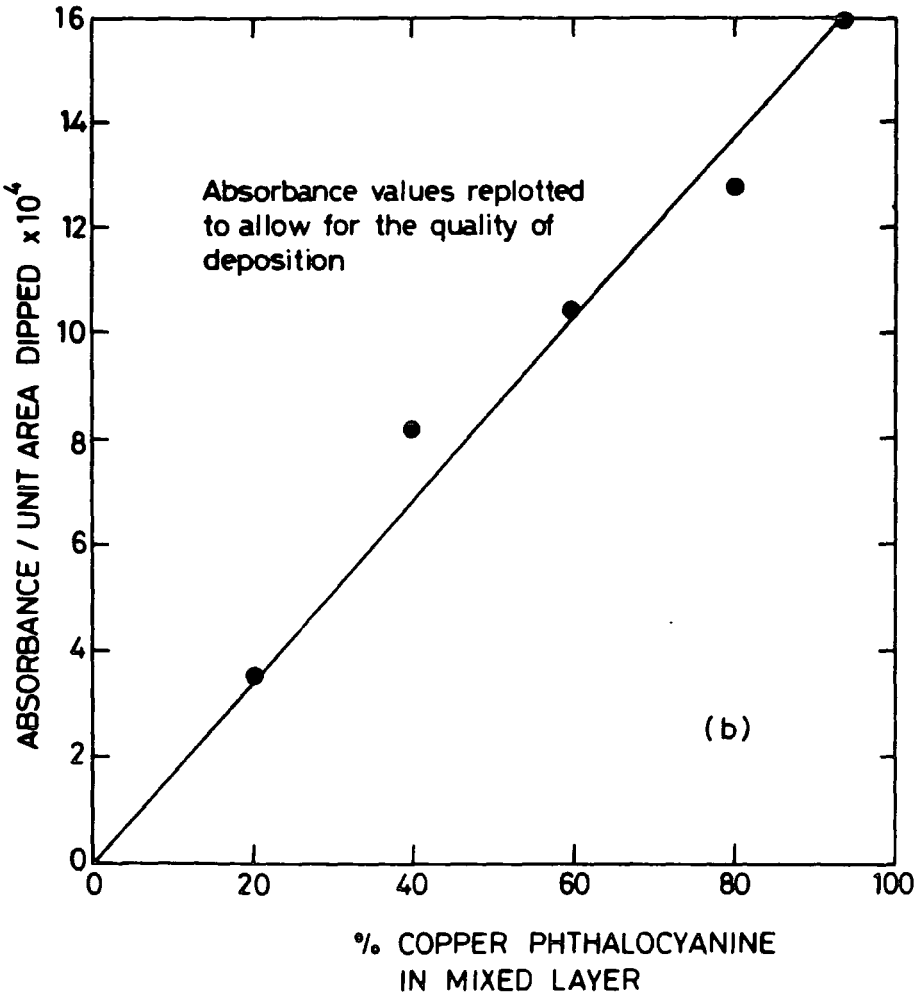

Figure 17. Absorbance values for a range of mixed layer samples containing various percentage mixtures of phthalocyanine, a) The absolute absorbance values plotted versus percentage composition, b) The absorbance values corrected to allow for the quality of deposition by normalising to unit area of

sample which contained only 1% phthalocyanine. The spectrum obtained is shown in fig. (6.18). as can be seen at this concentration the two peaks are now quite clearly resolved. Additional structuring also appears to be apparent but as this spectrum is taken right at the bottom of the lowest scale it is difficult to say whether they are true artifacts of the film. The resolution of the peaks can be attributed to a substantial reduction in the crystal field which is responsible for the broadening of the peaks in the more concentrated films.

The fact that the spectra observed still show the splitting of the 0-0 solution transition indicates that there is still significant dipole-dipole interaction taking place. This could be expected as, at this concentration, modelling of the packing in the layer demonstrates that, at most, the phthalocyanine molecules will be isolated from each other by only one layer of stearate molecules. Further work is to be carried out in preparing substrates of substantially lower concentrations in an effort to achieve isolation of the phthalocyanine molecules.

6.3 Electrical properties

This section describes the electrical characterisation of the phthalocyanine LB films. The data presented fall into the three areas; capacitance, lateral conduction and bulk conduction. The capacitance measurements were used to assess the reproducibility of the deposition process, by plotting the reciprocal capacitance against the thickness of the deposited

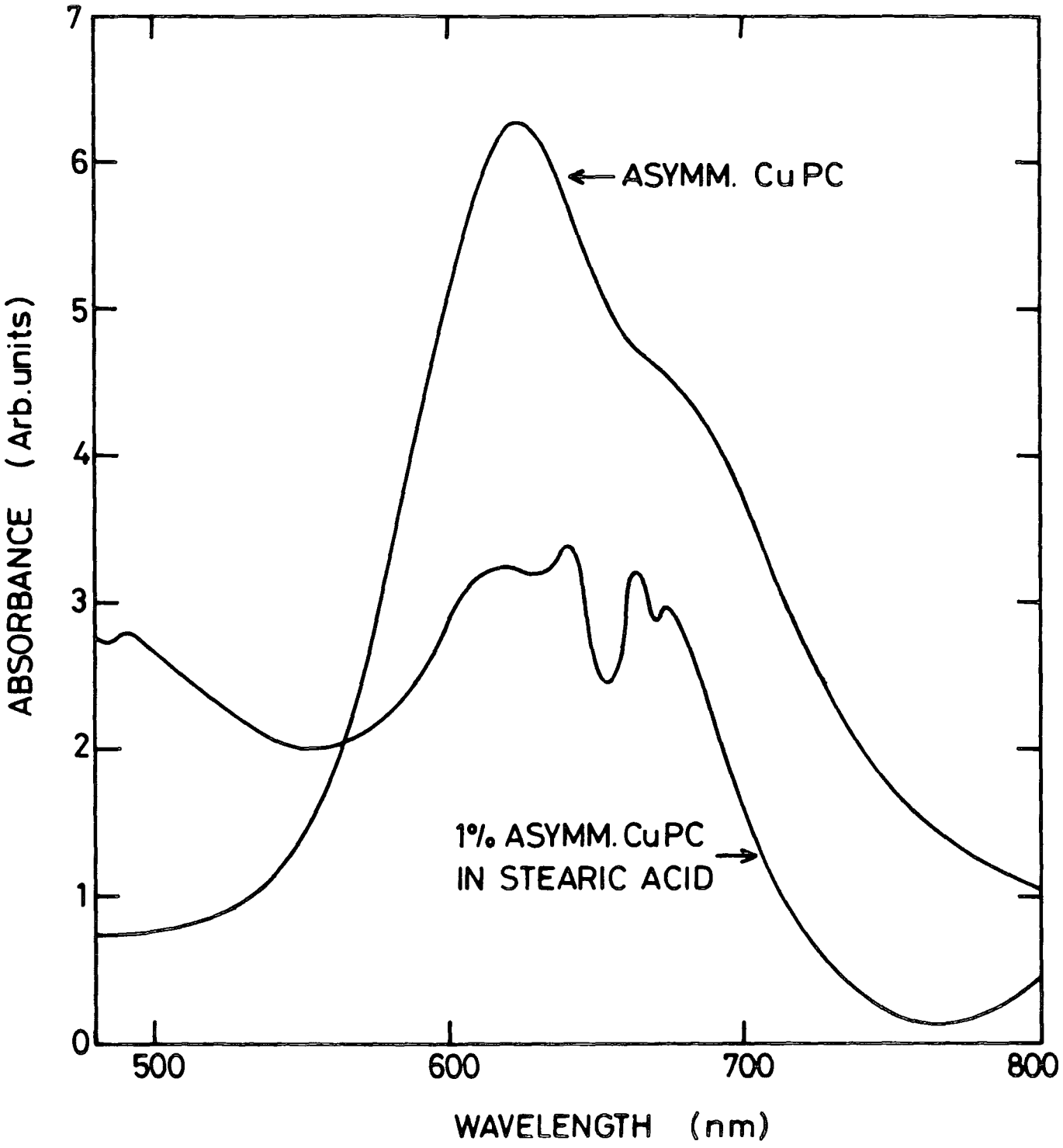

Figure 18. Absorbance spectra for both an LB film of ASY-CuPc and a mixed layer containing 1% ASY-CuPc in stearic acid.

film. These are relatively easy to interpret. However, the d.c. conduction mechanisms are more complex and require some knowledge of barrier-limited and bulk limited processes. The relevant background theory is briefly explained in the following sub-section.

6.3.1 Conduction Mechanisms in Organic Materials

The manner in which charge is transported through any material depends critically on the wave-function overlap between adjacent sites. Apart from the one-dimensional conductors such as polyacetylene, the transfer is less effective in organic compounds because of the weak inter-molecular forces involved. The phthalocyanines have relatively high mobilities for organic materials; it has been mentioned in chapter 2 that values close to 1.5 $cm^2/V.s$ are typical, depending on the quality of the material and the metal ion insertion. However, as far as the statistics of the charge carriers are concerned, it has been demonstrated conclusively by Sussman (4), Cox (5) and Barbe and Westgate (6) that a similar situation to that which exists in inorganic semiconductors, is valid. We can then distinguish two types of current-voltage characteristics depending whether bulk-limited or barrier-limited processes are involved.

Barrier-Limited

There are many types of barrier that can hinder the flow of electrons or holes across a sample. The most common is the Schottky barrier that is formed at the surface of a semiconductor and can lead to rectification. In forward bias one commonly observes a linear plot of log current versus voltage. However, with thin organic films the most common current-voltage relationship observed takes the form of log J proportional to $V^{1/2}$. This can arise due to either the Schottky or Poole-Frenkel effect.

The Schottky effect describes the situation where the conduction process is dominated by the emission of carriers directly into the extended conduction band or valence band states from the metal electrode. At the metal-semiconductor boundary, in the presence of a strong electric field, the barrier separating the electron states in the metal and the conduction band states can be approximated as:

$$\phi=\phi_{ms} - \frac{q^2}{(4\pi\varepsilon_o\varepsilon)4x + q^2/\phi_{ms}} - Fqx \qquad 6.1$$

The first term ϕ_{ms} is the metal-semiconductor work function and the second arises from the image forces on an electron leaving the metal and varies as $1/(4x)$. This term has the effect of rounding off the step barrier due to the metal-semiconductor work function; the third term is due to the electric field. It may be shown that this type of potential function leads to a relationship of the form

$$\text{Log } J = \gamma_S F^{1/2}/kT \qquad 6.2$$

where F is electric field and $\gamma_s = (q^3/4\pi\varepsilon\varepsilon_o)^{1/2}$ is termed the Schottky constant.

A similar result to that of the Schottky effect is found for the Poole-Frenkel effect, but there are some important differences in concept between the two processes. In this case conduction is due to charge movement between impurities or defect levels in the bulk of the material. The electrons can be considered to be sited at donor levels which basically form a series of potential wells. In the presence of an electric field the potential of these wells is altered so as to lower the energy required for an electron to transfer to a neighbouring atom. The barrier, separating the localized level from the transport band is

$$\Phi(x) = \Phi - \frac{q^2}{4\pi\varepsilon\varepsilon_o x} - Fqx \qquad 6.3$$

Where ϕ is the energy difference between the levels and the band in the absence of the field. The second term is again a Coulombic term but in this case, since the remaining positive donor level is fixed in space, it only varies as $1/x$. Thus, a similar log J proportional to $V^{1/2}$ current-voltage relationship is observed, but the constant of proportionality is different. In the Poole-Frenkel case, the relationship is

$$\text{Log}J = \gamma_{pf} F^{1/2}/kT \qquad 6.4$$

where $\gamma_{pf} = 2\gamma_s$

Bulk-Limited

The classical case of bulk limited conduction is Ohms Law. However, there are several situations where the addition of injected charge can result in super-linear current-voltage characteristics. The most common of these results from the injection of these charge carriers at a planar metal-semiconductor contact and is termed space-charge-limited-conduction (SCLC). There is a close analogy between space charge conduction in solids and in a thermionic diode. The fundamental difference occurs because in a vacuum electrons can be treated as obeying simple particle dynamics but in a solid the mobile charge carriers are continually interacting with the crystal lattice. A thermodynamic equilibrium is maintained between the space charge and the crystal lattice so that there is a linear relationship between the applied electric field and the drift velocity of the carriers. Accordingly, SCLCs in a solid medium are lower than the corresponding ones in a vacuum by several orders of magnitude. The presence of trapping sites, recombination and the possibility in a solid that, with a suitable choice of contacts, hole injection as well as electron injection can occur, brings in added complications.

The complete analysis of time independent SCLC in solids is complex but a relatively simple expression can be derived relating the current, voltage, and thickness in a trap free insulator. It is;

$$J = 9/8\, \sigma_n \varepsilon \mu_e (V^2/L^3) \qquad 6.5$$

In this equation μ_e is the electron mobility, ε is the permittivity and ϕ_n is the fraction of total carriers which are free. Equation (6.5) is a special case of the general scaling law for bulk space charge currents in a homogeneous medium which is

$$J = L(V/L^2)^m \qquad 6.6$$

where m is a constant which need not necessarily be an integer. For example in the trap free insulator case m=2, while for double injection m=3, and for recombinative space charge injection m=1/2

6.3.2 Capacitance measurements

The capacitance was measured as described in chapter 4, and the reciprocal capacitance plotted against the number of layers deposited, the linearity of the resulting plot is indicative of the quality of the deposited layers. The results described here are for the asymmetric copper phthalocyanine, on both aluminised glass slides and on semiconductor substrates. In all cases there is inevitably a surface layer on the substrate before deposition of the film. The thickness of the native oxide layer is not known but can often be inferred from the intercept of the reciprocal capacitance versus number of layers plot. An aluminium slide was oxidised by anodically growing an oxide layer on its surface whose thickness could be estimated from the voltage used to grow it. Figure (6.19) shows a diagram of

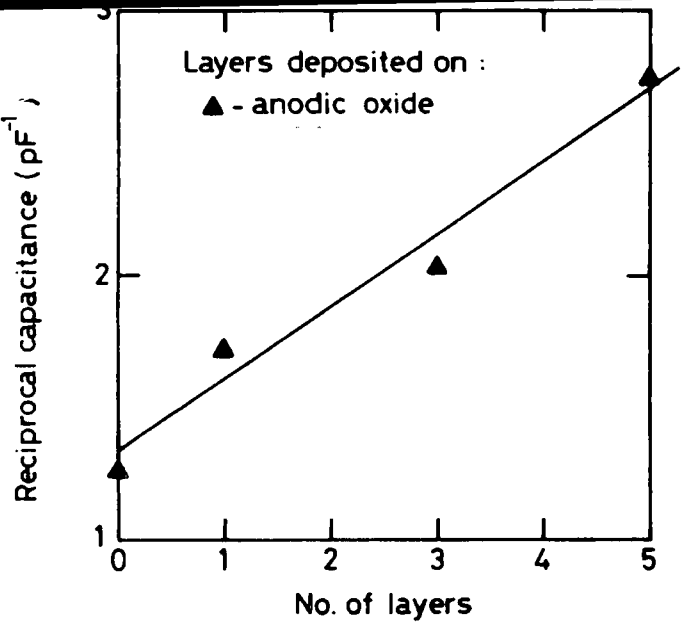

Figure 19.

A plot of the reciprocal capacitance versus the number of layers of ASY-CuPc deposited on an aluminium/anodic oxide substrate.

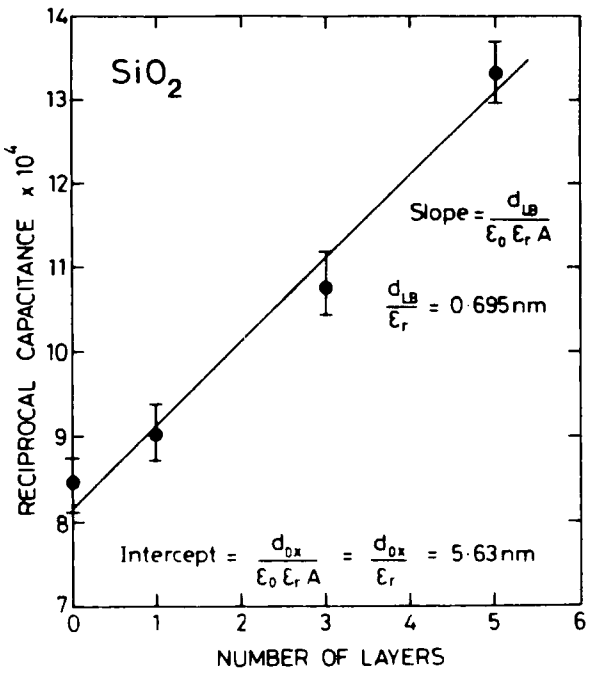

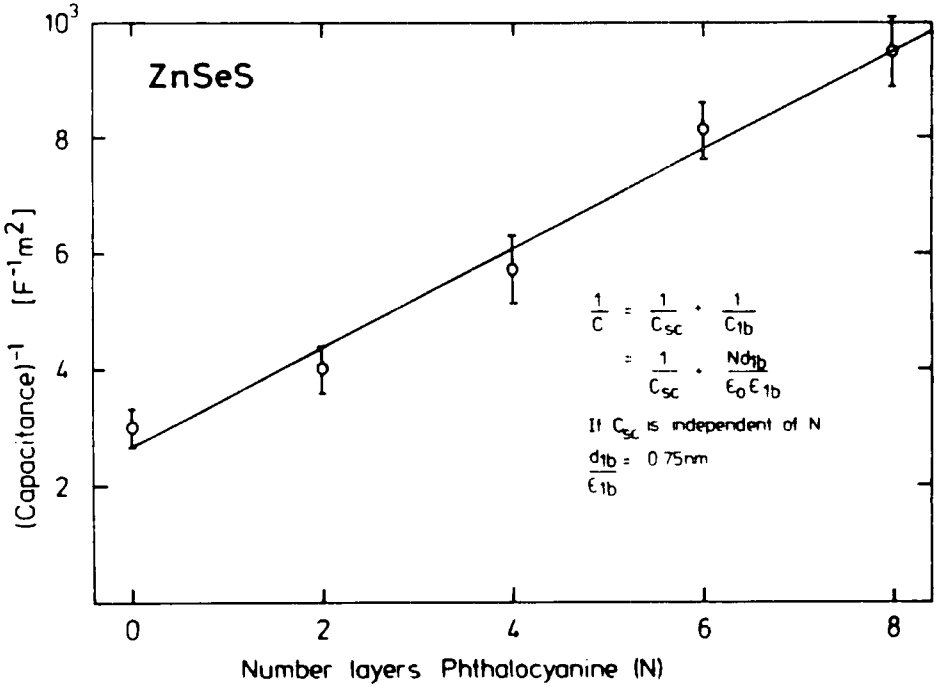

Figure 20. A plot of the reciprocal capacitance versus the number of layers of ASY-CuPc dipped for layered structures on both Sio_2 and ZnSeS.

reciprocal capacitance versus the number of phthalocyanine layers dipped. The value of dielectric thickness per layer obtained from the plot is 0.30nm. Assuming a value of 2.7 for the dielectric constant, leads to a molecular thickness of 0.8nm. This value is much less than that expected if the molecules were stacked edge ways on the substrate (a value of the order of 2nm might be expected for this configuration). One explanation is that the molecules are orientated differently upon the substrate to when they are compressed upon the trough; that is, a change in orientation occurs when the film is transferred. Such an explanation has been used by Hann et al (1) for films of zinc 4-ter-butyl phthalocyanine. In this related research investigation, he reports a thickness of 0.9nm per deposited layer from similar capacitance measurements. From the intercept of the reciprocal capacitance versus number of layers deposited plot in fig. (6.19), assuming a value of 8 for the dielectric constant of Al_2O_3, we obtain a thickness of 10nm, in good agreement with that expected based on the anodic growth conditions.

Measurements were also performed for ASY-CuPc layered structures deposited onto both Si and ZnSeS structures. Figure (6.20) shows the plots obtained. As can be seen, both cases give better linear behavior than that achieved for the aluminised substrate. The calculated values of dielectric thickness obtained per layer are 0.70 and 0.75 nm, respectively for the Si and ZnSeS substrates. Again, assuming a value of 2.7 for the dielectric constant for the phthalocyanine, this gives

respective thicknesses per molecule of 1.88 and 2.03nm. These values are now consistent with edge-on stacking of the molecules.

With the Si substrate the oxide thickness was known to be about 30nm. The intercept in fig. (6.20) gives a value of 5.63nm for the dielectric thickness and hence, using the literature value of 4.5 for the dielectric constant of SiO_2, an oxide thickness of 25.3nm is obtained in reasonable agreement with the stated value.

In addition, a phthalocyanine LB film was prepared on a silicon/silicon dioxide substrate and examined using a commercial ellipsometer. The measurements indicated a consistent layer thickness of 2.4nm. This is in good agreement with the value obtained from capacitance measurements on the silicon and ZnSeS substrates.

The thickness values obtained for the films deposited on semiconductor substrates, together with the area/molecule values obtained from the pressure area curves reported in chapter 5, indicate that the film formed is a monolayer and that the molecules are stacked edge-on with respect to the substrate. It is interesting to note that SiO_2 has a hydrophobic surface whilst ZnSeS is hydrophillic, yet good deposition is achieved with both. The determining factor in obtaining good deposition then, may well be the use of a high order surface as possesed by the polished semiconductor substrates used. The anodic oxide substrate, however, gave a lower value for the thickness per layer. This is indicitive of a large degree of tilt in the

structure of the deposited film. It is quite likely that the Al_2O_3 is interacting in some way with the centre of the phthalocyanine molecule. Chemical bond formation of this type is known to take place with the fatty acids.

6.3.3 Lateral conductivity measurements

The lateral conduction structures used in our experiments have been described in chapter 4. Great care is required with such measurements because the conductivity of the Langmuir-Blodgett film is relatively low and thus they must be deposited onto well insulated substrates. A rigorous cleaning procedure was required to remove any foreign matter which may have constituted a leakage path for the charge carriers. In some cases, especially at high fields, a correction factor was required. In addition, gold electrodes were used to obviate any difficulties associated with aluminium contacts. Figure (6.21) shows a plot of the lateral conduction observed through five and ten layers of metal-free unsubstituted phthalocyanine. The current is found to scale both with voltage and thickness, indicating ohmic conduction; such behaviour is to be anticipated in view of the relatively low electric fields involved (10^3V/cm). The value of lateral conductivity is calculated to be $\sim 10^{-7}\,\Omega^{-1}.m^{-1}$ Figure (6.22) shows a similar plot obtained for asymmetrically substituted copper phthalocyanine. Once again, Ohm's law is observed, but the conductivity is approximately a factor of 5 higher. Both the conductivities mentioned are

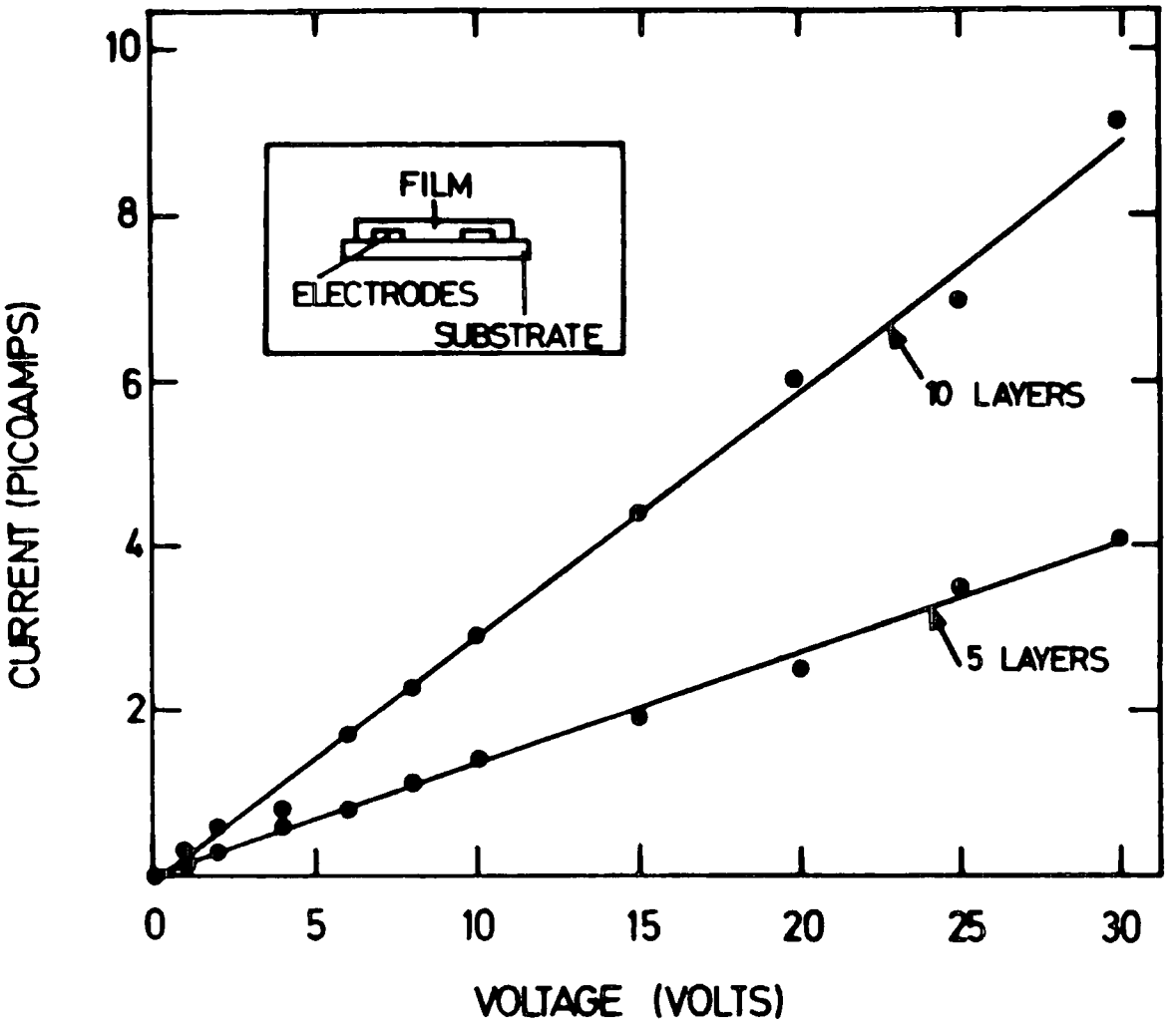

Figure 21. A plot of the lateral conduction observed through five and ten layers of metal-free unsubstituted phthalocyanine.

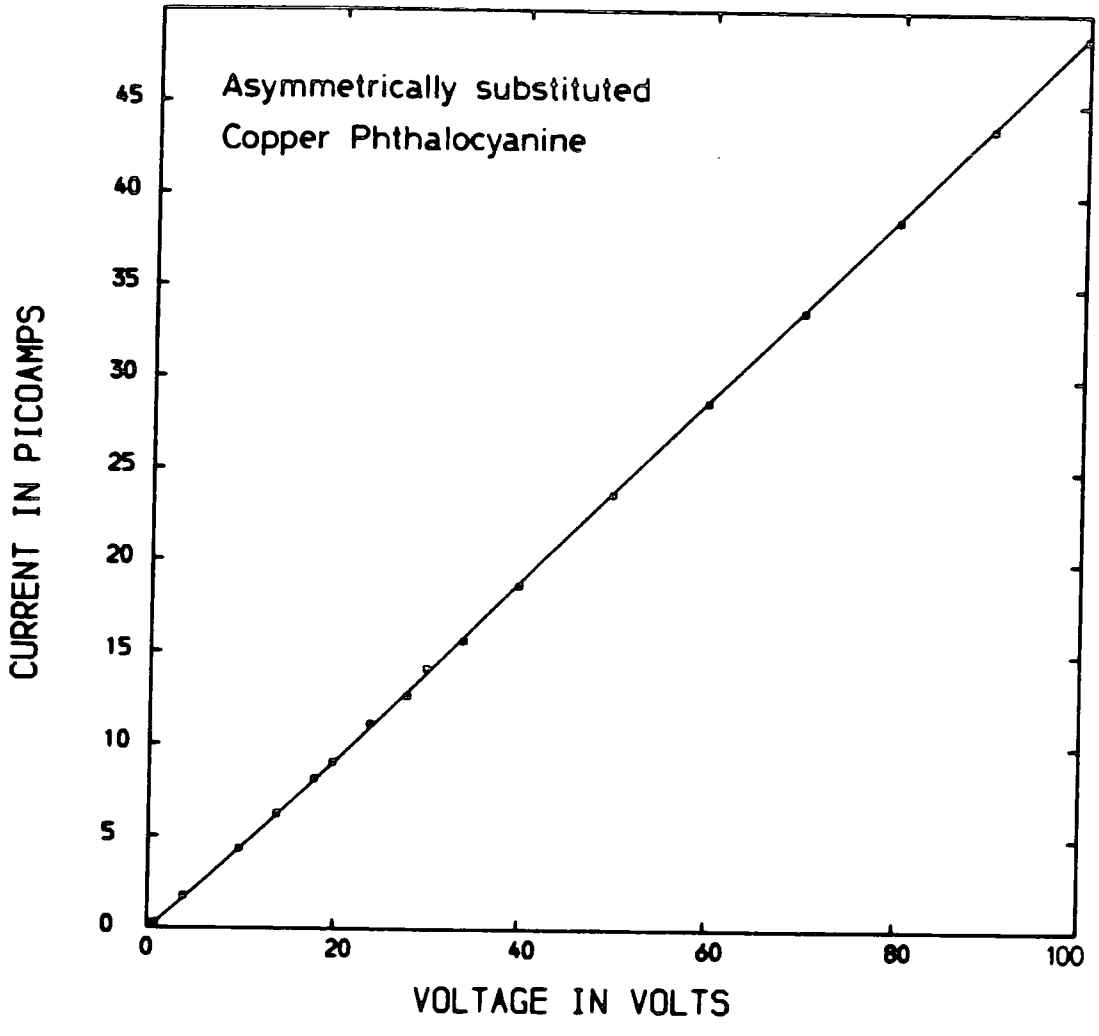

Figure 22. A plot of the lateral conduction observed through five layers of ASY-CuPc.

higher than those commonly observed for single crystals. This is not altogether surprising in view of the different crystalline structure involved; moreover, our method of preparation could well entail the incorporation of solvent, thus creating a charge transfer complex. In summary, the lateral conduction measurements show that the in-plane conductivity of phthalocyanine is approximately 10^{-7} Ω^{-1} m^{-1} and is not enormously sensitive to metal ion incorporation. Despite the improved structure of the ASY-CuPc film compared with the unsubstituted metal-free layers, only a marginal difference in conductivity is observed. The lateral conduction structures, because of their ease of fabrication, have been used in the gas detection experiments described in the next chapter. A greater degree of success was obtained with the Nesa/phthalocyanine LB film/palladium structure.

6.3.4 Bulk conductivity measurements

The majority of conductivity experiments using LB films have been carried out using aluminium as the substrate. Such data are extremely suspect because of the oxide layer associated with this electrode material. Figure (6.23) shows a typical plot obtained for an aluminium-gold sandwich structure containing a few LB layers of metal-free phthalocyanine. The characteristic falls into two distinct straight-line regions when plotted as log J versus $V^{1/2}$. Earlier in this chapter we have described how such behavior can arise when barrier-limited

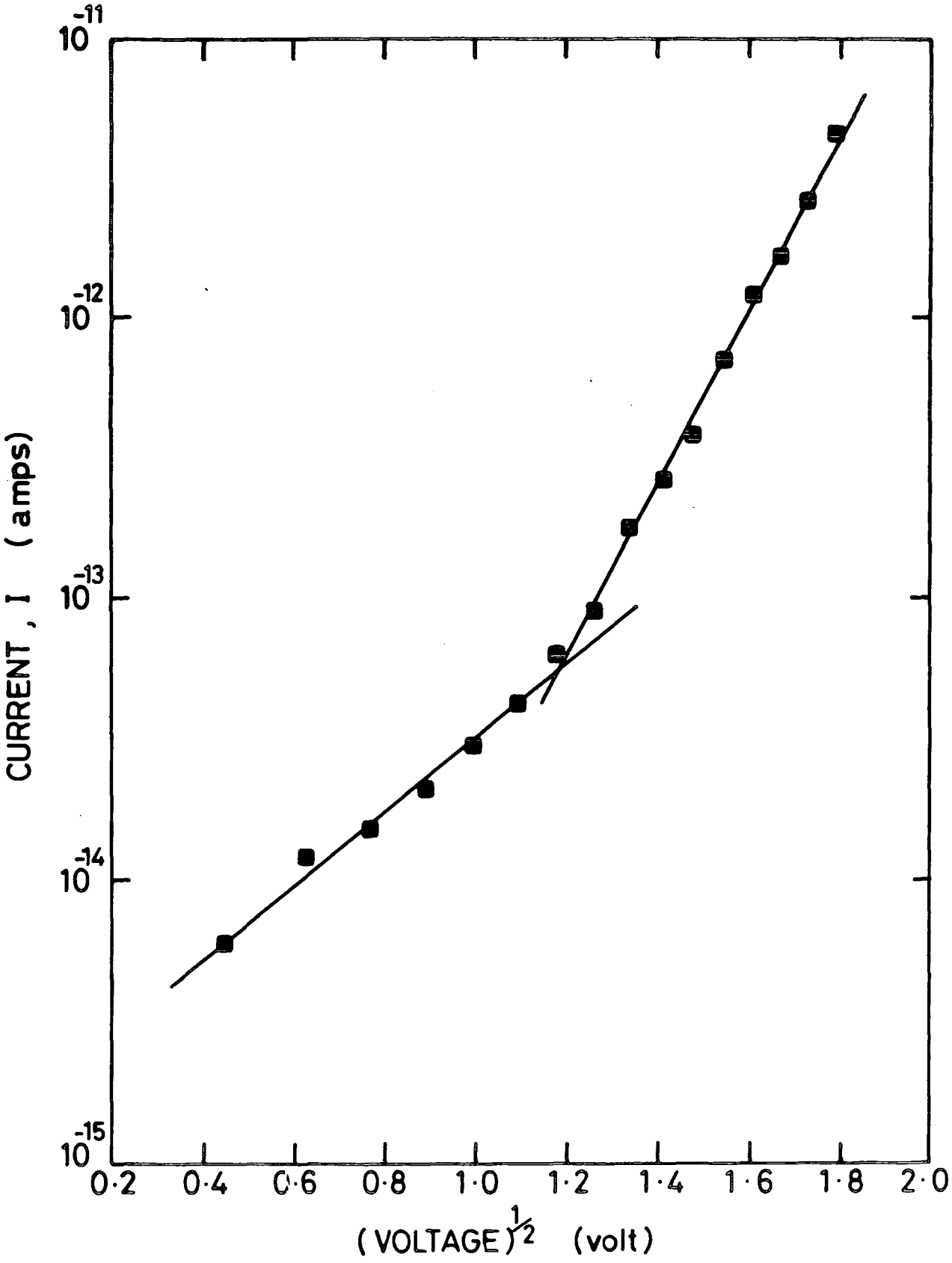

Figure 23. A typical plot obtained for an aluminium/H_2Pc/aluminium/ gold sandwich structure.

conduction processes are involved. Great care, however, must be taken in interpreting these data as being due to Schottky or Poole-Frenkel conduction though the phthalocyanine film. This is because almost identical results were obtained with different thicknesses and indeed, with no phthalocyanine. It would appear that the role of the phthalocyanine, if any, is merely to improve the breakdown strength of the underlying oxide. Thus, the observed characteristics reflect a barrier-limited process involving aluminium oxide rather than the Langmuir-Blodgett film. It is difficult to be certain about the nature of the interface and thus the thickness of the insulating layer. However, using the accepted dielectric constant for the Al_2O_3, and assuming that the entire electric field is dropped across the oxide layer, we calculated, using equation (6.4), a thickness of 1.9 nm. The break point in the log J versus $V^{1/2}$ curve is assumed to be due to a transition from a Schottky to a Poole-Frenkel mechanism as one slope is exactly twice the other. An alternative explanation could be that both neutral and ionized impurity centres are involved; however this seems to be unlikely.

The message to be learnt from using aluminium electrodes is that they should be avoided if accurate conductivity measurements are to be obtained. Therefore, we have concentrated on Nesa glass substrates and have used palladium as the top contacts; the latter is to help avoid any diffusion penetration of gold into the LB film. Figure (6.24) shows a log current versus log voltage plot obtained for a structure

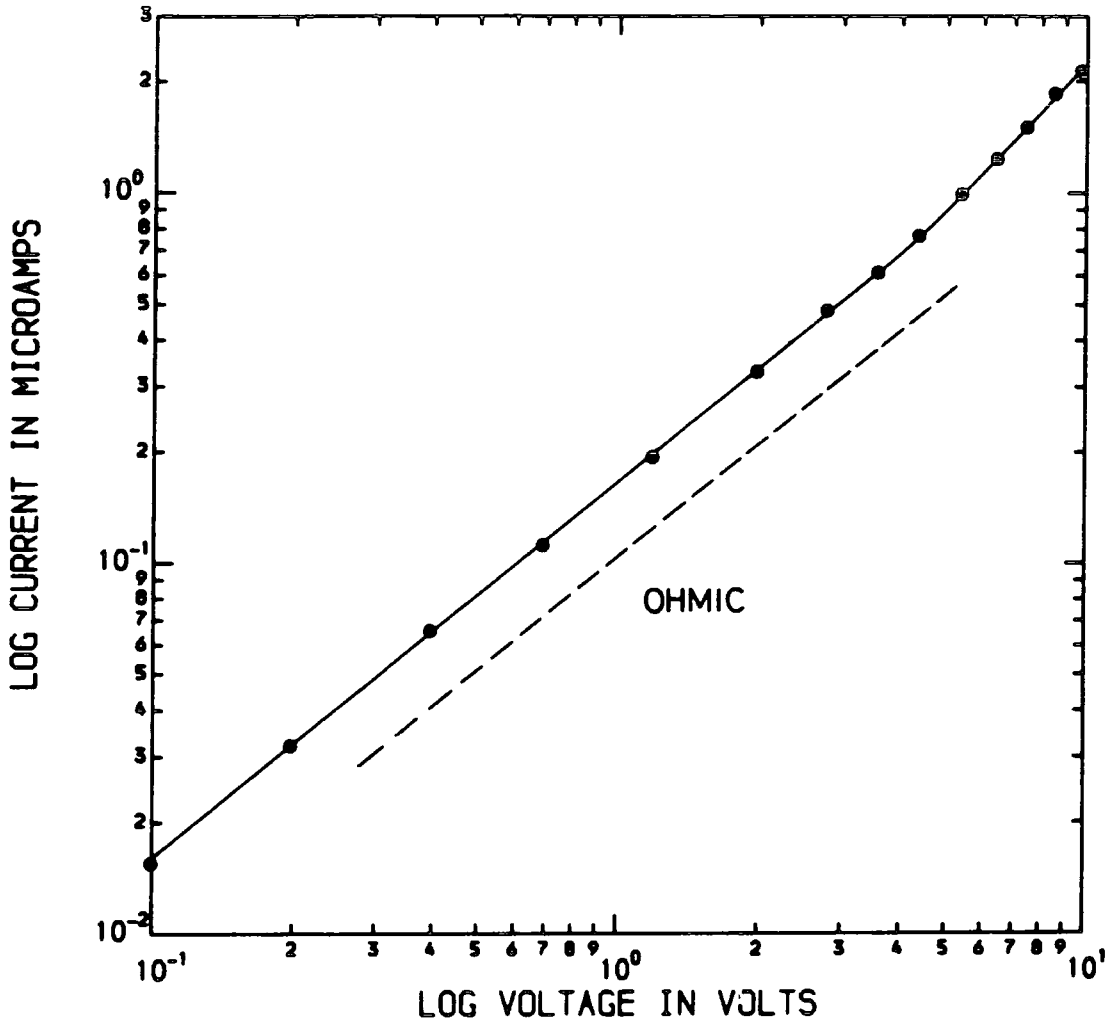

Figure 24. A log current versus log voltage plot obtained for a structure containing forty layers of ASY-CuPc.

containing forty layers of the asymmetrically substituted phthalocyanine. The first part of the plot is accurately linear with a slope of one, indicating ohmic conduction. The conductivity in the ohmic region is calculated to be 1.7×10^{-8} $\Omega^{-1}.M^{-1}$ and is thus similar to the values observed in lateral conduction experiments. At higher fields the slope increases slightly, probably due to the onset of charge injection.

A similar log current versus log voltage plot is shown in fig. (6.25) for forty layers of manganese 4-ter-butyl phthalocyanine. Again the initial values fit a straight line with a slope of one, indicating that in this regime the conduction is ohmic with a similar conductivity to that observed for the ASY-CuPc. However, in this case, at high electric fields (above approximately 2V) there is a better developed super-ohmic region. In fact, it conforms very well to the characteristic space charge limited conduction relationship described in equation (6.5). Time did not permit an extensive investigation to be carried cut of the thickness and temperature dependences of the bulk conductivity characteristics. However, it was observed that there was very little difference between the forward and reverse data. Thus, as in the case of the single crystals and evaporated film, it would appear that it is relatively easy to inject charge into phthalocyanine films. In the absence of drift mobility measurements we assume that it is hole conduction which is involved and that holes are being injected. It is disappointing to find that the copper and

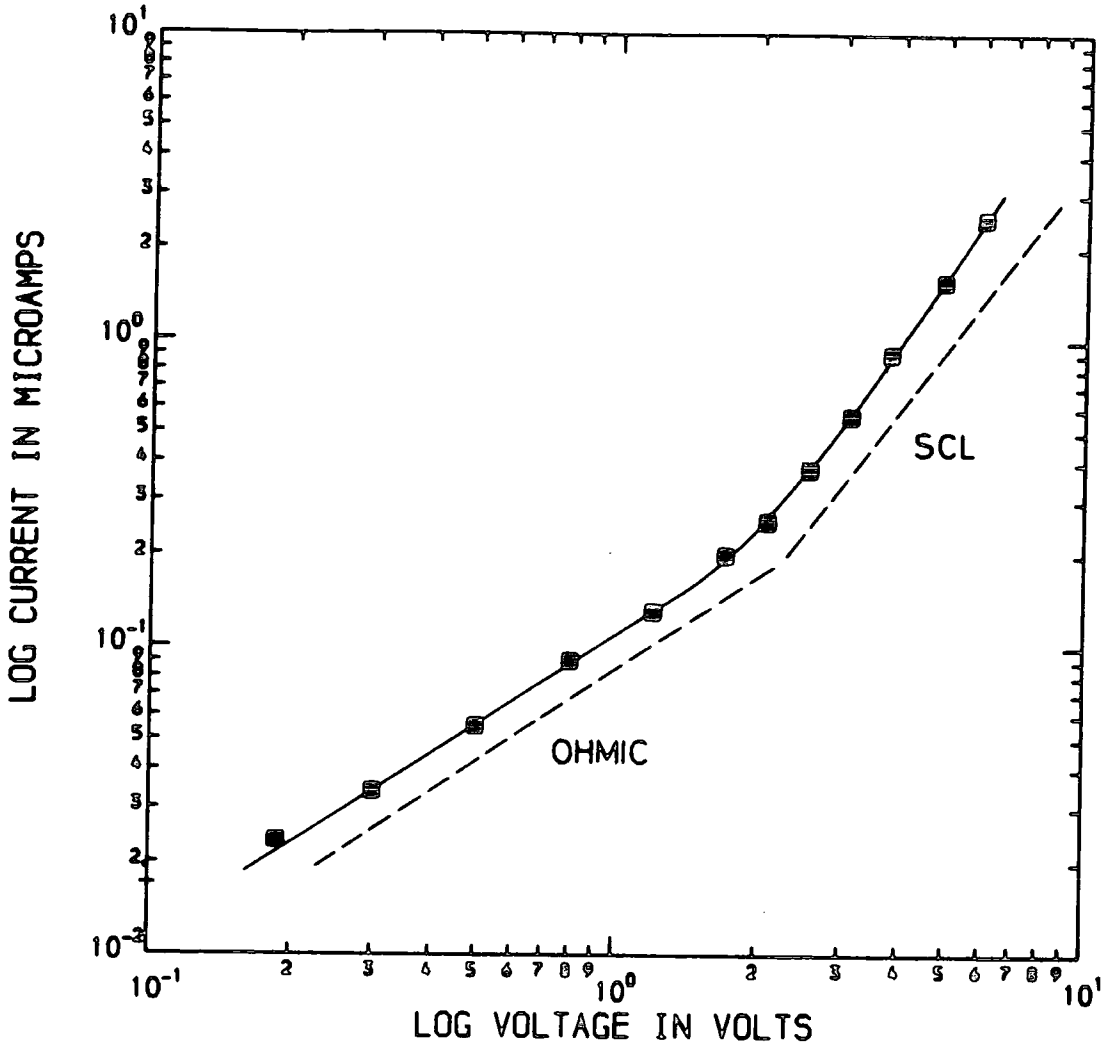

Figure 25. A log current versus log voltage plot obtained for a structure containing forty layers of Mn 4-ter-butyl Pc.

manganese films behave in a similar fashion because one might have expected the manganese compound, because of the different valency states involved, to show interesting and different characteristics. One explanation, of course, is that defects are dominating the proceedings and may be obscuring the interesting properties of the LB layers.

6.3.5 Photo electrical measurements.

It was possible with the metal-insulator-metal structures of both types to detect a very weak photoresponse. The photoconductivity took a long time (approximately one minute) to decay to its original value after the light source was removed, confirming the presence of deep traps in the layers. It is not altogether surprising that the films were virtually insensitive to illumination because even in the single crystal form it is only one specific configuration (the unusual X form) that displays reasonable photoconductivity.

The presence of the phthalocyanine film is much more apparent in a junction device involving a semiconductor. Experiments were carried out using both CdTe and InP but only the results of the latter are described here. Devices of the type Au/InP/Au and Au/InP/metal-free Pc/Au were constructed in order to gauge the influence of the LB film. The most dramatic effect was a decrease of two orders of magnitude in the conductivity of the structure; this probably arose due to an increase in barrier height due to the Pc film changing the

effective work function difference between the metal and the InP. Further evidence to support this hypothesis is the observation of a photovoltage in the phthalocyanine containing structure. The interesting spectral response shows that there is a generation of carriers within the InP ie. the large peak observed coincides with the maximum in the photoresponse curve for the inorganic semiconductor. The sample used was n-type and thus it was not surprising to see some rectification in our p-type containing structures.

CHAPTER 7

DEVICES APPLICATIONS

7.0 INTRODUCTION

During the course of this work we have described the production of various forms of phthalocyanine LB films. Their structural qualities have been shown to depend critically on the preparation of the Langmuir film and to a large extent on the substitution of the molecule. It is clear that there is considerable room for improvement as far as structural quality is concerned and yet there is evidence that monolayers are being formed. These are the most stable LB films yet discovered and as well as sticking tenaciously to substrates have high thermal and optical stability. It is thought that they might find use in many applications especially where crystalline perfection is not critical. Indeed this has been the case and many research colleagues in Durham have been able to use such layers in different devices.

The first and simplest application to be mentioned involves the ability of phthalocyanine film (a single layer is usually sufficient) to seal the leakage pathways in an underlying oxide on a substrate. The LB film adheres well to the surface and serves as a 'blanket' protecting the weak spots in the inorganic film where localized breakdown could occur. We have already seen the evidence for this in our work on aluminium substrates

containing an oxide layer. The effect of the LB film is to improve its resistance, and hence increase the voltage at which breakdown occurs. Phthalocyanine films have been prepared for a colleague Mr B.Holcroft; he has shown that the breakdown strength of other oxides including those on silicon and tantalum can be increased by more than one order of magnitude using this method. Another use of the phthalocyanine film has been as a protective layer on top of other LB film materials, e.g. to avoid damage during a metal evaporation stage. Films have also been coated on catheters prepared by Dr D.Parker, (University College, London). The purpose of the catheters is to measure the arterial oxygen concentration in preterm infants; this is a critical factor in regulating the amount of oxygen which they receive: too little, results in death from lack of oxygen and too much, often leads to terrible side-effects such as blindness. The phthalocyanine LB film is used as a membrane which limits conduction between the catheter electrodes through the blood (which acts as an electrolyte). However, it permits sufficient diffusion of oxygen to allow some conduction to take place. Preliminary results on the devices look hopeful, but optimisation of the material and thickness of the film is still required.

In this chapter, three different devices will be described that have benefitted from the inclusion of a phthalocyanine LB film. The first two involving electroluminescence and bistable switching have been investigated in Durham by Dr J.Batey and Mr N.Thomas. Their films were supplied by the author, although it

should be emphasized that this was during the period before preparation conditions had been optimized. These devices will not be discussed in detail in this thesis. However, the specimen data described in sections 7.1 and 7.2 should serve to emphasise the potential importance of depositing phthalocyanine LB films onto semiconductor surfaces. One of the virtues of the technique is that it is a low temperature process and hence, the semiconductor is left relatively undisturbed during the dipping. Other thin film methods such as vacuum evaporation or sputtering and plasma processing etc. are relatively energetic and can often introduce trapping levels at the semiconductor/insulator interface. On the other hand, semiconductor surfaces are invariably covered with a layer of ill-defined material. Thus, considerable care has to be exercised in etching and preparing the surfaces of the semiconductors before LB film deposition.

7.1 ELECTROLUMINESCENT DEVICES

In order to obtain electroluminescence (EL) from materials which are efficient phosphors but are poor amphoteric semiconductors, an alternative to the p-n junction is required. One possibility is to use a metal-semiconductor (Schottky barrier) structure. In such a device the minority carrier injection ratio is known to be small: however, it has been shown that this can be substantially increased by the incorporation of a thin insulator between the semiconductor and the metal electrode. In previous publications, Dr Batey has reported on

the use of the LB technique for fabricating MIS EL diodes incorporating fatty acid materials. However, because of the relatively low melting points of these materials it is unlikely that they will be useful in a practical device. Hence the interest in the use of phthalocyanine LB films to fulfil the role of the insulating layer. The device structure used is shown in fig. (7.1); the stepped structure adopted allows the evaluation of the thickness dependence to be carried out on the same substrate, thereby eliminating effects due to variations in substrate preparation etc.

Under the application of forward bias the devices emit a yellow/green EL, the spectrum of this emission being identical to that seen for the fatty acid based devices. Figure (7.2) shows a plot of the dc power conversion efficiency versus the number of layers. For an explanation of the optimum , the reader is referred to references (1) and (2).

The main incentive for using phthalocyanine in Dr Batey's work was the formation of a stable MIS EL device. Consequently part of his research covered an assessment of the device degradation. He had found previously using fatty acid LB films that insulator "forming" effects were observed at the high current levels required for EL operation; these effects eventually led to the degradation of the diode. For the diodes incorporating phthalocyanine, an initial decrease was noted but this levelled out to an intensity of approximately one-third of the maximum signal. This lower level was maintained even after several days of continuous operation. This is in marked

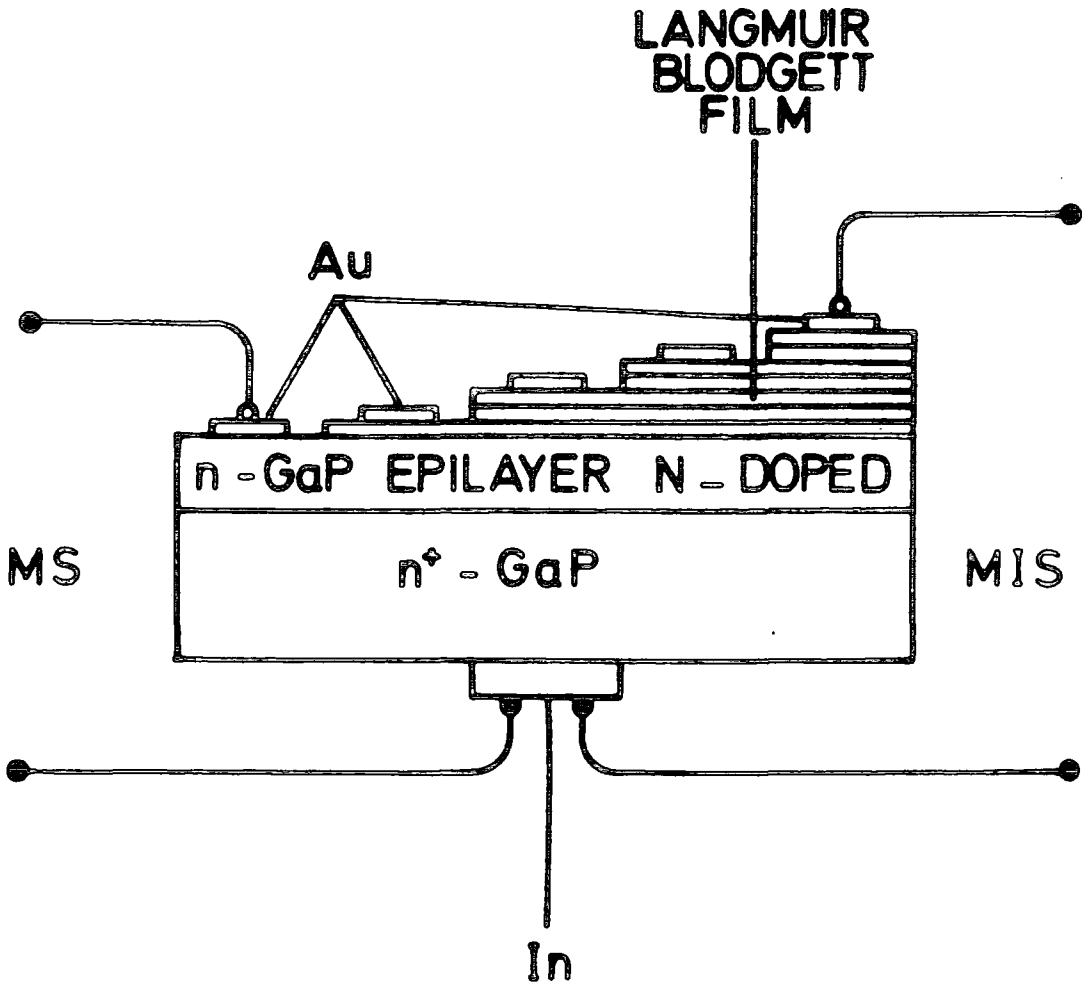

Figure 1. The device structure used for checking the effect of varying the number of phthalocyanine LB layers in a MIS electroluminescent diode.

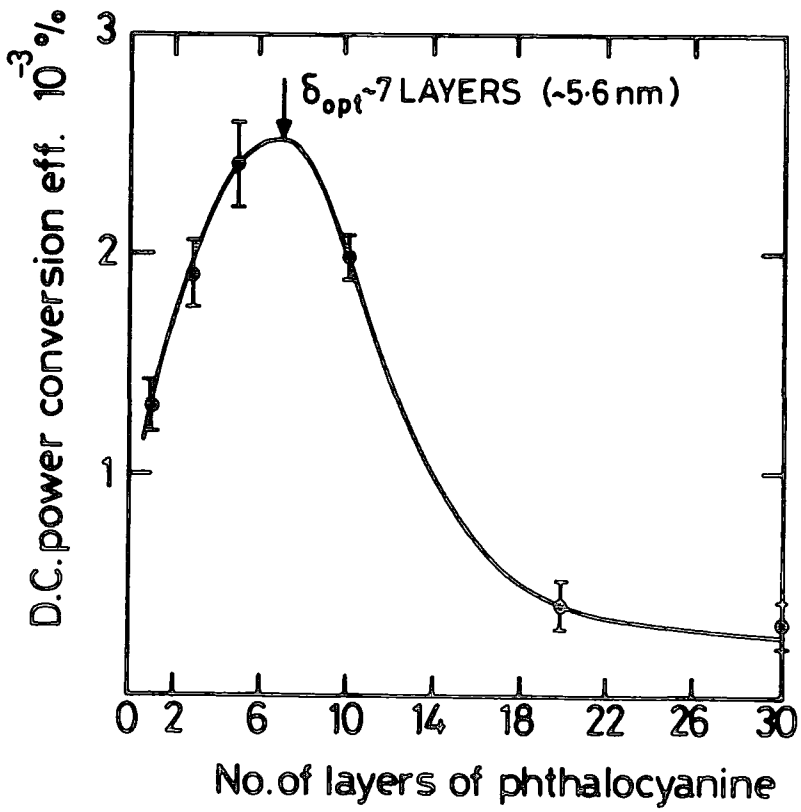

Figure 2. A plot of the dc power conversion efficiency versus the number of phthalocyanine layers obtained for the above structure.

contrast to the fatty acid based diode in which the EL output diminished to zero with time.

7.2 MISS bistable switching devices

A fundamental requirement of a metal insulator semiconductor switch or MISS device is that the insulator presents a semi-transparent barrier to minority carriers, thus enabling the device to be driven into deep depletion. This is normally performed by a semi-insulating silicon nitride layer, or with a thin "tunnelling oxide" of silicon dioxide. In the latter case problems are often encountered due to the difficulties in growing thin pin-hole free oxides of tunnelling dimensions. Additionally, with materials other than silicon, e.g. GaAs, where there is no natural insulating oxide, it is difficult to form adequate insulating layers. The LB technique adequately fulfils the requirements of providing a high quality, stable, thin insulating layer. The device structure used by Mr Thomas is shown in fig. (7.3); the methods used to deposit a film comprising four layers of ASY-CuPc, were as described in section 5.2.2. The devices were found to be stable and produced good switching characteristics. A typical result is shown in fig. (7.4). Operation for 10^7 cycles at 100Hz does not degrade the device characteristics. Both the holding and switching voltages are remarkably stable with time and are not sensitive to illumination. Research is in progress on device structures containing both GaAs and Si in order to optimize the insulator

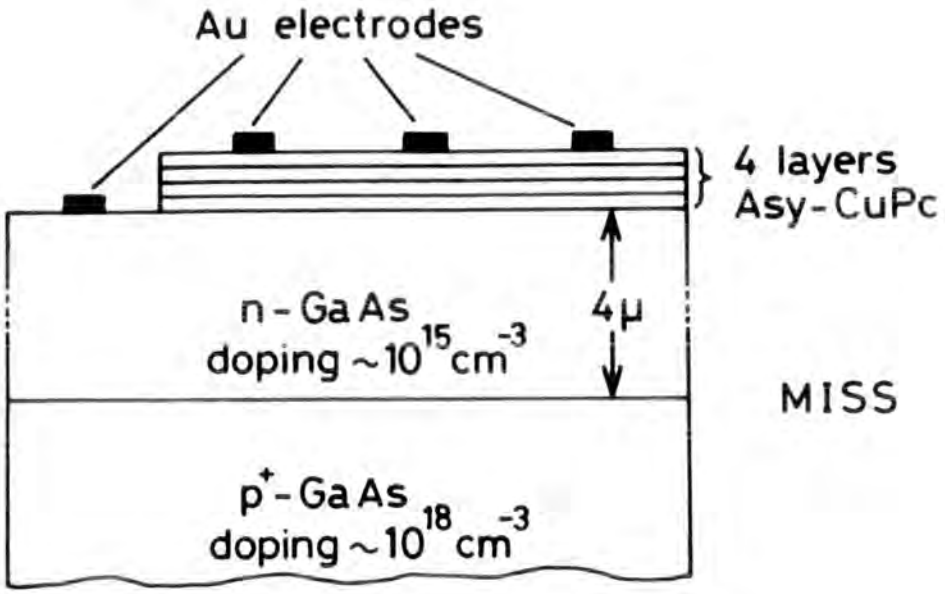

Figure 3. The device structure of the MISS devices fabricated with four layers of ASY-CuPc.

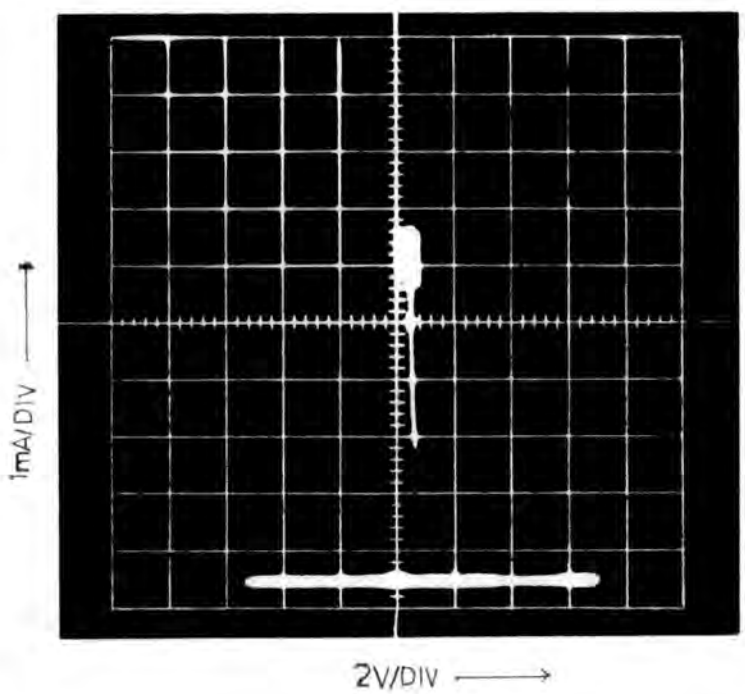

Figure 4. A typical device characteristic obtained for the above structure

thickness. Further mention is made of the MISS switch in the next section dealing with the effects of ambients on phthalocyanine containing devices.

7.3 GAS PROPERTIES

The sensitivity of the phthalocyanines to certain gas ambients is well established and has been reviewed in section 2.3.4 of this thesis. The work reported there shows that of the extensive range of gases which has been explored, only electron acceptors such as NO_2/N_2O_4, Cl_2, NO, and HCl have been found to have any significant effect. In particular, NO_2/N_2O_4 produces a highly marked response, several orders of magnitude greater than Cl_2, its closest rival. (It should be noted that although henceforth in the text reference will be made to NO_2, the gas even in low concentrations exhibits a degree of association and N_2O_4 will also be present.) This increase in conductivity, arising through exposure to the NO_2 .has been shown to be reversible, although to obtain effective removal of the NO_2 either evacuation and/ or elevated temperatures have had to be applied. For the single crystal and evaporated film samples reported to date, it is customary to use temperatures near 150° C; this allows desorption of the gas without any obvious degradation of the film.

In this work we have concentrated upon NO_2 for two main reasons; first, the large conductivity response facilitates characterisation at low gas concentrations and secondly, NO_2 is

a far easier gas to handle than the halogens. The effect of NO_2 on the phthalocyanine molecule can be readily observed by passsing the gas through a solution. Figure (7.5) shows the spectra obtained for ASY-CuPc before and after exposure to 50 ppm NO_2 for 10 minutes. It can be seen that the visible absorbance of the solution drops and a relative enhancement of the peak at 612nm occurs. These bands are associated with the -electron system of the phthalocyanine molecule. It is interesting to note that as the visible absorption was reduced a new red band was seen to emerge at 718nm. (The drop in absorbance is also reflected in absorption spectra of the deposited LB films.) The spectra obtained for ASY-CuPc before and after exposure to 200ppm are shown in fig. (7.6). The exposure of the film to 200ppm of nitrogen dioxide for half an hour reduces the peak absorbance value by 24%. When the film was allowed to recover in air for two hours at room temperature, the absorbance returned to within 9% of the original value. As for the solution spectra, a reduction in the strength of the visible spectrum is observed. This has also been observed by Honeybourne (see the references cited in section 2.3.4) and attributed to the formation of the organic radical cation and the NO_2 ion. The recovery of the sample indicates the regeneration of the neutral organic species and is reflected in the increase in the absorbance peak.

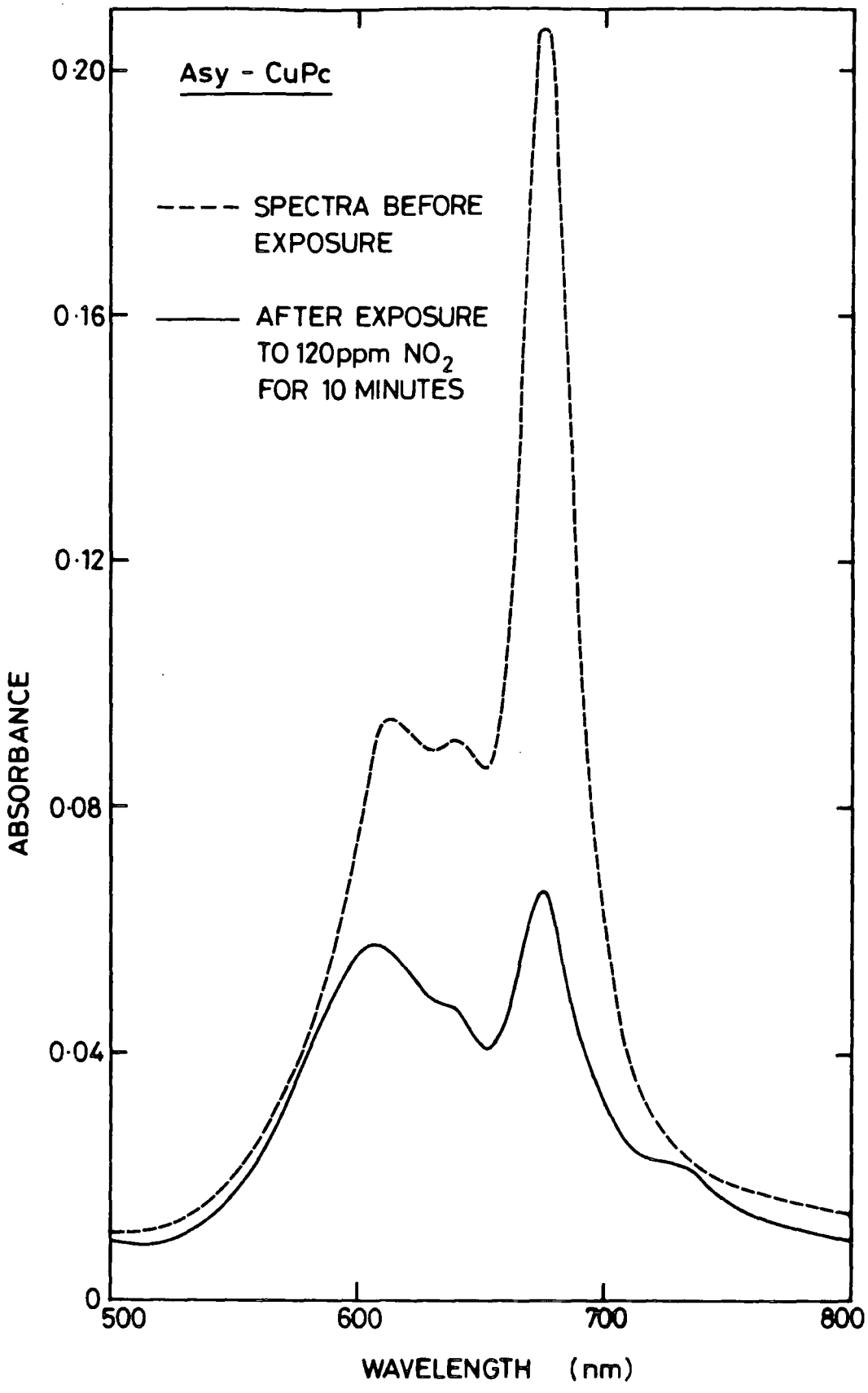

Figure 5. The solution spectra obtained for ASY-CuPc before and after exposure to 120ppm NO_2.

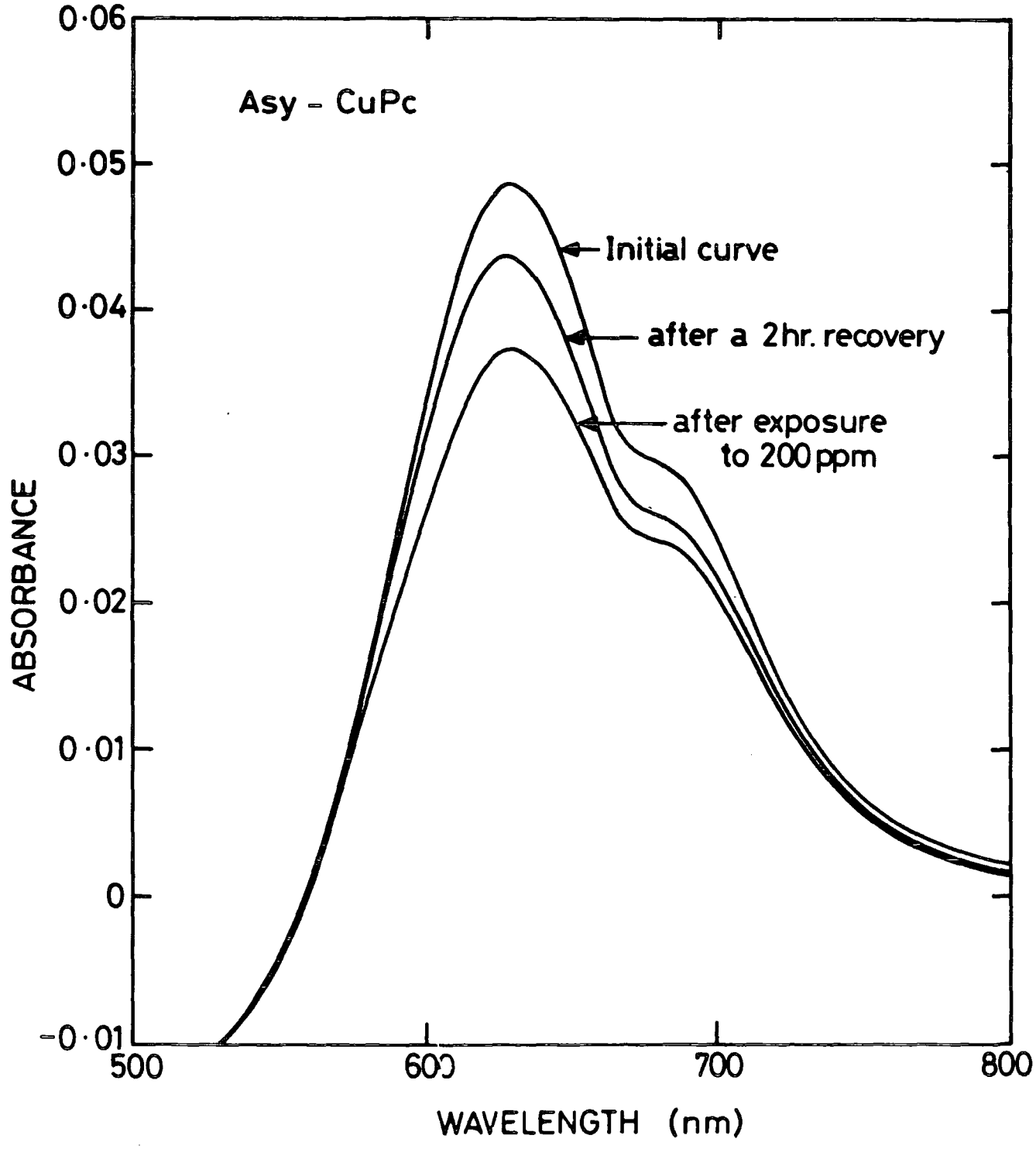

Figure 6. The spectra obtained for an LB film of ASY-CuPc before and after exposure to 200ppm NO_2.

7.4 LATERAL CONDUCTIVITY GAS DETECTING STRUCTURES

In the previous section we have described how the interaction of phthalocyanine with NO_2 can be recorded by simply observing the changes in the solution- or solid-state-spectra on exposure to a gas. An alternative method of investigating this interaction is to monitor the lateral conduction of the phthalocyanine in the presence of electron acceptor gases. The lateral conduction structures used in this work took the form of a set of interdigitated electrodes; a schematic diagram of the device is shown in fig. (7.7). All the measurements reported here are for the ASY-CuPc but similar data were obtained for the other phthalocyanine molecules described in this thesis.

Saturation effects

The first experiments involved monitoring the rise in conduction due to placing the sample in a 20ppm ambient of NO_2. A typical result is shown in fig. (7.8) for a sample incorporating one layer of ASY-CuPc. The response is very rapid and the current is seen to reach an equilibrium value within 70 minutes of the introduction of the gas into the chamber. The magnitude of the increase depends on the thickness of the film, but even for the single monolayer shown here, an increase of several orders of magnitude is observed. For example, a device incorporating five layers for the same gas concentration would typically involve an increase of six orders of magnitude. It

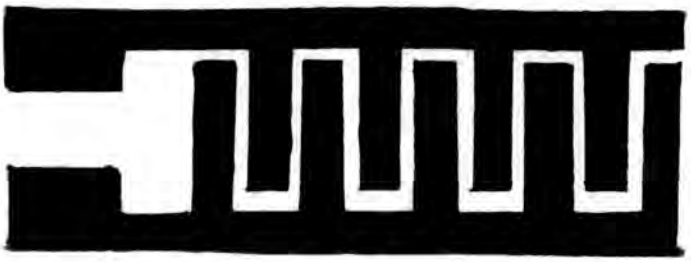

Figure 7. A schematic diagram of the interdigitated electrode structure used in the lateral conduction devices.

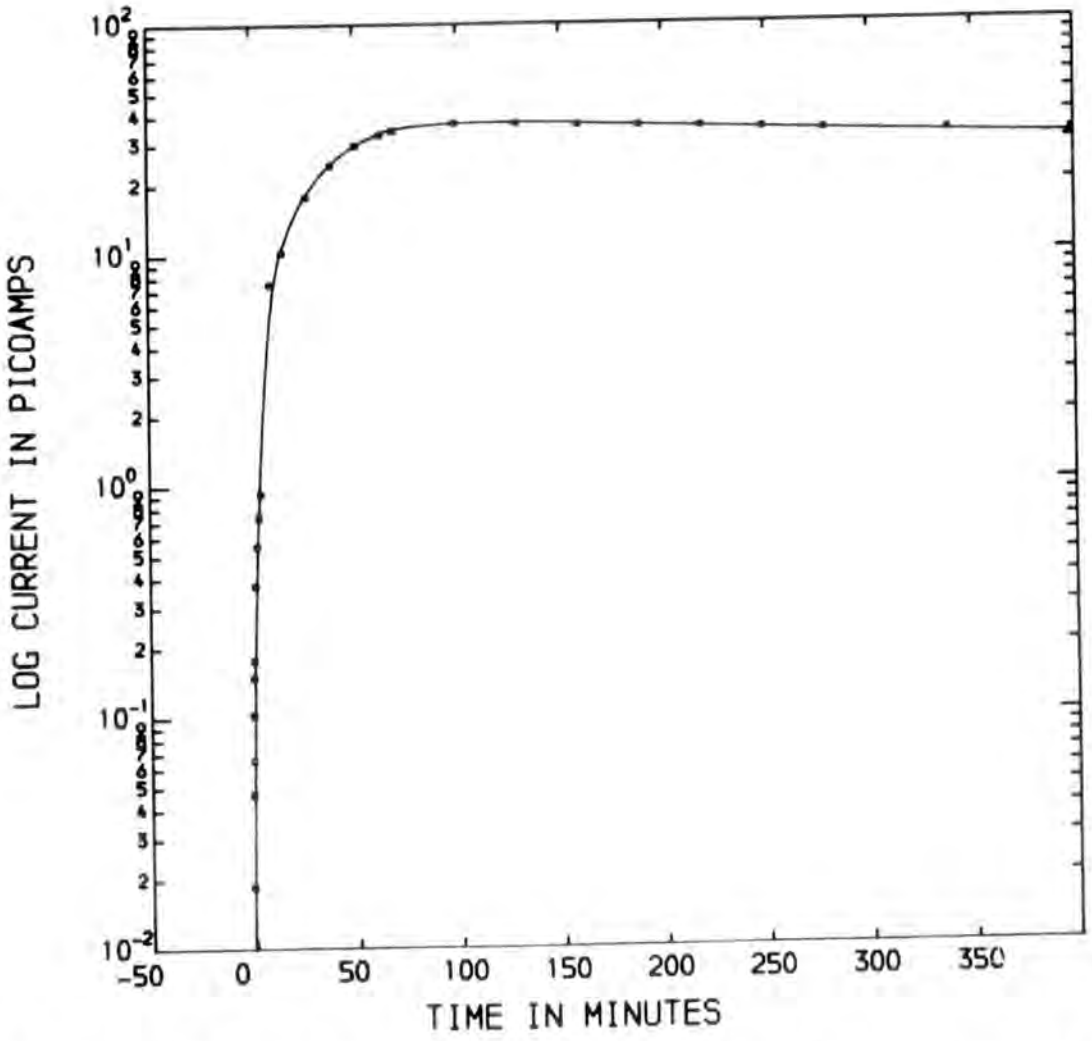

Figure 8. A typical result showing the rise in conduction due to placing a sample incorporating one layer of ASY-CuPc in a 20ppm ambient of NO_2.

can be noticed on closer inspection of fig. (7.8) that the saturation value displays a slight decay. Similar results have also been observed by Tredgold (3) on LB films of substituted porphyrins. Here he found the lateral conduction to increase by four orders of magnitude for a seven layer film of the copper complex of mesoporphyrin IX diol exposed to 10ppm NO_2. The decay in the saturation level with time has also been observed by Tredgold and other workers, for example Wright, and is attributed to an actual deterioration in the film. The current decay observed in our films is very slight but is accentuated at higher concentrations of NO_2. For devices incorporating thicker layers the decay is very marginal and is only apparent if a high saturation level is observed over a period of many hours.

The variation of the saturated current level with NO_2 concentration is given in fig.(7.9). A linear variation is observed, except at concentrations lower than 5ppm. In fig. (7.10) the data have been redrawn using a log-log scale. These plots were observed to produce a linear variation over the entire range.

In the case of NO_2 absorption on phthalocyanine each adsorbed molecule is believed to produce a carrier which is available for conduction. Therefore, the conductivity is proportional to the number of adsorbed gas molecules. The process thus conforms to the Freundlich adsorption isotherm which takes the form $\theta=kP^x$, Where θ is the fraction of surface covered, P is the pressure and k and x are constants. In our experiments we are relating the concentration of the NO_2 to the

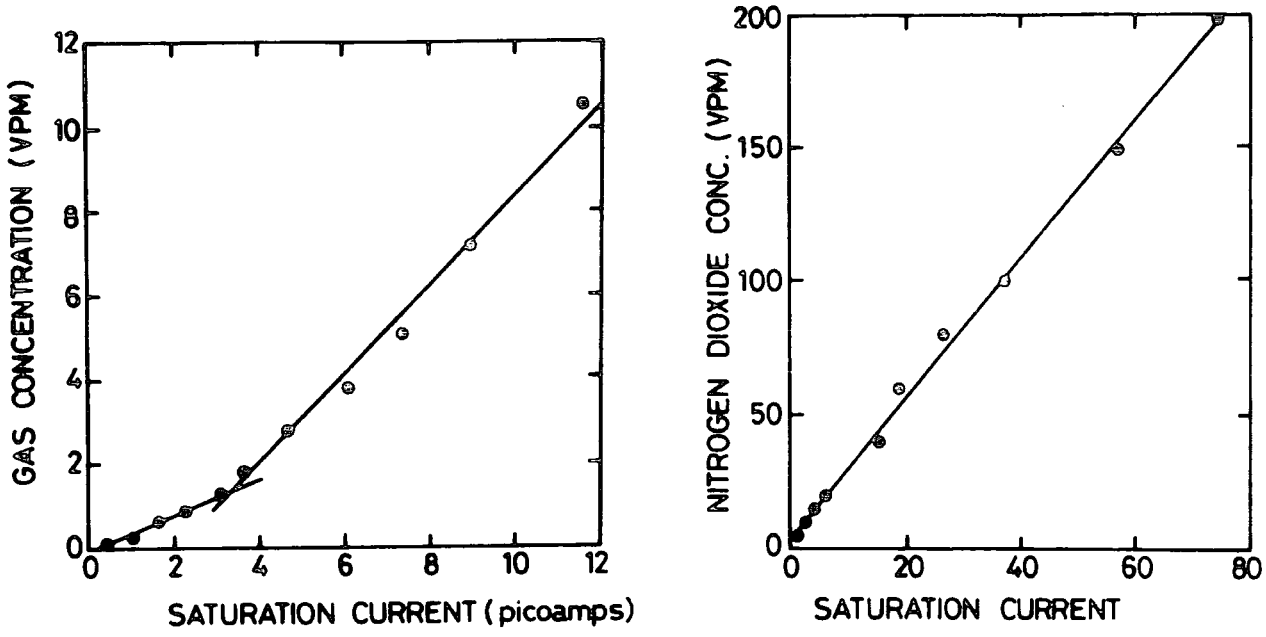

Figure 9. The variation of the saturated current level with NO_2 concentration.

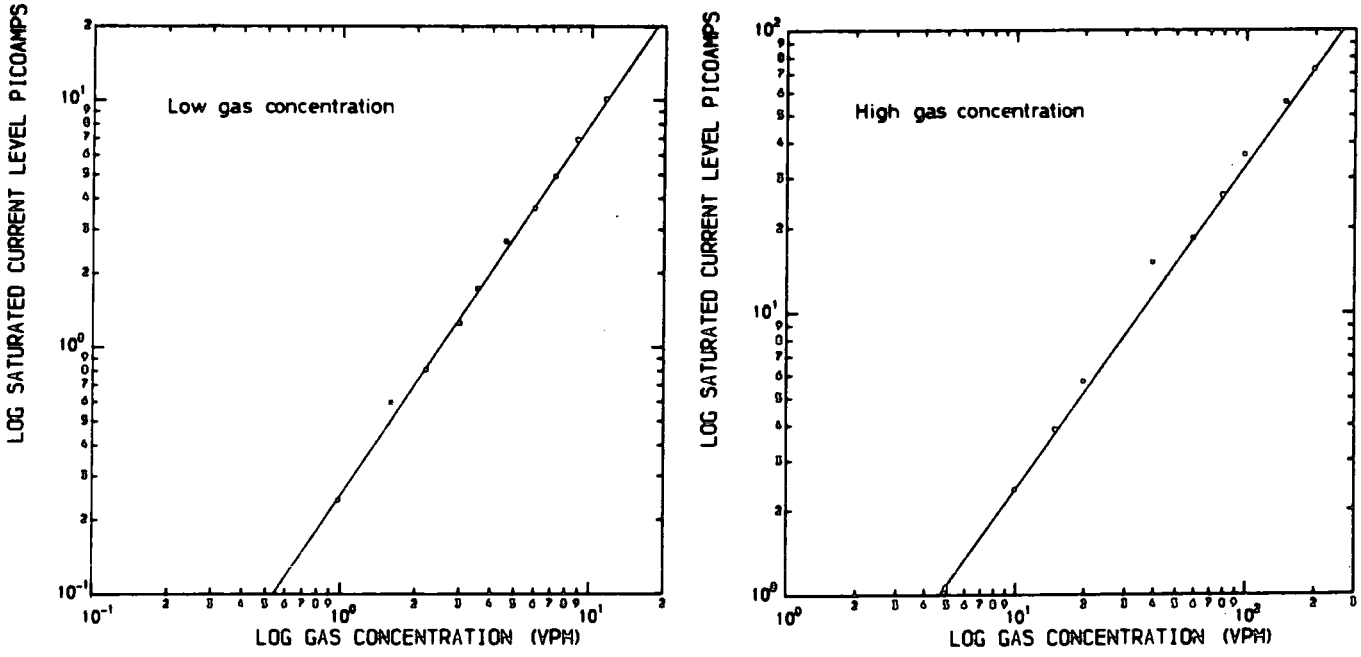

Figure 10. The data presented in fig. 9 replotted on a log-log scale.

partial pressure exerted by it. It is also to be expected that the saturation current should depend on the thickness of the phthalocyanine film. This is confirmed in fig. (7.11) which shows the variation of the saturation current level with the number of deposited layers. An approximate linear relationship is observed. The response for a single monolayer lies off this straight line suggesting that the structure of the first monolayer is different because of the influence of the substrate.

Transient phenomena

The recovery of the conductivity to its original value has been monitored as a function of time. Figure (7.12) shows the data obtained for a number of films of different thickness. The curves are plotted on a log-log scale to enable all the curves to be exhibited on the same graph. An alternative method of displaying the information is a semi logarithmic plot of current versus log time. This would be expected to give a linear relationship if the Elovich equation given below is obeyed.

$$\frac{d\theta}{dt} = a \exp(-b\theta)$$

Where a and b are constants. In deriving this equation it is again assumed that the conductivity increase is proportional to the number of adsorbed gas molecules on the phthalocyanine surface. Elovich plots for one to five layer samples are shown

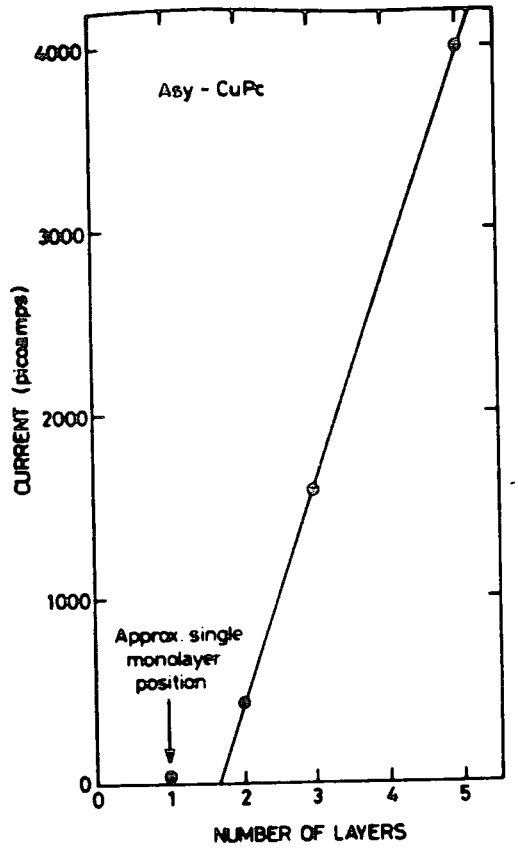

Figure 11. The variation of the saturation current level with the number of deposited layers.

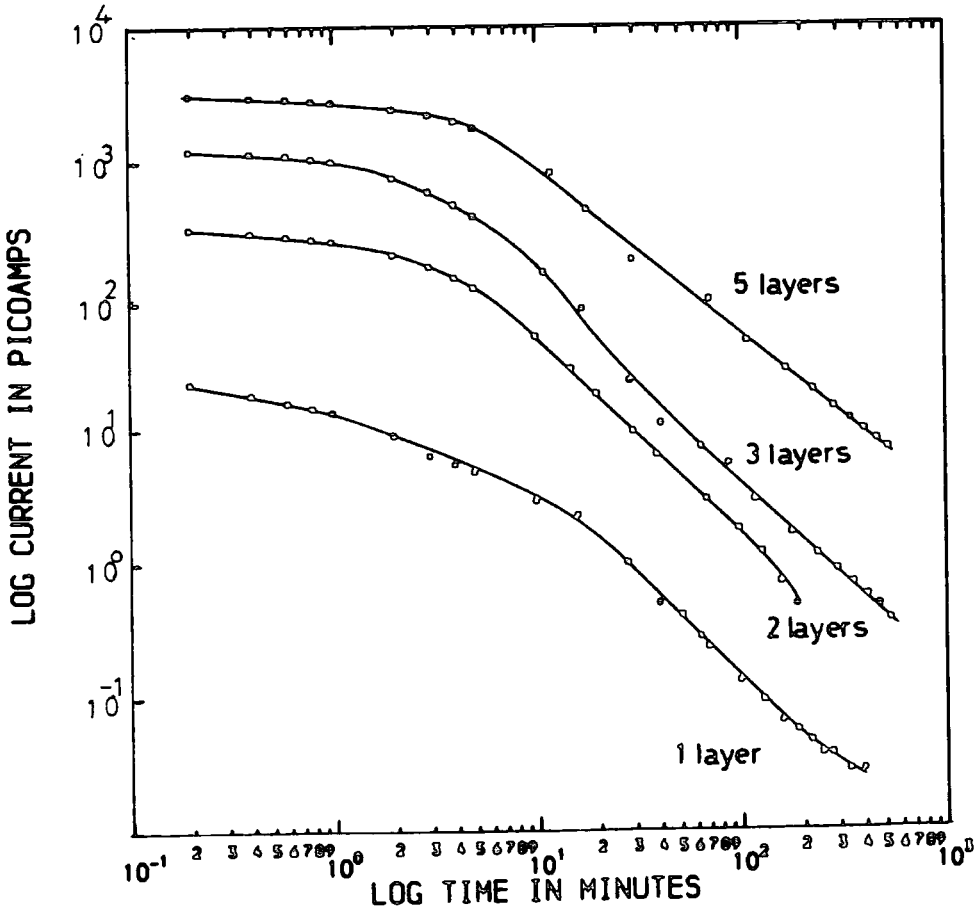

Figure 12. The recovery of the conductivity for a number of different thickness films.

together in fig. (7.13). The data for a single monolayer film are shown separately in fig. (7.14) and it can be seen that a linear relationship is observed. However, for films incorporating two or more layers, an increasing degree of curvature is introduced at the start of each plot. Similarly shaped characteristics have been observed by Misaik and Wright (4) for evaporated films of phthalocyanine. They have interpreted the curvature as being indicative of a complex surface structure with several types of adsorption site. That is, the Elovich equation predicts a linear plot if there is a single absorption site. However, for surfaces where there is more than one type of active site, curved Elovich plots would be expected. We favour a simpler interpretation and believe that the deviation from linearity can be explained as follows: the gas clearly desorbs first from the surface region of the film and presumably at a later stage there follows a reduction in the complex formation in the bulk. Most of the increased current results from the additional charge generated in the bulk regions and clearly, as we have indicated, it scales with the thickness of the film. Thus even though the desorption processes involved are the same in the cases shown in fig. (7.13), the initial effects are obscured in the early stages in figs (b), (c), and (d) due to the bulk conductivity. That is, the thicker the film, the higher the current density, and the less impact of the loss of the complex from the surface and the first few monolayers of the phthalocyanine. In fact Misaik and Wright report a delay which is of the order of a 100s before their

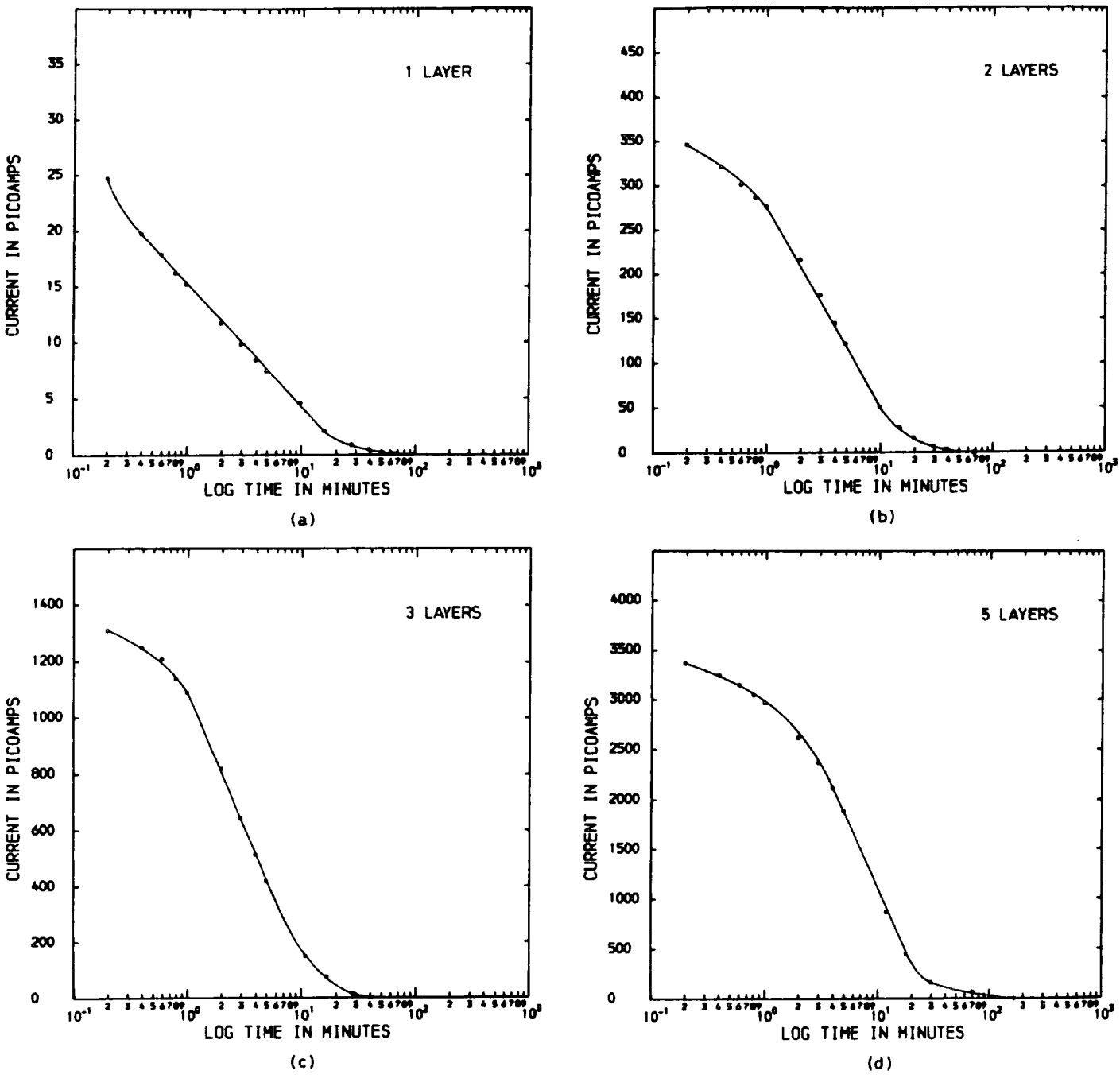

Figure 13. Elovich plots for one to five layer samples.

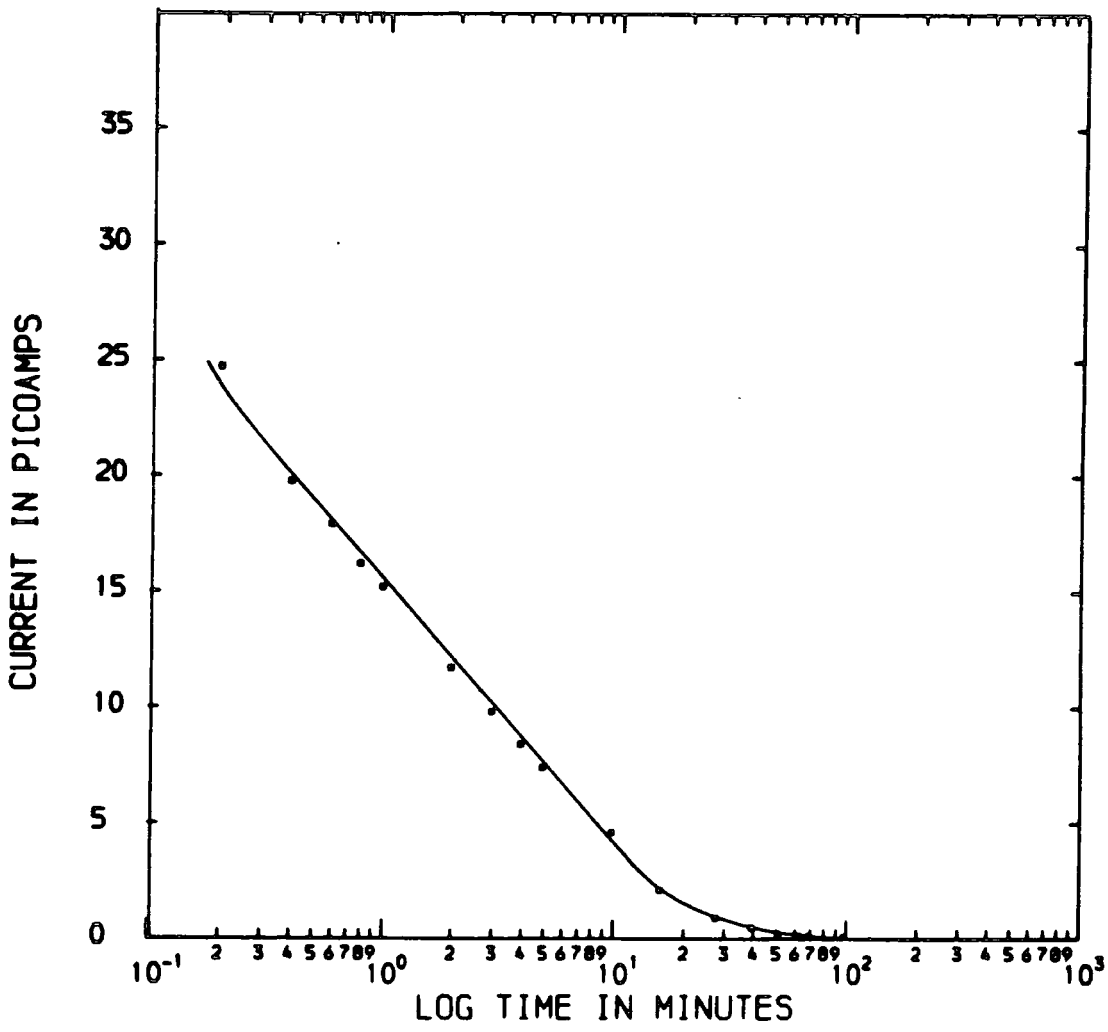

Figure 14. An enlarged diagram of the Elovich plot obtained for a 1 layer sample, showing the linear relationship observed.

devices respond to the removal of NO_2 from the gas flow. This long delay was not observed in our devices although the initial response is clearly seen to be slower for thicker samples. A further comparison between the evaporated films and our LB films can be made if the time taken for the current to fall to 90% of the saturation value is measured. In the evaporated film devices reported by Misaik and Wright, the 90% recovery time is found to be of the order of 250 minutes. We would again attribute this to a bulk conductivity effect as in our single layer devices this parameter was approximately 15 minutes.

Response to a NO_2 transient

To test the above hypothesis we decided to observe the transient effects due to (a) reduced exposure and (b) in a single monolayer. Figure (7.15) shows the influence of 120 ppm NO_2 in N_2 on an ASY-CuPc structure containing eight monolayers. It is different to those shown previously in that the gas supply was cut off before the saturation regime was reached. Figure (7.16) shows that the transient recovery is now very different in that straight line regions are observed in plots of log current versus time. From these it is possible to deduce time constants τ_1=126s and τ_2=258s using an equation of the form $\log J = -t/\tau + \text{const}$. Presumably they are associated with either two trapping sites on the surface of the film or, more probably, due to a surface desorption and a bulk process.

It is also interesting to note that the single monolayer

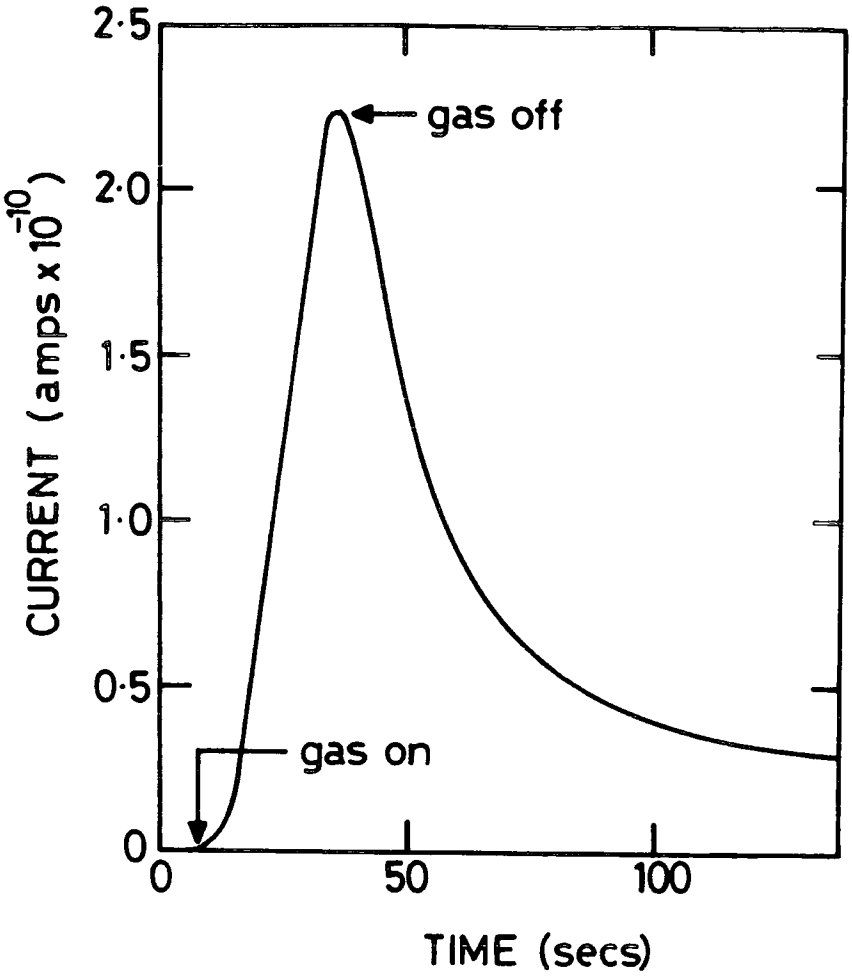

Figure 15. The influence of 120ppm NO_2 in N_2 on an ASY-CuPc structure containing eight monolayers.

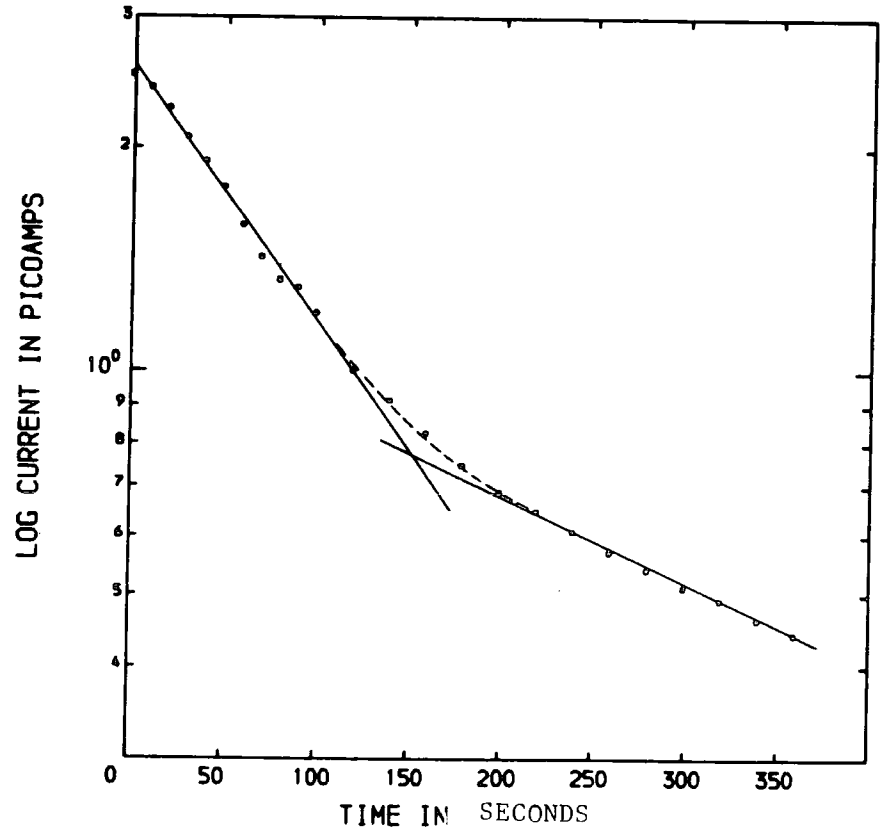

Figure 16. The recovery curve shown above replotted as log current versus time.

result shown previously in fig. (7.13a) and enlarged in fig. (7.14) yields a reasonably good Elovich type plot, confirming that only one surface site is associated with the desorption process. The linearity of this plot is progressively removed as more layers are incorporated due to bulk conduction effects.

7.5. MIS GAS DETECTING STRUCTURES

In this section results are reported on the use of MIS structures incorporating phthalocyanine LB films for the detection of nitrogen dioxide. The device structure used is shown in fig. (7.17). The silicon used was 14-20 Ωcm, 100 p-type, and two oxide thicknesses of 7 and 30 nm were available. Both structures were fabricated so that it was possible to evaluate at least ten contacts for each thickness of film used. The results of exposure to NO_2 were similar and therefore only the data for the thicker oxide film are presented here.

Figure (7.18) shows capacitance versus voltage curves for MIS structures containing 0,1,3 and 5 monolayers of ASY-CuPc. For clarity only the scans from negative to positive bias are shown. However, there is some slight hysteresis in the characteristics and these are displayed in figure (7.19) for the oxide only case. This diagram also contains an insert repeating some information shown previously in chapter 6; that is, the capacitance in the accumulation region scales correctly with number of additional monolayers. Figure (7.20) shows that our

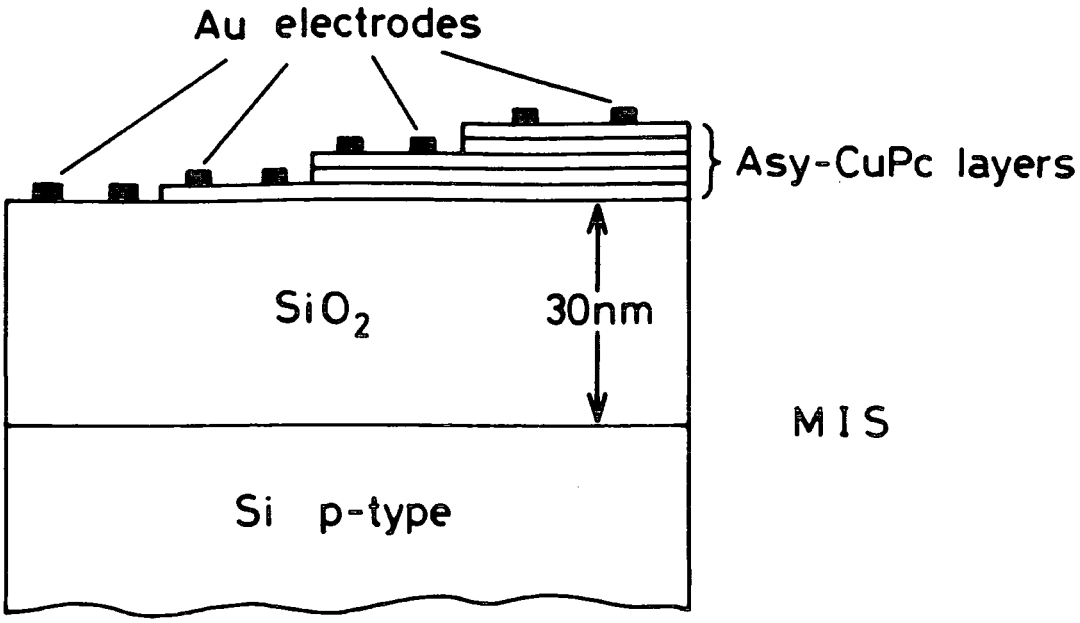

Figure 17. The MIS device used for gas detection.

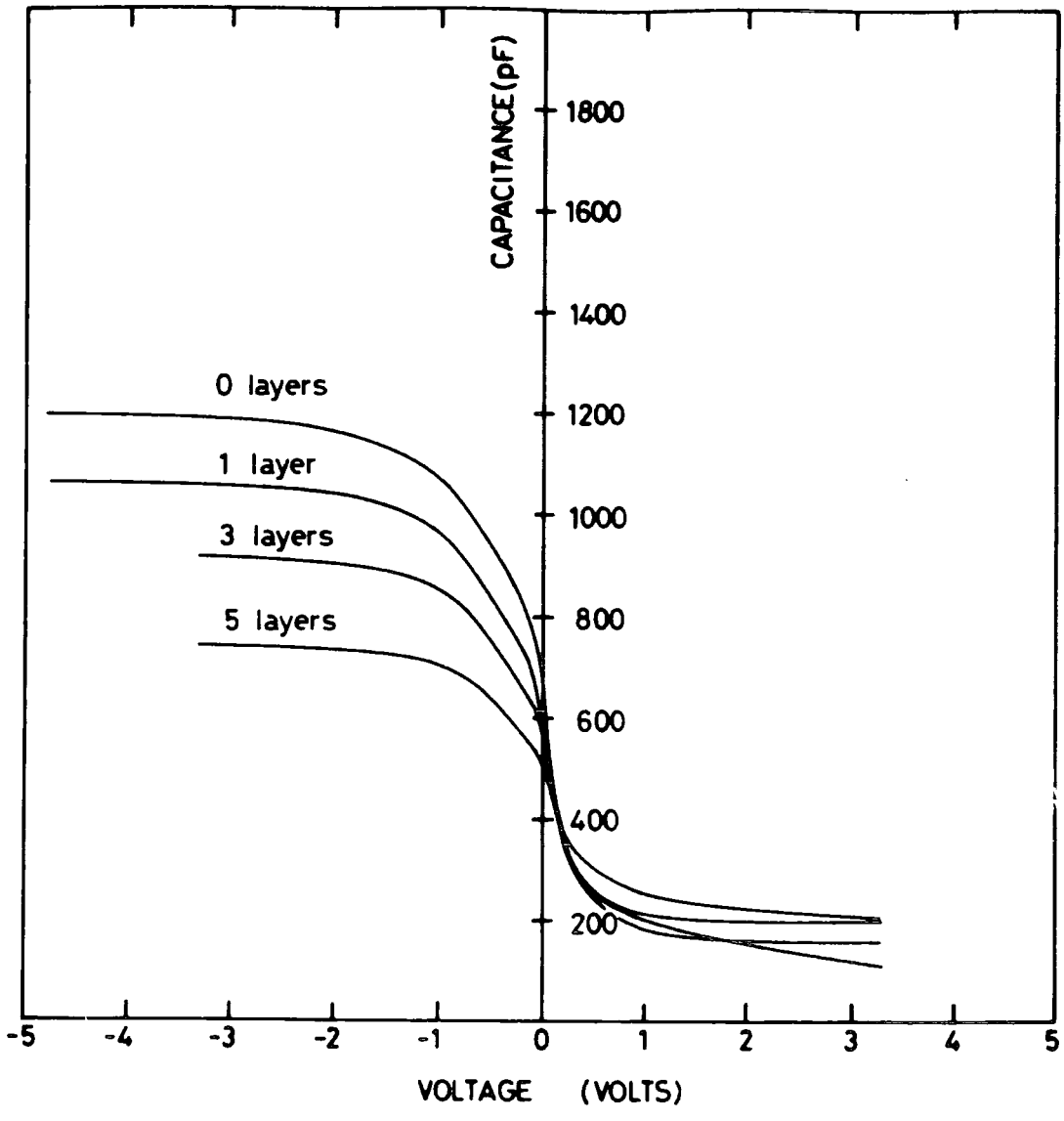

Figure 18. The capacitance voltage curves for MIS structures containing 0,1,3 and 5 monolayers of ASY-CuPc.

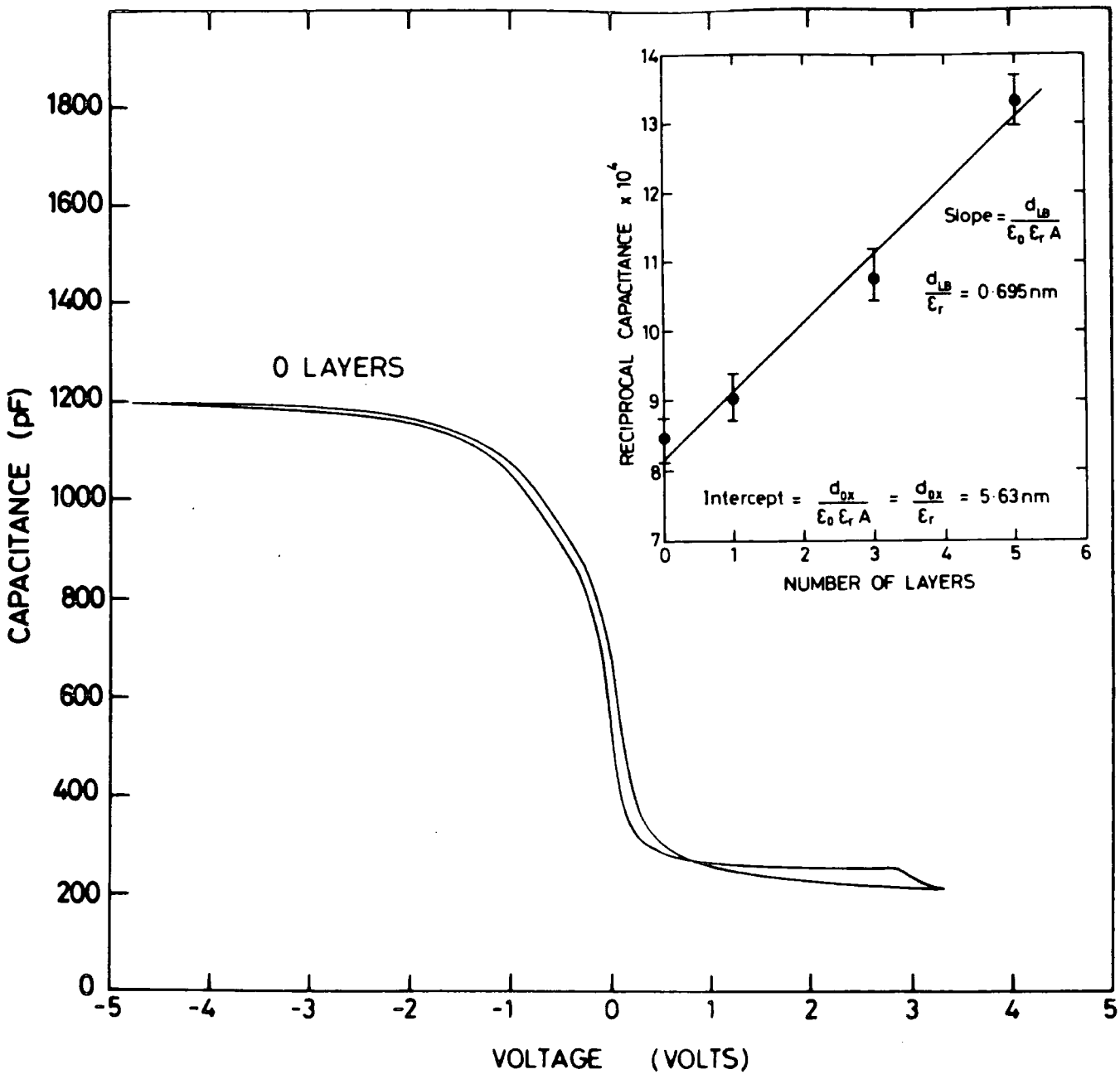

Figure 19. The capacitance voltage curve for the oxide only structure. The inset shows the variation of the reciprocal capacitance with the number of incorporated ASY-CuPc layers.

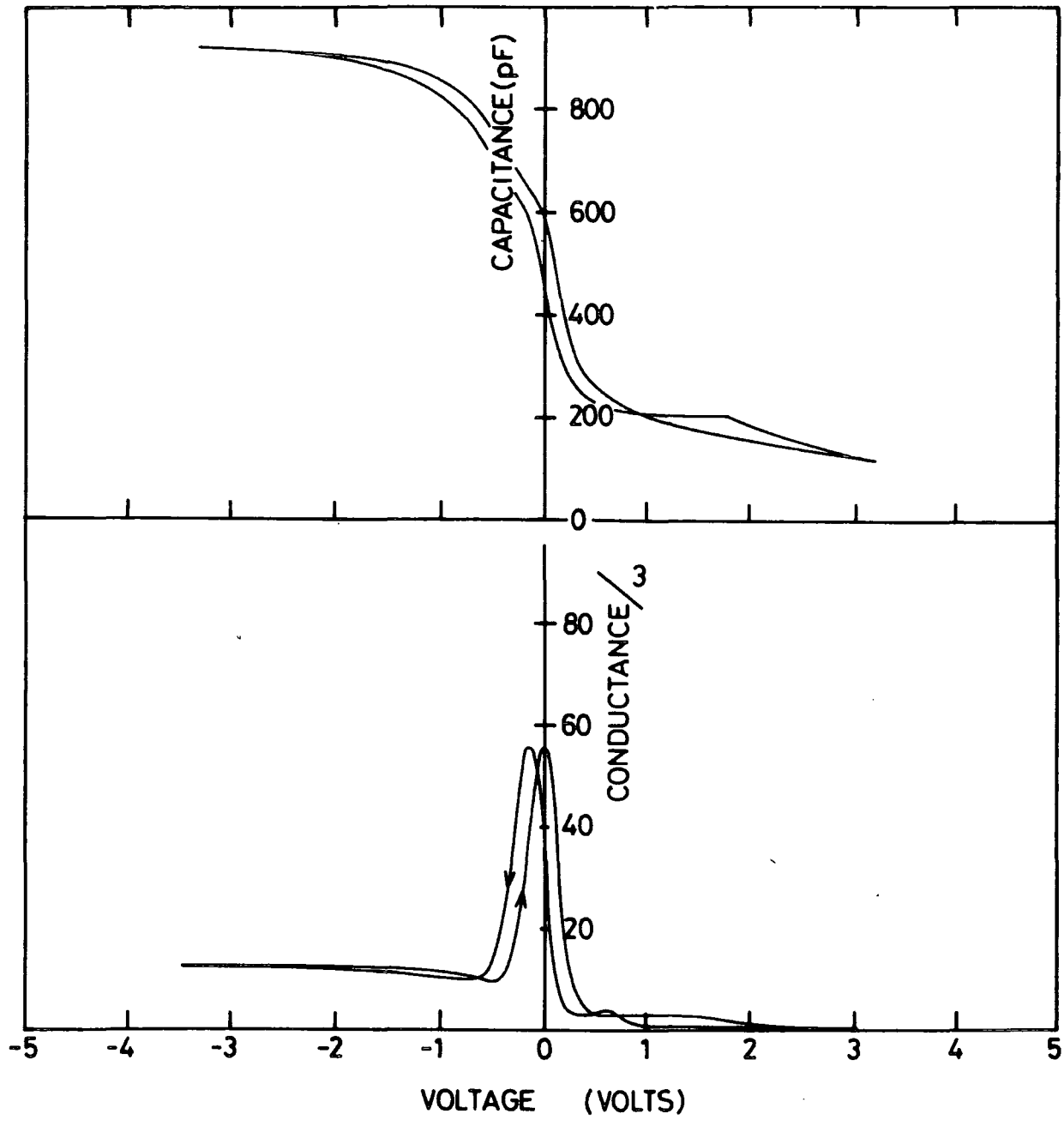

Figure 20. The curves obtained for the structure containing 3 layers of ASY-CuPc showing the capacitance and conductance as a function of bias.

device structures containing phthalocyanine also display classical metal-insulator-semiconductor behavior as far as the conductance is concerned. This particular curve is for three monolayers of ASY-CuPc, but similar features were observed without the organic film. The data in figs (7.18, 7.19 and 7.20) can be interpreted in the normal way. The capacitance characteristics fall into three distinct regions. For large negative voltages the surface of the p-type silicon is accumulated with holes and therefore only the oxide capacitance is measured. However, by applying positive voltages it also possible to deplete the surface of charge carriers and thus introduce an additional series capacitance. Thus the value of C drops until the band bending is so severe that an inversion layer is formed. Then the capacitance levels off and is invariant with voltage until breakdown occurs. Our measurements were carried out at 1kHz. Had we measured data at lower frequencies we would have observed an increase in the inversion region. However, at 1kHz the minority carriers cannot respond sufficiently quickly to the a.c. signal. The conductance curve reflects the presence of unsaturated bonds or surface states at the interface between the silicon and its oxide. Hysteresis can occur for a variety of reasons; for example, ion movement or trapping effects. The shape of the hysteresis curve in our case suggests that ion movement is responsible for this effect.

Figure (7.21) shows the influence of varying concentrations of gas on the silicon substrate passivated with 30nm of oxide. The areas of the device which did not contain a phthalocyanine

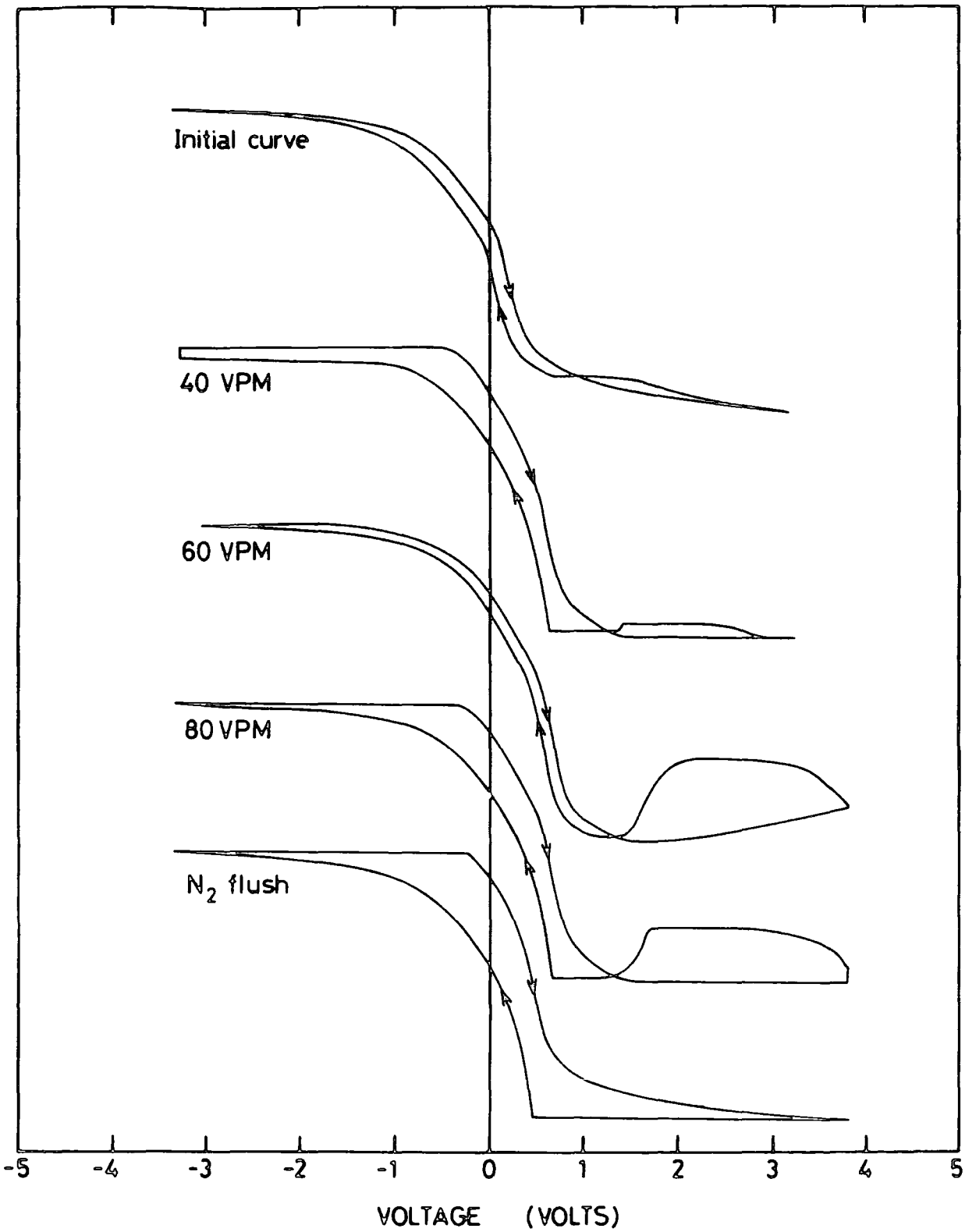

Figure 21. Capacitance-voltage curves for a structure containing 5 layers of ASY-CuPc showing the influence of varying concentrations of NO_2.

layer were insensitive to the presence of NO_2. There is a marginal increase in the hysteresis effect and a slight shift of the curves to higher positive voltages depending on gas concentration. A similar displacement along the voltage axis is observed for the conductance curves (fig 7.22). We interpret this as being due to a change in the effective work function of the top electrode. A more noticeable feature in the conductance data is the introduction of an additional peak whose magnitude is very sensitive to the ambient. Its appearance can be attributed to the onset of lateral conduction. It is known that an inversion layer is very sensitive to potential gradients along the oxide surface. Because most of the ac current flows laterally, the characteristics depend critically on the oxide surface potential around the field plate. Atalla et al (5) and Shockley et al (6) have both studied ion drift along the oxide surface and showed that a biased junction has a fringing field reaching to the surface of the oxide layer covering this junction. Atalla found that adsorbed molecules can be separated into ions which migrate along the surface trying to establish a uniform potential over the oxide surface. Shockley has described how the distribution of charge on the oxide surface is reflected by a charge build up at the semiconductor oxide interface; this charge is free to contribute to the lateral conduction. In the case of an oxide surface covered with a phthalocyanine layer we suggest that the phthalocyanine layer provides the conditions to allow such a charge distribution to occur. Thus the production of the new lateral conduction peak

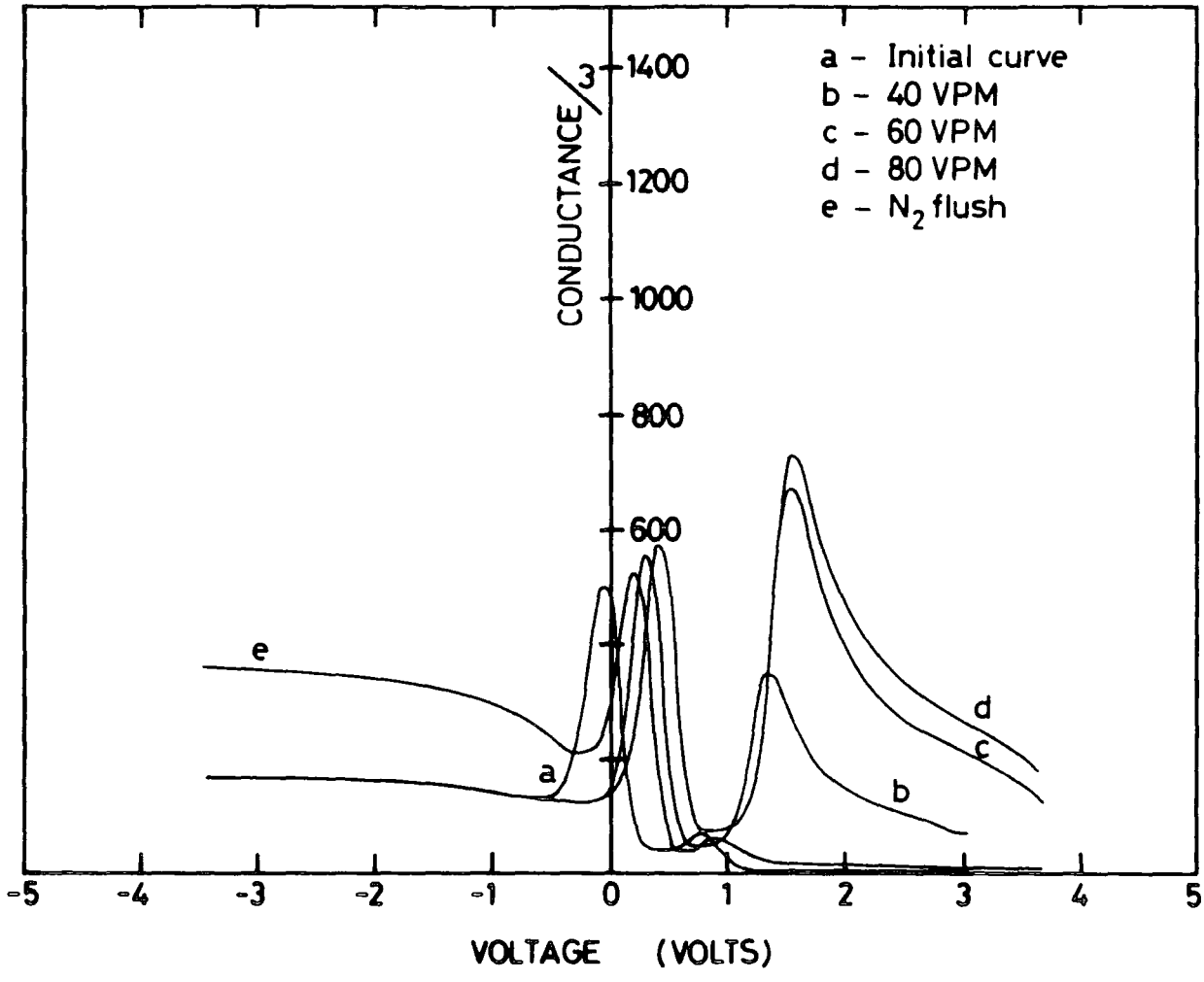

Figure 22. Conductance-voltage curves for a structure containing 5 layers of ASY-CuPc showing the influence of varying concentrations of NO_2.

directly reflects the additional charge introduced by the NO_2 at the oxide-phthalocyanine interface.

In this section we have presented data for both M-I-M and M-I-S structures incorporating ASY-CuPc LB layers. Essentially similar results have been observed in the simple conductivity measurements to those reported for single crystal of evaporated films. However, the advantage of the monolayers is that the recovery times are much shorter. We would anticipate that as film structures improve and defect densities are reduced, this feature will become even more noticeable and hence offer a tangible advantage in using LB films as gas detectors. Naturally, although we have only presented data here for phthalocyanine, it should be possible to envisage lock-key type mechanisms being usefully employed to make more sensitive and selective devices. The novel metal-insulator-semiconductor characteristics demonstrate that opportunities may exist for displaying ambient effects in more useful ways than simple conductivity measurements. More data on different semiconductor substrates and different LB film materials are required before one can assess any real advantage of using the semiconductor substrate. It seems clear, however, that there is more opportunity to capitalize on the presence of distinguishing features such as conductance peaks. For example, a sharp

threshold has been described earlier in this chapter for MISS devices. Mr Thomas using films prepared by us has indeed obtained preliminary results showing that his structures are sensitive to various ambients.

CHAPTER 8

SUMMARY AND CONCLUSIONS

8.1 SUMMARY

The main aim of this research has been to develop the materials and techniques for producing phthalocyanine LB films. A secondary aim has involved characterising the films and investigating their potential use in device structures.

It has been shown that phthalocyanine molecules with a low level of organic substitution can form the basis of LB film materials. In particular, both the metal substituted 4-ter-butyl and metal substituted asymmetric phthalocyanines are acceptable molecules for monomolecular assemblies. The isotherms for these materials give an area per molecule which is consistent with the molecular modelling of the packing in the film.

The importance of the Langmuir film preparation procedure has been highlighted, and in particular the role played by the spreading solvents. Results presented showing the optimisation achieved for certain spreading solvent combinations, specifically the improvement obtained for 4-ter-butyl manganese phthalocyanine, give a clear example of the value of such work. Similar important results have also been presented for phthalocyanine materials which have been incorporated into a matrix of cadmium stearate. Other novel features presented in

the thesis include techniques to enhance the LB deposition process, such as the incorporation of slowly evaporating liquids in the spreading solvent, deposition at a high pH, and the introduction of small quantities of alcohol into the subphase. All the phthalocyanines were found to transfer in the Z-type deposition mode; for this reason, a Langmuir trough was modified so as to incorporate an automatic cycle for transfer on the upward stroke only.

The structural, optical and electrical characterisation of our phthalocyanine films have been reported. Electron microscopy studies have shown that the majority of films are polycrystalline, of small domain size and with no preferred orientation to the grains. The asymmetric copper phthalocyanine is a valuable exception, however. Multilayer films of this molecule were found to have domains of the order of 3mm in size and to show a preferred orientation. Even so it has to be accepted that phthalocyanine films produced to date are not as structurally perfect as, for example, multilayers of w-tricosenoic acid. To offset this disadvantage, however, it should be stressed that our novel materials are far more stable and are indeed the only LB films to have survived the demanding 'cellotape' test. In all cases the molecules stick tenaciously to the substrate thus demonstrating good adhesion and cohesion properties.

The electrical assessment of the films included capacitance measurements; the linear behaviour observed in plots of C^{-1} versus N demonstrated the reproducibility of the layers. From

estimations of the layer thickness we conclude that the molecules are possibly stacked at an angle on aluminized substrates, but are oriented almost vertically on semiconductors. The values for the conductivity are broadly consistent with published data, for evaporated films.

The optical characteristics emphasise the low level of interaction between molecules, in that the spectra are of a similar form to those of the free molecule. However, it is shown that dipole-dipole interactions do occur between molecules as evidenced by the splitting of the absorption peak.

Because of their intrinsic stability the value of our phthalocyanine films has been demonstrated in several situations. Two examples of semiconductor devices incorporating LB films deposited by the author are the MISS switch and the electroluminescent device based on minority carrier injection. Similar results can be achieved with less stable compounds, but these deteriorate with time. Where phthalocyanine LB films are involved, relatively little degradation occurs even when relatively large current densities are involved. The films were also incorporated into a number of gas detecting devices and solar cell structures in order to evaluate their potential. The results from the use of the films in a lateral conduction device have indicated a high sensitivity to oxidising gases such as nitrogen dioxide. It was found that an increased level of response was obtained with thicker layers, but this was accompanied by a reduction in both the response and recovery times. Some data were also obtained for films incorporated in

an MIS structure. In this case exposure to nitrogen dioxide produced a secondary conduction peak associated with lateral conduction at the semiconductor interface. The preliminary gas measurements have provided some useful pointers to the future; it would appear that there may be some merit in using LB films in sensing devices because of the faster recovery times and their greater potential in terms of selectivity.

8.2 SUGGESTIONS FOR FURTHER WORK

One of the main areas for development and investigation is in the area of the production of LB film materials. In particular an investigation into the use of other substitutions, particularly asymmetrical ones would be of immense value. The materials used in this study were very much "off-the-shelf" materials or molecules which could be synthesised fairly easily. Future work in Durham will be carried out on certain "custom-made" materials with substitutions which should increase the degree of orientation of the film, and increase the ease with which the material can be handled. It is strongly felt that a good organic chemist working in conjunction with an LB film group is very much a pre-requisite for further developments in the materials field.

An impact in the materials will inevitably lead to an improvement in the film properties. This will in turn lead to films with fewer defects which may be of more use in, for

example, electronic devices. Naturally, one assumes that the substitution has been achieved without losing the stability of the phthalocyanine. It may well be that a compromise has to be reached between the film quality and the multilayer stability. Good results might also be achieved with other lightly substituted dye molecules. Contenders in this regard would be dithiolenes or porphyrins. Clearly, if LB films of sufficient quality and stability can be produced then there is enormous potential for them in several applications. We have concentrated on those involving semiconducting substrates; each device mentioned requires further research effort before a commercial product could be realised. For example, both the semiconductor surface preparation plus film thickness would need to be optimized in the MISS bistable switch. It is also possible to be more ambitious and plan 'active' applications of LB films involving LB films e.g. producing novel photoconductors involving p/n junctions. With exciting materials it is possible to construct heterojunctions e.g. using paraquat and merocyanine. What is desirable, however, is to make a homojunction where the same basic material is used for both p and n constituents. It may be possible by varying the metal ion to achieve this with phthalocyanines. Novel structures e.g. organic superlattices comprising alternate layers of p and n type phthalocyanine could also have interesting fundamental characteristics.

Figure Captions for Chapter 2

Figure 2.1 A schematic diagram showing the synthetic roots to phthalocyanine originally used by a) Braun and Tcherniac, b) de Diesbach and Von der Wied.

Figure 2.2 The molecular structure of phthalocyanine.

Figure 2.3 The unit cell of metal-free phthalocyanine, with cell parameters and positions of molecules indicated.

Figure 2.4 The idealized electronic transitions occurring in an organic material and an inorganic semiconductor, with the resultant absorption spectrum

Figure 2.5 The absorption spectra of metal-free phthalocyanine single crystal, evaporated film, and solution in 1-chloronapthalene (film and solution spectra by Assour, crystal spectra by Heilmeir).

Figure 2.6 The fluorescence spectra of compressed pellets of α-, β-, and X-metal-free phthalocyanine; (after Menzel and Jordon 1978).

Figure 2.7 Current density versus crystal thickness for the Ohmic region at 100V (o) and for the square-law region at 400V (▭) (after Barbe and Westgate)

Figure 2.8 Current density versus reciprocal temperature for the Ohmic region at 10V (o) and the space-charge-limited region at 4000V (▭) (after Barbe and Westgate).

Figure 2.9 A log-linear plot of the transient behaviour of photocurrent versus time (after Mizuggchi).

Figure 2.10 The absorption spectra of a) copper phthalocyanine and b) metal-free phthalocyanine films both undoped and doped with iodine.

Figure 2.11 The effects of NOX on the electronic spectrum of a-phthalocyanine: a) before NOX, b) after NOX, c) the film heated to 150 C, d) the film further heated to 200° C (after Honeybourne and Ewen).

Figure 2.12 The response of a zinc phthalocyanine film to a) a 4ppm NO_2 ambient, b) removal of the NO_2 from the gas stream (after Miasik).

Figure 2.13 Variation of conductance of lead phthalocyanine film with time following a step change of 50ppb NO_2 and return to air (after Bott).

Figure 2.14 a) schematic diagram of the gas sensor b) the decay of current level after exposure to the gas, c) the decay of current level after removal of the gas ambient (after Luars and Heiland).

Figure Captions for Chapter 3

Figure 3.1 Diagram showing a) the alignment of amphipathic materials with the subphase and b), c) and d) the successive steps in the formation of a multilayer.

Figure 3.2 The molecular structure of a) stearic acid, b) cadmium stearate and c) w-tricosenoic acid.

Figure 3.3 Isotherms for stearic acid showing the effect of both pH variation and the use of cadmium chloride in the subphase.

Figure 3.4 A typical isotherm for stearic acid obtained for the optimum subphase conditions.

Figure 3.5 A schematic representation of the pick-up of a monolayer and the subsequent build-up of a multilayer for a Y-type material.

Figure 3.6 A plot of film area versus time for the deposition of a Y-type material

Figure 3.7 A schematic diagram of the multilayer arrangement achieved with X and Z-type deposition.

Figure 3.8 Results showing X-ray diffraction data from a film of 43 layers of perdeuterated manganese stearate on a substrate of monocrystalline silicon (After Nicklow et al)

Figure 3.9 A photograph showing the diffraction pattern from 21 layers of w-tricosenoic acid. (After Peterson et al)

Figure 3.10 Capacitance data for cadmium stearate LB films on a highly doped InP substrate as a function of the number of deposited layers. (After Roberts et al)

Figure Captions for Chapter 4

Figure 4.1 A photograph of the LB trough system used in this work.

Figure 4.7 Schematic representations of a) the standard deposition of an LB film, where the film area is simply recorded as a function of time and b) an alternative method of monitoring the deposition, where the area is plotted as a function of the dipping head position

Figure 4.8 Schematic representations of a) a deposition plot of area versus dipping head position for a z-type material and b) the film/ dipping head position diagram for the complete autocycle used for z-type deposition.

Figure 4.9 A photograph of the sample chamber used to make capacitance and conductance measurements.

Figure 4.10 A photograph of the equipment used to measure the conductivity of the phthalocyanine films in the presence of various ambients.

Figure 4.11 A plot showing the calibration curve supplied for the gas blender

Figure Captions for Chapter 5

Figure 5.1 A schematic diagram of the "in line" filter used when spreading metal-free phthalocyanine

Figure 5.2 Variation of the area decay of a Langmuir film of ASY-CuPc with the pH of the subphase.

Figure 5.3 The variation of surface tension with various mixtures of water and ethanol.

Figure 5.4 A typical isotherm for metal-free phthalocyanine spread from acetone

Figure 5.5 A range of isotherms for metal-free phthalocyanine showing the variation with spreading solvent.

Figure 5.6 A range of isotherms showing the variation with percentage of incorporated stearic acid.

Figure 5.7 Isotherms for manganese phthalocyanine taken for both a fresh and a 9 hour old solution.

Figure 5.8 Isotherm for metal-free 4-ter-butyl phthalocyanine.

Figure 5.9 A typical isotherm for copper 4-ter-butyl phthalocyanine spread from xylene.

Figure Captions for Chapter 6

Figure 6.1 The RHEED diffraction pattern observed for three layers of metal-free phthalocyanine deposited on glass.

Figure 6.2 The RHEED diffraction pattern obtained for metal-free 4-ter-butyl phthalocyanine deposited on InP.

Figure 6.3 A TEM micrograph of asymmetrically substituted copper phthalocyanine showing a preferred orientation, indicated by the arcs of intensity which are present.

Figure 6.4 A scanning electron migrograph of a layered structure of metal-free phthalocyanine on InP.

Figure 6.5 An enhanced view of the layered structure shown in fig.4 showing the degree of aggregation present in the film.

Figure 6.6 A scanning electron micrograph for the asymmetrically substituted copper phthalocyanine.

Figure 6.7 a scanning electron micrograph of manganese 4-ter-butyl phthalocyanine, taken with a beam strength of, a)1.5kV and b) 7.5kV.

Figure 6.8 A plot of absorbance versus concentration for; a) dilithium phthalocyanine, b) manganese 4-ter-butyl phthalocyanine, c) asymmetrically substituted copper phthalocyanine.

Figure 6.9 The absorbance spectra for two solutions of concentration 8.6×10^{-6} and 71.1×10^{-6} moles/litre showing the growth of the dimer peak with increasing concentration.

Figure 6.10 A plot of the ratio of the heights of the monomer and dimer peaks versus concentration, showing the increase of dimer formation with increasing concentration.

Figure 6.11 Absorbance spectra for both a solution of dilithium phthalocyanine, and a deposited LB film of metal-free phthalocyanine.

Figure 6.12 A schematic representation of the changes in the electronic levels due to the crystal field and dipole-dipole interactions.

Figure 6.25 A log current versus log voltage plot obtained for a structure containing forty layers of Mn 4-ter-butyl Pc.

Figure Captions for Chapter 7

Figure 7.1 The device structure used for checking the effect of varying the number of phthalocyanine LB layers in a MIS electroluminescent diode

Figure 7.2 A plot of the dc power conversion efficiency versus the number of phthalocyanine layers obtained for the above structure.

Figure 7.3 The device structure of the MISS devices fabricated with four layers of ASY-CuPc.

Figure 7.4 A typical device characteristic obtained for the above structure .

Figure 7.5 The solution spectra obtained for ASY-CuPc before and after exposure to 120ppm NO_2.

Figure 7.6 The spectra obtained for an LB film of ASY-CuPc before and after exposure to 200ppm.

Figure 7.7 A schematic diagram of the interdigitated electrode structure used in the lateral conduction devices.

Figure 7.8 A typical result showing the rise in conduction due to placing a sample incorporating one layer of ASY-CuPc in a 20ppm ambient of NO_2.

Figure 7.9 The variation of the saturated current level with NO_2 concentration.

Figure 7.10 The data presented in fig. 9 replotted on a log-log scale.

Figure 7.11 The variation of the saturation current level with the number of deposited layers.

Figure 7.12 The recovery of the conductivity for a number of different thickness films.

Figure 7.13 Elovich plots for one to five layer samples.

Figure 7.14 An enlarged diagram of the Elovich plot obtained for a 1 layer sample, showing the linear relationship observed.

REFERENCES: CHAPTER 2

1. R.P.Linstead, Br. Assoc. Adv. Sci. Rep., (1933) 465

2. A.G.Dandridge, H.A.Drescher, J.Thomas, (to Scottish Dyes Ltd.), British Patent 322,169, November 18, 1929.

3. A.Braun, and J.Tcherniac, J., Ann. Ber., 40 (1907) 2709

4. H. De Diesbach, and E. Von der Wied, Helv. Chlim. Acta, 10, (1927) 886

5. F.H.Moser, and A.L.Thomas, 'The Phthalocyanines', Vol.2, 29, CRC Press.

6. J.M.Robertson, Chem. Soc., (1935) 615

7. J.M.Robertson, Chem. Soc., (1936) 1195

8. J.M.Robertson, R.P.Linstead, and C.E.Dent, Nature (London), (1935) 135

9. J.M.Robertson, and I.Woodward, Chem. Soc., (1937) 219

10. J.M.Robertson, and I.Woodward, Chem. Soc., (1940) 36

11. R.P.Linstead, and J.M.Robertson, J. Chem. Soc., (1936) 1195

12. F.W.Karasek and I.C.Decius, J. Am. Chem. Soc., 74 (1952) 4716

13. M.Fustoss-Wegner, Thermochim. Acta. 23 (1978) 93

14. N.Uyeda, T.Kobayashi, K.Ishizuka, and Y.Fujiyoshi, Chemica Scripta., 14, (1978) 47

15. T.Kobayashi, Y.Fujiyoshi, F.Iwatsu, and N.Uyeda, Acta Crysta. A37 (1981) 692

16. J.F.Byrne, P.F.Kurz, (to Xerox Corporation), U.S. Patent 3,357,989, December 12, 1967

17. J.F.Byrne, P.F.Kurz, (to Xerox Corporation), U.S.Reissue 27,117 of U.S. Patent 3,357,989, April 20, 1971

18. J.H.Sharp, and M.Lardon, J. Phys. Chem., 72 (1968) 3230

19. J.H.Sharp, and M.Abkowitz, J. Phys. Chem., 77 (1973) 477

20. Y.Abe, and T.Hosoda, Japanese Kokai., 43 (1971) 636

21. I.Kumano, M.Miyatake, S.Tamura, and S.Ishizuka, Japanese Kokai 74, 59 (1974) 136

22. R.L.Van Ewyk, Ph.d. Thesis, University of Kent (1978)

23. P.E.Fielding, Proc. U.S.-Japan Seminar (1973)

24. R.S.Kirk, Mol. Cryst., 5(2) (1968) 211

25. P.S.Vincettt, Z.D.Popovic and L.McIntyre, Thin Solid Films, 82 (1981) 357

26. R.Loutfy and C.Hsiao, Photographic Science and Engineering, 24 (1980) 156

27. H.Shirai, K.Kobayashi, Y.Takemae, and N.Hojo, J. Polm. Sci., Polym. Lett. Ed., 17 (1979) 343

28. H.Shirai, A.Maruyama, K.Kobayashi, and N.Hojo, J. Polm. Sci., Polym. Lett. Ed., 17 (1979) 661

29. H.Shirai, S.Higaki, K.Hanabusa, and N.Hojo, J. Polm. Sci., Polym. Lett. Ed., 21 (1983) 157

30. O.Hirabaru, T.Nakase, K.Hanabusa, H.Shirai, k.Takemoto, and N.Hojo, J. Chem. Soc. Dalton trans., (1984) 1485

31. G.J.Kovacs and P.S.Vincett, J. Vac. Sci., 20(3) (1982) 419

32. C.E.Dent, R.P.Linstead, J. Chem. Soc., (1934) 1027

33. L.S.Mai, B.A.Baranov, N.N.Gulyaev, V.N.Gorenko, Lakokrasoch.; Mater. Ikh Primen., 6 (1972) 57

34. P.Hauser, D.Horn, and R.Sappok, Fatipec Congr., 12 (1974) 191

35. M.J.Smith, J. Oil colour Chem. Assoc., 56(2), (1973) 126

36. J.Stabenow, Ber. Bunsenges. Phys. Chem., 72(3) (1968) 374

37. W.R.Graham, F.Hutchinson, and D.A.Reed, J. Appl. Phys., 44 (1973) 5155

38. F.H.Moser, and A.L.Thomas, The Phthalocyanines, CRC Press.

39. P.E.Fielding, A.G.MacKay. Aust. J. Chem, 28(7) (1975) 1445

40. G.H.Heilmeier and G.Warfield, J. Chem. Phys., 38 (1963) 893

41. B.D.Berezin, Izv. Vyssh. Ucheb. Zaved Khim. Tekhnol., 11 N 5 (1968) 537

42. K.Yoshino, M.Hikida, K.Tatsuno, K.Kaneto and Y.Inuishi., J. Phys. Soc. Jpn., 34(2) (1973) 441

43. R.E.Menzel, and K.J.Jordan, Chem. Phys. 32 (1978) 223

44. K.J.Beales, D.D.Eley, D.J.Hazeldine and T.F.Palmer, Katalyse an Phthalocyaninen, Symp., Hamburg, (1973) 1

45. S.E.Harrison and J.M.Assour, J. Chem. Phys., 40(2) (1964) 365

46. K.Wihksne and A.E.Newkirk, J. Chem. Phys., 34 (1961) 2184

47. S.E.Harrison and K.H.Ludewig, J. Chem. Phys., 45(1) (1966) 343

48. D.Kleitman, P.E.Fielding, and F.J.Gutman, J. Chem. Phys., 26, (1957) 411

49. G.H.Heilmeier, and G.Warfield, J. Chem. Phys., 38(1) (1963) 163

50. A.Sussman, J. App. Phys., 38(7) (1967) 2738

51. A.Sussman, J. App. Phys., 38(7) (1967) 2748

52. D.F.Barbe, and C.R.Westgate, Solid State Comm., 7 (1969) 563

53. D.F.Barbe, and C.R.Westgate, J. Chem. Phys., 52(8) (1970) 4046

54. T.G.Abdel-Malik and G.A.Cox., J. Phys. C: Solid State Phys., 10 (1977) 63

55. K.Ukei, J. Phys. Soc. Jpn., 40(1) (1976) 140

56. G.A.Cox and P.C.Knight, J. Phys. Chem. Solids, 34(10), (1973) 1655

57. G.A.Cox and P.C.Knight, J. Phys. Chem., 7(1), (1974) 146

58. Y.Aoyagi, K.Masuda, and S.Namba, Mol. Cryst. And Liq. Cryst., 22 (1973) 301

59. J.Mizuguchi, Jpn. J. Appl. Phys. 20 (1981) 293

60. G.A.Chamberlin, ORGANIC SOLAR CELLS - A REVIEW.

61. F.R.Fan, and L.R.Faulkner, J. Chem. Phys., 67 (1978) 3341

62. J.M.Assour, and S.E.Harrison, J. Phys. Chem. Solids, 26(3) (1965) 670

63. D.F.Barbe, and C.R.Westgate, J. Phys. Chem. Solids, 31 (1970) 2679

64. M.E.Musser and S.C.Dahlberg, Surface Science, 100 (1980) 605

65. J.Mizuguchi, Jpn. J. Appl. Phys. 20(4) (1981) 713

66. J.Mizuguchi, Jpn. J. Appl. Phys. 20(10) (1981) 1855

67. J.Mizuguchi, Jpn. J. Appl. Phys. 20(11) (1981) 2065

68. J.Mizuguchi, Jpn. J. Appl. Phys. 20(11) (1981) 2073

69. N.Yamamoto, S.Tonomura, and H.Tsubomura, J.Appl. Phys. 52(9) (1981) 5705

70. J.Curry and E.P.Cassidy, J. Chem. Phys., 37(9) (1962) 2154

71. Y.Yamamoto, K.Yoshino and Y.Inuishi, J. Phys. Soc. Jpn., 47(6) (1979) 1887

72. C.L.Honeybourne and R.J.Ewen, J. Phys. Chem. Solids, 44(8) (1983) 833

73. C.L.Honeybourne and R.J.Ewen, J. Phys. Chem. Solids, 44(3) (1983) 215

74. R.L.Van Ewyk, A.V.Chadwick and J.D.Wright., J.C.S. Faraday 1, 76 (1980) 2194

60. G.A.Chamberlin, Organic Solar Cells - a review presented to a meeting on "Thin film solar cells" held at Newcastle-on-Tyne Polytechnic, 14th-15th April 1981

75. R.L.Van Ewyk, A.V.Chadwick and J.D.Wright., J.C.S. Faraday 1, 77 (1981) 73

76. J.J.Miasic, Thesis, University of Kent (1981)

77. B.Bott and T.A.Jones, Sensors and Actuators, 5 (1984) 43

78. H.Luars, and G.Heiland, U.K. Patent application, GB 2 098 741 A

REFERENCES: CHAPTER 3

1. B.Franklin, Phil, Trans. Roy. Soc. 64 (1774) 445

2. A.Pockels, Nature, 43 (1891) 437

3. Lord Rayleigh, Phil.Mag., 48 (1899) 321

4. I.Langmuir, J.Am.Chem.Soc., 39 (1917) 1848

5. K.B.Blodgett and I.Langmuir, Phys.Rev., 51 (1937) 964

6. C.H.Giles and S.D.Forrester, Chem. Ind. (London) 1616(1969), 80 (1970), 42 (1971).

7. G.L.Gaines Jnr, 'Insoluble Monolayers at Liquid-Gas Interfaces', Wiley (1966)

8. First International Conference on Langmuir-Blodgett Films, Durham, 1982. Thin Solid Films 99 (1983)

9. G.G.Roberts, Contemp. Phys., 25 (1984) 109

10. C.W.Pitt and L.M.Walpita, Thin Solid Films, 68 (1980) 101

11. A.Barraud, Thin Solid Films, 99 (1983) 317

12. T.Ohnishi, M.Hatakeyama, N.D.Yamamoto and H.Tsubomura, Bull, Chem. Soc. Jpn.,51 (1978) 1714

13. A.Sen and G.S.Singhal, J. Coll, Interface Sci., 68 (1979) 471

14. H.Kuhn, J. Photochem., 10 (1979) 111

15. H.Kuhn, Pure Appl. Chem., 51 (1979) 341

16. M.Sugi, K.Nembach and D.Mobius, Thin solid Films, 27 (1975) 205

17. P.S.Vincett, W.A.Barlow, F.T.Boyle, J.A.Finney and G.G.Roberts, Thin Solid Films, 60 (1979) 265

18. R.Jones, R.H.Tredgold and P.Hodge. Thin Solid Films, 99 (1983) 25

19. A.Ruaudel-Teixier and A.Barraud. Thin solid Films, 99 (1983) 33

20. S.Kuroda, M.Sugi and S.Iizima. Thin Solid Films, 99 (1983) 21

21. M.Sugi, M.Saito, T.Fukui and S.Iizima, Thin Solid Films, 99 (1983) 17

22. M.Sugi and S.Iizima, Thin Solid Films, 68 (1980) 173

23. H.Kuhn, D.Mobius and H.Bucher, 'Spectroscopy of Monolayer Assemblies', in A.Weissberger and B.Rossiter (eds), Physical Methods of Chemistry, Vol.1, Part 3b, Wiley (1972)

24. I.Langmuir and V.J.Schaefer, J. Amer. Chem. Soc. 59 (1937) 2400

25. C.Sucher, Kolloid-z., 190 (1963) 146

26. P.Fromherz, Rev. Sci. Inst. 46 (1975) 1380

27. L.Blight, C.W.N.Cumper, and V.Kyte, J. Colloid Sci. 20 (1965) 393

28. A.Barraud, and M.Vandevyver, thin Solid Films, 99 (1983) 221

29. I.R.Peterson, G.J.Russell and G.G.Roberts, Thin Solid Films, 109 (1983) 371

30. R.M.Nicklow, M.Pomerantz and A.Segmuller, Physical Review, b,23, (1981) 1081

31. R.R.Highfield, and R.K.Thomas, Thin Solid Films, 99 (1983) 165

32. G.J.Russell, M.C.Petty, I.R.Peterson, G.G.Roberts, J.P.Lloyd and K.K.Kan, Journal of Materials Science (November) (1983)

33. D.T.Clark, Y.C.T.Fok, and G.G.Roberts, Journal of Electron Spectroscopy and Related Phenomena, 22, (1981) 173

34. G.G.Roberts, T.M.McGinnity, W.A.Barlow and P.S.Vincett, Thin Solid Films, 68 (1980) 223

35. M.Vandevyer,A.Ruaudel-Teixier, L.Brehamet and M.Lutz, Thin Solid Films, 99 (1983) 41

36. D.N.Batchelder, D.Bloor and I.R.J.Lyall, Thin Solid Films, 99 (1983) 118

37. P.A.Chollet and J.Messier, Thin Solid Films, 99 (1983) 197

38. T.M.Ginnai, D.P.Oxley and R.G.Pritchard, Thin Solid Films, 68 (1980) 241

39. R.P.Highfield and R.K.Thomas, Thin Solid Films, 99 (1983) 165

40. H.Kuhn, Thin Solid Films, 99 (1983) 1

41. C.Mori, H.Noguchi, M.Mizuno and T.Watanabe, Japanese Journal of Applied Physics, 19, (1980) 725

42. N.P.Franks, and K.A.Snook, Thin Solid Films, 99 (1983) 133

43. L.R.McLean, A.A.Durrani, M.A.Whittam, D.W.Johnston and D.Chapman, Thin Solid Films, 99 (1983) 127

44. G.G.Roberts, M.C.Petty and I.M.Dharmadasa, IEE Proc., 128 (1981) 197

45. J.Batey, G.G.Roberts, and M.C.Petty, Thin Solid Films, 99 (1983) 283

46. J.Batey, M.C.Petty, and G.G.Roberts, Proceedings of the International Conference on 'Insulating Films on Semiconductors' (North Holland) (1983) 141

47. K.K.Kan, G.G.Roberts and M.C.Petty, Thin Solid Films, 99 (1983) 291

48. G.G.Roberts, K.P.Pande and W.A.Barlow, Solid State Electron.Dev., 2 (1978) 169

REFERENCES: CHAPTER 4

1. L.Blight, C.W.N.Cumber, and V.Kyte, J. Colloid Sci. (1965) 393

2. W.Walkenhorst, Nature 34 (1947) 373

3. H.P.Zingsheim, Scanning Electron Microscopy 1 (1977) 357

4. G.J.Russell, M.C.Petty, I.R.Peterson, G.G.Roberts, J.P.Lloyd, K.K.Kan, Journal of Materials Science 3 (1984) 25

REFERENCES: CHAPTER 5

1. H.Kuhn, D.Mobius and H.Bucher, Spectroscopy of monomolayer assemblies. In A.Weissberger and B.Rossiter (eds.), Physical Methods of Chemistry, V1, Part 3B, Wiley, New York, 1972.

2. E.E.Polymeropoulos, D.Mobius and H.Kuhn, Thin Solid Films, 68 (1980) 173

3. P.S.Vincett and G.G.Roberts, Thin Solid Films, 68 (1980) 135

4. G.G.Roberts, K.P.Pande and W.A.Barlow, Proc. Inst. Electr. Eng., Part 1, 2 (1978) 169

5. G.G.Roberts, M.C.Petty and I.M.Dharmadasa, Proc. Inst. Electr. Eng., Part 1, 128 (1981) 197

6. J.Batey, G.G.Roberts, and M.C.Petty. Proc. 1st Int. Conf. On Langmuir Blodgett Films, Durham, September 20-22, 1982, in Thin Solid Films, 99 (1983) 283

7. S.Grammatica and J.Mort, Appl. Phys. Lett., 38 (1981) 445

8. G.A.Chamberlain and P.J.Cooney, Chem. Phys. Lett., 66 (1979) 88

9. M.Sugi and S.Iizima, Thin Solid Films, 68 (1980) 199

10. N.Yamamoto, T.Ohnishi, M.Hatakeyama and H.Tsubomura, Thin Solid Films, 68 (1980) 191

11. H.Killesreiter, Z. Naturforsch., Teil A, 34 (1979) 737

12. K.Venkataraman, The Chemistry of Synthetic Dyes, Vol. 2, Academic Press, New York, 1952, p. 1118; Vol. 5. Academic Press, New York, 1972, p. 241

13. S.A.Mikhalenko, S.V.Barkanova, O.L.Lebedev and E.A.Luk'Yanets, Zh. Obshch. Khim., 14 (1971) 2735

14. P.S.Vincett, W.A.Barlow, F.T.Boyle, T.A.Finney and G.G.Roberts, Thin Solid Films, 60 (1979) 265

15. M.T.Fowler, Ph.D thesis, Univ. Of Durham, 1985

16. R.Jones and R.H.Tredgold, Thin Solid Films, 99 (1983) 25

REFERENCES: CHAPTER 6

1. K.Bernauer, S.Fallab, Helv, Chim. Acta 44 (1961) 1287

2. P.D.W.Boyd, T.D.Smith, J. Chem. Soc., Dalton Trans (1972) 839

3. E.Schnabel, H.Nother, H.Kuhn. In "Chemistry of Natural and Synthetic Colouring Matters" Academic Press, New York, (1962), 561

4. A.Sussman, J. Appl. Phys. 30 (1967) 2738

5. G.A.Cox and P.C.Knight, Phys. Status Solidi 50B (1972) K135

6. D.F.Barbe and C.R.Westgate, J. Chem. Phys. 52 (1970) 4056

7. R.Hann, A.W.Barlow, J.H.Steven, B.L.Eyres, M.V.Twigg and G.G.Roberts, Proceedings Second Int. Workshop USA, apri1 1983

REFERENCES: CHAPTER 7

1. J.Batey, G.G.Roberts and M.C.Petty, Thin Solid films, 99 (1983) 283

2. J.Batey, M.C.Petty, and G.G.Roberts, Electronics Letters 20 (1984) 489

3. R.H.Tredgold and M.C.J.Young, Awaiting publication

4. J.D.Wright, A.V.Chadwick, B.Meadows and J.J.Miasik, Mol. Cryst. Liq. Cryst., 93 (1983) 315

5. M.M.Atalla, A.R.Bray and R.Linder, Suppl. Proc. IEE (London), pt B 106 (1959) 1130

6. W.Shockley, H.J.Queisser and W.W.Hooper, Phys. Rev. Letters, 11 (1963) 489